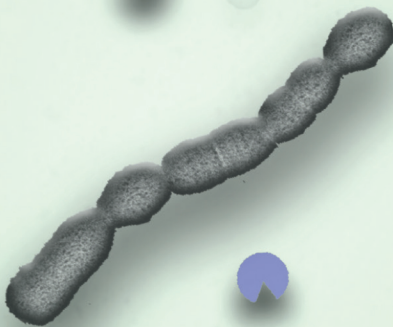


# Dissecting the intestinal mucosal niche with the pathobiont *Allobaculum mucolyticum*



Guus van Muijlwijk

**Dissecting the intestinal mucosal niche with the pathobiont  
*Allobaculum mucolyticum***

**Guus Hylke van Muijlwijk**

**Dissecting the intestinal mucosal niche with the pathobiont  
*Allobaculum mucolyticum***

Het ontleden van de intestinale mucosale niche met behulp van de  
pathobiont *Allobaculum mucolyticum*

(met een samenvatting in het Nederlands)

**Proefschrift**

ter verkrijging van de graad van doctor aan de  
Universiteit Utrecht  
op gezag van de  
rector magnificus, prof.dr. H.R.B.M. Kummeling,  
ingevolge het besluit van het college voor promoties  
in het openbaar te verdedigen op

donderdag 19 mei 2022 des middags te 4.15 uur

door

**Guus Hylke van Muijlwijk**

geboren op 15 maart 1990  
te Woerden

Dissecting the intestinal mucosal niche with the pathobiont *Allobaculum  
mucolyticum*

© Guus Hylke van Muijlwijk 2022

All rights reserved. No part of this thesis may be reproduced, stored, or  
transmitted in any form or by any means without prior permission of the author.

ISBN: 978-94-93270-62-6

Cover Design: Lodewijk Luken  
Layout: Guus Gijben. [www.proefschrift-aio.nl](http://www.proefschrift-aio.nl)  
Printing: [www.proefschrift-aio.nl](http://www.proefschrift-aio.nl)

Printing of this thesis was financially supported by: Infection & Immunity  
Utrecht; Department of Medical Microbiology, UMC Utrecht; Department  
of Biomolecular Health Sciences, Faculty of Veterinary Medicine, Utrecht  
University; Netherlands.

**Promotor:**

Prof. dr. J.P.M. van Putten

**Copromotor:**

Dr. M.R. de Zoete

**TABLE OF CONTENTS**

<b>Chapter 1.</b> General Introduction	7
<b>Chapter 2.</b> <i>Allobaculum mucolyticum</i> sp. nov. and <i>Allobaculum filumensis</i> sp. nov., two novel members of the <i>Allobaculum</i> genus isolated from the human intestinal tract	37
<b>Chapter 3.</b> Identification of <i>Allobaculum mucolyticum</i> as a novel human intestinal mucin degrader	53
<b>Chapter 4.</b> Growth inhibition of <i>Akkermansia muciniphila</i> by a secreted pathobiont sialidase	89
<b>Chapter 5.</b> Desialylation of secretory IgA increases IgA-mediated neutrophil activation	125
<b>Chapter 6.</b> General Discussion	151
<b>Appendices</b>	
Summary	179
Nederlandse samenvatting	187
Dankwoord/acknowledgements	195
Curriculum vitae	203
Publications	207

# 01



## General Introduction

# 01

## HUMANS AND THEIR MICROBIOTA

The last two decades can be characterized as an age of exploration of our microbial self. Technological advances, such as the development of high-throughput DNA sequencing and other -omics technologies, have allowed us to explore and map the microbial terra incognita in great detail<sup>1,2</sup>.

Microbial communities that colonize other organisms are collectively referred to as microbiota, or the microbiome when referring to their total collection of genes. To date, thousands of microbial species and communities have been discovered and are known to exert profound effects on human physiology and health. Among many things, they are involved in the production of essential nutrients, the protection from pathogens and the development of the immune system<sup>3-5</sup>. Recent studies show that the influence of the microbiota even extends to our mental health<sup>6</sup>. The study of the human microbiota has massively transformed our understanding of human biology and our role as a holobiont.

While the microbiota consists of bacteria, viruses, fungi and archaea at various sites on and in our body, in this thesis the focus will be on the bacterial microbiota in the intestinal tract. The most commonly used technique to identify bacterial species in complex communities is through 16S rRNA gene sequencing. Although this technique generally does not allow detection to the species or strain level, this technique can be used to draw a rough map of the microbial landscape at a given site. Mapping of the bacterial microbiota composition at different body sites and in different persons demonstrated that each body site and each individual harbours distinct bacterial species organized in complex communities<sup>7</sup>. Like different geographical habitats harbour different plants and animals, so do different people and body sites harbour different microbes<sup>7-9</sup>. Even though each person and body site has a unique microbiota composition, the overall community structure and genomic functions often contain conserved patterns. By studying these conserved patterns in healthy people and comparing them to people suffering from diseases it was discovered that many diseases are characterized by changes in the microbiota composition.

## THE GUT MICROBIOTA AND INFLAMMATORY BOWEL DISEASE

The gut microbiota is the most well studied in relationship to human disease. One of the diseases in which the composition of the gut microbiota is altered is inflammatory bowel disease (IBD). IBD is an umbrella term for chronic relapsing and remitting inflammatory diseases of the intestine of which the aetiology is unclear. IBD includes Crohn's disease (CD) and ulcerative colitis (UC). CD can affect any site of the gastrointestinal (GI)-tract and is characterized by local inflammatory lesions which, in severe cases, can penetrate into the deeper layers of the intestine. Ulcerative colitis, on the other hand, is characterized by a single continuous site of inflammation that is restricted to the mucosa of the rectum and colon. Both CD and UC can be highly debilitating diseases that can develop into life-threatening complications.

IBD currently affects up to 0.5% of the population in North America and Europe. At these continents, the incidence rate seems to have stabilized after a rapid increase in prevalence over the last 50 years<sup>10,11</sup>. Although incidence rates in North America and Europe have stabilized, the incidence rates in newly industrialized countries in Asia, South America and the Middle East are rapidly increasing. IBD is a chronic disease often diagnosed early in life. Due

to the lack of curative therapies this will likely result in the cumulative addition of cases and an exponential increase in the number of IBD patients over the next decade<sup>11</sup>. This will not only come at a high individual cost for each patient but will also put a tremendous economic burden on health-care systems worldwide.

Current therapies for IBD are mainly directed at limiting inflammation, using immunosuppressant steroids, biologicals (e.g. TNF inhibitors), antibiotics or a combination of the three<sup>12-14</sup>. These therapies are often successful in inducing remission of disease symptoms; however, they are not a definitive cure. Moreover, these therapies can come with severe side-effects and a significant number of patients relapse overtime or fail to respond to therapy at all. Faecal microbial transplantation (FMT) is currently being explored for IBD and other diseases to restore altered microbiota. Although the first results are cautiously promising, we are still far from curing IBD<sup>15,16</sup>. In order to improve current therapies and one day find a cure for IBD, or prevent it altogether, a better mechanistic understanding of the processes underlying IBD development and pathogenesis is essential.

IBD pathogenesis is currently thought to occur from complex interactions involving genetic predisposition, environmental factors, aberrant immune responses, and alterations to the gut microbiota, also referred to as dysbiosis<sup>17-19</sup>. Genome wide association studies (GWAS) have identified over 200 genetic risk loci for IBD, many of which are related to the regulation of innate and adaptive immune responses involved in host-microbiota interactions<sup>19</sup>. Examples of these risk loci are NOD2 and IL-10. NOD2 was the first gene to be associated with IBD and functions as a cytosolic receptor for the bacterial peptidoglycan building-block muramyl dipeptide (MDP)<sup>20,21</sup>. Among other things, NOD2 regulates antigen presentation, induces antimicrobial peptide production by Paneth cells and promotes Th17-cell differentiation<sup>22</sup>. Homozygous defects in NOD2 confer a 20-40x increased risk of developing CD<sup>20,21</sup>. IL-10 is an important anti-inflammatory cytokine, and has been implicated in the pathophysiology of both CD and UC<sup>19</sup>. Despite the important roles of these genes and other loci, genetic mutations fail to account for more than 75% of IBD cases, suggesting an important role for environmental factors<sup>19</sup>.

Relevant environmental factors for IBD include smoking, antibiotic use, diet and the gut microbiota composition. In humans, the use of antibiotics, and especially the use of antibiotics in early life, is associated with a greatly

increased risk of CD<sup>23,24</sup>. These findings were corroborated in mice, in which early life exposure to antibiotics was shown to have long lasting effects on host metabolism and immunological imprinting, resulting in increased susceptibility to colitis later in life<sup>25-27</sup>. Others showed that antibiotics deplete the gut microbiota of butyrate-producing species. The lack of butyrate led to higher levels of epithelial oxygenation and the expansion of facultative anaerobes. This so-called dysbiotic microbiota can then act as a driver of inflammatory responses, e.g. through increased levels of bacterial translocation<sup>28-30</sup>. Importantly, antibiotic-induced dysbiosis can also be passed on from mother to offspring, which is an excellent demonstration of the far-reaching impact antibiotics may have.

Western-style diets have also been associated with increased risk of IBD. Such western diets are rich in saturated fatty acids and simple sugars such as glucose and fructose, but low in dietary fibre. In multiple epidemiological studies these nutrients were shown to be risk factors for IBD<sup>31</sup>. In mouse models of intestinal inflammation, diets low in dietary fibre or high in simple sugars or saturated fats resulted in a microbiota-mediated degradation of the mucus layer and increased susceptibility to various forms of colitis<sup>32-34</sup>.

It is important to note that environmental factors such as diet and antibiotics also greatly impact the gut microbiota composition, and it is likely that some, if not most, of their influence on IBD is exerted through an altered gut microbiota. The gut microbiota composition of IBD patients is often less diverse than in healthy controls<sup>35-37</sup>. General patterns include a reduction in the relative abundance of the *Firmicutes* and *Bacteroidetes* phyla and an increase in the number of *Enterobacteriaceae*. Other notable changes include the increased number of encroaching, mucosa-associated bacteria as well as changes in the IgA-coated bacterial communities<sup>38,39</sup>. Some of these immunogenic, IgA-coated commensals are thought to have increased pathogenic potential compared to other symbionts, and are referred to as pathogenic symbionts or pathobionts<sup>39,40</sup>. Although many associations and correlations between the gut microbiota composition, pathobionts and IBD susceptibility have been reported to date, it has often been difficult to establish causality outside of mouse models. This is likely due to the complex, multifactorial nature of the disease. Moreover, a deeper understanding of these complex interactions is often hampered by the fact that most bacteria within the gut remain functionally unexplored. Therefore, if we aim to

elucidate novel mechanisms that drive IBD development, a more detailed and functional characterization of dysbiosis-associated microbes and their interaction with the host is warranted.

In this thesis I will explore the interaction of pathobionts with several critical components of the mucosal barrier. To understand the complex host-microbiota interactions in the mucosal niche, a thorough understanding of key components of the mucosal barrier is required. In the following section two critical elements of the mucosal barrier will be discussed: the mucus layer and secretory IgA, as well as their interactions with the bacterial microbiota

## THE INTESTINAL MUCUS LAYER

As the name implies all mucosae are covered by a mucus layer. This highly viscous and slimy mucus layer is an important part of the innate immune system and a first line of defence<sup>41,42</sup>. It protects the underlying epithelium from dehydration, functions as a lubricant, and acts as a barrier to protect the epithelial cells and lamina propria from excessive exposure to foreign antigens and pathogens, including bacteria. The mucus layer is mainly composed of water, lipids and (glyco)proteins. The main glycoproteins are mucins, which be grouped in either secreted or transmembrane mucins. Transmembrane mucins, including the most common transmembrane mucin MUC1, are an important part of the glycocalyx expressed on the apical side of epithelial cells. These mucins not only form a barrier but can also play important roles in cell signalling pathways. The role of transmembrane mucins has been extensively described by others<sup>43</sup>.

In the intestine, the largest part of the mucus layer is composed of the secreted and gel-forming mucin MUC2<sup>44</sup>. MUC2 is produced in goblet cells as a multimeric protein and stored within tightly packed granules. Upon release, this firm network of MUC2 proteins attracts water and massively expands in size forming a large and highly viscous gel<sup>44</sup>. This gel initially remains attached to the epithelial cells, but through combined effects of increasing pH and an endogenous protease is eventually released to form a more loose, detached mucus layer. The mucus layer is continuously renewed and mixed with defence molecules like antimicrobial peptides and IgA. Combined these components form an important barrier against pathogen invasion and as such are crucial for maintaining intestinal homeostasis<sup>41</sup>.

The GI tract is highly compartmentalized, and each compartment serves different functions. This differentiation is not only reflected by a distinct microbiota within each compartment, but also by a distinct mucus layer composition<sup>45</sup>. In the stomach and colon, the mucus layer is composed of two distinct mucus layers: a thin inner mucus layer and a much thicker, more loose outer mucus layer. In contrast the small intestinal mucus layer is composed of a single, thin and loose mucus layer (Figure 1). These differences are believed to reflect the different functions and different exposures to microbes<sup>44</sup>. Whereas the small intestine contains relatively few microbes and the mucus layer needs to facilitate the transport of nutrients towards the epithelial cells and the sampling of antigens by mucosal immune cells, the colon contains a much higher density of microbes and the mucus layer needs to physically protect the epithelium from excessive exposure to these microbes<sup>41,45,46</sup>. This notion is supported by the observation that the inner mucus layer of the colon is normally devoid of bacteria, whereas the outer mucus layer is colonized by multiple commensal bacteria<sup>47</sup>.

### MUC2 glycosylation

Mucins, including MUC2, are heavily decorated with glycans (Figure 2)<sup>41,42</sup>. The glycans on MUC2 determine up to 80% of its mass and give the mucin a bottlebrush-like structure<sup>44</sup>. These glycans have several important roles including the ability to attract water, prevent proteolytic cleavage of the mucin backbone, form a physical barrier to microbes as well as facilitate interactions with the microbiota. The MUC2 protein backbone contains a large variable number of tandem repeats (VNTR) region that contains many serine and threonine residues in a proline-rich context. These serine and threonine residues are the site for the attachment of *O*-glycans. *O*-glycosylation takes place in the Golgi and is initiated by the transfer of the monosaccharide GalNAc from its nucleotide sugar donor, UDP-GalNAc, to serine or threonine residues<sup>49</sup>. This reaction is catalysed by the family of polypeptide GalNAc transferases (GalNAcT)<sup>49</sup>. This creates the so-called Tn-antigen, which can be further extended by a combination of glycosyl transferases, each with a distinct activity and substrate specificity, using various combinations of monosaccharides, such as N-acetylglucosamine (GlcNAc) and galactose. This gives rise to several distinct core *O*-glycans<sup>49,50</sup>. These core *O*-glycans can be elongated further to form more complex linear and branched glycan structures that are often terminated by the addition of fucose, sialic acid residues or sulphate. Despite the limited number of monosaccharides used, variation in the order and linkages used can give rise to a tremendous diversity in glycan structures of several hundred different glycans<sup>49,50</sup>. Which glycan is



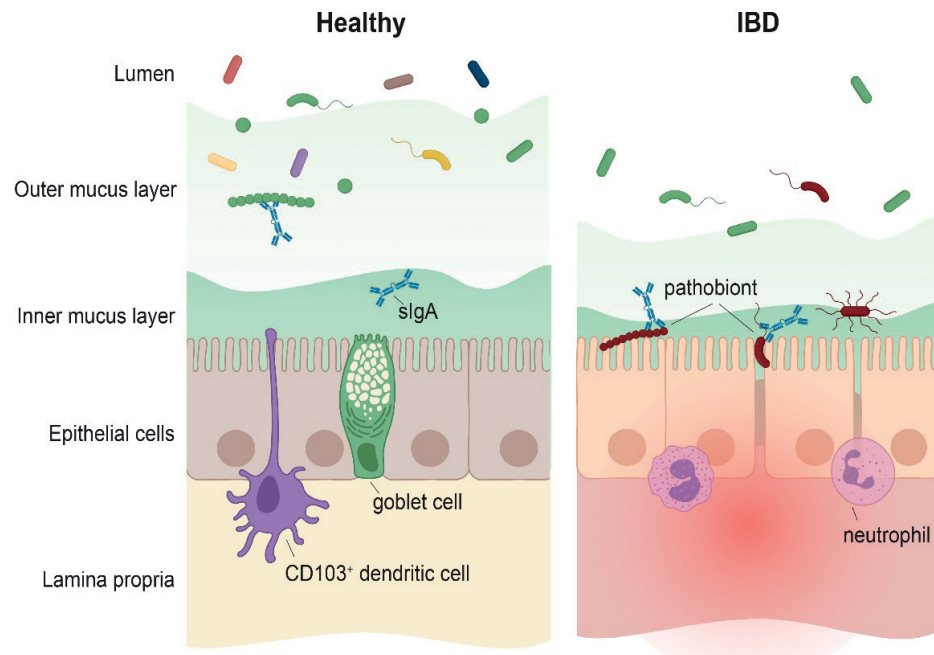


**Figure 1. Colonic mucosal barrier in health and disease.** Schematic representation of the colonic mucosal barrier. A healthy colonic mucosal barrier is characterized by an intact epithelial monolayer and sufficient mucus production by goblet cells. The thin inner mucus layer is normally impenetrable to the microbiota while the thicker and more loose outer mucus layer and lumen are colonized by a diverse microbiota. Dendritic cells sample the lumen for the presence of antigens and bacteria. In IBD patients the microbiota composition is less diverse, and the colonic mucus layer is thinner. The inner mucus layer is penetrable to bacteria which allows bacteria, including IgA-coated pathobionts, to encroach the epithelium and trigger an inflammatory response which involves the recruitment of pro-inflammatory neutrophils<sup>48</sup>.

synthesized depends on a combination of factors, including the sequence of the polypeptide backbone, the expression of glycosyl transferases, their relative abundance, specificity and activity, as well as the concentration of sugars present. These factors contribute to different patterns of *O*-glycosylation at different body sites and for example can be changed upon the stimulation by external stimuli like bacterial colonization<sup>50-53</sup>. It is also important to note that there are profound differences in intestinal glycosylation patterns between mice and humans. In humans the terminal epitopes of *O*-glycans form a proximal-distal gradient. When going from the stomach to the rectum the amount of terminal fucosylation decreases while increases in sialylation and

sulphation are observed<sup>54</sup>. In contrast, in mice this gradient is inverted<sup>55</sup>. These differences in epithelial and mucin glycosylation will almost certainly affect host-microbiota interactions but are not often fully appreciated, in particular when studying mice that are colonized with a human gut microbiota.

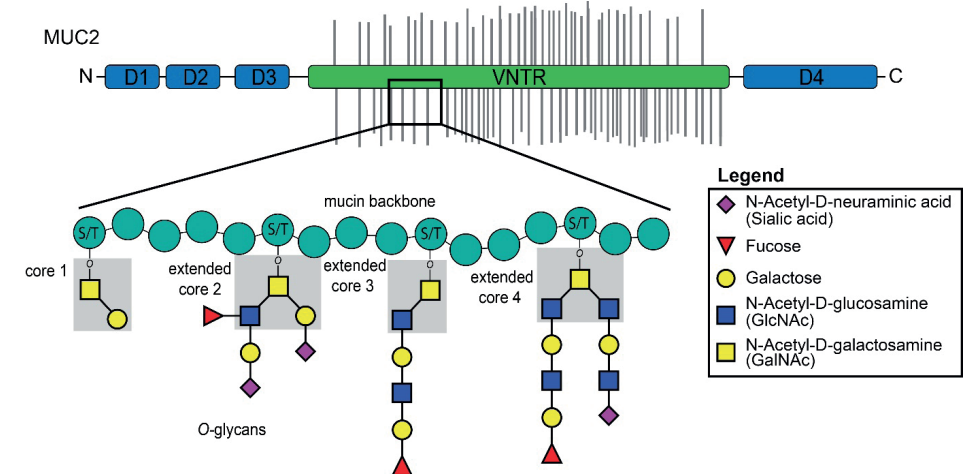


**Figure 2. MUC2 domain structure and -glycosylation.** Schematic representation of MUC2 domain structure. MUC2 contains N- and C-terminally located cysteine-rich D domains that are involved in MUC2 multimerization. The variable number of tandem repeats (VNTR) region is rich in serine (S) and threonine (T) residues to which *O*-glycans can be attached giving the glycosylated MUC2 protein a bottle brush-like structure. Four typical extensible mucin *O*-glycan cores are displayed to which various monosaccharides are attached. Carbohydrate legend is shown to the right.

### Interactions between mucins and bacteria

Multiple bacterial species have evolved strategies to interact with mucins<sup>46,56-58</sup>. For example, bacterial species from all major bacterial phyla have been shown to employ surface structures to adhere to the mucin glycans<sup>59</sup>. The ability to adhere to mucus may allow bacteria to colonize the mucus layer, while on the other hand, the host can select for specific microbes through control of mucus flow<sup>60</sup>. Moreover, some bacterial species have evolved systems to feed on mucin glycans as a key nutrient source<sup>56</sup>. The mucus layer is a unique nutrient niche and the ability of certain species to utilize host-derived mucins offers a competitive advantage over bacteria that lack this trait<sup>61,62</sup>. Mucin-utilizing bacteria often degrade mucin *O*-glycans through the concerted action of carbohydrate active enzymes (CAZymes), which include a wide array of

glycosidases that attack the glycosidic bonds within the glycan chain<sup>56</sup>. After release from the glycan the liberated monosaccharides can be taken up and catabolized to facilitate bacterial growth. Such interactions also influence the formation of complex ecological networks, in which certain glycosidase-producing bacteria facilitate the growth of other bacteria which lack the enzymatic machinery required to release the glycans. Such cross-feeding events have been described for bacteria from multiple genera, including many *Bacteroides* species<sup>63-65</sup>. It is thought that, as the mucus layer is produced by the host and as such is a relatively stable nutrient source for mucolytic bacteria, it enables the host to select for and retain certain beneficial bacteria during periods of nutrient deprivation, e.g., due to seasonal variations in food availability, by providing a continuous source of glycans<sup>61,66,67</sup>.

Perhaps the most well-known example of a mucus-degrading bacterium is *Akkermansia muciniphila*. This bacterium not only degrades mucins, but also stimulates the release of mucins<sup>68,69</sup>. Some other species also seem to employ this strategy in the intestinal tract. In fact, a study using germ-free mice demonstrated that the production and release of mucins largely depends on the presence of the microbiota<sup>52</sup>. The microbiota signals through the TLR-MyD88 axis, activating NLRP6 which subsequently induces the secretion of mucin from goblet cells<sup>70,71</sup>. Other seminal studies indicate that bacteria can alter the glycosylation of mucin glycans. For example, *Bacteroides thetaiotamicron* increases the fucosylation of mucin *O*-glycans and thereby facilitates its own colonization<sup>72,73</sup>. Such increases in fucosylation have also been observed in response to infection with enteropathogens<sup>53,74</sup>.

### Mucus-bacterial interactions in IBD

The fact that the mucus layer is at the centre of important reciprocal interactions between bacteria and the host indicates its importance as a mediator of intestinal homeostasis. Considering the intricate balance between the mucus layer and microbiota it is not surprising that defects or alterations of the mucus layer have been associated with IBD. For instance, the *O*-glycosylation profile of MUC2 in IBD patients with active disease was found to be markedly different from the glycosylation of MUC2 in healthy controls, with a reduction in *O*-glycan length and complexity. These changes were correlated with disease severity<sup>75</sup>. Also, mice deficient in MUC2 were shown to be much more likely to develop spontaneous colitis as well as dextran sodium sulfate (DSS-) and pathogen-induced colitis<sup>76,77</sup>. Another often used mouse model of colitis is the IL-10 knockout mouse. Although the thickness of the mucus layer in these mice is normal, the inner mucus layer is easily penetrated

by a dysbiotic microbiota and these mice are prone to developing spontaneous colitis<sup>78</sup>. Moreover, mutations in the IL-10 pathway have been in patients with early-onset enterocolitis<sup>79</sup>.

The processes that result in reduced mucus layer thickness in IBD are not completely understood. One factor could be the malfunction or depletion of goblet cells, a feature often observed in IBD patients during periods of active inflammation. Based on *in vitro* studies it was hypothesized that goblet cell depletion is caused by an inflammation-induced hypersecretion of MUC2. The prolonged overexpression induced ER stress and misfolding of MUC2, which culminates in increased levels of goblet cell apoptosis<sup>80</sup>. A reduced mucus layer thickness could also be due to low levels of short-chain fatty acids (SCFAs). SCFAs, like acetate and butyrate, are produced by the microbiota through fermentation of dietary fibre and are an important energy source for colonic epithelial cells, including goblet cells. A reduced intake of dietary fibre or an antibiotic-induced loss of SCFA-producing bacteria may therefore result in lower levels of SCFAs and thus goblet cell dysfunction and mucus layer defects<sup>32,81,82</sup>.

As mentioned above, IBD patients often have a reduced mucus layer thickness and an increased load of mucosa-associated bacteria<sup>38</sup>. This encroachment of the microbiota towards the intestinal epithelium increases the chance of translocation of bacteria or foreign antigens into the lamina propria where it may trigger or exacerbate inflammation. Examples of mucosa-associated bacteria include the aforementioned *A. muciniphila*, but also *Bacteroides fragilis* and *B. thetaiotamicron*, *Ruminococcus torques* and *Ruminococcus gnavus*, and several *Bifidobacterium* species. All these bacteria can degrade mucins by producing CAZymes that either fully or partially degrade mucin *O*-glycans. It is important to note that many of these species are also immunogenic and targeted by the secretory IgA, as will also be discussed below.

Interestingly, in IBD patients *A. muciniphila* is often reduced in abundance whereas other mucolytic bacteria like *R. gnavus* and *R. torques* are increased<sup>83</sup>. Although it is clear that the ability to degrade mucins enables colonization of the mucus layer, it is yet unclear to what extent the mucolytic activity of these bacteria contributes to mucus layer degradation that is seen in IBD patients. In mice, there have been clear correlations between mucolytic activity, mucus layer degradation and intestinal inflammation, but from the limited studies in humans the detected mucolytic enzyme activity found in faeces does not

always correlate with disease activity<sup>32,84,85</sup>. The observation that one species is displaced by another species residing in the same niche can likely be explained by their competition for the same limiting nutrient, in this case host-derived mucin<sup>83</sup>, and as such would be a beautiful illustration of natural selection and the struggle for existence. It is likely that the smallest of changes to the factors that govern the interactions between two competing species will already be sufficient to tip the balance to favour one species over the other, and as such alter the microbial landscape. Although evidently nutrient availability is such a critical factor, little is known about the molecular mechanisms that underly such interactions between nutrients and competing bacterial species.

## SECRETORY IGA

Secretory IgA (sIgA) is the most abundant immunoglobulin class in our body and is ubiquitously secreted at mucosal surfaces<sup>86</sup>. The highest concentration of IgA-producing plasma cells is found in the intestine. This is not surprising, given the fact that the production of sIgA depends on the presence of the microbiota<sup>87</sup>. Bacterial species dramatically differ in their ability to induce sIgA and these differences can even be observed between two different strains of the same species, as has been demonstrated for *Bacteroides ovatus*<sup>39,88-90</sup>. As opposed to serum IgA, which is mostly monomeric, most of the sIgA is produced as a dimer or multimer. Most of the sIgA is produced by plasma cells in the intestinal lamina propria, where two or more IgA monomers are joined together by the joining chain and translocated across the epithelial cells by the polymeric Ig receptor (pIgR)<sup>91</sup>. Part of this receptor, the secretory component, is proteolytically cleaved and donated to the IgA dimer upon secretion into the lumen (Figure 3).

### IgA subclasses and glycosylation

In humans, there are two subclasses of IgA: IgA1 and IgA2 (Figure 3). In serum, IgA1 is the dominant subclass whereas IgA2 is more dominant in secretions. The subclasses are differentiated by the extended hinge region of IgA1 and differences in glycosylation. Multiple bacterial pathogens exploit this difference and evade immune recognition through specific proteolytic cleavage of the IgA1 hinge region<sup>92</sup>. This extended IgA1 hinge region also contains five *O*-glycosylation sites that are absent in IgA2<sup>92</sup>. These *O*-glycans are thought to play important roles in multiple diseases, such as IgA nephropathy<sup>93,94</sup>. Moreover, the amount of GalNAc residues in the IgA *O*-glycans of CD patients is lower than in UC patients or controls and the decrease of GalNAc residues correlated with CD disease severity<sup>95</sup>. sIgA also contains multiple

N-glycosylation sites, present on the heavy chain, joining chain and the secretory component. These N-glycans are often complex and branched and terminally sialylated or fucosylated<sup>96</sup>. The N-glycans affect sIgA effector functions. An example of this is the localization of sIgA in the mucus layer; Phalipon *et al.*<sup>97</sup> demonstrated that the N-glycans on the secretory component are critical for anchoring it to the mucus layer in the respiratory tract and its protective effect against bacterial infection. Another function of sIgA that is dependent on its sialoglycans is its ability to neutralize sialic-acid binding bacteria and viruses, such as S-fimbriated *Escherichia coli* and influenza A<sup>98,99</sup>. A recent report by Steffen *et al.*<sup>100</sup> also demonstrated a differential neutrophil activation capacity between serum IgA1 and IgA2. Interestingly, this was also related to the level of sialylation of the IgA N-glycans. Removal of sialic acid from serum IgA1 increased its pro-inflammatory potential through increased neutrophil activation, which correlated with higher disease activity in rheumatoid arthritis patients<sup>100</sup>.

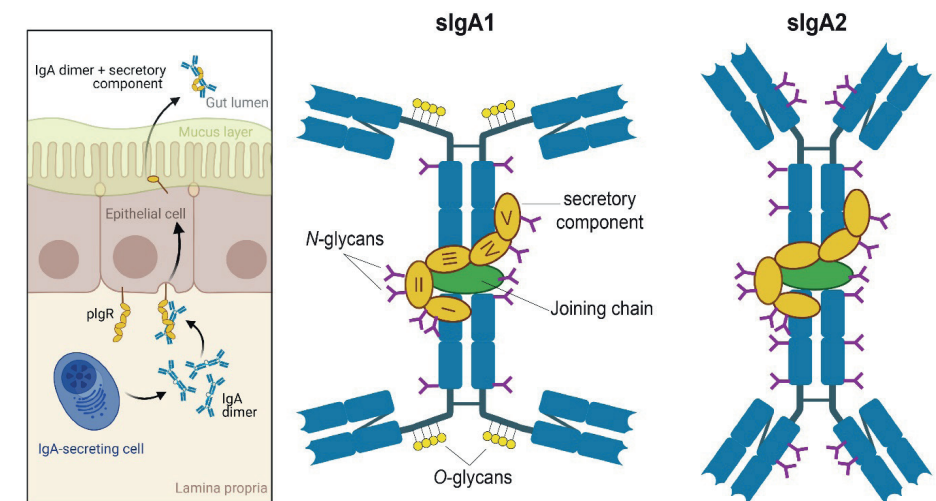


**Figure 3. Secretory IgA production and structure.** The left side is a schematic depiction of the dimeric IgA secretion pathway in the gut. IgA secreting cells in the lamina propria secrete dimeric IgA, which consists of two IgA monomers joined by a joining (J) chain. This complex binds to the polymeric IgA receptor (pIgR) on the basolateral side of epithelial cells and is transported to the apical side. Here, dimeric IgA is released into the lumen together with a cleaved part of the pIgR, the secretory component, which remains covalently attached to the IgA dimer. On the right, the two subclasses of secretory IgA are depicted. Shown are the IgA molecule (blue), joining chain (green), secretory component (orange), and the N-glycans (purple Y-shapes). Furthermore, IgA1 is characterized by an extended hinge region containing multiple *O*-glycosylation sites (yellow circles). Adapted from Royle *et al.*<sup>96,101</sup>

## Functions of sIgA

sIgA can exert a wide variety of functions. Most importantly, sIgA contributes to intestinal homeostasis by limiting microbial overgrowth and preventing microbes from invading underlying tissue. sIgA neutralizes toxins, limits bacterial motility, blocks adhesins and leads to immune exclusion through bacterial enchainment<sup>102-104</sup>. The importance of these events is illustrated by the overgrowth of inflammatory bacteria during sIgA deficiency<sup>105</sup>. IgA is also important for establishing a diverse and balanced microbiota early in life and shaping appropriate mucosal immune responses<sup>106,107</sup>. sIgA binds a wide variety of commensal intestinal bacteria but inflammatory bacteria are especially highly IgA coated<sup>39,90,108</sup>. These sIgA-bacteria interactions are mediated by highly specific, Fab-dependent as well as non-specific interactions. Particularly towards widely conserved glycan epitopes, affinity-matured monoclonal sIgA can display cross-species reactivity of phylogenetically unrelated bacterial species<sup>109</sup>. Interestingly, some bacteria, such as *B. fragilis* and *Lactobacillus*, exploit sIgA binding to facilitate colonization of the mucosal niche<sup>110,111</sup>. Through expression of specific capsular polysaccharides, *B. fragilis* induces specific IgA responses which result in increased levels of IgA coating. Binding of sIgA then results in increased expression of a polysaccharide utilization locus and increases bacterial adherence to epithelial cells<sup>110,112,113</sup>. Another recent report demonstrates that the binding of sIgA can induce the expression of *LEE* encoded virulence genes by enterohemorrhagic *Escherichia coli*, which drives pathogenicity and is required for transmissibility<sup>114</sup>. The exact mechanism(s) through which these bacteria sense binding of sIgA remain unclear. This could be due to expression of yet unidentified IgA receptors or, for example, through alterations in bacterial metabolic functions, as has recently been described by Rollenske *et al.*<sup>115</sup>

Beside its direct effects on bacteria, sIgA also forms a bridge between the adaptive and innate immune response. IgA-opsonized bacteria or antigens can be sensed by a variety of IgA-receptor expressing cells present in the intestine or at more distal sites, such as M-cells, dendritic cells, monocytes and neutrophils<sup>116</sup>. Notably, resident intestinal macrophages do not express the main receptor for IgA, FcαRI (CD89), which likely contributes to the maintenance of intestinal homeostasis<sup>117</sup>. The interactions between sIgA and its receptors are crucial for IgA-mediated antigen sampling and the initiation of both tolerogenic and inflammatory responses towards the gut microbiota and invasive pathogens<sup>116,118-121</sup>. The interactions between FcαRI and serum IgA

have been well characterized, as discussed in several excellent reviews<sup>122,123</sup>. However, the interactions of FcαRI with sIgA are relatively understudied and the role of several other, alternative IgA (co-)receptors remains to be elucidated.

Similar to differences in epithelial and mucin glycosylation patterns there are also important differences in IgA biology between mice and men. First of all, mice only have one IgA isotype. Secondly, mice lack the FcαRI (CD89), the major human IgA-receptor. Although transgenic mice expressing human CD89 have been generated<sup>124</sup>, one should be careful translating findings concerning the mechanistics of IgA biology in mouse models to human systems.

## IgA-coated pathobionts and inflammation

As described above, sIgA plays important roles in maintaining intestinal mucosal homeostasis by binding to pathogens as well as several select members of the microbiota. Some of these bacteria even deliberately elicit binding by sIgA through alterations of surface epitopes, which facilitates their colonization of the mucosal niche<sup>110,111</sup>. Examples of IgA-coated bacteria include *B. fragilis*, *Ruminococcaceae spp.*, *Lactobacilli spp.*, segmented filamentous bacterium (SFB), and several members of the *Erysipelotrichaceae* family and *Akkermansia* species<sup>39,89,108,125</sup>. It is interesting to note that many of these IgA-coated species are also considered mucus-colonizing and mucus-degrading bacteria. This suggests that colonization of the mucosal niche or the factors that influence colonization predispose these species to be targeted by sIgA.

Multiple studies provide evidence that especially inflammatory members of the microbiota are targeted by IgA. For example, in a cohort of undernourished Malawian children, *Enterobacteriaceae* were shown to be heavily bound by sIgA<sup>125</sup>. Moreover, IgA targeting correlated with the nutritional status of these children. When mice were colonized with these IgA-inducing *Enterobacteriaceae* they developed diet-dependent enteropathy characterized by a rapid deterioration of the intestinal epithelial barrier and even sepsis. Prior to that, Palm and De Zoete *et al.*<sup>39</sup> demonstrated that the percentage of sIgA-coated bacteria is increased in IBD patients when compared to healthy controls, and that the consortium of IgA-coated bacteria differs between healthy controls and IBD patients. They also showed that these dysbiosis-associated, IgA-inducing pathobionts can penetrate deep into the mucus layer and are capable of inducing severe inflammation in mouse models of colitis<sup>39</sup>. Even though these pathobionts elicit potent immune responses and

can contribute to intestinal inflammation, it is largely unknown how these IgA-inducing pathobionts differ from other bacteria and which traits underly their immunogenic and inflammatory potential.

## AIM AND OUTLINE OF THESIS

In order to advance our understanding of the role of the gut microbiota in IBD, the challenge of the field is to progress beyond association and correlation studies and to strive to attain new mechanistic insights into the factors that drive disease development. As described above many pathobionts interact with mucins, sIgA and each other, which makes them critical modulators of the mucosal niche. Moreover, by taking up residence close to or even in direct contact with the epithelium, they have an outsized influence on host immune responses and as such can modulate inflammatory conditions such as IBD. Currently, many of the pathobionts remain functionally unexplored and many of the molecular mechanisms that govern their interactions within the mucosal niche remain uncharacterized. Importantly, many of these interactions are influenced by or even fully depend on glycans, a factor that is often underappreciated. In this thesis we study pathobionts and their glycobiological interactions with critical components of the mucosal niche with the aim of identifying novel molecular mechanisms that help elucidate the pathways that drive pathological inflammatory conditions such as IBD.

**In Chapter 2** the microscopic, genetic and chemical characterization of two novel, immunogenic and inflammatory bacterial species from the *Allobaculum* genus: *A. filumensis* and *A. mucolyticum* are described.

**Chapter 3** describes the broad repertoire of mucolytic enzymes that are secreted by *A. mucolyticum* and their role in mucin degradation and the liberation of monosaccharides which can be used for growth.

**Chapter 4** addresses the interaction between *A. mucolyticum* and *Akkermansia muciniphila*. In particular, we tested the hypothesis that the NanH1 sialidase from *A. mucolyticum* is capable of altering components of the glycometabolic niche, thereby inhibiting *Akkermansia* growth.

**Chapter 5** focuses on the role of sIgA glycosylation and the role of sialic acids in regulating neutrophil responses. Particular attention was given to the potential role of bacterial sialidases, including the NanH1 sialidase from *A. mucolyticum*, as modulator of sIgA function.

Finally, in **Chapter 6** the findings presented in this thesis are placed in a broader context and the future perspectives and challenges are discussed.

## REFERENCES

1. Qin J, Li R, Raes J, Arumugam M, Burgdorf S, Manichanh C, Nielsen T, Pons N, Yamada T, Mende DR, *et al.* A human gut microbial gene catalog established by metagenomic sequencing. *Nature*. 2010;464(7285):59–65. doi:10.1038/nature08821.A
2. THMPC. Structure, Function and Diversity of the Healthy Human Microbiome. *Nature*. 2013;486(7402):207–214. doi:10.1038/nature11234.Structure
3. Sommer F, Bäckhed F. The gut microbiota-masters of host development and physiology. *Nature Reviews Microbiology*. 2013;11(4):227–238. doi:10.1038/nrmicro2974
4. Thaiss CA, Zmora N, Levy M, Elinav E. The microbiome and innate immunity. 2016. p. 65–74. doi:10.1038/nature18847
5. Gilbert JA, Blaser MJ, Caporaso JG, Jansson JK, Lynch S V., Knight R. Current understanding of the human microbiome. *Nature Medicine*. 2018;24(4):392–400. doi:10.1038/nm.4517
6. Morais LH, Schreiber HL, Mazmanian SK. The gut microbiota-brain axis in behaviour and brain disorders. *Nature Reviews Microbiology*. 2021;19(4):241–255. doi:10.1038/s41579-020-00460-0
7. Spor A, Koren O, Ley R. Unravelling the effects of the environment and host genotype on the gut microbiome. *Nature Reviews Microbiology*. 2011;9(4):279–290. doi:10.1038/nrmicro2540
8. Yatsunenko T, Rey FE, Manary MJ, Trehan I, Dominguez-Bello MG, Contreras M, Magris M, Hidalgo G, Baldassano RN, Anokhin AP, *et al.* Human gut microbiome viewed across age and geography. *Nature*. 2012;486(7402):222–227. doi:10.1038/nature11053
9. Tropini C, Earle KA, Huang KC, Sonnenburg JL. The Gut Microbiome: Connecting Spatial Organization to Function. *Cell Host & Microbe*. 2017;21(4):433–442. doi:10.1016/j.chom.2017.03.010
10. Kaplan GG, Ng SC. Understanding and Preventing the Global Increase of Inflammatory Bowel Disease. *Gastroenterology*. 2017;152(2):313–321.e2. doi:10.1053/j.gastro.2016.10.020
11. Kaplan GG. The global burden of IBD: From 2015 to 2025. *Nature Reviews Gastroenterology and Hepatology*. 2015;12(12):720–727. doi:10.1038/nrgastro.2015.150
12. Rubin DT, Kornbluth A. Role of antibiotics in the management of inflammatory bowel disease: A review. *Reviews in Gastroenterological Disorders*. 2005;5(SUPPL. 3):6.
13. Ledder O, Turner D. Antibiotics in IBD: Still a Role in the Biological Era? *Inflammatory Bowel Diseases*. 2018;24(9):1676–1688. doi:10.1093/ibd/izy067
14. Herrlinger KR, Stange EF. Twenty five years of biologicals in IBD: What’s all the hype about? *Journal of Internal Medicine*. 2021;290(4):806–825. doi:10.1111/joim.13345
15. Tabbaa OM, Aboelsoud MM, Mattar MC. Long-Term Safety and Efficacy of Fecal Microbiota Transplantation in the Treatment of *Clostridium difficile* Infection in Patients With and Without Inflammatory Bowel Disease: A Tertiary Care Center’s Experience. *Gastroenterology Research*. 2018;11(6):397–403. doi:10.14740/gr1091
16. Jeon SR, Chai J, Kim C, Lee CH. Current Evidence for the Management of Inflammatory Bowel Diseases Using Fecal Microbiota Transplantation. *Current Infectious Disease Reports*. 2018;20(8):21. doi:10.1007/s11908-018-0627-8
17. de Souza HSP, Fiocchi C, Iliopoulos D. The IBD interactome: an integrated view of aetiology, pathogenesis and therapy. *Nature Reviews Gastroenterology & Hepatology*. 2017;14(12):739–749. doi:10.1038/nrgastro.2017.110
18. Caruso R, Lo BC, Núñez G. Host-microbiota interactions in inflammatory bowel disease. *Nature Reviews Immunology*. 2020;20(7):411–426. doi:10.1038/s41577-019-0268-7
19. Khor B, Gardet A, Xavier RJ. Genetics and pathogenesis of inflammatory bowel disease. *Nature*. 2011;474(7351):307–317. doi:10.1038/nature10209
20. Hugot J-P, Chamaillard M, Zouali H, Lesage S, Cézard J-P, Belaiche J, Almer S, Tysk C, O’Morain CA, Gassull M, *et al.* Association of NOD2 leucine-rich repeat variants with susceptibility to Crohn’s disease. *Nature*. 2001;411(6837):599–603. doi:10.1038/35079107
21. Ogura Y, Bonen DK, Inohara N, Nicolae DL, Chen FF, Ramos R, Britton H, Moran T, Karaliuskas R, Duerr RH, *et al.* A frameshift mutation in NOD2 associated with susceptibility to Crohn’s disease. *Nature*. 2001;411(6837):603–606. doi:10.1038/35079114
22. Napier RJ, Lee EJ, Vance EE, Snow PE, Samson KA, Dawson CE, Moran AE, Stenzel P, Davey MP, Sakaguchi S, *et al.* Nod2 Deficiency Augments Th17 Responses and Exacerbates Autoimmune Arthritis. *The Journal of Immunology*. 2018;201(7):1889–1898. doi:10.4049/jimmunol.1700507
23. Hviid A, Svanstrom H, Frisch M. Antibiotic use and inflammatory bowel diseases in childhood. *Gut*. 2011;60(1):49–54. doi:10.1136/gut.2010.219683
24. Kronman MP, Zaoutis TE, Haynes K, Feng R, Coffin SE. Antibiotic Exposure and IBD Development Among Children: A Population-Based Cohort Study. *PEDIATRICS*. 2012;130(4):e794–e803. doi:10.1542/peds.2011-3886
25. Cox LM, Yamanishi S, Sohn J, Alekseyenko A V, Leung JM, Cho I, Rogers AB, Kim SG, Li H, Gao Z, *et al.* Altering the Intestinal Microbiota during a Critical Developmental Window Has Lasting Metabolic Consequences. *Cell*. 2014;158(4):705–721. doi:10.1016/j.cell.2014.05.052
26. Knoop KA, Gustafsson JK, McDonald KG, Kulkarni DH, Coughlin PE, McCrate S, Kim D, Hsieh CS, Hogan SP, Elson CO, *et al.* Microbial antigen encounter during a preweaning interval is critical for tolerance to gut bacteria. *Science Immunology*. 2017;2(18):1–12. doi:10.1126/sciimmunol.aao1314

27. Al Nabhani Z, Dulauroy S, Marques R, Cousu C, Al Bounny S, Déjardin F, Sparwasser T, Bérard M, Cerf-Bensussan N, Eberl G. A Weaning Reaction to Microbiota Is Required for Resistance to Immunopathologies in the Adult. *Immunity*. 2019;50(5):1276-1288.e5. doi:10.1016/j.immuni.2019.02.014
28. Lee JY, Cevallos SA, Byndloss MX, Tiffany CR, Olsan EE, Butler BP, Young BM, Rogers AWL, Nguyen H, Kim K, *et al.* High-Fat Diet and Antibiotics Cooperatively Impair Mitochondrial Bioenergetics to Trigger Dysbiosis that Exacerbates Pre-inflammatory Bowel Disease. *Cell Host and Microbe*. 2020;28(2):273-284.e6. doi:10.1016/j.chom.2020.06.001
29. Rivera-Chávez F, Zhang LF, Faber F, Lopez CA, Byndloss MX, Olsan EE, Xu G, Velazquez EM, Lebrilla CB, Winter SE, *et al.* Depletion of Butyrate-Producing *Clostridia* from the Gut Microbiota Drives an Aerobic Luminal Expansion of *Salmonella*. *Cell Host and Microbe*. 2016;19(4):443-454. doi:10.1016/j.chom.2016.03.004
30. Knoop KA, McDonald KG, Kulkarni DH, Newberry RD. Antibiotics promote inflammation through the translocation of native commensal colonic bacteria. *Gut*. 2016;65(7):1100-1109. doi:10.1136/gutjnl-2014-309059
31. Gentschew L, Ferguson LR. Role of nutrition and microbiota in susceptibility to inflammatory bowel diseases. *Molecular Nutrition & Food Research*. 2012;56(4):524-535. doi:10.1002/mnfr.201100630
32. Desai MS, Seekatz AM, Koropatkin NM, Kamada N, Hickey CA, Wolter M, Pudlo NA, Kitamoto S, Terrapon N, Muller A, *et al.* A Dietary Fiber-Deprived Gut Microbiota Degrades the Colonic Mucus Barrier and Enhances Pathogen Susceptibility. *Cell*. 2016;167(5):1339-1353.e21. doi:10.1016/j.cell.2016.10.043
33. Khan S, Waliullah S, Godfrey V, Khan AW, Ramachandran RA, Cantarel BL, Behrendt C, Peng L, Hooper L V, Zaki H. Dietary simple sugars alter microbial ecology in the gut and promote colitis in mice. *Science translational medicine*. 2020;6218(October).
34. Devkota S, Wang Y, Musch MW, Leone V, Fehlner-Peach H, Nadimpalli A, Antonopoulos DA, Jabri B, Chang EB. Dietary-fat-induced taurocholic acid promotes pathobiont expansion and colitis in IL10<sup>-/-</sup> mice. *Nature*. 2012;487(7405):104-108. doi:10.1038/nature11225
35. Caruso R, Lo BC, Núñez G. Host-microbiota interactions in inflammatory bowel disease. *Nature Reviews Immunology*. 2020;20(7):411-426. doi:10.1038/s41577-019-0268-7
36. Lloyd-Price J, Arze C, Ananthkrishnan AN, Schirmer M, Avila-Pacheco J, Poon TW, Andrews E, Ajami NJ, Bonham KS, Brislawn CJ, *et al.* Multi-omics of the gut microbial ecosystem in inflammatory bowel diseases. *Nature*. 2019;569(7758):655-662. doi:10.1038/s41586-019-1237-9
37. Alipour M, Zaidi D, Valcheva R, Jovel J, Martínez I, Sergi C, Walter J, Mason AL, Ka-Shu Wong G, Dieleman LA, *et al.* Mucosal barrier depletion and loss of bacterial diversity are primary abnormalities in paediatric ulcerative colitis. *Journal of Crohn's and Colitis*. 2016;10(4):462-471. doi:10.1093/ecco-jcc/jjv223
38. Johansson ME V, Gustafsson JK, Holmén-Larsson J, Jabbar KS, Xia L, Xu H, Ghishan FK, Carvalho FA, Gewirtz AT, Sjövall H, *et al.* Bacteria penetrate the normally impenetrable inner colon mucus layer in both murine colitis models and patients with ulcerative colitis. *Gut*. 2014;63(2):281-291. doi:10.1136/gutjnl-2012-303207
39. Palm NW, de Zoete MR, Cullen TW, Barry NA, Stefanowski J, Hao L, Degnan PH, Hu J, Peter I, Zhang W, *et al.* Immunoglobulin A Coating Identifies Colitogenic Bacteria in Inflammatory Bowel Disease. *Cell*. 2014;158(5):1000-1010. doi:10.1016/j.cell.2014.08.006
40. Chow J, Tang H, Mazmanian SK. Pathobionts of the gastrointestinal microbiota and inflammatory disease. *Current Opinion in Immunology*. 2011;23(4):473-480. doi:10.1016/j.coi.2011.07.010
41. Johansson MEV, Hansson GC. Immunological aspects of intestinal mucus and mucins. *Nature Reviews Immunology*. 2016;16(10):639-649. doi:10.1038/nri.2016.88
42. Hansson GC. Mucus and mucins in diseases of the intestinal and respiratory tracts. *Journal of Internal Medicine*. 2019;285(5):479-490. doi:10.1111/joim.12910
43. van Putten JPM, Strijbis K. Transmembrane Mucins: Signaling Receptors at the Intersection of Inflammation and Cancer. *Journal of Innate Immunity*. 2017;9(3):281-299. doi:10.1159/000453594
44. Johansson MEV, Holmén Larsson JM, Hansson GC. The two mucus layers of colon are organized by the MUC2 mucin, whereas the outer layer is a legislator of host-microbial interactions. *Proceedings of the National Academy of Sciences of the United States of America*. 2011;108(SUPPL. 1):4659-4665. doi:10.1073/pnas.1006451107
45. McGuckin MA, Lindén SK, Sutton P, Florin TH. Mucin dynamics and enteric pathogens. *Nature Reviews Microbiology*. 2011;9(4):265-278. doi:10.1038/nrmicro2538
46. Martens EC, Neumann M, Desai MS. Interactions of commensal and pathogenic microorganisms with the intestinal mucosal barrier. *Nature Reviews Microbiology*. 2018;16(8):457-470. doi:10.1038/s41579-018-0036-x
47. Johansson MEV, Phillipson M, Petersson J, Velcich A, Holm L, Hansson GC. The inner of the two Muc2 mucin-dependent mucus layers in colon is devoid of bacteria. *Proceedings of the National Academy of Sciences of the United States of America*. 2008;105(39):15064-15069. doi:10.1073/pnas.0803124105
48. Adapted from "Structure of Mucosal Barrier", by BioRender.com (2021). Retrieved from <https://app.biorender.com/biorender-templates>.
49. Bennett EP, Mandel U, Clausen H, Gerken TA, Fritz TA, Tabak LA. Control of mucin-type O-glycosylation: A classification of the polypeptide GalNAc-transferase gene family. *Glycobiology*. 2012;22(6):736-756. doi:10.1093/glycob/cwr182
50. Bergstrom KSB, Xia L. Mucin-type O-glycans and their roles in intestinal homeostasis. *Glycobiology*. 2013;23(9):1026-1037. doi:10.1093/glycob/cwt045

51. Theodoratou E, Campbell H, Ventham NT, Kolarich D, Pučić-Baković M, Zoldoš V, Fernandes D, Pemberton IK, Rudan I, Kennedy NA, *et al.* The role of glycosylation in IBD. *Nature reviews. Gastroenterology & hepatology.* 2014;11(10):588–600. doi:10.1038/nrgastro.2014.78
52. Johansson MEV, Jakobsson HE, Holmén-Larsson J, Schütte A, Ermund A, Rodríguez-Piñero AM, Arike L, Wising C, Svensson F, Bäckhed F, *et al.* Normalization of host intestinal mucus layers requires long-term microbial colonization. *Cell Host and Microbe.* 2015;18(5):582–592. doi:10.1016/j.chom.2015.10.007
53. Arabyan N, Park D, Foutouhi S, Weis AM, Huang BC, Williams CC, Desai P, Shah J, Jeannotte R, Kong N, *et al.* *Salmonella* Degrades the Host Glycocalyx Leading to Altered Infection and Glycan Remodeling. *Scientific Reports.* 2016;6:29525. doi:10.1038/srep29525
54. Robbe C, Capon C, Maes E, Rousset M, Zweibaum A, Zanetta J-P, Michalski J-C. Evidence of Regio-specific Glycosylation in Human Intestinal Mucins. *Journal of Biological Chemistry.* 2003;278(47):46337–46348. doi:10.1074/jbc.M302529200
55. Holmén Larsson JM, Thomsson KA, Rodríguez-Piñero AM, Karlsson H, Hansson GC. Studies of mucus in mouse stomach, small intestine, and colon. III. Gastrointestinal Muc5ac and Muc2 mucin O-glycan patterns reveal a regiospecific distribution. *American Journal of Physiology-Gastrointestinal and Liver Physiology.* 2013;305(5):G357–G363. doi:10.1152/ajpgi.00048.2013
56. Tailford LE, Crost EH, Kavanaugh D, Juge N. Mucin glycan foraging in the human gut microbiome. *Frontiers in Genetics.* 2015;6(FEB). doi:10.3389/fgene.2015.00081
57. Johansson MEV, Hansson GC. Immunological aspects of intestinal mucus and mucins. *Nature Reviews Immunology.* 2016;16(10):639–649. doi:10.1038/nri.2016.88
58. Ravcheev DA, Thiele I. Comparative genomic analysis of the human gut microbiome reveals a broad distribution of metabolic pathways for the degradation of host-synthesized mucin glycans and utilization of mucin-derived monosaccharides. *Frontiers in Genetics.* 2017;8(AUG). doi:10.3389/fgene.2017.00111
59. Ouwerkerk JP, De Vos WM, Belzer C. Glycobiome: Bacteria and mucus at the epithelial interface. *Best Practice and Research: Clinical Gastroenterology.* 2013;27(1):25–38. doi:10.1016/j.bpg.2013.03.001
60. McLoughlin K, Schluter J, Rakoff-Nahoum S, Smith AL, Foster KR. Host Selection of Microbiota via Differential Adhesion. *Cell Host & Microbe.* 2016;1–10. doi:10.1016/j.chom.2016.02.021
61. Martens EC, Chiang HC, Gordon JI. Mucosal Glycan Foraging Enhances Fitness and Transmission of a Saccharolytic Human Gut Bacterial Symbiont. *Cell Host & Microbe.* 2008;4(5):447–457. doi:10.1016/j.chom.2008.09.007
62. Pereira FC, Berry D. Microbial nutrient niches in the gut. *Environmental Microbiology.* 2017;19(4):1366–1378. doi:10.1111/1462-2920.13659
63. Rakoff-Nahoum S, Foster KR, Comstock LE. The evolution of cooperation within the gut microbiota. *Nature.* 2016;533(7602):255–259. doi:10.1038/nature17626
64. Ng KM, Ferreyra JA, Higginbottom SK, Lynch JB, Kashyap PC, Gopinath S, Naidu N, Choudhury B, Weimer BC, Monack DM, *et al.* Microbiota-liberated host sugars facilitate post-antibiotic expansion of enteric pathogens. *Nature.* 2013;502(7469):96–99. doi:10.1038/nature12503
65. Pacheco AR, Munera D, Waldor MK, Sperandio V, Ritchie JM. Fucose sensing regulates bacterial intestinal colonization. *Nature.* 2012;492(7427):113–117. doi:10.1038/nature11623
66. Smits SA, Leach J, Sonnenburg ED, Gonzalez CG, Lichtman JS, Reid G, Knight R, Manjurano A, Changalucha J, Elias JE, *et al.* Seasonal cycling in the gut microbiome of the Hadza hunter-gatherers of Tanzania. *Science.* 2017;357(6353):802–806. doi:10.1126/science.aan4834
67. Sonnenburg ED, Smits SA, Tikhonov M, Higginbottom SK, Wingreen NS, Sonnenburg JL. Diet-induced extinctions in the gut microbiota compound over generations. *Nature.* 2016;529(7585):212–215. doi:10.1038/nature16504
68. Derrien M, Vaughan EE, Plugge CM, de Vos WM. *Akkermansia muciniphila* gen. nov., sp. nov., a human intestinal mucin-degrading bacterium. *International Journal of Systematic and Evolutionary Microbiology.* 2004;54(5):1469–1476. doi:10.1099/ijs.0.02873-0
69. Derrien M, Belzer C, de Vos WM. *Akkermansia muciniphila* and its role in regulating host functions. *Microbial Pathogenesis.* 2017;106:171–181. (Microbiota and nutrition). doi:10.1016/j.micpath.2016.02.005
70. Włodarska M, Thaiss CA, Nowarski R, Henao-Mejia J, Zhang J-P, Brown EM, Frankel G, Levy M, Katz MN, Philbrick WM, *et al.* NLRP6 Inflammasome Orchestrates the Colonic Host-Microbial Interface by Regulating Goblet Cell Mucus Secretion. *Cell.* 2014;156(5):1045–1059. doi:10.1016/j.cell.2014.01.026
71. Birchenough GMH, Nyström EEL, Johansson MEV, Hansson GC. A sentinel goblet cell guards the colonic crypt by triggering Nlrp6-dependent Muc2 secretion. *Science.* 2016;352(6293):1535–1542. doi:10.1126/science.aaf7419
72. Pickard JM, Chervonsky A V. Intestinal Fucose as a Mediator of Host-Microbe Symbiosis. *The Journal of Immunology.* 2015;194(12):5588–5593. doi:10.4049/jimmunol.1500395
73. Sonnenburg JL, Xu J, Leip DD, Chen CH, Westover BP, Weatherford J, Buhler JD, Gordon JI. Glycan foraging in vivo by an intestine-adapted bacterial symbiont. *Science.* 2005;307(5717):1955–1959. doi:10.1126/science.1109051
74. Pickard JM, Maurice CF, Kinnebrew MA, Abt MC, Schenten D, Golovkina T V., Bogatyrev SR, Ismagilov RF, Pamer EG, Turnbaugh PJ, *et al.* Rapid fucosylation of intestinal epithelium sustains host-commensal symbiosis in sickness. *Nature.* 2014;514(7524):638–641. doi:10.1038/nature13823
75. Larsson JMH, Karlsson H, Crespo JG, Johansson MEV, Eklund L, Sjövall H, Hansson GC. Altered O-glycosylation profile of MUC2 mucin occurs in active ulcerative colitis and is associated with increased inflammation. *Inflammatory Bowel Diseases.* 2011;17(11):2299–2307. doi:10.1002/ibd.21625



76. Van der Sluis M, De Koning BAE, De Bruijn ACJM, Velcich A, Meijerink JPP, Van Goudoever JB, Büller HA, Dekker J, Van Seuning I, Renes IB, *et al.* Muc2-Deficient Mice Spontaneously Develop Colitis, Indicating That MUC2 Is Critical for Colonic Protection. *Gastroenterology*. 2006;131(1):117–129. doi:10.1053/j.gastro.2006.04.020
77. Bergstrom KSB, Kisson-Singh V, Gibson DL, Ma C, Montero M, Sham HP, Ryz N, Huang T, Velcich A, Finlay BB, *et al.* Muc2 Protects against Lethal Infectious Colitis by Disassociating Pathogenic and Commensal Bacteria from the Colonic Mucosa Roy CR, editor. *PLoS Pathogens*. 2010;6(5):e1000902. doi:10.1371/journal.ppat.1000902
78. Gunasekera DC, Ma J, Vacharathit V, Shah P, Ramakrishnan A, Uprety P, Shen Z, Sheh A, Brayton CF, Whary MT, *et al.* The development of colitis in IL10<sup>-/-</sup> mice is dependent on IL-22. *Mucosal Immunology*. 2020;13(3):493–506. doi:10.1038/s41385-019-0252-3
79. Glocker E-O, Kotlarz D, Boztug K, Gertz EM, Schäffer AA, Noyan F, Perro M, Diestelhorst J, Allroth A, Murugan D, *et al.* Inflammatory Bowel Disease and Mutations Affecting the Interleukin-10 Receptor. *New England Journal of Medicine*. 2009;361(21):2033–2045. doi:10.1056/NEJMoa0907206
80. Tawiah A, Cornick S, Moreau F, Gorman H, Kumar M, Tiwari S, Chadee K. High MUC2 Mucin Expression and Misfolding Induce Cellular Stress, Reactive Oxygen Production, and Apoptosis in Goblet Cells. *American Journal of Pathology*. 2018;188(6):1354–1373. doi:10.1016/j.ajpath.2018.02.007
81. Wrzosek L, Miquel S, Noordine ML, Bouet S, Chevalier-Curt MJ, Robert V, Philippe C, Bridonneau C, Cherbuy C, Robbe-Masselot C, *et al.* *Bacteroides thetaiotaomicron* and *Faecalibacterium prausnitzii* influence the production of mucus glycans and the development of goblet cells in the colonic epithelium of a gnotobiotic model rodent. *BMC Biology*. 2013;11:61. doi:10.1186/1741-7007-11-61
82. Rivera-Chávez F, Zhang LF, Faber F, Lopez CA, Byndloss MX, Olsan EE, Xu G, Velazquez EM, Lebrilla CB, Winter SE, *et al.* Depletion of Butyrate-Producing Clostridia from the Gut Microbiota Drives an Aerobic Luminal Expansion of Salmonella. *Cell Host and Microbe*. 2016;19(4):443–454. doi:10.1016/j.chom.2016.03.004
83. Png CW, Lindén SK, Gilshenan KS, Zoetendal EG, McSweeney CS, Sly LI, McGuckin MA, Florin THJ. Mucolytic bacteria with increased prevalence in IBD mucosa augment in vitro utilization of mucin by other bacteria. *American Journal of Gastroenterology*. 2010;105(11):2420–2428. doi:10.1038/ajg.2010.281
84. Dwarakanath AD, Campbell BJ, Tsai HH, Sunderland D, Hart CA, Rhodes JM. Faecal mucinase activity assessed in inflammatory bowel disease using 14C threonine labelled mucin substrate. *Gut*. 1995;37(1):58–62. doi:10.1136/gut.37.1.58
85. Rhodes JM, Gallimore R, Elias E, Allan RN, Kennedy JF. Alimentary tract and pancreas faecal mucus degrading glycosidases in ulcerative colitis and Crohn's disease. *Gut*. 1985;26(8):761–765. doi:10.1136/gut.26.8.761
86. Seikrit C, Pabst O. The immune landscape of IgA induction in the gut. *Seminars in Immunopathology*. 2021;43(5):627–637. doi:10.1007/s00281-021-00879-4
87. Benveniste J, Lespinats G, Adam C, Salomon JC. Immunoglobulins in intact, immunized, and contaminated axenic mice: study of serum IgA. *Journal of immunology (Baltimore, Md. : 1950)*. 1971;107(6):1647–55.
88. Yang C, Mogno I, Contijoch EJ, Borgerding JN, Aggarwala V, Li Z, Siu S, Grasset EK, Helmus DS, Dubinsky MC, *et al.* Fecal IgA Levels Are Determined by Strain-Level Differences in *Bacteroides ovatus* and Are Modifiable by Gut Microbiota Manipulation. *Cell Host and Microbe*. 2020;27(3):467–475.e6. doi:10.1016/j.chom.2020.01.016
89. Planer JD, Peng Y, Kau AL, Blanton L V., Ndao IM, Tarr PI, Warner BB, Gordon JI. Development of the gut microbiota and mucosal IgA responses in twins and gnotobiotic mice. *Nature*. 2016;534(7606):263–266. doi:10.1038/nature17940
90. Bunker JJ, Flynn TM, Koval JC, Shaw DG, Meisel M, McDonald BD, Ishizuka IE, Dent AL, Wilson PC, Jabri B, *et al.* Innate and Adaptive Humoral Responses Coat Distinct Commensal Bacteria with Immunoglobulin A. *Immunity*. 2015;43(3):541–553. doi:10.1016/j.immuni.2015.08.007
91. MacPherson AJ, McCoy KD, Johansen FE, Brandtzaeg P. The immune geography of IgA induction and function. *Mucosal Immunology*. 2008;1(1):11–22. doi:10.1038/mi.2007.6
92. de Sousa-Pereira P, Woof JM. IgA: Structure, Function, and Developability. *Antibodies*. 2019;8(4):57. doi:10.3390/antib8040057
93. Kokubo T, Hiki Y, Iwase H, Tanaka A, Toma K, Hotta K, Kobayashi Y. Protective role of IgA1 glycans against IgA1 self- aggregation and adhesion to extracellular matrix proteins. *Journal of the American Society of Nephrology*. 1998;9(11):2048–2054.
94. Iwase H, Tanaka A, Hiki Y, Kokubo T, Sano T, Ishii-Karakasa I, Toma K, Kobayashi Y, Hotta K. Aggregated human serum immunoglobulin A1 induced by neuraminidase treatment had a lower number of O-linked sugar chains on the hinge portion. *Journal of Chromatography B: Biomedical Sciences and Applications*. 1999;724(1):1–7. doi:10.1016/S0378-4347(98)00552-0
95. Inoue T, Iijima H, Tajiri M, Shinzaki S, Shiraishi E, Hiyama S, Mukai A, Nakajima S, Iwatani H, Nishida T, *et al.* Deficiency of N-acetylgalactosamine in O-linked oligosaccharides of IgA is a novel biologic marker for Crohn's disease. *Inflammatory Bowel Diseases*. 2012;18(9):1723–1734. doi:10.1002/ibd.22876
96. Royle L, Roos A, Harvey DJ, Wormald MR, Van Gijlswijk-Janssen D, Redwan ERM, Wilson IA, Daha MR, Dwek RA, Rudd PM. Secretory IgA N- and O-glycans provide a link between the innate and adaptive immune systems. *Journal of Biological Chemistry*. 2003;278(22):20140–20153. doi:10.1074/jbc.M301436200
97. Phalipon A, Cardona A, Kraehenbuhl JP, Edelman L, Sansonetti PJ, Corthésy B. Secretory component: A new role in secretory IgA-mediated immune exclusion in vivo. *Immunity*. 2002;17(1):107–115. doi:10.1016/S1074-7613(02)00341-2

98. Maurer MA, Meyer L, Bianchi M, Turner HL, Le NPL, Steck M, Wyrzucki A, Orlowski V, Ward AB, Crispin M, *et al.* Glycosylation of Human IgA Directly Inhibits Influenza A and Other Sialic-Acid-Binding Viruses. *Cell Reports*. 2018;23(1):90–99. doi:10.1016/j.celrep.2018.03.027
99. Schrotten H, Stapper C, Plogmann R, Köhler H, Hacker J, Hanisch F-G. Fab-Independent Antiadhesion Effects of Secretory Immunoglobulin A on S-Fimbriated *Escherichia coli* Are Mediated by Sialyloligosaccharides. *Infection and Immunity*. 1998;66(8):3971–3973. doi:10.1128/IAI.66.8.3971-3973.1998
100. Steffen U, Koeleman CA, Sokolova M V., Bang H, Kleyer A, Rech J, Unterweger H, Schicht M, Garreis F, Hahn J, *et al.* IgA subclasses have different effector functions associated with distinct glycosylation profiles. *Nature Communications*. 2020;11(1). doi:10.1038/s41467-019-13992-8
101. Adapted from “IgA Transport Across Type I Epithelia”, by BioRender.com (2021). Retrieved from <https://app.biorender.com/biorender-templates>.
102. Moor K, Diard M, Sellin ME, Felmy B, Wotzka SY, Toska A, Bakkeren E, Arnoldini M, Bansept F, Co AD, *et al.* High-avidity IgA protects the intestine by enchainning growing bacteria. *Nature*. 2017;544(7651):498–502. doi:10.1038/nature22058
103. Perrier C, Sprenger N, Corthésy B. Glycans on secretory component participate in innate protection against mucosal pathogens. *Journal of Biological Chemistry*. 2006;281(20):14280–14287. doi:10.1074/jbc.M512958200
104. Ost KS, O’ Meara TR, Zac SW, Chiaro T, Zhou H, Penman J, Bell R, Catanzaro J, Song D, Singh S, *et al.* Adaptive immunity induces mutually beneficial interactions with gut fungi. *Nature*. 2021;Accepted(June 2020). doi:10.1038/s41586-021-03722-w
105. Wang S, Charbonnier LM, Noval Rivas M, Georgiev P, Li N, Gerber G, Bry L, Chatila TA. MyD88 Adaptor-Dependent Microbial Sensing by Regulatory T Cells Promotes Mucosal Tolerance and Enforces Commensalism. *Immunity*. 2015;43(2):289–303. doi:10.1016/j.immuni.2015.06.014
106. Rogier EW, Frantz AL, Bruno MEC, Wedlund L, Cohen DA, Stromberg AJ, Kaetzel CS. Secretory antibodies in breast milk promote long-term intestinal homeostasis by regulating the gut microbiota and host gene expression. *Proceedings of the National Academy of Sciences of the United States of America*. 2014;111(8):3074–3079. doi:10.1073/pnas.1315792111
107. Koch MA, Reiner GL, Lugo KA, Kreuk LSM, Stanbery AG, Ansaldo E, Seher TD, Ludington WB, Barton GM. Maternal IgG and IgA Antibodies Dampen Mucosal T Helper Cell Responses in Early Life. *Cell*. 2016;165(4):827–841. doi:10.1016/j.cell.2016.04.055
108. Huus KE, Frankowski M, Pučić-Baković M, Vučković F, Lauc G, Mullish BH, Marchesi JR, Monaghan TM, Kao D, Finlay BB. Changes in IgA-targeted microbiota following fecal transplantation for recurrent *Clostridioides difficile* infection. *Gut Microbes*. 2021;13(1):1–12. doi:10.1080/19490976.2020.1862027
109. Bunker JJ, Erickson SA, Flynn TM, Henry C, Koval JC, Meisel M, Jabri B, Antonopoulos DA, Wilson PC, Bendelac A. Natural polyreactive IgA antibodies coat the intestinal microbiota. *Science*. 2017;358(6361):eaan6619. doi:10.1126/science.aan6619
110. Donaldson GP, Ladinsky MS, Yu KB, Sanders JG, Yoo BB, Chou WC, Conner ME, Earl AM, Knight R, Bjorkman PJ, *et al.* Gut microbiota utilize immunoglobulin A for mucosal colonization. *Science*. 2018;360(6390):795–800. doi:10.1126/science.aaq0926
111. Huus KE, Bauer KC, Brown EM, Bozorgmehr T, Woodward SE, Serapio-Palacios A, Boutin RCT, Petersen C, Finlay BB. Commensal Bacteria Modulate Immunoglobulin A Binding in Response to Host Nutrition. *Cell Host & Microbe*. 2020;27(6):909–921.e5. doi:10.1016/j.chom.2020.03.012
112. Nakajima A, Vogelzang A, Maruya M, Miyajima M, Murata M, Son A, Kuwahara T, Tsuruyama T, Yamada S, Matsuura M, *et al.* IgA regulates the composition and metabolic function of gut microbiota by promoting symbiosis between bacteria. *Journal of Experimental Medicine*. 2018;215(8):2019–2034. doi:10.1084/jem.20180427
113. Donaldson GP, Chou WC, Manson AL, Rogov P, Abeel T, Bochicchio J, Ciulla D, Melnikov A, Ernst PB, Chu H, *et al.* Spatially distinct physiology of *Bacteroides fragilis* within the proximal colon of gnotobiotic mice. *Nature Microbiology*. 2020;5(May). doi:10.1038/s41564-020-0683-3
114. Platt JL, de Mattos Barbosa MG, Huynh D, Lefferts AR, Katta J, Kharas C, Freddolino P, Bassis CM, Wobus C, Geha R, *et al.* TNFRSF13B polymorphisms counter microbial adaptation to enteric IgA. *JCI Insight*. 2021;6(14):1–14. doi:10.1172/jci.insight.148208
115. Rollenske T, Burkhalter S, Muerner L, Gunten S Von, Lukasiewicz J, Wardemann H, Macpherson AJ. Parallelism of intestinal secretory IgA shapes functional microbial fitness. *Nature*. 2021;598(7882):657–661. doi:10.1038/s41586-021-03973-7
116. van Gool MMJ, van Egmond M. IgA and Fc RI: Versatile Players in Homeostasis, Infection, and Autoimmunity. *ImmunoTargets and Therapy*. 2021;Volume 9:351–372. doi:10.2147/ITT.S266242
117. Smith PD, Smythies LE, Mosteller-Barnum M, Sibley DA, Russell MW, Merger M, Sellers MT, Orenstein JM, Shimada T, Graham MF, *et al.* Intestinal Macrophages Lack CD14 and CD89 and Consequently Are Down-Regulated for LPS- and IgA-Mediated Activities. *The Journal of Immunology*. 2001;167(5):2651–2656. doi:10.4049/jimmunol.167.5.2651
118. Rochereau N, Drocourt D, Perouzel E, Pavot V, Redelinghuys P, Brown GD, Tiraby G, Roblin X, Verrier B, Genin C, *et al.* Dectin-1 Is Essential for Reverse Transcytosis of Glycosylated SIgA-Antigen Complexes by Intestinal M Cells Nemazee D, editor. *PLoS Biology*. 2013;11(9):e1001658. doi:10.1371/journal.pbio.1001658

119. Rios D, Wood MB, Li J, Chassaing B, Gewirtz AT, Williams IR. Antigen sampling by intestinal M cells is the principal pathway initiating mucosal IgA production to commensal enteric bacteria. *Mucosal Immunology*. 2016;9(4):907–916. doi:10.1038/mi.2015.121
120. Hoepel W, Golebski K, van Drunen CM, den Dunnen J. Active control of mucosal tolerance and inflammation by human IgA and IgG antibodies. *Journal of Allergy and Clinical Immunology*. 2020;146(2):273–275. doi:10.1016/j.jaci.2020.04.032
121. van der Steen L, Tuk CW, Bakema JE, Kooij G, Reijkerkerk A, Vidarsson G, Bouma G, Kraal G, de Vries HE, Beelen RHJ, *et al*. Immunoglobulin A: FcRI Interactions Induce Neutrophil Migration Through Release of Leukotriene B4. *Gastroenterology*. 2009;137(6):2018–2029.e3. doi:10.1053/j.gastro.2009.06.047
122. Breedveld A, Van Egmond M. IgA and FcRI: Pathological roles and therapeutic opportunities. 2019. doi:10.3389/fimmu.2019.00553
123. Kamada N, Núñez G. Regulation of the immune system by the resident intestinal bacteria. *Gastroenterology*. 2014;146(6):1477–1488. doi:10.1053/j.gastro.2014.01.060
124. van Egmond M, van Vuuren AJ, Morton HC, van Spriel AB, Shen L, Hofhuis FM, Saito T, Mayadas TN, Verbeek JS, van de Winkel JG. Human immunoglobulin A receptor (FcalphaRI, CD89) function in transgenic mice requires both FcR gamma chain and CR3 (CD11b/CD18). *Blood*. 1999;93(12):4387–94.
125. Kau AL, Planer JD, Liu J, Rao S, Yatsunencko T, Trehan I, Manary MJ, Liu T-C, Stappenbeck TS, Maleta KM, *et al*. Functional characterization of IgA-targeted bacterial taxa from undernourished Malawian children that produce diet-dependent enteropathy. *Science Translational Medicine*. 2015;7(276):276ra24–276ra24. doi:10.1126/scitranslmed.aaa4877

# 02

---

## ***Allobaculum mucolyticum* sp. nov. and *Allobaculum filumensis* sp. nov., two novel members of the *Allobaculum* genus isolated from the human intestinal tract**

Guus H. van Muijlwijk<sup>1</sup>, Tyler Rice<sup>2</sup>, Richard A. Flavell<sup>3</sup>, Noah W. Palm<sup>2\*</sup> and Marcel R. de Zoete<sup>1</sup>

<sup>1</sup> Department of Medical Microbiology, University Medical Center Utrecht, Utrecht, the Netherlands

<sup>2</sup> Human and Translational Immunobiology Program, Yale University School of Medicine, New Haven, CT 06519, USA

<sup>3</sup> Department of Immunobiology, Yale University School of Medicine, New Haven, CT 06510, USA

## 02

## ABSTRACT

As part of a culturomics study to identify bacterial species associated with inflammatory bowel disease, a large collection of bacteria was isolated from patients with ulcerative colitis. Two of these isolates were tentatively identified as members of the *Erysipelotrichaceae* family. Following phylogenetic analysis based on 16S rRNA gene sequence and whole genome sequence, both strain 128<sup>T</sup> and 539<sup>T</sup> were found to be most closely related to *Allobaculum stercoricanis*, with G+C contents of 48.6 mol% and 50.5 mol%, respectively, and the genome sizes of 2 864 314 and 2 580 362 base pairs, respectively. Strains 128<sup>T</sup> and 539<sup>T</sup> were strict anaerobe rods that grew in long chains between 37°C and 42°C. Scanning electron microscopy did not reveal flagella, fimbriae or visible endospores. Biochemical analysis showed nearly identical results for both strains with enzymatic activity of C4 and C8 esterases, acid phosphatase, Naphthol-AS-BI-phosphohydrolase, β-Glucuronidase, N-Acetyl-β-Glucosaminidase and Arginine Arylamidase. In addition, both strains produced indole and reduced nitrate. Major fatty acids were identified as C<sub>18:1</sub> ω9c (oleic acid, 64.06% in 128<sup>T</sup> and 74.35% in 539<sup>T</sup>), C<sub>18:1</sub> ω7c/C<sub>18:1</sub> ω9t/C<sub>18:1</sub> ω12t/UN17.834 (16.18% in 128<sup>T</sup> and 6.22% in 539<sup>T</sup>) and C<sub>16:0</sub> (6.23% in 128<sup>T</sup> and 7.37% in 538<sup>T</sup>). Based on these analyses two novel species are proposed, *Allobaculum mucolyticum* sp. nov. with as the type strain 128<sup>T</sup> (=NCTC 14626=DSMZ 112815) and *Allobaculum filumensis* sp. nov. with as the type strain 539<sup>T</sup> (=NCTC 14627=DSMZ 112814).

## INTRODUCTION

The family *Erysipelotrichaceae* was originally proposed by Verbarg *et al.*<sup>1</sup> in 2004 and named after the family's original genus *Erysipelothrix*—best known for the member *Erysipelothrix rhusiopathiae*, which is an animal and zoonotic pathogen<sup>2</sup>. To date, the *Erysipelotrichaceae* family has expanded to more than 30 (proposed) genera according to the List of Prokaryotic names with Standing in Nomenclature (LPSN, <http://www.bacterio.net>), including *Allobaculum*<sup>3</sup>, *Bulleidia*<sup>4</sup>, *Catenisphaera*<sup>5</sup>, *Dubosiella*<sup>6</sup>, *Faecalibaculum*<sup>7</sup>, *Faecalicoccus*<sup>8</sup>, *Holdemania*<sup>9</sup>, *Ileibacterium*<sup>6</sup> and *Solobacterium*<sup>10</sup>. Members of the *Erysipelotrichaceae* family are Gram-positive, mostly anaerobic, non-motile, slender rods. In addition, several members have been described to have the tendency to form long filaments and contain a B-type peptidoglycan with a unique peptide cross-linking<sup>1</sup>. The vast majority of the *Erysipelotrichaceae* family members have been isolated from the feces or the intestinal tract of humans or animals and, with the recent advances in microbiota research, have been increasingly associated with metabolic syndrome and intestinal inflammatory disorders in both humans and mice. *Erysipelotrichaceae* therefore form an interesting but functionally still largely understudied family of bacteria.

The genus *Allobaculum* (“the other small rod”) currently consist of the sole species *Allobaculum stercoricanis*, described by Greetham *et al.* in 2004 after being isolated from the feces of a dog<sup>3</sup>. *A. stercoricanis* grows strictly anaerobic in pairs or chains, is non-spore-forming and non-motile, and was shown to be present in the intestinal tract of all dogs examined, suggesting it is widely dispersed without an obvious association with canine pathogenesis. Since then, 16S rRNA gene profiling of the microbiota of humans, mice and rats has often identified the *Allobaculum* genus in the context of dietary interventions<sup>11</sup>, aging<sup>12</sup>, intestinal inflammation<sup>13</sup> or experimental autoimmune encephalitis<sup>14</sup>, but thus far no new additions to the *Allobaculum* genus have been proposed.

In this article, we describe two novel, strictly anaerobic *Allobaculum* strains 128<sup>T</sup> and 539<sup>T</sup> isolated from the feces of humans with inflammatory bowel disease (IBD). While being closely related to *A. stercoricanis*, the 16S rRNA gene sequences of isolates 128<sup>T</sup> and 539<sup>T</sup> shows 91.95% and 93.25% similarity (95.49% similar to each other) and therefore phylogenetically cluster separately. We propose to designate 128<sup>T</sup> as *Allobaculum mucolyticum* sp. nov. and 539<sup>T</sup> as *Allobaculum filumensis* sp. nov.

### Isolation and Morphology

Strains 128<sup>T</sup> and 539<sup>T</sup> were isolated from fecal samples of two patients with inflammatory bowel disease as part of an IBD culturomics study. Both strains were isolated under strict anaerobic culturing conditions (5% H<sub>2</sub>, 10% CO<sub>2</sub> and 85% N<sub>2</sub>) using nonselective Gut Microbiota Medium (GMM)<sup>15</sup> culture plates, on which visible bacteria appeared after 2-3 days as opaque to white, mainly round, flat colonies with undulating margins and a dry mucoid appearance. Strains 128<sup>T</sup> and 539<sup>T</sup> are strict anaerobes as no growth was observed when grown on GMM plates in the presence of 1%, 5% or 20% oxygen. Both strains showed limited growth at 30°C but grew readily between 37°C and 42°C, with a generation time of ~130 minutes in GMM broth at 37°C under anaerobic conditions. Gifu Anaerobic Medium showed moderate growth as compared to GMM media, while BHI did not support growth at all. Scanning electron microscopy (SEM) of strains 128<sup>T</sup> and 539<sup>T</sup>, cultured in GMM broth for 48 hours under anaerobic conditions at 37°C, revealed rods with tapering ends and varying lengths (~1-2 μm x ~0.7 μm) that grew in long chains and appeared to have one or more symmetrical ring-like structures that resemble Z-rings that drive septum constriction (Figure 1). SEM did not reveal flagella or fimbriae. No visible endospores were observed, similar to what has been previously reported for other members of the *Erysipelotrichaceae* family<sup>1,16</sup>.

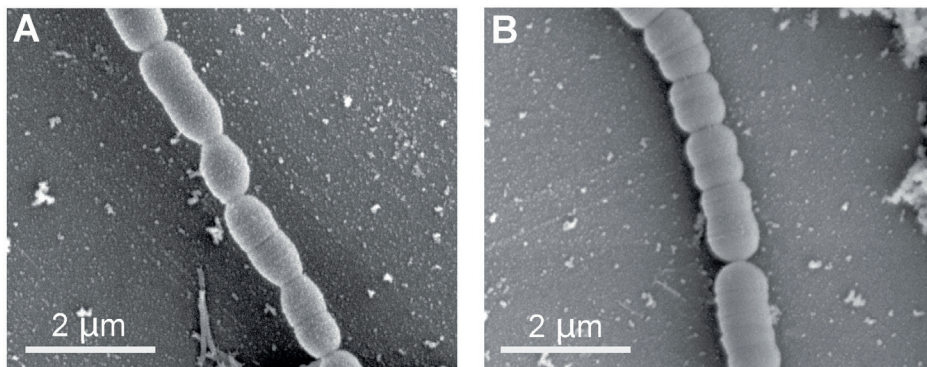


**Figure 1.** Scanning electron microscopy of strains 128<sup>T</sup> (a) and 539<sup>T</sup> (b).

### Physiology and Chemotaxonomy

*Allobaculum* strains 128<sup>T</sup> and 539<sup>T</sup> were characterized phenotypically using API Rapid ID32A and API ZYM (bioMérieux) according to the manufacturers' instructions (Table 1). Similar to the closest relative *A. stercoricanis*, both strains 128<sup>T</sup> and 539<sup>T</sup> exhibited weak C4 and C8 esterases activity,

acid phosphatase activity and lacked most arylamidase activity except for arginine arylamidase, which was present in strains 128<sup>T</sup> and 539<sup>T</sup>, as well as in *A. stercoricanis*. β-galactosidase, β-glucosidase and N-acetyl-β-glucosaminidase was also present in all strains. In contrast to *A. stercoricanis*, strains 128<sup>T</sup> and 539<sup>T</sup> showed β-glucuronidase activity and were able to reduce nitrate and produce indole, but did not exhibit alkaline phosphatase activity. Overall, strains 128<sup>T</sup> and 539<sup>T</sup> were very similar, although minor variations in detected levels of enzymatic activity did occur.

The fatty acids contents from bacterial cultures grown for 48 h in GMM media at 37°C under anaerobic conditions were identified by the Sherlock Microbial Identification System (MIDI) using Gas Chromatographic Analysis of Fatty Acid Methyl Esters (GC-FAME)<sup>17</sup> and was carried out by the Identification Service, Leibniz-Institut DSMZ – Deutsche Sammlung von Mikroorganismen und Zellkulturen GmbH, Braunschweig, Germany (Table 2). The major fatty acids of strain 128<sup>T</sup> were C<sub>18:1</sub> ω9c (oleic acid, 64.06%), C<sub>18:1</sub> ω7c/C<sub>18:1</sub> ω9t/C<sub>18:1</sub> ω12t/UN17.834 (16.18%) and C<sub>16:0</sub> (6.23%). For strain 539<sup>T</sup> the major fatty acids were C<sub>18:1</sub> ω9c (oleic acid, 74.35%), C<sub>16:0</sub> (7.37%) and C<sub>18:1</sub> ω7c/C<sub>18:1</sub> ω9t/C<sub>18:1</sub> ω12t/UN17.834 (6.22%). Minor fatty acids present in strains 128<sup>T</sup> and 539<sup>T</sup> are shown in Table 2. The major fatty acids in the membrane of *Allobaculum stercoricanis* were reported to be C<sub>16:0</sub>, C<sub>18:1</sub> ω9c and C<sub>18:0</sub>, which were also detected in strains 128<sup>T</sup> and 539<sup>T</sup>, and C<sub>18:2</sub> n-6 (linoleic acid), which was absent from both strains. The high level of oleic acid in the membrane of both strains was noticeable; while *Dakotella fusiforme* was shown to contain 29.82% oleic acid<sup>16</sup>, lower amounts of membrane oleic acid have been reported for various *Erysipelotrichaceae* family members, including *Ileibacterium valens*, *Dubosiella newyorkensis*, *Erysipelothrix rhusiopathiae*, *Coprobacillus cateniformis* and *Turicibacter sanguinis*.

**Table 1. Characteristics of strains 128<sup>T</sup> and 539<sup>T</sup> compared to the closely related *Erysipelotrichaceae* family members *A. stercoricanis* and *I. valens*.** Data from *A. stercoricanis* from Verbarq *et al.*<sup>1</sup> Data from *I. valens* from Cox *et al.*<sup>6</sup>; +, positive; -, negative; w, weakly positive; v, variable; nd, not determined.

Characteristic	128 <sup>T</sup>	539 <sup>T</sup>	<i>Allobaculum stercoricanis</i> DSM 13633 <sup>T</sup>	<i>Ileibacterium valens</i> NYU-BL-A3 <sup>T</sup>
Alkaline Phosphatase	-	-	+	-
Esterase (C4)	w	w	+	nd
Esterase Lipase (C8)	w	w	+	nd
Lipase (C14)	-	-	-	nd
Arginine Arylamidase	+/-	+	+	-
Leucine Arylamidase	-	-	-	-
Proline Arylamidase	-	-	-	-
Leucyl Glycine Arylamidase	-	-	-	-
Phenylalanine Arylamidase	-	-	-	-
Pyroglutamic acid Arylamidase	-	-	-	-
Tyrosine Arylamidase	-	-	-	-
Alanine Arylamidase	-	-	-	-
Glycine Arylamidase	-	-	-	-
Histidine Arylamidase	-	-	-	-
Glutamyl Glutamic acid Arylamidase	-	-	-	-
Serine Arylamidase	-	-	-	-
Valine Arylamidase	-	-	-	nd
Cystine Arylamidase	-	-	nd	nd
Trypsin	-	-	-	nd
α-Chymotrypsin	-	-	-	nd
Acid Phosphatase	+	+	+	nd
Naphthol-AS-BI-phosphohydrolase	+	+	nd	nd
α-Galactosidase	-	-	-	+
β-Galactosidase	+	+	+	+
β-Galactosidase-6-phosphate	-	-	-	-
β-Glucuronidase	w	-	-	-
α-Glucosidase	w	w	+	-/w
β-Glucosidase	-	-	-	+
α-Arabinosidase	-	-	-	-
N-Acetyl-β-Glucosaminidase	+	+	w	-
α-Mannosidase	-	-	-	nd
α-Fucosidase	-	-	-	-
Urease	-	-	-	-
Glutamic acid Decarboxylase	-	-	-	-
Arginine Dihydrolase	-	-	-	-
Mannose fermentation	-	-	-	v
Raffinose fermentation	-	-	-	v
Indole production	+	+	-	-
Nitrate reduction	w	w	-	-

**Table 2. Fatty acid composition of strains 128<sup>T</sup> and 539<sup>T</sup> compared to the closely related *Erysipelotrichaceae* family members *A. stercoricanis* and *I. valens*.** Data from *A. stercoricanis* from Verbarq *et al.*<sup>1</sup> Data from *I. valens* from Cox *et al.*<sup>6</sup> Fatty acids that could not be separated using the microbial identification system (Microbial ID) were considered summed features. <sup>1</sup>MIDI analysis designation "Summed in feature 10", which contains C<sub>18:1</sub> ω7c/ω9t/ω12t and/or an unknown fatty acid of ECL 17.834; <sup>2</sup>MIDI analysis designation "Summed in feature 8", which contains C<sub>17:1</sub> ω8c and/or C<sub>17:2</sub> and/or an unknown fatty acid of ECL 16.801; <sup>3</sup>MIDI analysis designation "Summed feature 12", which contains C<sub>19:0</sub> iso and/or an unknown fatty acid of ECL 18.622. UNx, unknown fatty acid of ECL x; DMA, dimethyl acetal.

Fatty acid	128 <sup>T</sup>	539 <sup>T</sup>	<i>Allobaculum stercoricanis</i> DSM 13633 <sup>T</sup>	<i>Ileibacterium valens</i> NYU-BL-A3 <sup>T</sup>
C <sub>9:0</sub>	-	-	1.3	2.6
C <sub>10:0</sub>	-	0.11	9.8	4.5
C <sub>11:0</sub>	-	-	-	2.3
C <sub>12:0</sub>	-	-	2.7	4.9
C <sub>13:0</sub>	-	-	-	2.2
C <sub>14:0</sub>	0.27	0.36	5.8	6.0
C <sub>15:0</sub>	-	-	1.0	2.8
C <sub>16:0</sub>	6.23	7.37	33.7	34.2
C <sub>17:0</sub>	-	-	1.0	3.4
C <sub>18:0</sub>	3.64	3.82	12.0	18.9
C <sub>16:1</sub> ω7c	1.62	1.67	-	-
C <sub>16:1</sub> ω7c/ω6c	-	-	1.5	-
C <sub>18:1</sub> ω9c	64.07	74.35	15.2	9.4
C <sub>18:1</sub> ω7c	-	-	3.5	-
C <sub>20:1</sub> ω9c	0.54	0.41	-	-
C <sub>18:2</sub> ω6,9c and/or C <sub>18:0</sub> anteiso	-	-	12.5	2.8
UN18.199 and/or C <sub>18:2</sub> ω7c/ω9c DMA	2.36	2.14	-	-
C <sub>18:1</sub> ω7c DMA	2.35	1.82	-	-
C <sub>18:1</sub> ω7c/ω9t/ω12t and/or UN17.834 <sup>1</sup>	16.18	6.22	-	-
C <sub>17:1</sub> ω8c and/or C <sub>17:2</sub> <sup>2</sup>	-	0.26	-	-
UN18.622 and/or C <sub>19:0</sub> iso <sup>3</sup>	2.73	1.47	-	-

## Genomic characterization

Whole genome sequence of strains 128<sup>T</sup> and 539<sup>T</sup> were obtained using Illumina MiSeq sequencing with a 2x250 bp paired-end configuration. The resulting sequencing reads were assembled using SPAdes version 3.11.1<sup>19</sup> using k-mer lengths of 57, 97 and 127. Quality control of the genome assemblies was performed using the quality assessment tool for genome assemblies (QUAST)<sup>20</sup>. The genome sizes of strains 128<sup>T</sup> and 539<sup>T</sup> were 2 864 314 base pairs (412 contigs) and 2 580 362 base pairs (201 contigs), respectively. The DNA G+C content was calculated at 48.6 mol% for 128<sup>T</sup> and 50.5 mol% for 539<sup>T</sup>, which was markedly higher than *A. stercoricanis* DSM 13633 (37.8 mol%) and the closely related *Ileibacterium valens* NYU-BL-A3<sup>T</sup> (41.1 mol%) and *Dubosiella newyorkensis* NYU-BL-A4<sup>T</sup> (42.5 mol%), but slightly lower than *Faecalibaculum rodentium* NYU-BL-K8 (53.7 mol%)<sup>6</sup>. Genomes were annotated using PROKKA 1.14.6<sup>21</sup>, which yielded a predicted 2253 coding sequences (CDS) for strain 128<sup>T</sup> and 2049 CDS for strain 539<sup>T</sup>. The NCBI accession numbers of strain 128<sup>T</sup> and 539<sup>T</sup> are JAHUZH000000000 and JAHDSX000000000, respectively.

## 16S RNA and whole genome-based phylogeny

The near-complete 16S rRNA gene sequences of strain 128<sup>T</sup> and 539<sup>T</sup> were obtained by PCR using the universal primers 27F (5'-AGA GTT TGA TCM TGG CTC AG-3') and 1492R (5'-CGG TTA CCT TGT TAC GAC TT-3'), Sanger sequenced (Macrogen) and deposited under GenBank accession numbers MZ153114 and MZ153115, respectively. The EzBioCloud 16S-based ID database<sup>22</sup> was searched for the closest homologues for strains 128<sup>T</sup> and 539<sup>T</sup>, which was an uncultured bacterium from the feces of a rat for both strains (accession FJ880578, 95.10% and 99.72% similarity, respectively). Based on 16S rRNA sequence similarity alone this uncultured bacterial clone FJ880578, designated '*Allobaculum*' in the EzBioCloud 16S Database, likely belongs to the same species as strain 539<sup>T</sup>. The 16S rRNA gene sequence similarity between strain 128<sup>T</sup> and 539<sup>T</sup> was 95.49% (EzBioCloud Pairwise Nucleotide Sequence Alignment for Taxonomy tool), suggesting they are distinct species from likely the same genus.

When 16S rRNA gene sequence similarity of strain 128<sup>T</sup> and 539<sup>T</sup> was compared to *A. stercoricanis* DSM 13633, the only previously classified *Allobaculum* species, 128<sup>T</sup> had a similarity of 91.95%, while 539<sup>T</sup> was 93.25% similar.

In order to further examine their phylogeny, type strains 128<sup>T</sup> and 539<sup>T</sup>, a neighbour-joining dendrogram that contained the 16S rRNA gene sequences of all *Erysipelotrichaceae* family members was constructed using MEGA

X<sup>23</sup>, with bootstrap values based on 500 repetitions (Figure 2). To root the phylogenetic tree, the 16S rRNA gene sequence of *Escherichia coli* strain DSM 30083<sup>T</sup> was used as an outgroup. Strains 128<sup>T</sup> and 539<sup>T</sup> were placed within the family of *Erysipelotrichaceae* and were most closely related to *A. stercoricanis* (91.95% and 93.25% sequence similarity, respectively) and *Ileibacterium valens* (89.56% and 90.25%, respectively). Guidelines for sequence-based grouping of taxa into the same genus are not strictly defined and can vary greatly among different taxa. This may pose a particular challenge for the family of *Erysipelotrichaceae*, which displays high phylogenetic heterogeneity and is characterized by many monotypic genera<sup>18</sup>. For instance, >94.5% similarity based on 16S rRNA gene sequence was recently proposed as a genus cutoff<sup>24</sup>, which would place strains 128<sup>T</sup> and 539<sup>T</sup> in the same genus but outside the *Allobaculum* genus when compared to *A. stercoricanis*. Notably, with 93.25% similarity strain 539<sup>T</sup> is phylogenetically markedly closer to the *Allobaculum* genus than strain 128<sup>T</sup> while both strains genetically belong to the same genus, highlighting the limits of using cutoff for genus classification based on 16S rRNA gene sequences.

Using the whole genome sequences of type strains 128<sup>T</sup> and 539<sup>T</sup> and closely related *Erysipelotrichaceae* family members based on the 16S phylogenetic analysis depicted in Figure 2, average sequence identities of shared genes (ANI) was calculated using ANI/AAI-Matrix Genome-based distance calculator<sup>25</sup>. These calculations again show that strains 128<sup>T</sup> and 539<sup>T</sup> do not belong to the same species and do not cluster with other known *Erysipelotrichaceae* species, as all ANI values were not within the proposed 83%-95% range<sup>26</sup>; 128<sup>T</sup> and 539<sup>T</sup> had ANI values of 82%, and 77% and 76% as compared to *A. stercoricanis*, respectively. An alternative method to delineate genera and estimate their evolutionary and phenotypic distance uses the percentage of conserved proteins (POCP<sup>27</sup>). POCP values between 128<sup>T</sup> and *A. stercoricanis*, and 539<sup>T</sup> and *A. stercoricanis* were 54.5% and 57.2%, respectively, which is well above the proposed genus boundary of 50%. We therefore conclude that, while the 16S rDNA gene sequence of strains 128<sup>T</sup> and 539<sup>T</sup> differ significantly from that of *A. stercoricanis*, both strains belong to the *Allobaculum* genus as based on the POCP values.



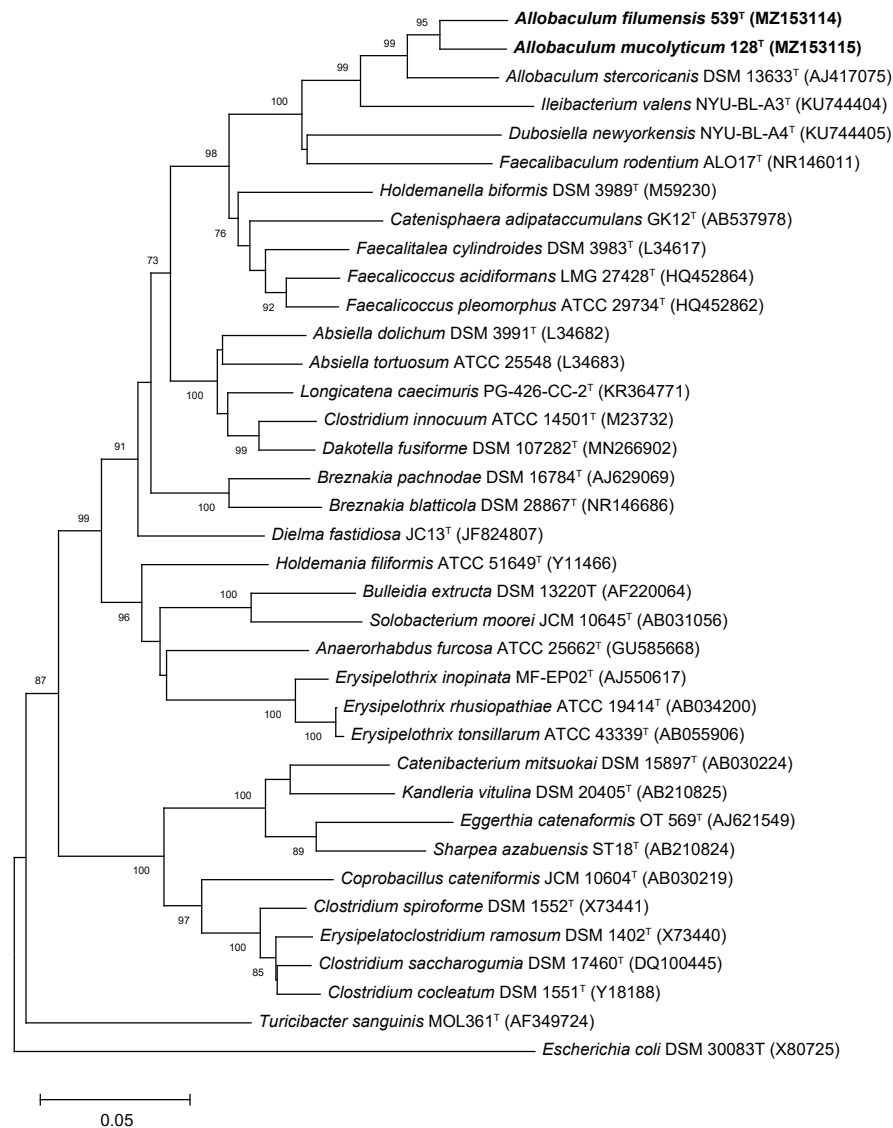


**Figure 2. Neighbour-joining phylogenetic dendrogram based on 16S rRNA gene sequences of strains 128<sup>T</sup> and 538<sup>T</sup> with related members of the *Erysipelotrichaceae* family.** 16S rRNA gene sequences accession numbers are given in parentheses. The sequences were aligned using the neighbour-joining method in MEGA7 and evolutionary distances were computed using the Kimura 2-parameter method. The phylogenetic tree was obtained using MEGA X (percentage of 500 bootstrap tests are shown at the branching point) with branch lengths measured in the number of base substitutions per site. Bar represents 0.05 substitutions per nucleotide position. *Escherichia coli* DSM 30083<sup>T</sup> was used as an outgroup.

### Description of *Allobaculum mucolyticum* sp. nov.

*Allobaculum mucolyticum* (mu.co.'ly.ti.cum. L. neut. n. mucus; Gr. adj. lyticos, causing degradation; N.L. neut. n. mucolyticum, mucus-degrading). Cells are rod-shaped with tapering ends of an average of ~1-2 μm in length and ~0.7 μm in width that stain Gram-positive. Cells grow under strict anaerobic conditions between 30°C and 42°C in long chains, are non-motile and show no visible fimbriae. Best growth is observed with Gut Microbiota Medium, while Gifu Anaerobic Media showed limited growth. With the API Rapid ID32A and API ZYM systems, positive reactions were observed for C4 and C8 esterases activity (weak activity), acid phosphatase activity, Naphthol-AS-BI-phosphohydrolase activity, Arginine Arylamidase activity, β-Glucuronidase activity, N-Acetyl-β-Glucosaminidase activity, indole production and nitrate reduction. Major fatty acids are C<sub>18:1</sub> ω9c (64.06%), C<sub>18:1</sub> ω7c/C<sub>18:1</sub> ω9t/C<sub>18:1</sub> ω12t/UN17.834 (16.18%) and C<sub>16:0</sub> (6.23%). The type strain is 128<sup>T</sup> (=NCTC 14626=DSMZ 112815), isolated from the intestinal tract of a patient with ulcerative colitis. Its G+C content is 48.6 mol% and the genome size is 2 864 314 base pairs.

### Description of *Allobaculum filumensis* sp. nov.

*Allobaculum filumensis* (fi.lu.'men.sis. L. neut. n. filum, string; N.L. neut. adj. filumensis, belonging to or part of a string). Cells stain Gram-positive and are rod-shaped with tapering ends of an average of ~1-2 μm in length and ~0.7 μm in width. Grows in long chains and is restricted to anaerobic conditions with a temperature range between 30°C and 42°C, are non-motile and show no visible fimbriae. Optimal growth is observed with Gut Microbiota Medium, while Gifu Anaerobic Media showed limited growth. With the API Rapid ID32A and API ZYM systems, positive reactions were observed for C4 and C8 esterases activity (weakly positive), Arginine Arylamidase activity, acid phosphatase activity, Naphthol-AS-BI-phosphohydrolase activity, β-Glucuronidase activity, N-Acetyl-β-Glucosaminidase activity, indole production and nitrate reduction. Major fatty acids are C<sub>18:1</sub> ω9c (74.35%), C<sub>16:0</sub> (7.37%) and C<sub>18:1</sub> ω7c/C<sub>18:1</sub> ω9t/C<sub>18:1</sub> ω12t/UN17.834 (6.22%). The type strain is 539<sup>T</sup> (=NCTC 14627=DSMZ 112814), isolated from the intestinal tract of a patient with ulcerative colitis. Its G+C content is 50.5 mol% and the genome size is 2 580 362 base pairs.

## Protologue

The GenBank/EMBL/DDBJ accession numbers for the 16S rDNA gene sequences of *Allobaculum mucolyticum* strain<sup>T</sup> and *Allobaculum filumensis* strain<sup>T</sup> are MZ153114 and MZ153115, respectively. Whole-genome sequences have been deposited under NCBI bioproject number PRJNA730514.

## AUTHOR STATEMENTS

### Authors and contributors

M.R.d.Z., N.W.P., T.R., R.A.F. and G.H.v.M. conceived and designed the study and co-wrote the manuscript. G.H.v.M performed all experiments.

### Conflicts of interest

The authors declare that there are no conflicts of interest.

### Acknowledgements

We would like to acknowledge Moniek Salomons for assisting with the phenotypical characterizations and Marco Viveen for assisting with scanning electron microscopy.

## REFERENCES

1. Verborg S, Rheims H, Emus S, Frühling A, Kroppenstedt RM et al. *Erysipelothrix inopinata* sp. nov., isolated in the course of sterile filtration of vegetable peptone broth, and description of Erysipelotrichaceae fam. nov. *Int J Syst Evol Microbiol* 2004;54(Pt 1):221-225.
2. Wang Q, Chang BJ, Riley TV. *Erysipelothrix rhusiopathiae*. *Vet Microbiol* 2010;140(3-4):405-417.
3. Greetham HL, Gibson GR, Giffard C, Hippe H, Merkhoffer B et al. *Allobaculum stercoricanis* gen. nov., sp. nov., isolated from canine feces. *Anaerobe* 2004;10(5):301-307.
4. Downes J, Olsvik B, Hiom SJ, Spratt DA, Cheeseman SL et al. *Bulleidia extracta* gen. nov., sp. nov., isolated from the oral cavity. *Int J Syst Evol Microbiol* 2000;50 Pt 3:979-983.
5. Kanno M, Katayama T, Morita N, Tamaki H, Hanada S et al. *Catenisphaera adipataaccumulans* gen. nov., sp. nov., a member of the family Erysipelotrichaceae isolated from an anaerobic digester. *Int J Syst Evol Microbiol* 2015;65(Pt 3):805-810.
6. Cox LM, Sohn J, Tyrrell KL, Citron DM, Lawson PA et al. Description of two novel members of the family Erysipelotrichaceae: *Ileibacterium valens* gen. nov., sp. nov. and *Dubosiella newyorkensis*, gen. nov., sp. nov., from the murine intestine, and emendation to the description of *Faecalibaculum rodentium*. *Int J Syst Evol Microbiol* 2017;67(5):1247-1254.
7. Chang DH, Rhee MS, Ahn S, Bang BH, Oh JE et al. *Faecalibaculum rodentium* gen. nov., sp. nov., isolated from the faeces of a laboratory mouse. *Antonie Van Leeuwenhoek* 2015;108(6):1309-1318.
8. De Maesschalck C, Van Immerseel F, Eeckhaut V, De Baere S, Cnockaert M et al. *Faecalicoccus acidiformans* gen. nov., sp. nov., isolated from the chicken caecum, and reclassification of *Streptococcus pleomorphus* (Barnes et al. 1977), *Eubacterium bifforme* (Eggerth 1935) and *Eubacterium cylindroides* (Cato et al. 1974) as *Faecalicoccus pleomorphus* comb. nov., *Holdemanella biformis* gen. nov., comb. nov. and *Faecalitalea cylindroides* gen. nov., comb. nov., respectively, within the family Erysipelotrichaceae. *Int J Syst Evol Microbiol* 2014;64(Pt 11):3877-3884.
9. Willems A, Moore WE, Weiss N, Collins MD. Phenotypic and phylogenetic characterization of some *Eubacterium*-like isolates containing a novel type B wall murein from human feces: description of *Holdemanella filiformis* gen. nov., sp. nov. *Int J Syst Bacteriol* 1997;47(4):1201-1204.
10. Kageyama A, Benno Y. Phylogenetic and phenotypic characterization of some *Eubacterium*-like isolates from human feces: description of *Solobacterium moorei* Gen. Nov., Sp. Nov. *Microbiol Immunol* 2000;44(4):223-227.
11. Ravussin Y, Koren O, Spor A, LeDuc C, Gutman R et al. Responses of gut microbiota to diet composition and weight loss in lean and obese mice. *Obesity (Silver Spring)* 2012;20(4):738-747.

12. Thevaranjan N, Puchta A, Schulz C, Naidoo A, Szamosi JC et al. Age-Associated Microbial Dysbiosis Promotes Intestinal Permeability, Systemic Inflammation, and Macrophage Dysfunction. *Cell Host Microbe* 2017;21(4):455-466.e454.
13. Palm NW, de Zoete MR, Cullen TW, Barry NA, Stefanowski J et al. Immunoglobulin A coating identifies colitogenic bacteria in inflammatory bowel disease. *Cell* 2014;158(5):1000-1010.
14. Miyauchi E, Kim SW, Suda W, Kawasumi M, Onawa S et al. Gut microorganisms act together to exacerbate inflammation in spinal cords. *Nature* 2020;585(7823):102-106.
15. Goodman AL, Kallstrom G, Faith JJ, Reyes A, Moore A et al. Extensive personal human gut microbiota culture collections characterized and manipulated in gnotobiotic mice. *Proc Natl Acad Sci U S A* 2011;108(15):6252-6257.
16. Ghimire S, Wongkuna S, Scaria J. Description of a new member of the family Erysipelotrichaceae : *Dakotella fusiforme* gen. nov., sp. nov., isolated from healthy human feces. *PeerJ* 2020;8:e10071.
17. M S. Identification of bacteria by gas chromatography of cellular fatty acids. MIDI Technical Note 101 1990.
18. Verbarq S, Göker M, Scheuner C, Schumann P, Stackebrandt E. The families Erysipelotrichaceae emend., Coprobacillaceae fam. nov., and Turicibacteraceae fam. nov. *The prokaryotes: Firmicutes and Tenericutes 4th ed Berlin-Heidelberg: Springer-Verlag* 2014:79-105.
19. Bankevich A, Nurk S, Antipov D, Gurevich AA, Dvorkin M et al. SPAdes: a new genome assembly algorithm and its applications to single-cell sequencing. *J Comput Biol* 2012;19(5):455-477.
20. Gurevich A, Saveliev V, Vyahhi N, Tesler G. QUAST: quality assessment tool for genome assemblies. *Bioinformatics* 2013;29(8):1072-1075.
21. Seemann T. Prokka: rapid prokaryotic genome annotation. *Bioinformatics* 2014;30(14):2068-2069.
22. Yoon S-H, Ha S-M, Kwon S, Lim J, Kim Y et al. Introducing EzBioCloud: a taxonomically united database of 16S rRNA gene sequences and whole-genome assemblies. *International Journal of Systematic and Evolutionary Microbiology* 2017;67(5):1613-1617.
23. Kumar S, Stecher G, Li M, Knyaz C, Tamura K. MEGA X: Molecular Evolutionary Genetics Analysis across Computing Platforms. *Mol Biol Evol* 2018;35(6):1547-1549.
24. Yarza P, Yilmaz P, Pruesse E, Glöckner FO, Ludwig W et al. Uniting the classification of cultured and uncultured bacteria and archaea using 16S rRNA gene sequences. *Nature Reviews Microbiology* 2014;12(9):635-645.
25. Rodriguez-R LM, Konstantinidis KT. The enveomics collection: a toolbox for specialized analyses of microbial genomes and metagenomes. *PeerJ Preprints* 2016;4:e1900v1.

26. Jain C, Rodriguez RL, Phillippy AM, Konstantinidis KT, Aluru S. High throughput ANI analysis of 90K prokaryotic genomes reveals clear species boundaries. *Nat Commun* 2018;9(1):5114.
27. Qin QL, Xie BB, Zhang XY, Chen XL, Zhou BC et al. A proposed genus boundary for the prokaryotes based on genomic insights. *J Bacteriol* 2014;196(12):2210-2215. *Allobaculum mucolyticum* sp. nov. and *Allobaculum filumensis* sp. nov.

# 03

---

## Identification of *Allobaculum mucolyticum* as a novel human intestinal mucin degrader

Guus H. van Muijlwijk<sup>1</sup>, Guido van Mierlo<sup>2\*</sup>, Pascal W.T.C. Jansen<sup>2</sup>, Michiel Vermeulen<sup>2</sup>, Nancy M.C. Bleumink-Pluym<sup>3</sup>, Noah W. Palm<sup>4</sup>, Jos P.M. van Putten<sup>3</sup> & Marcel R. de Zoete<sup>1</sup>

<sup>1</sup> Department of Medical Microbiology, University Medical Center Utrecht, Utrecht, Netherlands

<sup>2</sup> Department of Molecular Biology, Faculty of Science, Radboud Institute for Molecular Life Sciences, Oncode Institute, Radboud University Nijmegen, Nijmegen, the Netherlands

<sup>3</sup> Department of Biomolecular Health Sciences, Utrecht University, Utrecht, Netherlands

<sup>4</sup> Department of Immunobiology, Yale University School of Medicine, New Haven, CT, USA

\* Present address: Laboratory of Systems Biology and Genetics, Institute of Bioengineering, School of Life Sciences, Ecole Polytechnique Fédérale de Lausanne (EPFL), CH-1015 Lausanne, Switzerland

## 03

## ABSTRACT

The human gut microbiota plays a central role in intestinal health and disease. Yet, many of its bacterial constituents are functionally still largely unexplored. A crucial prerequisite for bacterial survival and proliferation is the creation and/or exploitation of an own niche. For many bacterial species that are linked to human disease, the inner mucus layer was found to be an important niche. *Allobaculum mucolyticum* is a newly identified, IBD-associated species that is thought to be closely associated with the host epithelium. To explore how this bacterium is able to effectively colonize this niche, we screened its genome for factors that may contribute to mucosal colonization. Up to 60 genes encoding putative Carbohydrate Active Enzymes (CAZymes) were identified in the genome of *A. mucolyticum*. Mass spectrometry revealed 49 CAZymes of which 26 were significantly enriched in its secretome. Functional assays demonstrated the presence of CAZyme activity in *A. mucolyticum* conditioned medium, degradation of human mucin O-glycans, and utilization of liberated non-terminal monosaccharides for bacterial growth. The results support a model in which sialidases and fucosidases remove terminal O-glycan sugars enabling subsequent degradation and utilization of carbohydrates for *A. mucolyticum* growth. *A. mucolyticum* CAZyme secretion may thus facilitate bacterial colonization and degradation of the mucus layer and may pose an interesting target for future therapeutic intervention.

## INTRODUCTION

The intestinal microbiota plays an important role in host health and disease. Due to their close association with the host epithelium, bacteria occupying the intestinal mucosal niche are thought to have a preponderant effect on host health. For example, their close proximity to the intestinal epithelium increases the chances of activating host immune responses, which may drive excessive inflammatory responses as seen in inflammatory bowel disease (IBD)<sup>1</sup>.

In order to provide protection and avoid excessive inflammatory responses, the intestinal epithelial cells are covered by a viscous mucus layer that protects them from direct contact with potentially harmful bacteria. This mucus layer primarily consists of heavily glycosylated mucin proteins, such as MUC2, that are highly decorated with branched O-glycans linked to serine/threonine-rich repeats in the polypeptide backbone. These mucin O-glycans retain large amounts of water (>90% of the mucin weight is due to water), which gives the mucus layer its lubricant properties. Furthermore, mucin glycans also protect the peptide backbone from proteolytic degradation by bacterial and host proteases, thereby safeguarding its main function as a mucosal firewall.

Many enteropathogenic bacteria have developed mechanisms to breach the mucus barrier, e.g., through flagella-driven propulsion. However, in recent years it has also become clear that several commensal bacteria, such as *Akkermansia muciniphila* and *Bacteroides thetaiotamicron*, have adopted a mucus-dwelling lifestyle and feed on the monosaccharides present in mucin O-glycans<sup>2-5</sup>. To enable this, these bacteria employ one or more mucin O-glycan specific glycoside hydrolases that release the monosaccharides that make up the glycan chain. The glycoside hydrolase families required for mucin O-glycan degradation have previously been described by Tailford *et al.*<sup>6</sup>

A decreased mucus layer thickness and increased bacterial invasion into the inner mucus layer are well-known phenomena in IBD pathology<sup>7</sup>. Our group has previously demonstrated that IgA-coated bacteria are inclined to encroach towards the intestinal epithelial cells and can cause intestinal inflammation in mouse models of colitis<sup>8</sup>. One of these highly IgA-coated bacteria is a newly identified bacterium from the *Allobaculum* genus: *Allobaculum mucolyticum* sp. nov. Little is known about bacteria from the *Allobaculum* genus, which are part of the *Erysipelotrichaceae* family and inhabitants of the intestinal microbiota. The first reported member of this genus is *Allobaculum*

*stercoricanis*, a Gram-positive rod shaped bacterium isolated from dog feces<sup>9</sup>. *Allobaculum* species are mainly identified on the basis of high throughput 16S rRNA gene sequencing, often in studies that focus on changes in gut microbiota composition of mice after dietary interventions. The relative abundance of *Allobaculum* species in mice and rats has been correlated with aging, high fat diets, and fatty acid metabolism<sup>10-16</sup>. Besides correlations with fatty acid metabolism, Herrmann *et al.* reported *Allobaculum* to be an active glucose utilizer and producer of lactate and butyrate<sup>13,14</sup>. These reports are in line with previous reports about bacteria from the *Erysipelotrichaceae* family, which are often associated with a western or high fat diet<sup>17,18</sup>.

*Allobaculum* species have also been implicated in playing a role in inflammatory processes. For example, Cox *et al.*<sup>16</sup> reported a positive correlation between *Allobaculum* relative abundance and levels of ileal ROR $\gamma$ T and IL-17 levels and protection from metabolic syndrome in mice. Another, more recent report by Miyauchi *et al.*<sup>19</sup> causatively linked an *Allobaculum* strain (OTU002) to increased susceptibility to experimental autoimmune encephalitis. This increased susceptibility was attributed to this bacterium's ability to adhere to small intestinal epithelial cells which induces the expansion of inflammatory intestinal T helper 17 cells. Finally, *A. mucolyticum* was originally isolated from an ulcerative colitis patient (UC) based on its high levels of IgA coating. Mice that were colonized with this strain as part of a microbial community also developed IgA responses towards this bacterium and developed much more severe colitis upon exposure to DSS<sup>8</sup>. This suggests that *A. mucolyticum* is immunogenic *in vivo* and could play an important role in the development of intestinal inflammation.

As the reports about *Allobaculum* species are increasing in number, and we and others have reported that bacteria within the *Allobaculum* genus belong to the immunogenic inhabitants of the intestinal mucosal niche, a more detailed characterization of bacteria belonging to this genus is warranted. Here, we subjected *A. mucolyticum* to a thorough genomic and functional characterization. We show that *A. mucolyticum* can secrete a wide repertoire of mucin *O*-glycan targeting carbohydrate active enzymes (CAZymes), which allow it to effectively degrade and feed on intestinal mucins. These potent mucolytic capabilities suggest it can effectively colonize and degrade the protective mucus layer of its host.

## RESULTS

### ***Allobaculum mucolyticum* utilizes both dietary- and host-derived glycans for growth**

*Allobaculum* species are inhabitants of the intestine and thus encounter multiple dietary- and host-derived nutrients. To investigate the nutrient requirements of *A. mucolyticum*, we assessed its growth over a period of 72 hours in the presence of a variety of substrates. Robust growth of *A. mucolyticum* was observed in an enriched gut microbiota medium (GMM), containing multiple mono- and disaccharides, such as glucose, fructose, maltose and cellobiose (Figure 1A). To examine whether other, dietary-derived sources of glycan can also be used for growth, *A. mucolyticum* was grown in a basal medium supplemented with the plant polysaccharide inulin (Figure S1). The basal medium alone, which lacks all glycans present in GMM, did not support the growth of *A. mucolyticum*. Supplementation of basal medium with inulin resulted in firm growth, demonstrating the bacterium's ability to utilize dietary-derived carbon sources.

As several other *Allobaculum* species have been reported to be closely associated with the intestinal mucosal niche, we next investigated whether *A. mucolyticum* could also use mucins for growth. Hereto, basal medium was supplemented with porcine gastric mucin (PGM, 0.5% w/vol) and this was sufficient to support *A. mucolyticum* growth (Figure 1A). To assess whether mucin *O*-glycans and/or the mucin peptide backbone promoted bacterial growth, bacteria were grown in basal medium supplemented with purified mucin *O*-glycans (10 mg/mL). After supplementation with these glycans *A. mucolyticum* was able to grow to a similar optical density as on complete porcine gastric mucin (0.5% w/vol) (Figure 1A). This showed that the *O*-glycans present on mucin are sufficient to support the growth of *A. mucolyticum* and indicates that, in addition to dietary-derived glycans, *A. mucolyticum* can also use host-derived mucin as a growth substrate.

### **The genome of *Allobaculum mucolyticum* predicts the presence of a wide range of -glycan-targeting carbohydrate active enzymes (CAZymes)**

To investigate how *A. mucolyticum* can utilize complex *O*-glycans, we interrogated the available *A. mucolyticum* genome for the presence of CAZymes using the dbCAN2 metaserver pipeline for automated CAZyme annotation<sup>20</sup>. This pipeline uses a combination of three different annotation

tools (Diamond, HMMER and Hotpep) to increase accuracy in predicting and annotating CAZymes within bacterial genomes. This analysis revealed a total of 102 putative ORFs with putative CAZY domains (Figure 1B).

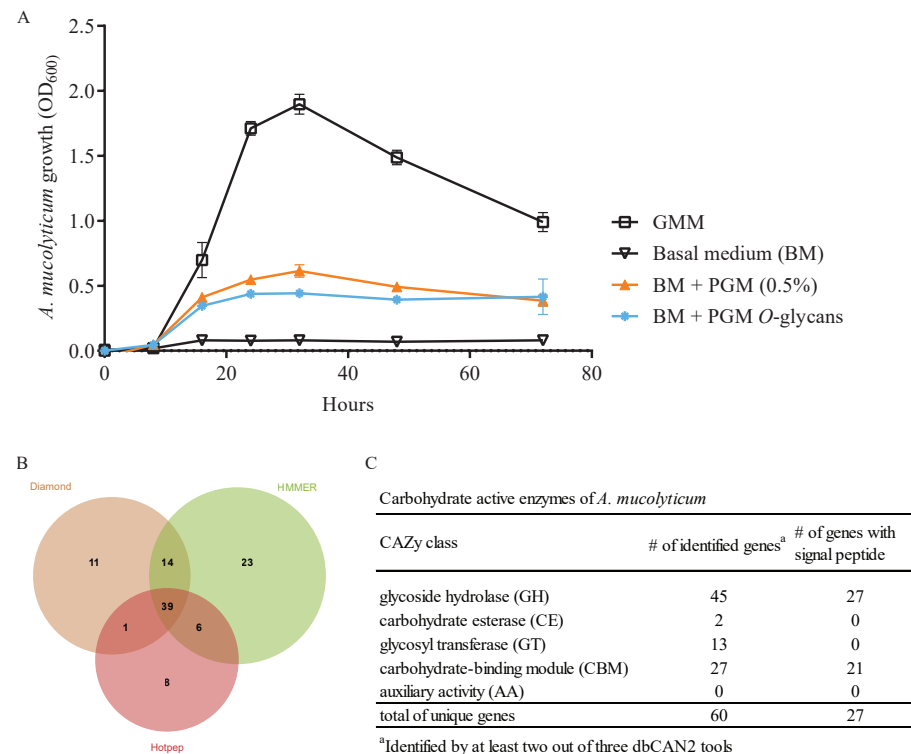


**Figure 1. *A. mucolyticum* growth on mucin and mucin O-glycans and identification of carbohydrate active enzymes (CAZymes) in its genome.** (A) *A. mucolyticum* growth was assessed over a 72 h period by measuring optical density at 600 nm (OD<sub>600</sub>). Bacteria were grown in Gut Microbiota Medium (GMM), basal medium (BM), or basal medium supplemented with porcine gastric mucin (0.5% w/vol) or purified PGM O-glycans (10 mg/mL). Data represent the mean ± SD of three independent experiments. (B) Proportional Venn diagram showing the number of identified CAZyme encoding genes using the Diamond, HMMER and Hotpep tools that are part of the dbCAN2 metaserver analysis. (C) The table shows the CAZymes and the presence of signal peptides, separated by CAZyme class, that were identified by at least two out of three dbCAN2 tools.

To increase accuracy, we discarded hits that were not identified by at least two out of three tools for further analysis. Among the remaining 60 ORFs multiple types of CAZY domains could be detected, such as glycoside hydrolase (GH), carbohydrate esterase (CE), glycosyl transferase (GT) domains and carbohydrate-binding modules (CBM), with some genes encoding a combination of multiple domains (Figure 2C). Many of the ORFs, especially those containing glycoside hydrolase domains, also encode signal peptides, suggesting that the proteins may be transferred to the bacterial surface or secreted into the environment. The wide repertoire of secreted and non-secreted CAZymes suggests that *A. mucolyticum* is highly adapted to living in the glycan rich mucus niche.

Closer inspection of the collection of CAZymes identified in the *A. mucolyticum* genome revealed at least 22 glycoside hydrolases that were predicted to specifically target O-glycans as found on mucins, of which the majority contains a signal peptide (Table 1). Among the 22 glycoside hydrolases are two sialidases (GH33) and three fucosidases (GH29/95), which target the monosaccharides often found at terminal positions of mucin O-glycans, and eight different galactosidases (GH2) and nine hexosaminidases (GH20/GH84/GH89), which are predicted to hydrolyze the underlying glycosidic linkages. The gene structure of the 22 putative enzymes, with the locations of the predicted glycoside hydrolase domains and additional domains (Figure 2), clearly demonstrates the great diversity in domains, domain organization and predicted protein sizes—also between genes predicted to encode the same class of enzymes. Transcription and translation of the entire repertoire of mucin-targeting CAZymes would allow degradation of the wide variety of linkages commonly found within mucin O-glycans.

### ***A. mucolyticum* secretes a large array of mucin glycan-targeting CAZymes**

In order to establish which of the predicted mucin-targeting CAZymes is produced and secreted by *A. mucolyticum* under *in vitro* culturing conditions, both the bacterial whole cell lysate and the conditioned medium from bacteria cultured for 24 h in complete GMM were subjected to proteomic analysis using mass spectrometry. In addition, the conditioned media from bacteria grown for 24 h in basal medium or basal medium supplemented with PGM were analyzed to investigate the effect of glycan availability on the regulation or secretion of CAZymes. Mapping of the detected peptide fragments to the *A. mucolyticum* genome revealed a total of 1005 proteins in the whole cell lysate and the

different conditioned media fractions. Since *A. mucolyticum* has a predicted 2255 genes, these results show that nearly 45% of all genes are translated under the conditions tested.

**Table 1. Putative mucin O-glycan targeting CAZymes of *A. mucolyticum***

Specificity	Gene_ID (putative activity)	CAZy family domains <sup>a</sup>	Signal peptide (aa)	Protein size (aa)
Sialidase	Allo_00594 (exo- $\alpha$ -sialidase)	CBM40,CBM40,GH33,CBM32	Y(1-25)	1762
	Allo_01388 (exo- $\beta$ -N-acetylgalactosaminidase, exo- $\alpha$ -sialidase)	GH123,GH33	Y(1-25)	1765
Fucosidase	Allo_00589 (exo- $\alpha$ -1,2-L-fucosidase)	GH95,CBM51	Y(1-29)	1675
	Allo_01711 (exo- $\alpha$ -1,2-L-fucosidase)	GH95,CBM51	Y(1-29)	1234
	Allo_01759 (exo- $\alpha$ -1,3/1,4-L-fucosidase)	GH29	Y(1-30)	1011
Galactosidase	Allo_00211 (exo- $\beta$ -galactosidase)	GH2,CBM51,CBM67	N	1203
	Allo_00263 (exo- $\beta$ -galactosidase)	GH2,CBM51,CBM51	N	1772
	Allo_00420 (exo- $\beta$ -galactosidase)	CBM32,GH2	Y(1-20)	1626
	Allo_00471 (exo- $\beta$ -galactosidase)	GH2,CBM32,CBM67,CBM71	Y(1-39)	1671
	Allo_00653 (exo- $\beta$ -galactosidase)	GH2,CBM32,CBM67,CBM71	Y(1-35)	1545
	Allo_01151 (exo- $\beta$ -galactosidase)	GH2,CBM57	N	761
	Allo_01556 (exo- $\beta$ -galactosidase)	GH2,GH2	Y(1-28)	2555
	Allo_02061 (exo- $\beta$ -galactosidase)	GH2,GH2	Y(1-31)	1766
	Hexosaminidase	Allo_00011 (exo- $\alpha$ -N-acetylglucosaminidase)	GH89,CBM32	Y(1-33)
Allo_00472 (exo- $\alpha$ -N-acetylglucosaminidase)		GH89	Y(1-33)	1468
Allo_00591 (exo- $\beta$ -N-acetylglucosaminidase)		GH84,CBM32	Y(1-42)	1117
Allo_00701 ( $\beta$ -N-acetylglucosaminidase)		GH20	Y(1-24)	1042
Allo_01227 (exo- $\beta$ -N-acetylglucosaminidase)		GH84,CBM32	Y(1-29)	1422
Allo_01229 (exo- $\beta$ -N-acetylglucosaminidase)		GH84,CBM32	Y(1-29)	1407
Allo_01236 (exo- $\beta$ -N-acetylglucosaminidase)		GH84,CBM32	Y(1-29)	514
Allo_01836 ( $\beta$ -N-acetylglucosaminidase)		CBM32,CBM32,GH20,CBM32	Y(1-35)	1567
Allo_01981 ( $\beta$ -N-acetylglucosaminidase)		GH84,CBM32,CBM32	Y(1-27)	1528

<sup>a</sup>Identified domains are listed from N to C terminus of the peptide chain

Since many CAZymes contain putative signal peptides and are predicted to be secreted, we next analyzed the total *A. mucolyticum* secretome by focusing on proteins enriched in the conditioned media compared to the whole cell lysate. This showed that 86 proteins were significantly enriched (>10 fold) in the conditioned medium of at least one of the three different growth conditions (Figure S2). For most proteins, the highest enrichment was detected in the conditioned medium of bacteria grown in GMM. Basal medium supplemented with PGM largely mimicked the protein secretion profile of complete GMM, suggesting that PGM provides similar regulatory cues or secretion signals. Basal medium did not result in a large number of significantly enriched secreted proteins, which correlated with the poor growth in this medium.

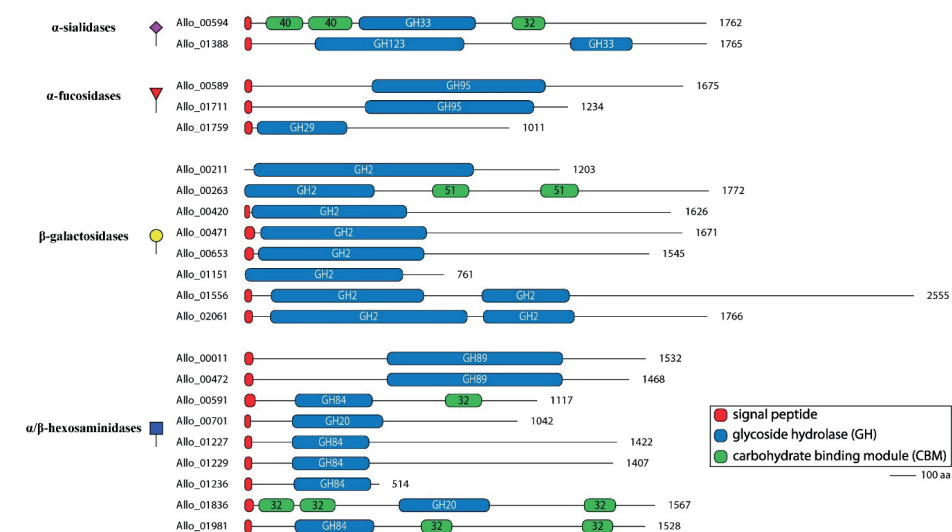


**Figure 2. Domain architecture of putative mucin O-glycan targeting CAZymes in genome of *A. mucolyticum*.** CAZymes are divided in groups based upon their predicted enzyme activity: from top to bottom,  $\alpha$ -sialidases,  $\alpha$ -fucosidases,  $\beta$ -galactosidases and  $\alpha/\beta$ -hexosaminidases. The displayed domains are those identified by HMMER and SignalP 4.0 and are drawn to scale with the size of the polypeptide backbone, in number of amino acids, indicated at the right side of each protein.

A closer inspection of the detected proteins revealed that out of the 60 putative CAZymes identified in the genome, 49 were detected using mass spectrometry of which 26 were significantly enriched in the conditioned medium of at least one of the growth conditions (Figure S3). Eighteen of these were predicted mucin-targeting CAZymes (Figure 3), indicating that over 80% (18 out of



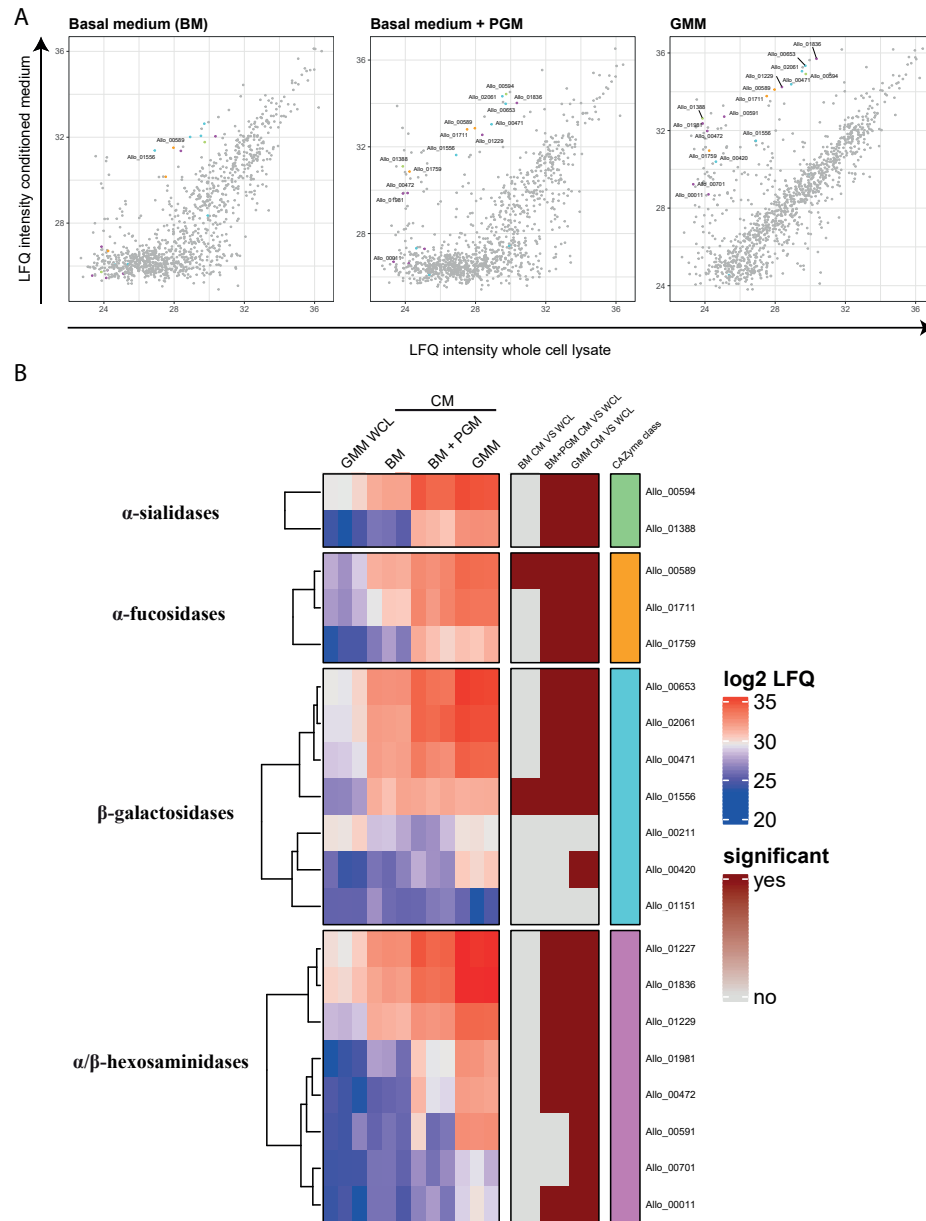


**Figure 3. Mass spectrometry analysis of the *A. mucolyticum* proteome demonstrates the presence of mucin glycan targeting CAZymes.** Legend on next page.

**Figure 3. Mass spectrometry analysis of the *A. mucolyticum* proteome demonstrates the presence of mucin glycan targeting CAZymes.** Conditioned media (CM) from 24 h cultures in basal medium (BM), basal medium + PGM and Gut Microbiota Medium (GMM) and a whole cell lysate (WCL) from the GMM culture were subjected to mass spectrometry analysis, with three biologically independent replicates per condition. (A) The scatter plots show the log<sub>2</sub> LFQ from whole cell lysate of the GMM culture (X-axis) and the secretomes from the three different media (Y-axis). The colored dots indicate the putative *O*-glycan targeting CAZymes with their color matching the color of their putative CAZyme class shown in the heat map. (B) The red/blue heat map displays the proteins and their relative enrichment in the three different secretomes compared to the GMM WCL. Significance (depicted in the brown heatmap) was calculated using a t-test and indicates a >10-fold enrichment in the respective secretome versus GMM WCL with an FDR < 0.05.

22) of the predicted mucin-targeting CAZymes were produced and secreted into the culture media. Strikingly, the 18 mucin-targeting CAZymes were among the most abundant proteins detected. This analysis demonstrates that *A. mucolyticum* produces and secretes a large array of putative mucin *O*-glycan targeting glycoside hydrolases which together are predicted to efficiently deglycosylate mucin proteins.

### Functional activity of the secreted CAZymes

Mucin *O*-glycans, such as the typical core 2 mucin *O*-glycan depicted in Figure 4F, are made up of multiple covalently linked monosaccharides. To degrade such glycans the linkages between the different monosaccharides need to be hydrolyzed by CAZymes with the correct linkage specificity. To verify whether the CAZymes secreted by *A. mucolyticum* are enzymatically active and able to hydrolyze linkages found in mucin *O*-glycans, conditioned medium or heat-inactivated conditioned medium (30 minutes at 98°C) from a 48 h culture was incubated with five different monovalent fluorescent or chromogenic substrates to detect the presence of sialidase, fucosidase, galactosidase, N-acetyl-glucosaminidase and N-acetyl-galactosaminidase activities. This resulted in clear signals for the presence of  $\alpha$ -sialidase,  $\beta$ -galactosidase,  $\beta$ -GlcNAcase and  $\alpha$ -GalNAcase activities in *A. mucolyticum* conditioned medium (Figure 4A-E). Although multiple fucosidases were detected in the secretome during the proteomics analysis, no fucosidase activity could be detected—even after concentrating the culture media 100 times. An alternative approach using chemoselective labelling of the fucosidases with an activity-based probe, which can detect fucosidase activity in enzymes with both GH29 and GH95 glycosyl hydrolase domains, also did not detect fucosidase activity.

Despite the lack of fucosidase activity, the combination of identified enzymatic activities would likely be able to effectively target and degrade *O*-linked glycans, such as found on mucins.

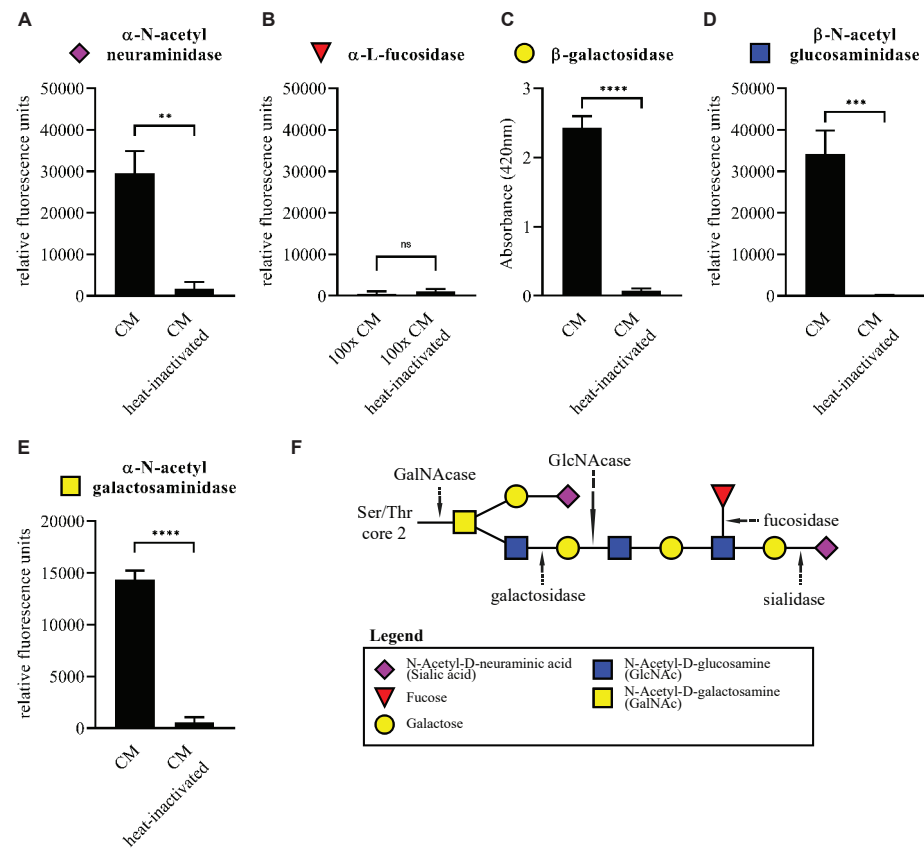


**Figure 4. Enzymatic activity of mucin-glycan-targeting CAZymes in conditioned medium of *A. mucolyticum*.** Filter-sterilized conditioned medium (CM) from a 48 h culture of *A. mucolyticum* grown in Gut Microbiota Medium was incubated for two hours at 37°C with fluorescent 4-methylumbelliferone linked (A)  $\alpha$ -N-acetylneuraminic acid (sialic acid), (B)  $\alpha$ -fucose, (D)  $\beta$ -GlcNAc and (E)  $\alpha$ -GalNAc or the chromogenic substrate (C) 2-Nitrophenyl  $\beta$ -D-galactopyranoside (ONPG) for the detection of enzymatic activities. A 100x concentrated conditioned medium was used with the  $\alpha$ -fucose substrate. (F) Schematic composition of a typical core 2 mucin *O*-glycan and the target site for each enzyme class. Data represent the mean  $\pm$  SD of three independent experiments. Statistical significance was determined by an unpaired *t* test using GraphPad Prism software. \*\*,  $P < 0.01$ ; \*\*\*,  $P < 0.001$ ; \*\*\*\*,  $P < 0.0001$ ; ns, not significant.

### Mucin degradation and utilization by *A. mucolyticum*

To assess whether secreted CAZymes in the *A. mucolyticum* conditioned medium are sufficient to degrade mucins, porcine gastric mucin (10 mg/mL) and human intestinal mucin (10 mg/mL) were treated with either control GMM, *A. mucolyticum* conditioned medium or heat-inactivated conditioned medium (30 min, 98°C). Following incubation (18 h), the mucins were separated using SDS-PAGE and then either stained in-gel with a Periodic acid-Schiff stain (PAS) or electroblotted onto a nitrocellulose membrane and detected with a SNA lectin or an antibody against human MUC2. The PAS-based detection, which detects polysaccharides, clearly demonstrated that both the porcine gastric mucin (Figure 5A) and human intestinal mucin (Figure 5B) were almost entirely degraded by the *A. mucolyticum* conditioned medium. Heat-inactivation completely abolished the mucin degradation activity. When detecting sialic acids at terminal positions in the glycan chain by probing with the lectin SNA, a clear reduction in signal was observed upon treatment with conditioned medium (Figure 5A-B). Interestingly, human intestinal mucin, which according to the PAS stain barely entered the gel, appeared as a MUC2-positive smear after treatment with the active conditioned medium. The smear pattern indicates degradation of MUC2 and an enhanced ability to be separated by SDS-PAGE.

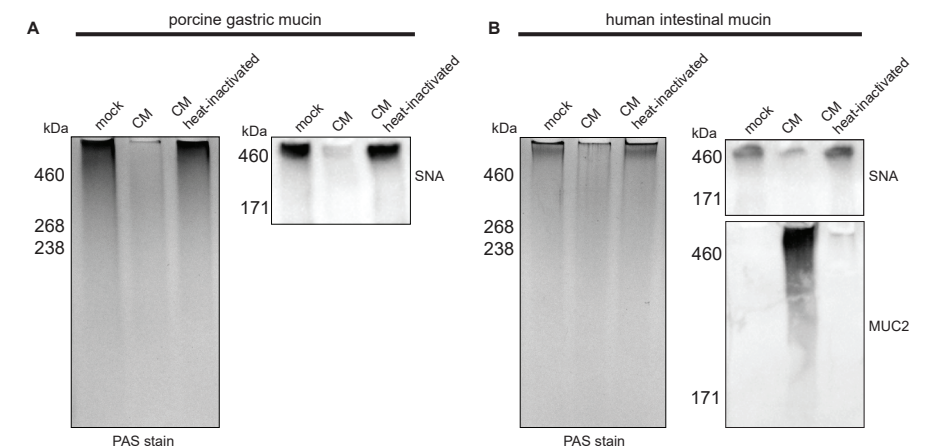


**Figure 5. Enzymatic activity within conditioned medium degrades porcine and human mucins.** (A) Porcine gastric mucin or (B) human intestinal mucin (both 10 mg/mL) were mixed 1:1 with GMM (mock) or active or heat-inactivated *A. mucolyticum* conditioned medium (CM) from a 48 h culture grown in GMM, and incubated overnight at 37°C. After separation using SDS-PAGE, mucins were either detected in-gel using a Periodic acid-Schiff (PAS) stain or electroblotted and detected using SNA lectin, and in the case of human intestinal mucin also with an anti-MUC2 antibody. Molecular masses are indicated in kilodaltons (kDa).

To assess whether mucin *O*-glycans products could be used as a substrate for bacterial growth, *A. mucolyticum* was cultured in a basal medium supplemented with 20 mM of the individual monosaccharides that are typically found within *O*-glycan chains: sialic acid, fucose, galactose, GlcNAc and GalNAc (Figure 6). The addition of sialic acid or fucose to basal medium did not support growth. In contrast, galactose, GlcNAc and GalNAc did support growth equal to growth levels observed in complete GMM. As sialic acid and fucose normally cap the *O*-glycans and protect the glycan chain from hydrolysis, this finding supports a model in which *A. mucolyticum* produces sialidases and fucosidases in order to gain access to and liberate underlying galactose, GlcNAc and GalNAc. Overall, these data demonstrate that *A. mucolyticum* can effectively degrade mucin *O*-glycans by secreting a wide repertoire of mucin-degrading enzymes after which it can use the liberated galactose, GlcNAc and GalNAc as substrates for growth.

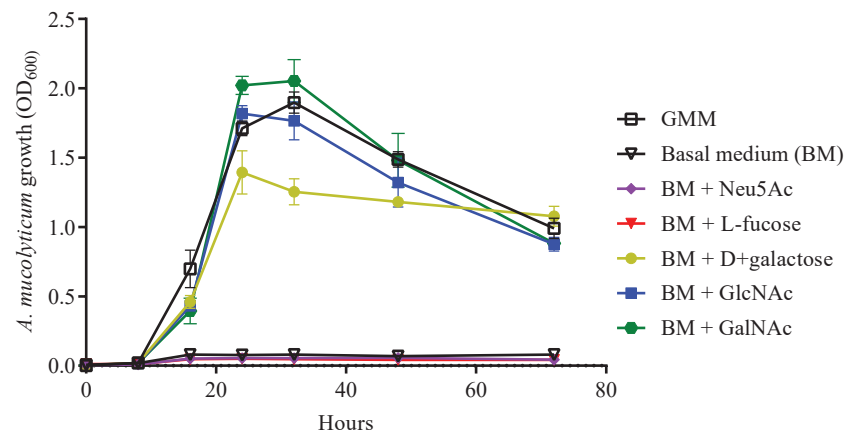


**Figure 6. *A. mucolyticum* uses mucin glycan monosaccharides as a substrate for growth.**

*A. mucolyticum* growth was assessed over a 72 h period by measuring optical density at 600 nm (OD<sub>600</sub>). Bacteria were grown in Gut Microbiota Medium (GMM), basal medium (BM) or basal medium supplemented with individually added monosaccharides (20 mM). Graphs depict the mean values  $\pm$  SD acquired from three independent experiments.

## DISCUSSION

While the intestinal mucus layer is designed as a barrier against bacterial invasion, some bacteria have adapted to living in the mucosal niche by feeding on mucin glycans. Through close proximity to intestinal epithelial cells these bacteria can have a dominant effect on host physiology and intestinal immune responses. Here we provide evidence that the recently classified bacterium *Allobaculum mucolyticum* produces a large repertoire of mucin *O*-glycan targeting enzymes that allow it to degrade mucins and forage on host-derived mucin *O*-glycans.

A search of CAZymes encoded in the *A. mucolyticum* genome revealed an array of 60 putative CAZymes of which many can target mucin *O*-glycans. With multiple glycoside hydrolases predicted to target similar glycosidic linkages, there appears to be a considerable redundancy in the *A. mucolyticum* CAZyme repertoire. For example, there are eight putative  $\beta$ -galactosidases and eight different hexosaminidases. Closer inspection of the proteins revealed that both the domain architecture and organization (Figure 2) and levels of protein production (Figure 3) are markedly different between different CAZymes that are predicted to target the same linkage. This redundancy may be explained by placing it in the perspective of the incredible diversity of glycans and glycan-linkages present in intestinal mucosal niche. Mucin glycans can be branched and contain various structures and modifications, which can greatly affect enzyme-substrate interactions. Having a diverse repertoire of CAZymes therefore allows *A. mucolyticum* to utilize a wide range of glycan substrates.

Large repertoires of CAZymes are also found in the genomes of other well-known mucolytic bacteria such as *Akkermansia muciniphila*, *Ruminococcus gnavus*, *Ruminococcus torques* and several *Bifidobacteria* and *Bacteroides* species, such as *Bacteroides thetaiotamicron*<sup>6</sup>. Glycan generalists such as *B. fragilis* and *B. thetaiotamicron* contain a very extensive repertoire of CAZymes, which allows utilization of a wide variety of substrates from both dietary- and host-derived sources. The total repertoire of CAZymes encoded within the *A. mucolyticum* genome is not as extensive as that of certain *Bacteroides* species, but *A. mucolyticum* seems to be highly specialized to target mucin *O*-glycans, with more than nearly half of its glycoside hydrolases directed to such glycans. This is comparable to the CAZyme repertoire detected in the mucin specialist *A. muciniphila* (Table S1). Even though the *A. mucolyticum* CAZyme repertoire is largely directed towards mucin glycans, *A. mucolyticum* can also use dietary-derived polysaccharide inulin as a substrate

for growth (Figure S1). This gives the bacterium the ability to switch between dietary- and host-derived glycans and adapt to fluctuations in nutrient availability as encountered in the dynamic environment of the gastrointestinal tract.

The plasticity of the CAZyme expression in response to changes in the nutritional environment is also evident from our proteomics analysis. This reveals that *A. mucolyticum* produces a limited set of CAZymes in basal medium, that contains no source of glycans. Under this condition, which allows for minimal growth, four CAZymes were found to be significantly enriched in the conditioned medium as compared to the whole cell lysate. The four enzymes (Allo\_589, 898, 1556 & 2010) are a putative  $\alpha$ -fucosidase, a carbohydrate esterase, a  $\beta$ -galactosidase and a N-acetyl- $\beta$ -galactosaminidase, respectively. Although the protein function and exact specificity of CAZymes are difficult to predict based on their amino acid sequence alone, the putative annotation suggests that under nutrient limited conditions *A. mucolyticum* is able to hydrolyze several host-associated glycans. For example, fucose is known to be abundant on mucin glycans, but also on glycans such as the Lewis antigens, which are known to play a role in regulating inflammation<sup>21</sup>. The N-acetyl- $\beta$ -galactosaminidase (GH123) could be involved in the degradation of glycosphingolipids on the membranes of the intestinal epithelial cells<sup>22</sup>.

When basal medium was supplemented with either mucin or the GMM carbohydrates glucose, fructose and the  $\alpha$ - and  $\beta$ -glucans maltose and cellobiose, production and secretion of CAZymes—in particular *O*-glycan targeting CAZymes—by *A. mucolyticum* was markedly increased. These results indicate that *A. mucolyticum* requires the presence of environmental glycans as stimuli to induce expression and secretion of the repertoire of glycosidases. Such regulatory mechanisms are also known from other bacteria that forage on mucin glycans<sup>4</sup>. While we have not yet determined in detail the individual components responsible for the induction of the CAZymes, the fact that both mucin and the combination of glucose, fructose, maltose and cellobiose are sufficient for glycosidase expression suggests that a similar glycosidase program is initiated by glycans of both host and dietary origin.

The annotation and detection of secreted *O*-glycan targeting CAZymes did not in all cases translate to the detection of the predicted enzymatic activity. For example, while three putative fucosidases were identified within the conditioned medium of *A. mucolyticum* by mass spectrometry, no detectable

fucosidase activity was observed in the conditioned medium using the monovalent 4-MU-fucose fluorescent substrate even though the validity of the assay was confirmed with a commercial fucosidase. Nor could fucosidase activity be detected using a novel activity-based probe. Although it is possible that all three fucosidases were annotated incorrectly by the dbCAN2 pipeline, the lack of detectable fucosidase activity is perhaps more likely caused by an incompatibility between the substrate specificity of the *A. mucolyticum* fucosidases and the monovalent substrates used in this study, as monovalent substrates are structurally different from the complex plant and host-derived glycans found in the intestine.

In contrast to the lack of detectable levels of fucosidase activity, we were able to detect N-acetyl- $\alpha$ -galactosaminidase activity, which was not expected on basis of the CAZyme annotation (Table 1). This might indicate that *A. mucolyticum* is capable of hydrolyzing the  $\alpha$ -linked GalNAc moiety that makes up the core of *O*-glycans, thereby enabling the complete degradation of mucin glycans. This hypothesis is supported by the finding that *A. mucolyticum* can effectively utilize GalNAc for growth (Figure 6). The enzyme(s) responsible for the N-acetyl- $\alpha$ -galactosaminidase activity remain to be identified.

Crost *et al.*<sup>23</sup> have previously demonstrated that the ability of *R. gnavus* to grow on PGM as a sole carbon source is strain-dependent, and was due to the presence of sialidases and fucosidases. These results highlight the necessity for both types of glycosidases to remove the terminal sialic acid and fucose residues in order to allow degradation and subsequent utilization of the underlying glycans. *A. mucolyticum* produces multiple sialidases and fucosidases that are suspected to be essential to access mucin glycans for growth. Media supplemented with sialic acid or fucose, however, were not able to support growth (Figure 6), which is in agreement with the absence of core genes in the *A. mucolyticum* genome normally found in canonical gene clusters for sialic acid or fucose catabolism. Interestingly, a curated blast search of the genome does show the presence of several genes predicted to be involved in the uptake of sialic acid, like genes encoding for sialic acid TRAP transporter SiaQ and sialic acid-binding protein SiaP (Allo\_00009 and Allo\_00087, respectively)<sup>24</sup>. Furthermore, there are several putative polysialyltransferases (e.g., Allo\_01518 and Allo\_02009) with homology to proteins from *Neisseria meningitidis* known to play a role the sialylation of lipooligosaccharide (LOS). Sialylation of the bacterial LOS or capsule glycans is known to contribute to host colonization and bacterial immune evasion<sup>25,26</sup>. When *A. mucolyticum* does not directly use host glycan-liberated sialic acid or fucose, they could

still have a major impact on the ecology of the mucosal niche and host health as free sialic acid and fucose has been shown to boost the expansion of enteric pathogens like *Salmonella typhimurium*, *Clostridium difficile*, *Campylobacter jejuni* and *Escherichia coli* under certain conditions<sup>27-30</sup>. In addition, removal of sialic acid from mucin glycans was shown to affect rotavirus adhesion and infection<sup>31,32</sup>. Whether *A. mucolyticum* decorates its surface glycans with endogenous sialic acid or fucose, or affects the microbiota composition indirectly by releasing them into the environment remains to be investigated.

Increased bacterial penetration and degradation of the intestinal mucus layer are major features of IBD. Understanding the mechanisms that drive these processes may thus be key to treating or preventing disease. It has been reported that a diet deprived of dietary fiber enhances the expression of mucin targeting CAZymes of the gut microbiota and promotes the expansion of mucin-degrading bacteria such as *A. muciniphila* and *Bacteroides caccae*<sup>33</sup>. As mucin also seems to be an important nutrient source for *A. mucolyticum*, it may be that a similar expansion might be observed for this bacterium. Bacterial mucus degradation may cause erosion of the mucus layer and an increased susceptibility to lethal colitis by the enteric pathogen *Citrobacter rodentium*, as was shown in mice<sup>33</sup>. This finding highlights the delicate balance between the microbiota, an intact mucus layer and invading pathogens.

Mucus layer degradation, as observed in IBD patients, is linked to an increased prevalence of mucosa-associated mucolytic bacteria like *R. gnavus* and *R. torques*<sup>34</sup>. Since *A. mucolyticum* was isolated from a patient with ulcerative colitis and, as described here, is able to effectively forage on mucins, it is likely that it operates in the same niche as other mucolytic bacteria. It would therefore be of great interest to investigate the interactions with other known mucus-degrading bacteria and to investigate to what extent the mucolytic capacities of *A. mucolyticum* can contribute to the pathogenesis of IBD.

## MATERIALS AND METHODS

### General

All commercial chemicals were purchased from Sigma-Aldrich unless stated otherwise. Data visualization was performed using Adobe Illustrator 2021, GraphPad Prism 7, and R.

### Carbohydrate-active enzyme (CAZyme) annotation

CAZymes within the Prokka-annotated genome of *A. mucolyticum* (Genbank accession number: JAHUZH010000000) and *A. muciniphila* ATCC BAA-835 (NCBI Reference Sequence: NC\_010655.1) were annotated using the dbCAN2 metasever <http://bcb.unl.edu/dbCAN2/> in February 2021<sup>20,35</sup>. CAZymes identified by at least two out of three tools were considered for further analysis and are displayed in Figure 1. The putative mucin-targeting glycoside hydrolases, as displayed in Table 1, Figure 2, and supplementary Table 1, were selected based on the mucin targeting CAZyme classes reported by Tailford *et al.*<sup>6</sup>

### Mucin and mucin O-glycan purification

Porcine gastric mucin (PGM type III, Sigma-Aldrich) was purified by ethanol precipitation as described previously by Ottman *et al.*<sup>36</sup>, with minor modifications. Briefly, 10 g of mucin was dissolved in 500 ml 2X PBS with pH 7.8 (NaCl: 274 mM, KCl: 5.4 mM, Na<sub>2</sub>HPO<sub>4</sub>: 20 mM, KH<sub>2</sub>PO<sub>4</sub>: 3.6 mM) and 100 µL of toluene for 24 h at 4°C, under continuous stirring. After the first hour, the pH was adjusted to 7.2 with 2 M NaOH. After 24 h, the solution was centrifuged at 10,000 x *g* for 20 min at 4°C, after which the supernatant containing the dissolved mucin was collected, cooled to 0°C and ice-cold (0°C) ethanol was added to a final concentration of 60% (vol/vol). The resulting precipitate was dissolved in 0.1 M NaCl and precipitated again with ice-cold ethanol to 60% (vol/vol). The precipitate was then washed with 100% ice-cold ethanol and dissolved in distilled water (~180 mL). Thereafter, the mucin solution was dialyzed against 5 L of distilled water for 24 h at 4°C, lyophilized, resuspended in Milli-Q ultrapure water, and sterilized by autoclaving (15 min at 121°C).

Porcine gastric mucin O-glycans were purified according to a protocol by Desai *et al.*<sup>33</sup> In short, PGM (Type III, Sigma-Aldrich) was suspended at 2.5% w/v in 100 mM Tris (pH 7.4) and autoclaved immediately (15 min at 121°C). Proteinase K (Sigma) was added to a final concentration of 100 µg/mL and incubated for 16 h at 55°C with slow shaking. The proteolyzed solution was centrifuged at 21,000 x *g* for 30 min at 4°C to remove insoluble material. Next, NaOH and NaBH<sub>4</sub> were added to final concentration of 0.1 M and 1 M, respectively. This solution was incubated for 18 h at 65°C to promote selective release of mucin O-glycans from mucin glycopeptides by alkaline β-elimination. The solution was neutralized to pH 7.0 with 2 M HCl, centrifuged at 21,000 x *g* for 30 min at 4°C, and filtered with a 0.2 µm filter to remove remaining insoluble material. After extensive dialysis (4 x 4 h with a 100X

volume of Milli-Q Ultrapure water, 1 kDa MWCO dialysis tube), the dialyzed mucin *O*-glycan solution was lyophilized and resuspended in Milli-Q Ultrapure water at desired concentrations.

Human small intestinal mucins were harvested from the urine (~100 mL per batch) of a patient with an orthotopic neobladder reconstruction. Crude mucin was collected by centrifugation (30,000 x g, 4°C, 30 min) and pellets were washed twice with PBS. Washed mucin was purified further using ethanol precipitation, as described for PGM, and redissolved in 5 mL Milli-Q Ultrapure water. Instead of lyophilization, the mucin was directly transferred to a 100 kDa MWCO Amicon Ultra filter (Thermo Fisher Scientific), washed twice with 5 mL Milli-Q and concentrated. Protein concentration was determined using a NanoDrop One UV-Vis Spectrophotometer (Thermo Fisher Scientific) and set to 10 mg/mL in Milli-Q Ultrapure water.

### Bacterial culture conditions

*A. mucolyticum* was routinely cultured at 37°C under anaerobic conditions in a vinyl anaerobic chamber (Coy Labs) with the following gas mix: 85% N<sub>2</sub>, 10% CO<sub>2</sub> and 5% H<sub>2</sub>. Gut Microbiota Medium (GMM) (Table S2) was the default growth medium and is essentially an enriched Gut Microbiota Medium, devoid of isovaleric acid, as described by Goodman *et al.*<sup>37</sup>

### Bacterial growth curves

Gut Microbiota Medium and basal medium were prepared according to recipe in described in Table S2. All media supplements were prepared in Milli-Q Ultrapure water and, if required, solutions were brought to neutral pH using 1 M NaOH. Supplemented media were prepared with supplements at following final concentrations: D+glucose (2 mg/ml, Sigma), D-fructose (1 mg/mL, Sigma), D+maltose (1 mg/ml, Sigma), D+cellobiose (1 mg/ml, Sigma), N-Acetylneuraminic acid (20 mM, Carbosynth), L-Fucose (20 mM, Sigma), D+Galactose (20 mM, Mikrobiologie), N-acetyl-D-glucosamine (20 mM, Sigma), N-acetyl-D-galactosamine (20 mM, Carbosynth), inulin (10 mg/mL, Sigma), purified porcine gastric mucin (PGM, 0,5% w/vol) or purified PGM *O*-glycans (10 mg/mL). All solutions, except PGM solution, were filter-sterilized and prerduced in the anaerobic chamber prior to use.

*A. mucolyticum* was grown on GMM agar plates for 72 h at 37°C under anaerobic conditions. Static liquid starter cultures were inoculated with three separate bacterial colonies each and grown for 16 h at 37°C under anaerobic conditions. Bacterial growth was assessed by measuring absorbance (600 nm). Bacteria

were collected by centrifugation (3,000 x g, 5 min), gently washed twice and resuspended in 2X basal medium. Washed bacteria were diluted to the desired OD and combined with an equal volume of MilliQ Ultrapure water or medium supplements to a total volume of 200 µL per well with a final starting OD of 0.01. For each time point (0, 8, 16, 24, 32, 48 and 72 h) a 96-Well Multiwell Plate (Corning Costar) was used with duplicate wells per condition. At each time point one plate was removed from the anaerobic chamber and final absorbance values (600 nm) were recorded using a FLUOstar Omega plate reader (BMG Labtech). Values were corrected for background levels in respective negative controls. Experiments were performed in triplicates, using three biologically independent *A. mucolyticum* starter cultures.

### Bacterial conditioned media and whole cell lysate preparation

Bacterial conditioned media and whole cell lysates for mass spectrometric analysis were harvested from static liquid *A. mucolyticum* cultures that were grown in Gut Microbiota Medium, basal medium or basal medium supplemented with 0.5% PGM for 24 h at 37°C under anaerobic conditions. For each condition, 4 mL cultures were inoculated from three independent starter cultures and grown as described above. After 24 h, bacteria were harvested by centrifugation at 15,000 x g for 2 min, washed twice with 2 mL of PBS and resuspended in 4 mL of ice-cold lysis buffer (PBS containing cOmplete EDTA-free protease inhibitor cocktail (Roche)). The conditioned media were collected and filter-sterilized using 0.2 µm filter. Bacteria were lysed by sonication (3 x 10 sec on ice). Large bacterial fragments were removed by centrifugation at 15,000 x g for 1 min, after which cleared lysate was collected. To remove possible media components all bacterial cell lysates and conditioned media were transferred to a 5 kDa MWCO filter (Pierce concentrator, PES, 5K MWCO, 6 mL, Thermo Fisher Scientific), washed with 5 mL of Milli-Q and concentrated to 1 mL.

The conditioned media used for glycosidase enzymatic activity assays were collected from three independent static liquid *A. mucolyticum* cultures grown in Gut Microbiota Medium for 48 h at 37°C under anaerobic conditions. The conditioned media were filter-sterilized using 0.2 µm filter and stored at -20°C prior to use. The 100X concentrated conditioned media used for fucosidase assays were obtained using a 10 kDa MWCO Amicon Ultra filter (Thermo Fisher Scientific).

### Mass spectrometry sample preparation

Whole cell lysates and conditioned media were processed using Filter Aided Sample Preparation (FASP), as described by Wiśniewski *et al.*<sup>38</sup> In brief, samples were denatured at 95°C in the presence of DTT, mixed with 8 M urea and loaded onto Centrifugal Filters (Microcon, cat. no MRCF0R030). This was followed by two washes with 8 M urea, treatment with 0.05 M iodoacetamide in 8 M urea, and three 8 M urea washes. After washing out the urea with three washes with 0.05 M ammonium bicarbonate, samples were digested overnight with trypsin at 37°C. The next day, samples were acidified and desalted using Stagetips<sup>39</sup>. Half of each of the digested samples was injected into an LTQ-Orbitrap QExactive mass spectrometer (Thermo Fisher Scientific) and measured using a 120-minute gradient.

### Mass spectrometry analyses

Thermo Raw files were analysed using MaxQuant versions 1.5.1.0 using default parameters, with the inclusion of the match between runs and IBAQ features<sup>40,41</sup>. Initial analyses were performed in Perseus.<sup>42</sup> Proteins flagged as contaminants, reverse or only identified by site were filtered out. Triplicates were grouped and only proteins reproducibly quantified in at least one of the sets of triplicates were retained. Missing values were imputed using default parameters. Differential proteins were determined using a t-test with adjustment for multiple testing (FDR < 0.05). To call proteins enriched in the secreted fractions, they additionally required at least a 10-fold higher LFQ value compared to the whole cell lysates. Data visualization and downstream processing was performed in R.

### Glycosidase activity assays

*A. mucolyticum* conditioned media used for enzymatic assays were collected as described above. The following substrates were used: 4-MU-Neu5Ac (Cayman), 4-MU-Fucose (Carbosynth), 4-MU-GlcNAc (Carbosynth), 4-MU-GalNAc (Carbosynth), and ortho-Nitrophenyl- $\beta$ -galactoside (ONPG, Sigma). Stocks of the 4-MU linked substrates were diluted to 200  $\mu$ M in Milli-Q Ultrapure water and ONPG was diluted to 1 mg/mL in Milli-Q Ultrapure water, after which 50  $\mu$ L of diluted substrates were added to a 96-Well Multiwell flat-bottom Plate (Corning Costar). Next, 50  $\mu$ L of either Gut Microbiota Medium (negative control), conditioned medium or heat-inactivated conditioned medium (98°C for 30 min) were added in duplicates. Plates were incubated for 2 h at 37°C shielded from light and transferred to a FLUOstar Omega plate reader (BMG labtech). For the 4-MU linked substrates, signal was detected using a 340 ex. / 460 em. filter set. For the ONPG substrate, absorbance was

measured at a wavelength of 420 nm. Chemoselective labelling of fucosidases using an activity-based probe was performed as described by Luijckx and Henselijn *et al.*<sup>43</sup>

### Detection of mucin degradation by Periodic acid-Schiff (PAS) stain and western blotting

PGM or human mucin (10 mg/mL in Milli-Q Ultrapure water) were combined at a 1:1 ratio with medium controls or the same *A. mucolyticum* conditioned medium that was used for the glycosidase activity assays. This mixture was incubated for 16 h at 37°C after which samples were mixed with one volume of 3x Laemmli sample buffer and boiled for 5 min. Subsequently 25  $\mu$ L per sample was loaded onto a gel and separated using SDS-PAGE. For SDS-PAGE separation and immunoblotting of large mucin proteins, a Boric acid-Tris gel system was used, as previously described by Li *et al.*<sup>44</sup>, with minor modifications. A 5% acrylamide gel (5% Acryl/Bis acryl solution, Bio-Rad 161-0144; 26% 1.5 M Tris pH 8.8; 0.1% SDS; 0.1% ammonium persulfate; 0.1% TEMED) was prepared in a Mini Protean II chamber (Bio-Rad) using 1.5 mm spacer plates. Gels were run in Boric acid-Tris buffer (192 mM Boric acid; 1 mM EDTA; 0.1% SDS, set to pH 7.6 with Tris) at 25 mA per gel for 3 h. To detect glycoproteins, gels were stained using a Periodic acid-Schiff stain (Pierce glycoprotein staining kit, Thermo Fisher Scientific). For detection of MUC2 and sialic acids, mucins were separated as described above and transferred onto nitrocellulose membranes using a wet transfer system with transfer buffer (25 mM Tris; 192 mM glycine; 20% methanol,) for 3 h at 90 V at 4°C. Subsequently, membranes were blocked with 5% bovine serum albumin (BSA, Sigma-Aldrich) in TSMT buffer (20 mM Tris, 150 mM NaCl, 1 mM CaCl<sub>2</sub>, 2 mM MgCl<sub>2</sub>, 0.1% Tween 20, adjusted to pH 7 with HCl) overnight at 4°C and then incubated with an anti-human MUC2 rabbit serum (a gift from Dr. Karin Strijbis) at a 1:200 dilution in TSMT containing 1% BSA, or with biotinylated SNA lectin (2 mg/mL stock, Vector Labs) at a dilution of 1:1000 in TSMT containing 1% BSA. After incubation for 1 h at room temperature, blots were washed 4 times with an excess of TSMT and incubated with  $\alpha$ -rabbit IgG (A4914, 1:10,000 dilution, Sigma-Aldrich) in TSMT containing 1% BSA for the detection of MUC2, or Streptavidin-HRP0 (1mg/mL stock, 1:10,000 dilution, Jackson ImmunoResearch) in TSMT containing 1% BSA for the detection of sialic acids. Blots were developed with the Clarity Western ECL kit (Bio-Rad) and imaged in a Gel-Doc system (Bio-Rad).

## REFERENCES

1. Honda K, Littman DR. The microbiota in adaptive immune homeostasis and disease. *Nature*. 2016;535(7610):75–84. doi:10.1038/nature18848
2. Derrien M, Vaughan EE, Plugge CM, de Vos WM. *Akkermansia muciniphila* gen. nov., sp. nov., a human intestinal mucin-degrading bacterium. *International Journal of Systematic and Evolutionary Microbiology*. 2004;54(5):1469–1476. doi:10.1099/ijs.0.02873-0
3. van Passel MWJ, Kant R, Zoetendal EG, Plugge CM, Derrien M, Malfatti SA, Chain PSG, Woyke T, Palva A, de Vos WM, et al. The Genome of *Akkermansia muciniphila*, a Dedicated Intestinal Mucin Degrader, and Its Use in Exploring Intestinal Metagenomes. *PLoS ONE*. 2011;6(3):e16876. doi:10.1371/journal.pone.0016876
4. Sonnenburg JL, Xu J, Leip DD, Chen C-H, Westover BP, Weatherford J, Buhler JD, Gordon JI. Glycan Foraging in Vivo by an Intestine-Adapted Bacterial Symbiont. *Science*. 2005;307(5717):1955–1959. doi:10.1126/science.1109051
5. Martens EC, Chiang HC, Gordon JI. Mucosal Glycan Foraging Enhances Fitness and Transmission of a Saccharolytic Human Gut Bacterial Symbiont. *Cell Host & Microbe*. 2008;4(5):447–457. doi:10.1016/j.chom.2008.09.007
6. Tailford LE, Crost EH, Kavanaugh D, Juge N. Mucin glycan foraging in the human gut microbiome. *Frontiers in Genetics*. 2015;6(FEB). doi:10.3389/fgene.2015.00081
7. Johansson ME V, Gustafsson JK, Holmén-Larsson J, Jabbar KS, Xia L, Xu H, Ghishan FK, Carvalho FA, Gewirtz AT, Sjövall H, et al. Bacteria penetrate the normally impenetrable inner colon mucus layer in both murine colitis models and patients with ulcerative colitis. *Gut*. 2014;63(2):281–291. doi:10.1136/gutjnl-2012-303207
8. Palm NW, de Zoete MR, Cullen TW, Barry NA, Stefanowski J, Hao L, Degnan PH, Hu J, Peter I, Zhang W, et al. Immunoglobulin A Coating Identifies Colitogenic Bacteria in Inflammatory Bowel Disease. *Cell*. 2014;158(5):1000–1010. doi:10.1016/j.cell.2014.08.006
9. Greetham HL, Gibson GR, Giffard C, Hippe H, Merkhoffer B, Steiner U, Falsen E, Collins MD. *Allobaculum stercoricanis* gen. nov., sp. nov., isolated from canine feces. *Anaerobe*. 2004;10(5):301–307. doi:10.1016/j.anaerobe.2004.06.004
10. Bárcena C, Valdés-Mas R, Mayoral P, Garabaya C, Durand S, Rodríguez F, Fernández-García MT, Salazar N, Nogacka AM, Garatachea N, et al. Healthspan and lifespan extension by fecal microbiota transplantation into progeroid mice. *Nature Medicine*. 2019;25(8):1234–1242. doi:10.1038/s41591-019-0504-5
11. Thevaranjan N, Puchta A, Schulz C, Naidoo A, Szamosi JC, Verschoor CP, Loukov D, Schenck LP, Jury J, Foley KP, et al. Age-Associated Microbial Dysbiosis Promotes Intestinal Permeability, Systemic Inflammation, and Macrophage Dysfunction. *Cell Host and Microbe*. 2017;21(4):455–466.e4. doi:10.1016/j.chom.2017.03.002
12. Ravussin Y, Koren O, Spor A, LeDuc C, Gutman R, Stombaugh J, Knight R, Ley RE, Leibel RL. Responses of Gut Microbiota to Diet Composition and Weight Loss in Lean and Obese Mice. *Obesity*. 2012;20(4):738–747. doi:10.1038/oby.2011.111
13. Herrmann E, Young W, Rosendale D, Reichert-Grimm V, Riedel CU, Conrad R, Egert M. RNA-Based Stable Isotope Probing Suggests *Allobaculum* spp. as Particularly Active Glucose Assimilators in a Complex Murine Microbiota Cultured in Vitro. *BioMed Research International*. 2017;2017. doi:10.1155/2017/1829685
14. Pujo J, Petitfils C, Le Faouder P, Eeckhaut V, Payros G, Maurel S, Perez-Berezo T, Van Hul M, Barreau F, Blanpied C, et al. Bacteria-derived long chain fatty acid exhibits anti-inflammatory properties in colitis. *Gut*. 2020;1917:gutjnl-2020-321173. doi:10.1136/gutjnl-2020-321173
15. Liu S, Qin P, Wang J. High-fat diet alters the intestinal microbiota in streptozotocin-induced type 2 diabetic mice. *Microorganisms*. 2019;7(6):176. doi:10.3390/microorganisms7060176
16. Cox LM, Yamanishi S, Sohn J, Alekseyenko A V, Leung JM, Cho I, Rogers AB, Kim SG, Li H, Gao Z, et al. Altering the Intestinal Microbiota during a Critical Developmental Window Has Lasting Metabolic Consequences. *Cell*. 2014;158(4):705–721. doi:10.1016/j.cell.2014.05.052
17. Kaakoush NO. Insights into the Role of *Erysipelotrichaceae* in the Human Host. *Frontiers in Cellular and Infection Microbiology*. 2015;5(November):1–4. doi:10.3389/fcimb.2015.00084
18. Turnbaugh PJ, Ridaura VK, Faith JJ, Rey FE, Knight R, Gordon JI. The effect of diet on the human gut microbiome: A metagenomic analysis in humanized gnotobiotic mice. *Science Translational Medicine*. 2009;1(6):1–12. doi:10.1126/scitranslmed.3000322
19. Miyauchi E, Kim S, Suda W, Kawasumi M, Onawa S, Taguchi-Atarashi N, Morita H, Taylor TD, Hattori M, Ohno H. Gut microorganisms act together to exacerbate inflammation in spinal cords. *Nature*. 2020;585(7823):102–106. doi:10.1038/s41586-020-2634-9
20. Zhang H, Yohe T, Huang L, Entwistle S, Wu P, Yang Z, Busk PK, Xu Y, Yin Y. dbCAN2: A meta server for automated carbohydrate-active enzyme annotation. *Nucleic Acids Research*. 2018;46(W1):W95–W101. doi:10.1093/nar/gky418
21. Kudelka MR, Stowell SR, Cummings RD, Neish AS. Intestinal epithelial glycosylation in homeostasis and gut microbiota interactions in IBD. *Nature Reviews Gastroenterology and Hepatology*. 2020;17(10):597–617. doi:10.1038/s41575-020-0331-7
22. Sumida T, Fujimoto K, Ito M. Molecular cloning and catalytic mechanism of a novel glycosphingolipid-degrading  $\beta$ -N-acetylgalactosaminidase from *Paenibacillus* sp. TS12. *Journal of Biological Chemistry*. 2011;286(16):14065–14072. doi:10.1074/jbc.M110.182592
23. Crost EH, Tailford LE, Le Gall G, Fons M, Henrissat B, Juge N. Utilisation of Mucin Glycans by the Human Gut Symbiont *Ruminococcus gnavus* Is Strain-Dependent. *PLoS ONE*. 2013;8(10). doi:10.1371/journal.pone.0076341



24. Price MN, Arkin AP. Curated BLAST for Genomes Greene CS, editor. *mSystems*. 2019;4(2):1–7. doi:10.1128/mSystems.00072-19
25. Carlin AF, Uchiyama S, Chang YC, Lewis AL, Nizet V, Varki A. Molecular mimicry of host sialylated glycans allows a bacterial pathogen to engage neutrophil Siglec-9 and dampen the innate immune response. *Blood*. 2009;113(14):3333–3336. doi:10.1182/blood-2008-11-187302
26. Lewis LA, Gulati S, Burrowes E, Zheng B, Ram S, Rice PA.  $\alpha$ -2,3-Sialyltransferase Expression Level Impacts the Kinetics of Lipooligosaccharide Sialylation, Complement Resistance, and the Ability of *Neisseria gonorrhoeae* to Colonize the Murine Genital Tract. *mBio*. 2015;6(1):1–11. doi:10.1128/mBio.02465-14. Editor
27. Ng KM, Ferreyra JA, Higginbottom SK, Lynch JB, Kashyap PC, Gopinath S, Naidu N, Choudhury B, Weimer BC, Monack DM, *et al.* Microbiota-liberated host sugars facilitate post-antibiotic expansion of enteric pathogens. *Nature*. 2013;502(7469):96–99. doi:10.1038/nature12503
28. Huang YL, Chassard C, Hausmann M, Von Itzstein M, Hennet T. Sialic acid catabolism drives intestinal inflammation and microbial dysbiosis in mice. *Nature Communications*. 2015;6:1–11. doi:10.1038/ncomms9141
29. Pacheco AR, Munera D, Waldor MK, Sperandio V, Ritchie JM. Fucose sensing regulates bacterial intestinal colonization. *Nature*. 2012;492(7427):113–117. doi:10.1038/nature11623
30. Luijckx YMCA, Bleumink NMC, Jiang J, Overkleeft HS, Wösten MMSM, Strijbis K, Wennekes T. *Bacteroides fragilis* fucosidases facilitate growth and invasion of *Campylobacter jejuni* in the presence of mucins. *Cellular Microbiology*. 2020;22(12). doi:10.1111/cmi.13252
31. Engevik MA, Banks LD, Engevik KA, Chang-Graham AL, Perry JL, Hutchinson DS, Ajami NJ, Petrosino JF, Hyser JM. Rotavirus infection induces glycan availability to promote ileum-specific changes in the microbiome aiding rotavirus virulence. *Gut Microbes*. 2020;11(5):1324–1347. doi:10.1080/19490976.2020.1754714
32. Alfajaro MM, Kim J-Y, Barbé L, Cho E-H, Park J-G, Soliman M, Baek Y-B, Kang M-I, Kim SH, Kim G-J, *et al.* Dual Recognition of Sialic Acid and  $\alpha$ Gal Epitopes by the VP8\* Domains of the Bovine Rotavirus G6P[5] WC3 and of Its Mono-reassortant G4P[5] RotaTeg Vaccine Strains López S, editor. *Journal of Virology*. 2019;93(18). doi:10.1128/JVI.00941-19
33. Desai MS, Seekatz AM, Koropatkin NM, Kamada N, Hickey CA, Wolter M, Pudlo NA, Kitamoto S, Terrapon N, Muller A, *et al.* A Dietary Fiber-Deprived Gut Microbiota Degrades the Colonic Mucus Barrier and Enhances Pathogen Susceptibility. *Cell*. 2016;167(5):1339–1353.e21. doi:10.1016/j.cell.2016.10.043
34. Png CW, Lindén SK, Gilshenan KS, Zoetendal EG, McSweeney CS, Sly LI, McGuckin MA, Florin THJ. Mucolytic bacteria with increased prevalence in IBD mucosa augment in vitro utilization of mucin by other bacteria. *American Journal of Gastroenterology*. 2010;105(11):2420–2428. doi:10.1038/ajg.2010.281
35. Yin Y, Mao X, Yang J, Chen X, Mao F, Xu Y. dbCAN: A web resource for automated carbohydrate-active enzyme annotation. *Nucleic Acids Research*. 2012;40(W1):W445–W451. doi:10.1093/nar/gks479

36. Ottman N, Davids M, Suarez-Diez M, Boeren S, Schaap PJ, dos Santos VAPM, Smidt H, Belzer C, de Vos WM. Genomescale model and omics analysis of metabolic capacities of *Akkermansia muciniphila* reveal a preferential mucin-degrading lifestyle. *Applied and Environmental Microbiology*. 2017;83(18):1–15. doi:10.1128/AEM.01014-17
37. Goodman AL, Kallstrom G, Faith JJ, Reyes A, Moore A, Dantas G, Gordon JI. Extensive personal human gut microbiota culture collections characterized and manipulated in gnotobiotic mice. *Proceedings of the National Academy of Sciences*. 2011;108(15):6252–6257. doi:10.1073/pnas.1102938108
38. Wiśniewski JR, Zougman A, Nagaraj N, Mann M. Universal sample preparation method for proteome analysis. *Nature Methods*. 2009;6(5):359–362. doi:10.1038/nmeth.1322
39. Rappsilber J, Mann M, Ishihama Y. Protocol for micro-purification, enrichment, pre-fractionation and storage of peptides for proteomics using StageTips. *Nature Protocols*. 2007;2(8):1896–1906. doi:10.1038/nprot.2007.261
40. Cox J, Mann M. MaxQuant enables high peptide identification rates, individualized p.p.b.-range mass accuracies and proteome-wide protein quantification. *Nature Biotechnology*. 2008;26(12):1367–1372. doi:10.1038/nbt.1511
41. Cox J, Hein MY, Lubner CA, Paron I, Nagaraj N, Mann M. Accurate Proteome-wide Label-free Quantification by Delayed Normalization and Maximal Peptide Ratio Extraction, Termed MaxLFQ. *Molecular & Cellular Proteomics*. 2014;13(9):2513–2526. doi:10.1074/mcp.M113.031591
42. Tyanova S, Temu T, Sinitcyn P, Carlson A, Hein MY, Geiger T, Mann M, Cox J. The Perseus computational platform for comprehensive analysis of (prote)omics data. *Nature Methods*. 2016;13(9):731–740. doi:10.1038/nmeth.3901
43. Luijckx YMCA, Henselijn AJ, Bosman GP, Cramer DAT, Giesbers CAP, van 't Veld EM, Boons GJPH, Heck AJR, Reiding KR, Strijbis K, *et al.* Detection of bacterial  $\alpha$  - L -fucosidases with an ortho -quinone methide-based probe and mapping of the probe-protein adducts. Manuscript submitted for publication.
44. Li X, Bleumink-Pluym NMC, Luijckx YMCA, Wubbolts RW, van Putten JPM, Strijbis K. MUC1 is a receptor for the *Salmonella* SiiE adhesin that enables apical invasion into enterocytes. *PLoS Pathogens*. 2019;15(2):e1007566. doi:10.1371/journal.ppat.1007566
45. Perez-Riverol Y, Csordas A, Bai J, Bernal-Llinares M, Hewapathirana S, Kundu DJ, Inuganti A, Griss J, Mayer G, Eisenacher M, *et al.* The PRIDE database and related tools and resources in 2019: Improving support for quantification data. *Nucleic Acids Research*. 2019;47(D1):D442–D450. doi:10.1093/nar/gky1106

### Data availability

The mass spectrometry proteomics data have been deposited to the ProteomeXchange Consortium via the PRIDE partner repository with the dataset identifier PXD024919<sup>45</sup>. Data can be accessed via <https://www.ebi.ac.uk/pride/> using dataset identifier above.

The *A. mucolyticum* Whole Genome Shotgun project has been deposited at DDBJ/ENA/GenBank under the accession JAHUZH000000000. The version described in this paper is version JAHUZH010000000.

### Acknowledgements

We would like to kindly thank Dr. Karin Strijbis for providing the anti-human MUC2 rabbit serum.

We would like to kindly thank Dr. Yvette Luijkx and Dr. Tom Wennekes for providing the activity-based probe and advice on experimental setup.

### Funding

M.R.d.Z. was supported by a VIDI grant from the Netherlands Organization for Scientific Research (NWO, grant 91715377) and the Utrecht Exposome Hub of Utrecht Life Sciences ([www.uu.nl/exposome](http://www.uu.nl/exposome)), funded by the Executive Board of Utrecht University.

### Declaration of interests

M.R.d.Z and N.W.P are co-founders of and hold equity in Artizan Biosciences.

## SUPPLEMENTARY DATA

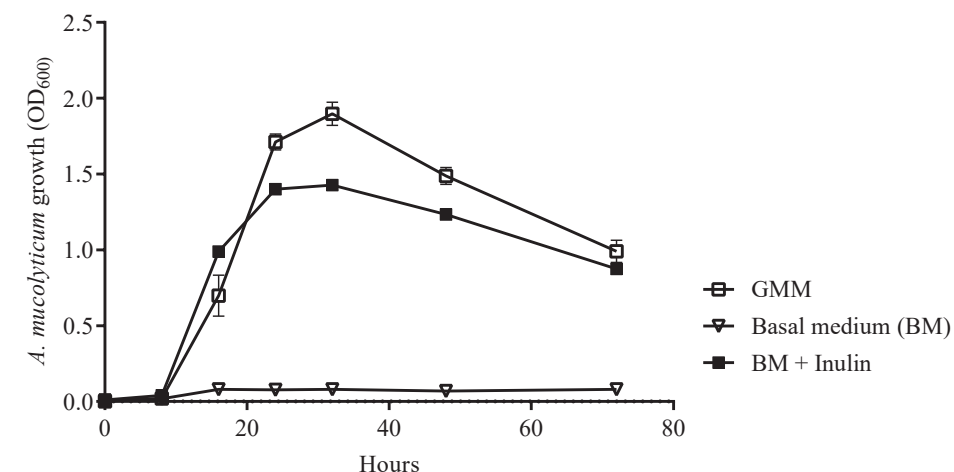


**Figure S1. *A. mucolyticum* can use inulin as substrate for growth.** *A. mucolyticum* growth was assessed over a 72 h period by measuring optical density at 600nm (OD<sub>600</sub>). Bacteria were grown in Gut Microbiota Medium (GMM), basal medium (BM) or basal medium supplemented with inulin (10mg/mL). Graphs depict the mean values ± SD acquired from three independent experiments.

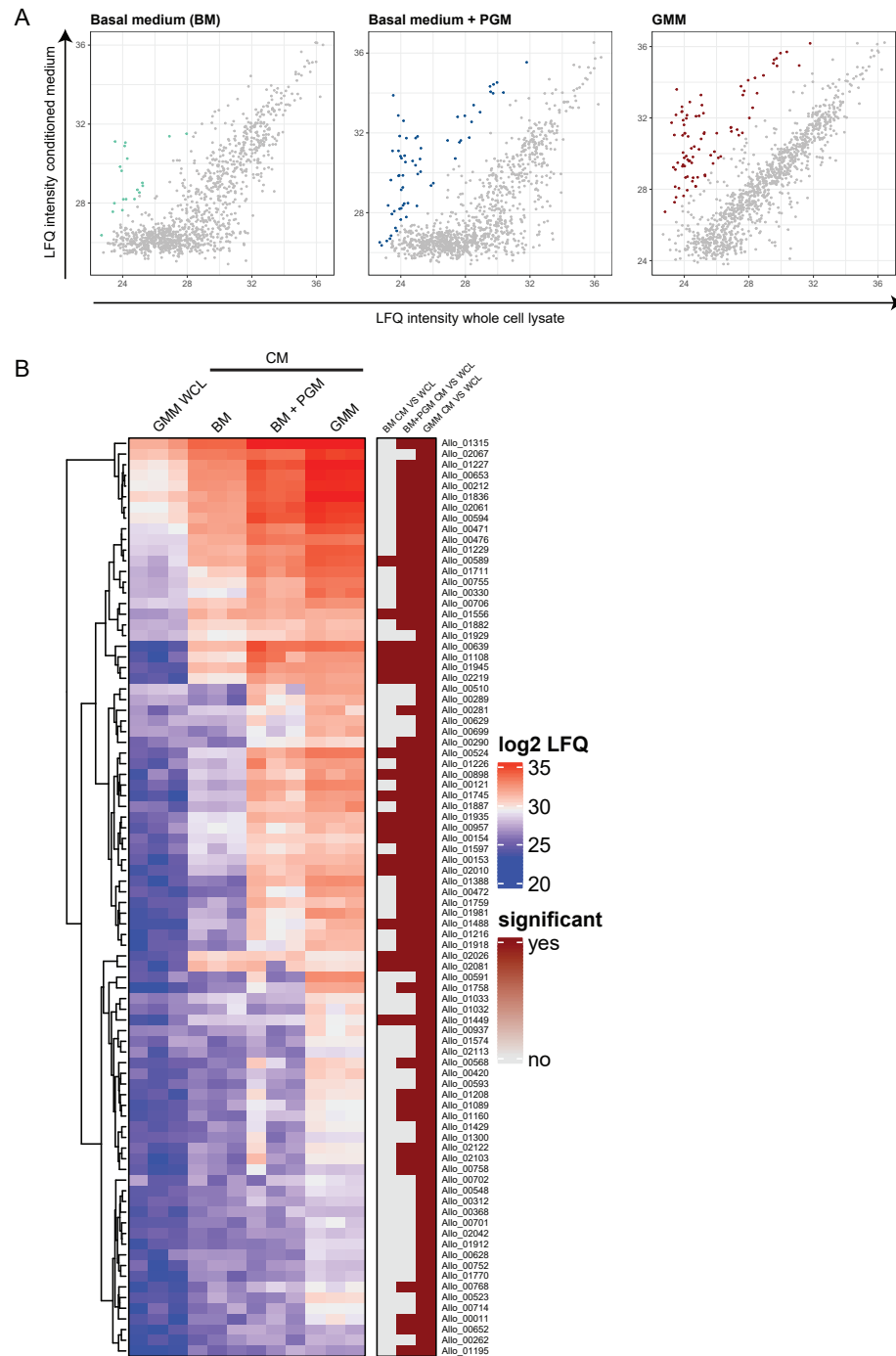


**Figure S2. Mass spectrometry analysis of proteome.** Conditioned media from 24 h old cultures in basal medium (BM), basal medium + PGM and Gut Microbiota Medium (GMM) and a whole cell lysate (WCL) from the GMM culture were subjected to mass spectrometry analysis, with three biologically independent replicates per condition. (A) The three scatter plots show the log<sub>2</sub> LFQ from whole cell lysate of the GMM culture (X-axis) and the secretomes from the three different media (Y-axis). The colored dots indicate the proteins with >10-fold enrichment in the secretome versus GMM WCL. (B) The red/blue heatmap displays the proteins and their relative enrichment in the three different secretomes compared to the GMM WCL. Significance (depicted in the brown heatmap) was calculated using a t-test and indicates a >10 fold enrichment in the respective secretome versus GMM WCL with a FDR < 0.05.

**Figure S2. Mass spectrometry analysis of proteome.** Legend on next page.

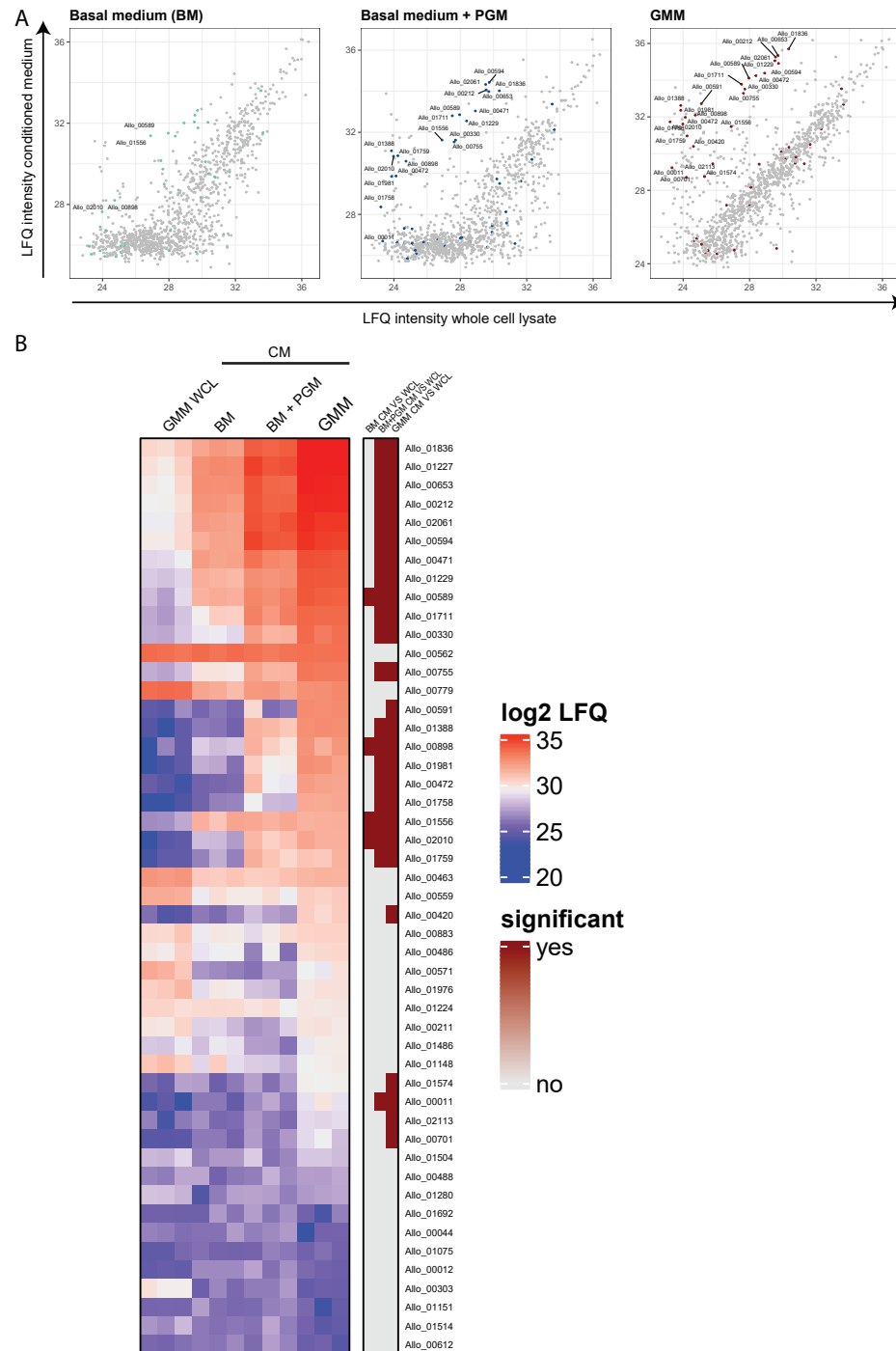


**Figure S3. Mass spectrometry analysis of CAZymes.** Conditioned media from 24 h old cultures in basal medium (BM), basal medium + PGM and Gut Microbiota Medium (GMM) and a whole cell lysate (WCL) from the GMM culture were subjected to mass spectrometry analysis, with three biologically independent replicates per condition. (A) The three scatter plots show the log<sub>2</sub> LFQ from whole cell lysate of the GMM culture (X-axis) and the secretomes from the three different media (Y-axis). The colored dots indicate the CAZymes. (B) The red/blue heatmap displays all the putative CAZymes and their relative enrichment in the three different secretomes compared to the GMM WCL. Significance (depicted in the brown heatmap) was calculated using a t-test and indicates a >10-fold enrichment in the respective secretome versus GMM WCL with a FDR < 0.05.

**Table S1. Comparison of number of putative mucin O-glycan targeting CAZymes of *A. mucolyticum* and *A. muciniphila* ATCC BAA-835.**

Putative CAZYme activity (GH domains)	# of genes in genome <sup>a</sup>	
	<i>A. mucolyticum</i>	<i>A. muciniphila</i> ATCC BAA-835
α-sialidases (GH33)	2	4
α-fucosidases (GH29/95)	3	6
β-galactosidases (GH2/42)	8	6
α/β-N-acetylglucosaminidase (GH20/84/85/89)	9	14
α/β-N-acetylgalactosaminidase (GH101/129)	0	0
total of unique genes	22	30

<sup>a</sup>Identified by at least two out of three dbCAN2 tools

**Figure S3. Mass spectrometry analysis of CAZymes.** Legend on next page

Table S2. Recipe for enriched Gut Microbiota Medium (GMM).

Component	Amount (500 mL)	Concentration	Comments	Vendor
Tryptone Peptone	5 g	10 g/L		BBL Trypticase Peptone BD (211921)
Yeast Extract	2.5 g	5 g/L		Bacto Yeast Extract BD (212750)
D-(+)-glucose - absent from basal medium	1 g	11 mM		Sigma (G8270-1KG)
L-cysteine HCL	0.5 g	6.4 mM		Sigma (C-1276)
D-(+)-Cellobiose - absent from basal medium	0.5 g	2.9 mM		Sigma
D-(+)-Maltose - absent from basal medium	0.5 g	2.8 mM		Sigma
D-(-)-Fructose - absent from basal medium	0.5 g	2.2 mM		Sigma
Meat Extract	2.5 g	5 g/L		Sigma
Phosphate buffer (see below)	100 mL	100 mM	1 M stock solution pH 7.2	
TYG salts solution (see below)				
CaCl <sub>2</sub>	0.5 mL	0.8%	8 mg/mL stock solution	Sigma
Vitamin K (menadione)	0.5 mL	5.8 mM	1 mg/mL stock solution	Sigma
FeSO <sub>4</sub> ·7H <sub>2</sub> O	0.5 mL	1.44 mM	0.4 mg FeSO <sub>4</sub> ·7H <sub>2</sub> O/mL stock solution	Sigma
Histidine Hematin Solution (see below)	0.5 mL	0.1%	1.2 mg hematin/mL in 0.2 M histidine solution	Sigma
Tween 80	1 mL	0.05%	25% stock solution	Sigma
ATCC Vitamin Supplement	5 mL	1%		ATCC
ATCC Trace Mineral Supplement	5 mL	1%		ATCC
Short-chain fatty acid supplement (see below)	3.75 mL			
Resazurin	2 mL	4 mM	0.25 mg/mL stock solution	Sigma

**Potassium Phosphate buffer recipe (1 M, pH 7.2)**

1 M KH<sub>2</sub>PO<sub>4</sub> (68.045 g/500 mL)

1 M K<sub>2</sub>HPO<sub>4</sub> (174.18 g/L) 1 L

add monobasic to dibasic to achieve pH 7.2, autoclave, store at room temperature

**TYG salts solution recipe** Amount (1 L)

MgSO<sub>4</sub>·7H<sub>2</sub>O 0.5 g Sigma

NaHCO<sub>3</sub> 10 g Sigma

NaCl 2 g Sigma

**Histidine solution recipe (0.2 M, pH 8)**

histidine 2.1 g Sigma

MilliQ bring to 40 mL

Set pH to 8.0 with 5 M NaOH, then bring to 40 mL

**Histidine-Hematin recipe (0.2 M)**

hematin 24 mg Sigma

histidin solution (0.2 M, pH 8) - see above

Cover in aluminum foil, rotate overnight at 4°C. Filter sterilize, aliquot in 0.5 mL, store at -20°C

**Short-chain fatty acid supplement recipe** Amount (50 mL)

Acetic acid 11.33 mL

Sodium propionate Na salt 5.21 g Sigma

Sodium butyrate Na salt 3.21 g Sigma

MilliQ bring to 50 mL

# 04

## **Growth inhibition of *Akkermansia muciniphila* by a secreted pathobiont sialidase**

Guus H. van Muijlwijk<sup>1</sup>, Emma C.R. Bröring<sup>2</sup>, Guido van Mierlo<sup>3</sup>, Pascal W.T.C. Jansen<sup>3</sup>, Michiel Vermeulen<sup>3</sup>, Piet C. Aerts<sup>1</sup>, Jos P.M. van Putten<sup>2</sup>, Noah W. Palm<sup>4</sup> & Marcel R. de Zoete<sup>1</sup>

<sup>1</sup>Department of Medical Microbiology, University Medical Center Utrecht, Utrecht, Netherlands

<sup>2</sup>Department of Biomolecular Health Sciences, Utrecht University, Utrecht, Netherlands.

<sup>3</sup>Radboud University, Faculty of Science, Department of Molecular Biology, Radboud Institute for Molecular Life Sciences (RIMLS), 6500HB Nijmegen, Netherlands

<sup>4</sup>Department of Immunobiology, Yale University School of Medicine, New Haven, CT 06520, USA

## 04 |

**ABSTRACT**

*Akkermansia muciniphila* is considered a key constituent of a healthy gut microbiota. In inflammatory bowel disease (IBD), *A. muciniphila* has a reduced abundance while other, putative pathogenic, mucus colonizers bloom. We hypothesized that interbacterial competition may contribute to this observation. By screening the supernatants of a panel of enteric bacteria, we discovered that a previously uncharacterized *Allobaculum* species potently inhibits the growth of *A. muciniphila*. Mass spectrometry analysis identified a secreted *Allobaculum* sialidase as inhibitor of *A. muciniphila* growth. The sialidase targets sialic acids on casein *O*-glycans, thereby altering the accessibility of nutrients critical for *A. muciniphila* growth. The altered glycometabolic niche results in distorted *A. muciniphila* cell division and efficiently arrests its growth. The identification of a novel mechanism of *A. muciniphila* growth inhibition by a competing bacterial pathobiont may provide a rationale for interventions aimed at restoring and maintaining a healthy microbiota symbiosis in patients with intestinal disease.

**INTRODUCTION**

The human intestinal tract is a highly dynamic ecosystem that is home to trillions of microbes, known as the gut microbiota<sup>1</sup>. Throughout our lives, the gut ecosystem is subject to various disturbing influences driven by external factors like changes in diet, exposure to antibiotics and competition with newly acquired commensals or invading enteropathogens<sup>2-4</sup>. All these events are reflected in the composition of the intestinal microbiota, and changes in this composition have been associated with numerous diseases<sup>5-10</sup>.

Intestinal bacteria can significantly affect host physiology, dependent on their metabolism and lifestyle<sup>11-13</sup>. Due to their position in the gut ecosystem, mucus-colonizing and mucosa-associated bacteria are more likely to affect host immune responses and have a dominant effect on host physiology and the development of intestinal disease<sup>14-18</sup>. One of the species known to reside in the mucus layer and to affect host immune responses is *Akkermansia muciniphila*<sup>19,20</sup>. This mucin-degrading bacterium plays an important role in the maintenance of gut immune homeostasis as it has been reported to improve mucus layer thickness and epithelial barrier function<sup>20</sup>. Furthermore, it induces immune tolerance through the induction of Tregs and is often highly coated by secretory IgA, suggesting close interactions with the intestinal immune system.<sup>18,20-23</sup> Notably, a reduced abundance of *A. muciniphila* has been reported in inflammatory bowel disease (IBD) patients and several other inflammatory diseases such as type 2 diabetes and metabolic syndrome, but the reasons for this reduced abundance remain unclear<sup>20,24,25</sup>. Identification of the factors that negatively impact the abundance of *A. muciniphila* may provide important new insights into the mucosal bacterial ecosystem and its effects on the host.

Multiple factors may contribute to the loss of *A. muciniphila*, such as changes in diet or the excessive use of antibiotics<sup>26-29</sup>. Another factor that is often overlooked, and which may act in synchrony with other factors, is the possibility of direct interbacterial antagonism by bacteria occupying the same niche. Given that many such interactions are known to exist in the bacterial kingdom, we investigated the possibility that distinct bacteria present in the gut of IBD patients have the ability to inhibit *A. muciniphila* directly.

By screening the interaction of *A. muciniphila* with a panel of IBD-associated bacteria we discovered that a secreted protein from the pathobiont *Allobaculum mucolyticum* potently inhibits the growth of *A. muciniphila*. This protein

was identified to be a sialidase that desialylates *O*-glycans on substrates required for *A. muciniphila* growth. The alteration of the glycometabolic niche efficiently arrests bacterial growth through distorted bacterial cell division. The identification of a novel mechanism of *A. muciniphila* growth inhibition by a competing bacterial pathobiont may pave the road for therapies aimed at restoring and maintaining microbiota homeostasis in patients with intestinal disease.

## MATERIALS & METHODS

### Bacterial culturing conditions

All bacteria were routinely cultured at 37°C under strict anaerobic conditions at an atmosphere of 5% H<sub>2</sub>, 10% CO<sub>2</sub> and 85% N<sub>2</sub>. Unless stated otherwise, bacteria were cultured in enriched Gut Microbiota Medium (GMM) broth, of which the recipe is described in Chapter 3 of this thesis. The defined minimal medium (DMM) was derived from GMM and prepared using the following basal ingredients at similar concentrations as in GMM: Phosphate buffer, Vitamin K solution, TYG salts, CaCl<sub>2</sub>, FeSO<sub>4</sub>·7H<sub>2</sub>O, Resazurin, Histidin-Hematin solution, Trace Mineral supplement, Vitamin supplement and L-Cysteine HCl. This basal medium was supplemented with trypticase peptone (10 g/L) and glucose (10 mM). Prior to use for bacterial growth, all media were prereduced in the anaerobic chamber for at least 12 h, unless stated otherwise.

### Bacterial conditioned media (CM)

Bacterial conditioned media (CM) were collected from a panel of 14 different enteric bacterial isolates previously isolated from IBD patients<sup>18</sup>. For each strain, conditioned medium was collected from three biologically independent broth cultures started from a glycerol stock. Cultures were grown statically for 48 h after which the conditioned media were harvested by centrifugation, filter-sterilized using 0.2 µm filter and stored at -20°C prior to use.

### A. *muciniphila* growth inhibition experiments

*Akkermansia muciniphila* (ATCC BAA-835) and an independent *A. muciniphila* clinical isolate were routinely cultured at 37°C under anaerobic conditions as described above.

**A. *muciniphila* starter cultures.** All growth assays were preceded by growing *A. muciniphila* broth starter cultures. For this, 3 mL of prereduced GMM broth was inoculated with *A. muciniphila* from a glycerol stock. After 48 h of growth, bacteria were pelleted by centrifugation (3,000 x g, 5 min) and gently washed twice with the desired medium used in the growth assay.

For all the following experiments *A. muciniphila* was diluted in the desired medium and cultured in a 96-Well Multiwell Flat Bottom Plate (Corning Costar) with a final volume of 200 µL per well and a starting optical density (600 nm) of 0.01. After 48 h, or unless otherwise stated, the plate was removed from the anaerobic chamber and final absorbance values (600 nm) were recorded using a FLUOstar Omega plate reader (BMG Labtech). Values were corrected for background levels in respective negative controls.

**A. *muciniphila* cultured with bacterial conditioned media.** Sterile bacterial CM were divided into two fractions. One fraction was kept at room temperature (21°C), while the other fraction was heat-inactivated (98°C, 30 min), after which both fractions were transferred to the anaerobic chamber. 50 µL of the active and heat-inactivated fractions were transferred to a 96-Well Multiwell Plate (Corning Costar) per well in duplicates to which *A. muciniphila* starter cultures were added for final volume of 200 µL.

### Treatments and supplementation of *Allobaculum mucolyticum* conditioned medium

For clarity *Allobaculum mucolyticum* will hereafter solely be referred to as *Allobaculum*. All treatments were performed prior to addition of CM to *A. muciniphila* cultures, unless otherwise stated.

**Proteinase K treatment.** *Allobaculum* CM or GMM control media were treated with Proteinase K (1 mg/mL), PMSF (1 mM) or PMSF-inactivated Proteinase K (1 mM and 1 mg/mL, respectively) for 16 h at 37°C, after which the Proteinase K-treated samples were supplemented with PMSF (1 mM).

**Size-fractionation.** *Allobaculum* CM was fractionated based on size through successive use of 50, 30, and 3 kDa MWCO Amicon Ultra filters (Thermo Fisher Scientific). Intermediate retentates were reconstituted to the starting volume using GMM.



**Size-fractionation by high-resolution chromatography.** Twenty mL of *Allobaculum* CM was concentrated to 0.5 mL using a 50 kDa MWCO Amicon Ultra filter (Thermo Fisher Scientific), reconstituted to 20 mL using PBS and reconcentrated once more to 0.5 mL. Fast Protein Liquid Chromatography (FPLC) of this fraction was conducted using a Superdex® 200 Increase 10/300 GL on the ÄKTA pure protein purification system (GE Healthcare, Uppsala, Sweden). The proteins were eluted with PBS (pH 7.4) at a flow rate of 0.75 mL/min, detected by absorbance at 280 nm, and collected in 0.5 mL fractions. Fractions containing protein peaks (fractions 13-56) were tested for growth inhibition of *A. muciniphila*. For this, 100 µL of each size-exclusion fraction was combined with *A. muciniphila* diluted in 2x concentrated GMM and cultured as described above. The surplus of the size-exclusion fractions was stored at -20°C prior to further fractionation.

**Fractionation by anion-exchange chromatography.** Inhibiting size-exclusion fractions (fractions 17-28) were pooled to a total volume of 3 mL. Pooled fractions were dialyzed overnight at 4°C, against starting buffer A (20 mM Bis-Tris, pH 6) using a 10 kDa MWCO dialysis tube. Fast Protein Liquid Chromatography (FPLC) was conducted using a HiTrap Q XL 1 mL Sepharose column on the ÄKTA pure protein purification system (GE Healthcare, Uppsala, Sweden). Proteins were eluted with starting buffer A followed by a gradually increasing concentration of buffer B (20 mM Bis-Tris, 1 M NaCl, pH 6) at a flow rate of 0.75 mL/min, detected by absorbance at 280 nm, and collected in 0.5 mL fractions. Fractions or matching NaCl molarity controls in TBS pH 6 were tested for growth inhibition of *A. muciniphila*. For this, 50 µL of each anion-exchange fraction was diluted with 50 µL MilliQ and combined with *A. muciniphila* diluted in 2x concentrated GMM and cultured as described above. The surplus of the size-exclusion fractions was stored at -20°C prior to further processing.

**Supplementation with defined monosaccharides.** L-Fucose (Sigma), D-Galactose (Sigma), N-Acetylneuraminic acid (Carbosynth), N-acetyl-D-glucosamine (GlcNAc, Sigma), and N-acetyl-D-galactosamine (GalNAc, Carbosynth) were dissolved in MilliQ to a final concentration of 100 mM, adjusted to pH 7.2 using 1 M NaOH or HCl if necessary, and filter-sterilized using 0.2 µm filter. Zero, 25 or 50 µL of active or heat-inactivated *Allobaculum* CM or GMM control, for a final concentration of 0%, 12.5% and 25% supernatant, respectively, were combined with 50 µL of each monosaccharide

solution, a dilution thereof, or MilliQ control for a final concentration of 0 mM, 1 mM, 5 mM or 25 mM monosaccharide. Mixtures were combined with *A. muciniphila* previously diluted in 2X concentrated GMM.

### NanH1 pretreatment of GMM and DMM

Recombinant NanH1 or heat-inactivated NanH1 (2.5 µg/mL) or an equal volume of PBS (mock) as control were added to GMM or DMM. Mixtures were incubated for 16 h at 37°C after which they were heat-inactivated (98°C, 30 min) prior to use.

### *A. muciniphila* growth with recombinant *Allobaculum* NanH1 sialidase and other bacterial sialidases

Recombinant NanH1, heat-inactivated NanH1 (98°C, 30 min) and the mutant NanH1ΔRIP (see below) were diluted to desired concentration in 100 µL MilliQ or MilliQ supplemented with sialic acid (Neu5Ac) and combined with *A. muciniphila* in 2x concentrated GMM. Recombinant *Allobaculum* NanH2, CPNA (Sigma), VCNA (Roche), and AUNA (Roche) were also diluted in MilliQ and the concentration was adjusted to equal the sialidase activity of NanH1 on the 4-MU-NANA substrate (see below).

### Sialidase activity assays

Fifty µL of *Allobaculum* CM or GMM control were added to a 96-Well Multiwell flat bottom plate (Corning Costar). Recombinant *Allobaculum* NanH1, NanH1ΔRIP, NanH2 (all at 500 µg/mL), and CPNA (25 U/mL), VCNA (16 U/mL) and AUNA (10 U/mL) were diluted to a range of different concentrations in GMM after which 50 µL was added to the wells. Next, 50 µL of 4-MU-Neu5Ac substrate (200 µM in MilliQ, Cayman) was added to each well after which the plate was transferred to the FLUOstar Omega plate reader (BMG labtech), which was kept at 37°C. Fluorescence was recorded over time or as an endpoint measurement (indicated in graph) using the 340 ex / 460 em filter set. Relative sialidase activities in GMM for stock solutions of NanH1 / NanH1ΔRIP / NanH2 / CPNA / VCNA / AUNA are 100% / 0% / 8.4% / 78.5% / 118.9% / 99.5%, respectively, relative to NanH1.

### Mass spectrometric analysis of fractionated *Allobaculum* conditioned media.

**In-gel digestion.** The strongest inhibiting anion-exchange fraction (fraction 50), and a non-inhibiting fraction (fraction 12) were analysed using LC-MS/MS. Protein mixtures were denatured in 1X Nu-PAGE LDS sample buffer (NP0007, Invitrogen) and separated using a SDS PAGE gel. Gels were fixed

with 10% acetic acid and 50% methanol, and stained with the Colloidal Blue Staining Kit (Invitrogen), followed by staining with colloidal Blue (20% stainer A (Invitrogen 46-7015) and 5% stainer B (Invitrogen 46-7016) in the presence of 20% methanol. Gels were destained with an excess of deionized water for 30 min at RT. Bands of interest were excised and at the same time control pieces of unstained gel fractions were taken along as controls. Each slice was transferred to a 1.5 ml Eppendorf tube and further destained in a mixture of 25 mM ammonium bicarbonate (ABC) and 50% ethanol. Slices were then washed with 1 mL Acetonitril (ACN) for 10 min at, 1 mL ABC (50 mM) and again twice with ACN. All liquid was removed and tubes were air dried using a speedvac for 10 min. Then 200  $\mu$ L of 10 mM dithiothreitol (DTT) in ABC was added and tubes were incubated for 45 min at 50 °C. This solution was removed and the gel was resuspended in 300  $\mu$ L of 50 mM IAA in ABC followed by a 30 min incubation in the dark. After a wash with ABC and two washes with ACN, tubes were air dried once more using a speedvac and gel slices were covered in a Trypsin / ABC mixture followed by overnight digestion. Next, digested peptides were extracted using two 15 min incubations in a 100  $\mu$ L mixture of 30% ACN and 3% formic acid in water, and two 15 min incubations in 100  $\mu$ L of ACN. Resulting supernatants were combined (yielding ~500  $\mu$ L) and concentrated to 100  $\mu$ L using a speedvac. The resulting peptide was desalted using StageTips<sup>30</sup>.

**LC-MS/MS measurements and data analysis.** Digested peptides were analysed using an Easy-nLC1000 (Thermo) connected to a LTQ-Orbitrap-Fusion (Thermo). Raw files were analysed using standard settings of MaxQuant 1.5.1.0. Options LFQ, iBAQ and match between runs were selected. Perseus 1.5.1.0.15 was used to filter out proteins flagged as contaminant, reverse or only identified by site.

### Fluorescence confocal microscopy

*A. muciniphila* was grown for 48 h in GMM with 25% active or heat-inactivated *Allobaculum* conditioned medium or in either mock or NanH1 pretreated GMM, as described above. Bacteria were pelleted (3,000  $\times g$ , 5 min, at room temperature (RT)), washed once in PBS pH 7.4, resuspended in PBS + 4% paraformaldehyde (PFA) and fixed for 15 min at RT. Bacteria were washed as described above, twice in PBS, once in MilliQ water, and stained for 10 min at RT with 5  $\mu$ M SYTO-9 dye (ThermoFisher) in MilliQ, while shielded from light. Five  $\mu$ L of each sample was spread on a poly-L-lysine-coated coverslip, air dried for 20-30 min at RT, mounted on a microscope slide using ProLong Diamond Antifade Mountant (Invitrogen) and allowed to dry overnight, while

shielded from light. Samples were imaged on a Leica SPE-II laser confocal microscope using 63.0x 1.40 objective, and images were processed using Leica LAS AF software.

### Scanning electron Microscopy (SEM)

*A. muciniphila* was grown for 48 h in either mock or NanH1 pretreated GMM, as described above. Five  $\mu$ L of each culture was spread on a poly-L-lysine-coated coverslip and air dried for 20-30 min at RT. Bacteria were then fixed for 72 h with 1 mL of primary fixative: 2% (v/v) formaldehyde + 0.5% (v/v) Glutaraldehyde + 0.15% (w/v) Ruthenium Red in 0.1 M phosphate buffer pH 7.4. After two washes with 0.1 M phosphate buffer, pH 7.4, this was followed by a 2 h fixation in a post-fixative: 1% Osmium tetroxide + 1.5% (w/v) Ferrocyanide in 0.065 M phosphate buffer pH 7.4. After a single wash with MilliQ, samples were dehydrated during consecutive 30 min steps with increasing concentrations of ethanol per step: 50%, 70%, 80%, 95%, and twice with 100% ethanol, respectively. This was followed by 50% hexamethyldisilazane (HMDS) in ethanol and twice with 100% HMDS. Following fixation and dehydration, samples were air dried overnight at RT and placed on EM thuds, coated with 6 nm gold and imaged using a FEI Scios FIB - Dual Beam SEM (ThermoFisher) at 5 kV.

### Bacterial length measurements

After acquisition of the fluorescent images, as described above, the length of 5 individual bacteria per field of view (FOV) was measured using Fiji software.<sup>31</sup> For each biologically independent experimental replicate, 5 FOVs were assessed for a total of 75 bacteria per condition.

### Recombinant sialidase cloning and expression

**Cloning of NanH1 in an expression vector.** The NanH1 coding sequence (Allo\_00594) of *Allobaculum mucolyticum* (Genbank accession number: JAHUZH010000000) lacking the predicted signal peptide (amino acids 1-29) was amplified from genomic DNA (isolated using the High Pure Template kit, Roche) by PCR using the Phusion Hot start II High Fidelity DNA Polymerase (Thermo Fisher Scientific) and primers NanH1-rec-F and NanH1-rec-R, both encoding a BsiWI restriction site (Table 1). The resulting PCR product was digested with BsiWI and ligated in frame with a N-terminal 3  $\times$  FLAG-tag and a C-terminal 6  $\times$  histidine tag into a modified and BsiWI-digested pET101/D-TOPO expression vector (Thermo Scientific), yielding pET101-NanH1.

**Cloning of NanH1ΔRIP.** The NanH1 sequence was annotated using the Conserved Domains NCBI database (available at: [www.ncbi.nlm.nih.gov/Structure/cdd/wrpsb.cgi](http://www.ncbi.nlm.nih.gov/Structure/cdd/wrpsb.cgi)). Seven putative catalytic amino acid residues within the sialidase domain likely form the active pocket and were identified based on similarity with other available sequences. Based on literature, the RIP motif (Arg449-Ile450-Pro451) was deemed part of a catalytic arginine triad important for the catalytic activity of the protein.<sup>32</sup> Therefore, this site was selected for deletion. An inverse PCR was designed, using primers NanH1-RIP-rec-F NanH1-RIP-rec-R, with the forward primer inducing a 9-bp deletion in the DNA sequence encoding the RIP motif (CGAATCCCA). The inverse PCR product was amplified from pET101-NanH1, after which the template was removed by treatment 20 U of DpnI (NEB), a methylation-sensitive restriction enzyme. The DpnI-treated PCR products were further purified using agarose gel electrophoresis. Bands of the correct size were excised from the gel and purified using the GeneJET Gel Purification Kit (ThermoFisher Scientific), following manufacture's protocol. The purified DNA fragment was blunt-end ligated using a T4 DNA ligase (ThermoFisher) resulting in plasmid pET101 - NanH1ΔRIP.

**Cloning of NanH2.** The NanH2 coding sequence (Allo\_01388) was PCR amplified in similar fashion as NanH1, also lacking the predicted signal peptide (amino acids 1-29), using PCR primers NanH2-rec-F and NanH2-rec-R, both encoding a SmaI restriction site (Table 1). The resulting PCR product was digested with SmaI and ligated in frame with a N-terminal 3xFLAG-tag and a C-terminal 6xhistidine tag into a modified and SmaI-digested pET101/D-TOPO expression vector (Thermo Scientific), yielding pET101-NanH2.

All plasmids were checked for a correct orientation of the insert and sequences were confirmed by Sanger sequencing (Macrogen).

**Protein expression and purification.** The NanH1, NanH1ΔRIP and NanH2 expression vectors were transformed into *E. coli* BL21 (DE3) (Thermo Scientific) by heat-shock and plated on LB plates with 100 µg/mL ampicillin. Transformants were cultured in LB with 100 µg/mL ampicillin at 37°C and 160 RPM to an OD<sub>600</sub> of 0.5 after which protein expression was induced by adding 1 mM IPTG (Thermo Scientific) for 4 h. Recombinant protein was purified using established lab protocols. In short, bacteria were pelleted (4,000 x g, 15 min, 4°C) and resuspended in 10 mL native buffer (50 mM Tris, 300 mM NaCl, pH8, 4°C). Lysozyme (200 µg/mL) and PMSF (1 mM) were added and mixtures were incubated for 15 min on ice. RNase and DNase (Roche, both at 5 µg/mL)

were added and the mixture was incubated for another 10 min. Bacteria were subjected to three consecutive rounds of sonication, snap-freezing in liquid nitrogen and thawing (waterbath, 37°C). Sonication consisted of 3 x 10 s per round. Next, intact cells and cell debris were removed by centrifugation (4,000 x g, 30 min, 4°C) and imidazole was added (10 mM) to the supernatant. Fast protein liquid chromatography (FPLC) of this fraction was conducted using a 5 mL HiTrap Chelating HP Sepharose column on the ÄKTA FPLC protein purification system (GE Healthcare, Uppsala, Sweden). The proteins were eluted with 10 mL of starting buffer A (native buffer + 10 mM imidazole) followed by a gradient of buffer B (native buffer + 500 mM imidazole) at a flow rate of 5 mL/min, detected by absorbance at 280 nm, and collected in 1.8 mL fractions. Collected fractions were checked for purity using SDS-PAGE. Pure fractions were pooled and dialyzed overnight at 4°C against 5 L of PBS buffer. Glycerol was added at a final concentration of 10%, protein concentration was measured on Nanodrop, adjusted to 500 µg/mL and stored at -20°C until use.

**Table 1. Primers used in this study**

Product	Template	Name	5'to 3' sequence
NanH1	<i>A. mucolyticum</i> genomic DNA	NanH1-rec-F	CGCCGTACGCGAAGAAGTCACTGCGAAGG
		NanH1-rec-R	CGCCGTACGCGATCAAGAAGAGCAGAATTGTC
NanH1 ΔRIP	pET101-NanH1	NanH1-RIP-rec-F	CTCTGCAGCCTATTCCATGATTACGAC
		NanH1-RIP-rec-R	ATAGGCTGCAGAGTTGTCATAGCCGAC
NanH2	<i>A. mucolyticum</i> genomic DNA	NanH2-rec-F	AAGCACCCGGGCCGAAATGATGAACATACC
		NanH2-rec-R	TAAGCACCCGGCGTTCAGTTTGTCTCGAGCTTGTC

## RESULTS

### Growth of *A. muciniphila* is inhibited by conditioned medium from *Allobaculum*

Direct competition with other intestinal bacterial species may contribute to the reduced abundance or absence of *A. muciniphila* in the intestinal tract. To identify inhibitory factors released by competing intestinal bacterial species, *A. muciniphila* cultures were supplemented with cell-free conditioned culture

media from a panel of fourteen mucosal bacterial species isolated from patients with IBD that covered all major bacterial phyla (Figure 1A).

In order to differentiate between active growth inhibition and passive inhibition through selective nutrient depletion from the added conditioned culture media, a parallel set of *A. muciniphila* cultures were supplemented with heat-inactivated conditioned culture media from the fourteen bacterial species (Figure 1B). While the addition of heat-inactivated conditioned culture media from most bacterial species resulted in similar diminished growth of *A. muciniphila*, only one species, *Allobaculum mucolyticum* (for clarity, hereafter referred to as *Allobaculum*), showed strong inhibitory activity against *A. muciniphila* that was neutralized by heat-inactivation (Figure 1C). Closer inspection of the kinetics of the inhibition revealed that *A. muciniphila* did not enter the early-logarithmic growth phase in the presence of *Allobaculum* conditioned media, with minimal growth observed after culturing for 48 h. In the presence of heat-inactivated conditioned medium the growth of *A. muciniphila* was similar to growth in GMM control medium in which *A. muciniphila* entered a logarithmic growth phase after 9-12 h before reaching a maximum optical density after about 36-48 h (Figure 1D). *A. muciniphila* cultured in control GMM media or in media supplemented with heat-inactivated *Allobaculum* conditioned media displayed the typical

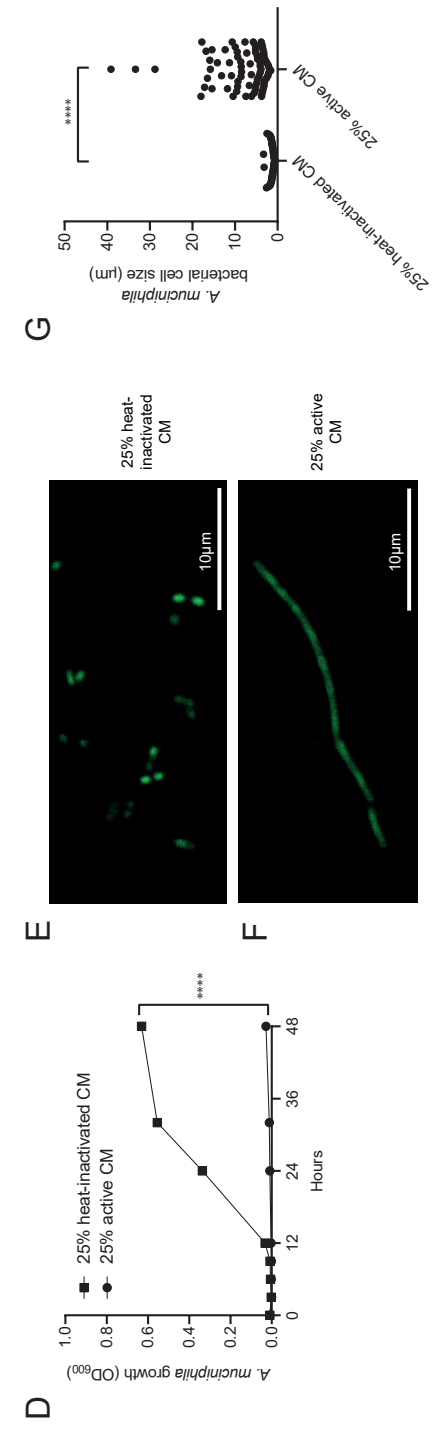
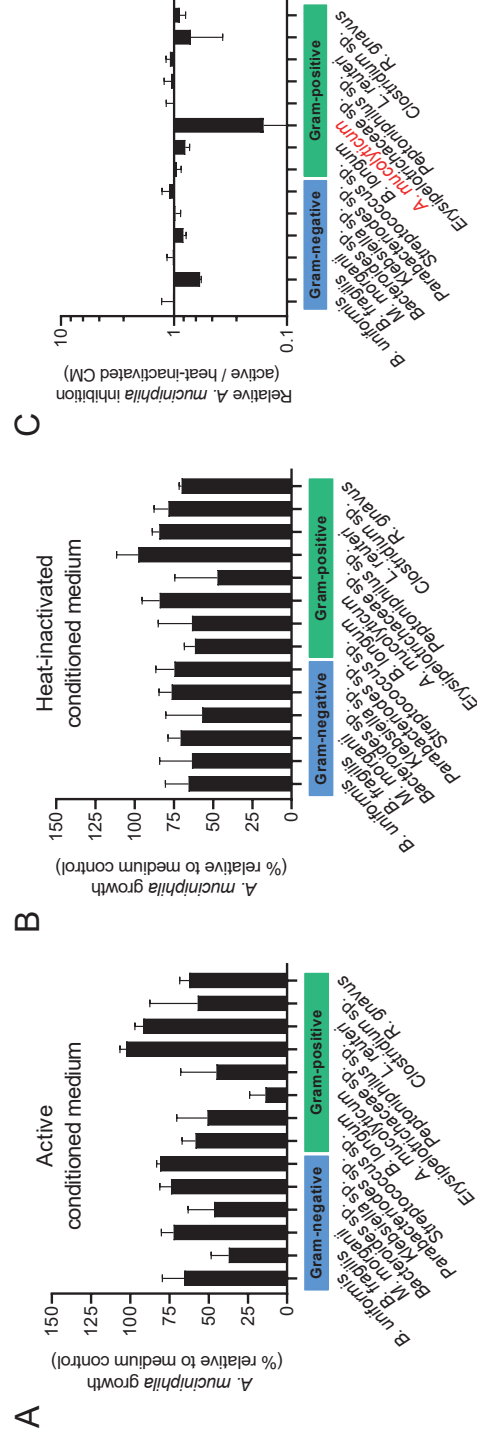


**Figure 1. *A. muciniphila* is inhibited by *Allobaculum* conditioned medium.** A. *A. muciniphila* growth was assessed after 48 h by measuring optical density at 600 nm (OD<sub>600</sub>). Bacteria were grown in Gut Microbiota Medium (GMM) supplemented with either active (A) or heat-inactivated (B) conditioned media (CM) from 14 different bacteria at a final concentration of 25%. The ratio between the final optical density values obtained with active or heat-inactivated media is displayed (C). (D) *A. muciniphila* growth curve showing growth over a 48 h period in the presence of active or heat-inactivated *Allobaculum* CM. Morphology of *A. muciniphila* was assessed after 48 h of growth in either heat-inactivated (E) or active (F) *Allobaculum* CM using confocal microscopy on syto-9 nuclear stained bacteria. Bars indicate 10 µm. Confocal images were used to measure bacterial cell length using ImageJ software (G). Per condition the length of 75 bacteria was recorded; five bacteria from five different fields of view per independent bacterial culture. Graphs depict the mean values ± SD acquired from three independent experiments. Statistical significance in D was determined for the 48 h time point by a t test. In G, statistical significance was determined using a Mann-Whitney U test. \*\*\*\*,  $P < 0.0001$ .

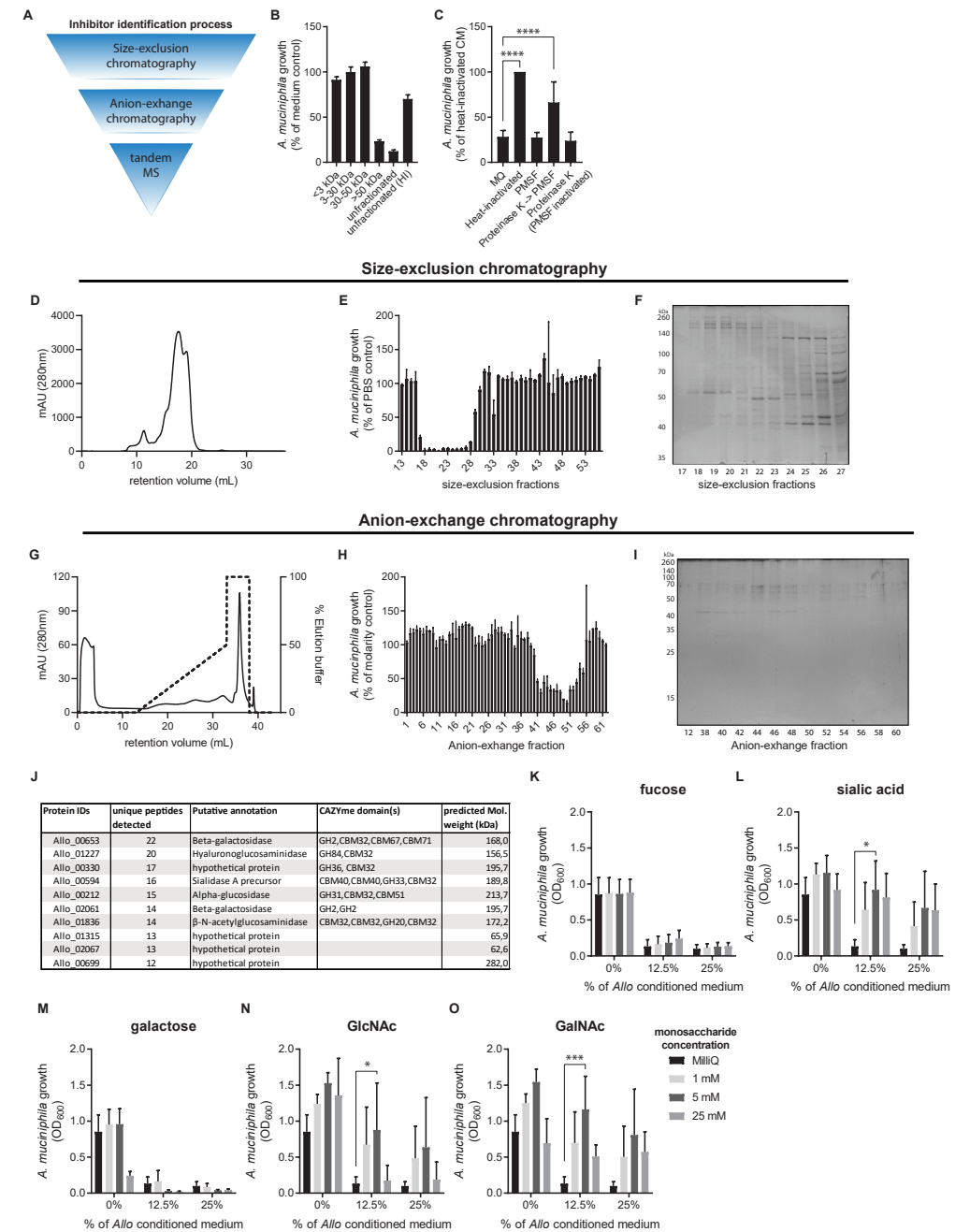
rod-shaped morphology with an average bacteria lengths of 1.21  $\mu\text{m}$  (Figure 1E,G). In contrast, *A. muciniphila* cultured in active *Allobaculum* conditioned media for 48 h displayed a severely elongated cell morphology with median bacterial length almost four times as long as control bacteria (5.73  $\mu\text{m}$ ), with some bacteria even reaching lengths of >30  $\mu\text{m}$  (Figure 1F,G). Combined, these results suggests that *Allobaculum* releases a heat-sensitive inhibitory factor that severely hampers the growth of *A. muciniphila*.

### The inhibitory fraction of *Allobaculum*-conditioned media is enriched in glycolytic enzymes

Given the potent effects of *Allobaculum* conditioned medium on *A. muciniphila* growth and morphology, we set out to identify the inhibitory factor(s) secreted by this bacterium. To assess the approximate molecular size of the growth inhibitory factor(s) in the *Allobaculum* conditioned medium, size-fractionation using Amicon spin filters was performed. Testing of the different fractions for *A. muciniphila* growth inhibitory activity demonstrated potent inhibition for >50 kDa fractions (Figure 2B). As the size and heat-sensitivity of the inhibitory factor(s) may indicate a proteinaceous nature, we pre-treated the *Allobaculum* conditioned medium with proteinase K. This treatment rescued the growth of *A. muciniphila* (Figure 2C). Together, these results show that the growth of *A. muciniphila* is severely inhibited by one or more heat-sensitive proteins that are larger than 50 kDa.

In order to identify the inhibitory protein(s), a 40x concentrated >50 kDa *Allobaculum* supernatant fraction was subjected to high-resolution size-exclusion chromatography (Figure 2D). Separate fractions were collected and added to *A. muciniphila* cultures to a final volume of 50% after which *A. muciniphila* growth was assessed after 48 h. This experiment showed that fractions 17 to 28, corresponding to retention volumes between 7.5 and 13.6 mL, had the strongest inhibitory effect on *A. muciniphila* growth (Figure 2E). These fractions corresponded with a minor single peak in the chromatogram but still contained a variety of different proteins as shown by SDS-PAGE analysis (Figure 2F).

Figure continues on next page



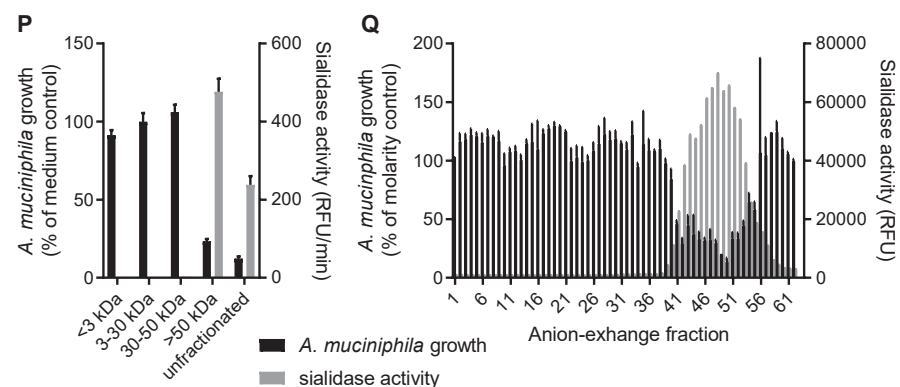


**Figure 2. Identification of inhibitors in *Allobaculum* conditioned medium.** (A) Overview of different steps in *Allobaculum* conditioned medium fractionation and inhibitor identification. (B) *A. muciniphila* growth was assessed after 48 h in the presence of 25% size-fractionated *Allobaculum* CM. Growth is depicted as a percentage of Gut Microbiota Medium (GMM) control. Size-fractionation was performed on Amicon spin-columns. (C) *A. muciniphila* growth ( $OD_{600}$ ) after 48 h in presence of 25% *Allobaculum* CM that was pretreated with Proteinase K. A 40x concentrated, >50 kDa fraction of *Allobaculum* CM was further fractionated using a size-exclusion column. (D) Chromatogram of size-exclusion fractionation showing retention volume (X-axis) and protein concentration as determined by measuring absorbance at 280 nm (Y-axis). (E) *A. muciniphila* growth at 48 h, as a percentage of PBS control, in the presence of the different size-exclusion fractions at a final concentration of 50%. Inhibiting fractions 17-27 were separated using SDS-PAGE and stained with a Coomassie stain (F). Inhibiting size-exclusion fractions 17 to 28 were pooled and separated further using anion-exchange chromatography. (G) Chromatogram of anion-exchange fractionation showing retention volume (X-axis) and protein concentration as determined by measuring absorbance at 280 nm (Y-axis). (H) *A. muciniphila* growth at 48 h, as a percentage of molarity control, in the presence of the different anion-exchange fractions at a final concentration of 25%. Inhibiting and non-inhibiting anion-exchange fractions were separated using SDS-PAGE and stained with a Coomassie stain (I). The strongest inhibiting anion-exchange fraction 50, and a non-inhibiting fraction 12 were analysed using LC-MS/MS and the detected peptides were aligned against the *Allobaculum* genome. The table (J) shows the ten most abundant proteins, as determined by the number of unique peptides per protein and their putative annotation based on automated annotations using Prokka and the dbCAN2 metaserver. *A. muciniphila* growth ( $OD_{600}$ ) after 48 h in presence of 0, 12.5 or 25% *Allobaculum* CM and 0, 1, 5 or 25 mM of either (K) D+fucose, (L), sialic acid (Neu5Ac), (M) D+galactose, (N) N-acetylglucosamine (GlcNAc) or (O) N-acetylgalactosamine

(GalNAc). (P) The size-fractionated and (Q) anion-exchange fractions from a 48 h culture of *Allobaculum* grown in Gut Microbiota Medium, matching the fractions in figure 2B and 2H, respectively, were incubated with fluorescent 4-methylumbelliferone linked  $\alpha$ -N-acetylneuraminic acid (sialic acid) for 30 minutes at 37°C. Fluorescence was recorded over time (P) or at the end-point (Q). All results are based on at least three experimentally independent replicates, each with two or three technical replicates per condition. Bar plots represent the mean  $\pm$  SD. Statistical analysis was performed using GraphPad Prism, using a one-way (C) or two-way (K-O) ANOVA with Dunnett's multiple comparison test. \* =  $P < 0.05$ , \*\* =  $P < 0.01$ , \*\*\* =  $P < 0.001$ , \*\*\*\* =  $P < 0.0001$ .

As a next step, the inhibiting size-exclusion fractions 17 to 28 were pooled and separated further using anion-exchange chromatography (Figure 2G). Again, fractions were collected and tested for *A. muciniphila* growth inhibition at a final concentration of 25% (v/v). As successive fractions contained increasing amounts of eluting buffer and therefore a higher concentration of NaCl, appropriate molarity medium controls were used to compare each fraction. This showed that anion-exchange fractions 41 to 55, corresponding to retention volumes between 27 and 34.5 mL, reduced growth of *A. muciniphila*, with fraction 50 causing the strongest growth reduction of more than 85% (Figure 2H). The inhibitory fractions corresponded with the third rather small peak in the anion-exchange chromatogram. SDS-PAGE analysis of the inhibitory fractions showed several bands (Figure 2I) but noticeably fewer than in Figure 2F, highlighting the effectiveness of the anion-exchange chromatography.

To learn more about the composition of the inhibitory fractions, the anion-exchange fraction with the strongest inhibitory activity (fraction 50) and a non-inhibiting fraction (fraction 12) were analysed using mass spectrometry. Detected peptides were aligned against the *Allobaculum* genome. The ten most abundant proteins detected in fraction 50, as determined by the number of unique peptides per protein, are displayed in Figure 2J. All these proteins had a molecular mass larger than 100 kDa. Automated annotation of the detected proteins suggested that three proteins were of unknown function, and a majority (7 out of 10) were putative glycosidases that contain one or multiple carbohydrate active enzyme (CAZY) domains. We have previously demonstrated that a number of these *Allobaculum* glycosidases are likely to be involved in mucin glycan degradation (Thesis Chapter 3).

### The secreted *Allobaculum* sialidase NanH1 inhibits the growth of *A. muciniphila*

To test whether glycosidases in the *Allobaculum* supernatant contributed to the inhibition of *A. muciniphila* growth, *A. muciniphila* was grown in the presence of 25% *Allobaculum* conditioned medium supplemented with one of five different monosaccharides often found in host-derived *O*-glycans: D+fucose, sialic acid (Neu5Ac), D+galactose, N-acetylglucosamine (GlcNAc) or N-acetylgalactosamine (GalNAc) (Figure 2K-O). We hypothesized that by adding these monosaccharides at high concentrations glycosidases present in the *Allobaculum* supernatant could be (partially) inhibited, leading to a rescue of *A. muciniphila* growth. In the presence of the highest concentration tested, D-(+)-fucose and D-(+)-galactose did not alleviate growth inhibition of *A. muciniphila* (Figure 2K & M). On the other hand, the presence of 5 mM Neu5Ac, GlcNAc or GalNAc rescued *A. muciniphila* growth (Figure 2L, N, O). Notably, when the concentration of either GlcNAc or GalNAc was increased to 25 mM, this again reduced the growth of *A. muciniphila*, suggesting potential toxicity/growth inhibitory effects of these substrates at higher concentrations. This effect was not seen with 25 mM of Neu5Ac. The consistent effect of sialic acid supplementation and the abundant presence of a sialidase in the inhibitory fraction as detected by MS (Figure 2J) led us to test for the presence of sialidase activity in the *Allobaculum* conditioned medium. Using the fluorescent 4-MU-NANA substrate, high levels of sialidase activity could indeed be detected in the inhibiting size-exclusion and anion-exchange fractions (Figure 2P & Q). Moreover, the levels of sialidase activity highly correlated with the level of inhibition of *A. muciniphila* growth. This combination of data suggests that the *Allobaculum* sialidase could play a role in the inhibition of *A. muciniphila* growth.

### Inhibition of *A. muciniphila* growth by the *Allobaculum* sialidase NanH1 and other bacterial sialidases

Inspection of the sequence of the sialidase gene (Allo\_00594) of *Allobaculum* demonstrated that it encodes a 1,762 amino acid protein with six domains including a non-viral sialidase domain (Figure 3A). This sialidase is further referred to here as NanH1. The *Allobaculum* NanH1 protein and NanH1 $\Delta$ RIP, a generated construct with a mutation in the active site, were expressed in *E. coli* after which sialidase activity was assessed using the 4-MU-NANA substrate (Figure 3B-C). Recombinant *Allobaculum* NanH1 demonstrated potent sialidase activity on this substrate, whereas this was completely absent

after heat-inactivation or in NanH1 $\Delta$ RIP. Moreover, the sialidase activity could be inhibited in a dose-dependent manner using 25 mM Neu5Ac or the sialic acid analogue oseltamivir phosphate (Figure 3C).

Next, we checked whether the recombinant sialidase was capable and sufficient to inhibit the growth of *A. muciniphila*. Culturing *A. muciniphila* for 48 hours in media supplemented with recombinant NanH1 greatly reduced the growth of *A. muciniphila*, whereas heat-inactivated NanH1 or NanH1 $\Delta$ RIP did not (Figure 3D). To confirm that the growth inhibition was caused by the sialidase activity rather than by one of the other domains present in NanH1, Neu5Ac was supplemented to the culture medium. This rescued the growth of *A. muciniphila* in a dose-dependent manner (Figure 3E), similar to what was seen for complete *Allobaculum* supernatant (Figure 2L). In order to test whether this sialidase-mediated inhibition is conserved across different strains of *A. muciniphila*, the type strain (ATCC BAA-835) was compared to a second, clinical *A. muciniphila* isolate. When recombinant NanH1 was added to a culture of this clinical isolate the growth of the isolate was also efficiently inhibited, suggesting that the mechanism underlying the growth inhibition is conserved among multiple strains. Together, these findings strongly suggest that the sialidase activity identified in the *Allobaculum* conditioned medium is due to NanH1 and that the sialidase activity is sufficient to inhibit *A. muciniphila* growth.

To assess the uniqueness of the inhibitory effect of the *Allobaculum* NanH1 on *A. muciniphila* growth, we tested four other bacterial sialidases for growth inhibitory activity: three commercially available bacterial sialidases from *Clostridium perfringens* (CPNA), *Vibrio cholerae* (VCNA), and *Arthobacter ureafaciens* (AUNA) and NanH2, which originates from the same *Allobaculum* strain as NanH1. Notably, when added to *A. muciniphila* cultures at equal levels of enzyme activity, these sialidases demonstrated differential inhibitory activities. CPNA and AUNA inhibited the growth of *A. muciniphila* to a similar extent as *Allobaculum* NanH1, whereas *Allobaculum* NanH2 and VCNA were much less efficient inhibitors (Figure 3G). These results show that the inhibition of *A. muciniphila* is not restricted to the *Allobaculum* NanH1 sialidase and that differences in substrate specificity of sialidases likely determines the efficiency with which they can inhibit the growth of *A. muciniphila*.

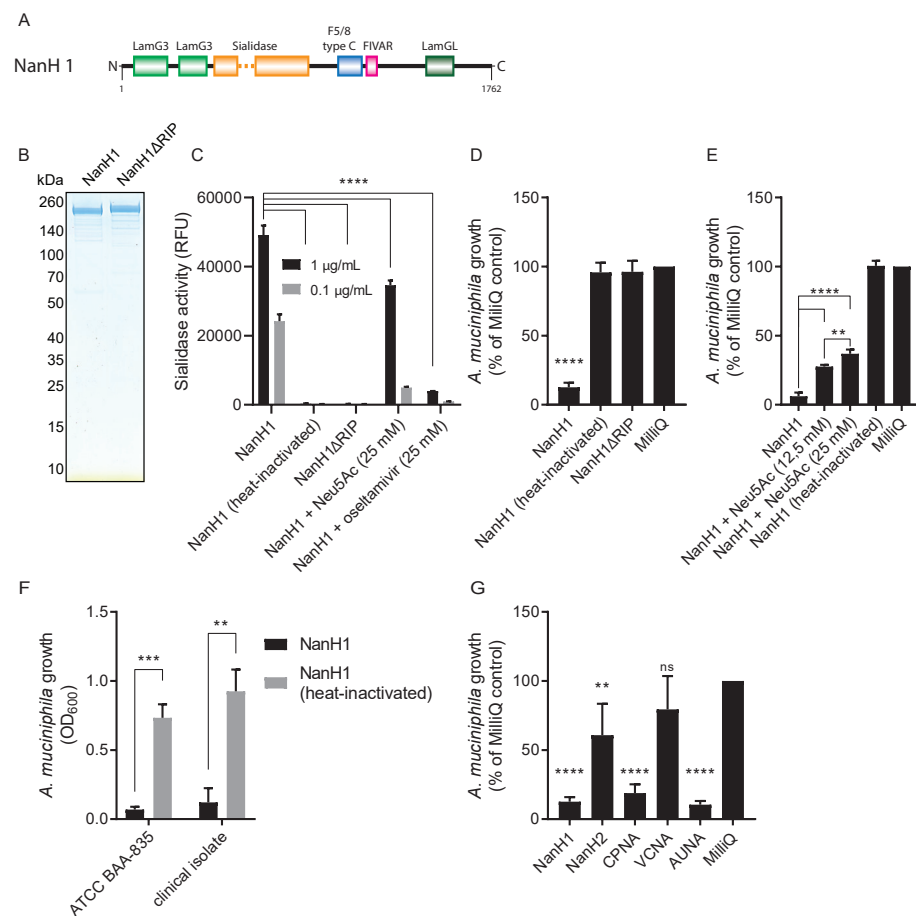


**Figure 3. *Allobaculum* sialidase NanH1 and other bacterial sialidase inhibit the growth of *A. muciniphila*.** (A) Domain architecture of NanH1. The displayed domains are those identified by BLAST search and are drawn to scale with polypeptide backbone. The number of amino acids in the backbone is indicated at the bottom. (B) Coomassie stain of recombinant NanH1 and NanH1ΔRIP separated by SDS-PAGE. (C) Sialidase activity of recombinant sialidases was determined by incubation with 4-methylumbelliferone linked  $\alpha$ -N-acetylneuraminic acid (sialic acid) for 30 minutes at 37°C. Fluorescence was recorded over time. Figures D-G all indicate the growth of *A. muciniphila* after 48 h in GMM with following experimental conditions: (D) Growth as percentage of control in presence of recombinant NanH1 constructs (2.5  $\mu$ g/mL). (E) Growth as percentage of control in presence of recombinant NanH1 (2.5  $\mu$ g/mL) and sialic acid (Neu5Ac). (F) Growth ( $OD_{600}$ ) of *A. muciniphila* type strain (ATCC BAA-835) and clinical *A. muciniphila* isolate in the presence of active or heat-inactivated NanH1 (2.5  $\mu$ g/mL). (G) Growth as percentage of control in presence of a panel of sialidases of which the enzyme activities were normalized to match the sialidase activity of NanH1 (2.5  $\mu$ g/mL) on the 4-MU-NANA substrate. All results are based on at least three

experimentally independent replicates, each with two or three technical replicates per condition. Bar plots represent the mean  $\pm$  SD. Statistical analysis was performed using GraphPad Prism, using a two-way (C) or one-way (D, E, G) ANOVA with Tukey's multiple comparison test. In figure F statistical significance was determined using an unpaired *t* test \* =  $P < 0.05$ , \*\* =  $P < 0.01$ , \*\*\* =  $P < 0.001$ , \*\*\*\* =  $P < 0.0001$ .

### The *Allobaculum* sialidase NanH1 inhibits *A. muciniphila* growth through nutrient modification

Next, we investigated how sialidases inhibit the growth of *A. muciniphila*. While sialic acid may be present on the surface of *A. muciniphila*, the culture medium represents the largest source of sialylated substrates that could serve as target for the NanH1 sialidase. To examine whether nutrients within the culture medium were the prime target for NanH1 and its inhibiting effects on *A. muciniphila* growth, culture medium was pretreated for 16 h at 37 °C with NanH1 or heat-inactivated NanH1 as a control. After all remaining sialidase activity was eliminated by heat-inactivation, the treated culture medium was examined for its effect on *A. muciniphila* growth. Sialidase pretreatment of the culture medium inhibited the growth of *A. muciniphila* to the same extent as when active NanH1 was present during growth (Figure 4A). Additionally, both the growth kinetics and the morphological changes of *A. muciniphila* that were observed with *Allobaculum* conditioned medium, could be recapitulated by sialidase pretreatment of the culture medium (Figure 4A-C). In sialidase pretreated medium, the median length of *A. muciniphila* was 4.23  $\mu$ m versus 1.31  $\mu$ m in mock treated medium (Figure 4C). Together, these results indicate that *Allobaculum* NanH1 targets one or more components of the culture medium and that desialylation of this component results in *A. muciniphila* growth inhibition.

### NanH1 sialidase inhibits *A. muciniphila* growth through desialylation of casein O-glycans

Gut microbiota medium contains many different components, but only three components that are predicted to contain sialylated glycans: trypticase peptone (a pancreatic digest of milk casein), yeast extract and meat extract. To first identify whether these and other components in the medium are required for *A. muciniphila* growth, different media were formulated, each lacking one component. This demonstrated that, in addition to a basal medium, glucose and trypticase peptone are essential medium components, in contrast to yeast extract and meat extract, which were dispensable for *A. muciniphila* growth (Figure 5A).



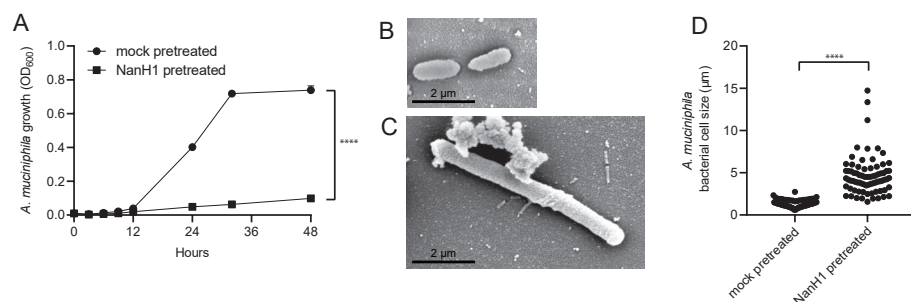


**Figure 4. Growth of *A. muciniphila* is inhibited by pretreatment of growth medium with *Allobaculum* sialidase.** (A) *A. muciniphila* growth curve over a 48 h period in the presence of NanH1 pretreated or mock pretreated Gut Microbiota Medium (GMM). Morphology of *A. muciniphila* was assessed after 48 h of growth in either (B) mock pretreated or (C) NanH1 pretreated GMM using scanning electron microscopy. Bars indicate 10 µm. *A. muciniphila* cell size was measured in confocal images of syto 9 nuclear stained bacteria grown for 48 h, using ImageJ software (D). Per condition the length of 75 bacteria was recorded: five bacteria from five different fields of view per independent bacterial culture. Graph depicts the mean values  $\pm$  SD acquired from three independent experiments. Statistical significance in A was determined for the 48 h time point by a *t* test. In D, statistical significance was determined using a Mann-Whitney U test. \*\*\*\*,  $P < 0.0001$ .

A more defined version of the gut microbiota medium was formulated with a combination of trypticase peptone and glucose as the only major glycan and carbon sources. This defined minimal medium (DMM) was sufficient to support *A. muciniphila* growth, albeit to a lower maximum OD (Figure 5B). Pretreatment of DMM with NanH1 resulted in reduced growth of *A. muciniphila*, similar to what was seen with treatment of complete gut microbiota medium (Figure 5B). This indicates that the trypticase peptone is not only an essential nutrient source for *A. muciniphila* but also that the *Allobaculum* NanH1 sialidase likely targets sialylated glycans on casein, resulting in inhibition of *A. muciniphila* growth. To investigate whether the inhibitory effect is caused by a loss of sialic acid from trypticase peptone glycans or is the result of increased levels of free sialic acid, the NanH1-pretreated or mock-pretreated DMM was fractionated into <3 kDa and >3 kDa fractions. Multiple on-column wash steps ensured removal of any free sialic acid from the >3 kDa fractions. *A. muciniphila* was able to grow in either unfractionated or the >3 kDa fraction of untreated

DMM, but not on NanH1-pretreated DMM or the <3 kDa fractions (Figure 5B). Moreover, when free sialic acid was supplemented to either the NanH1 or mock pretreated >3 kDa fraction, this did neither rescue nor inhibit the growth of *A. muciniphila* (Figure 5C). This demonstrates that the growth inhibition of *A. muciniphila* is not due to increased levels free sialic acid but rather due to the loss of sialic acid from casein glycans. Combined, these results demonstrate that *Allobaculum* inhibits *A. muciniphila* by secreting a sialidase that targets sialylated casein glycans that are critical for *A. muciniphila* growth.

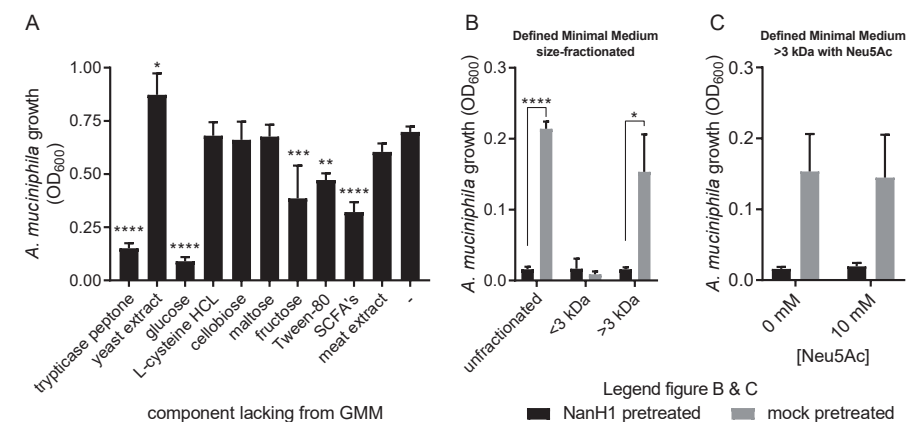


**Figure 5. Identification of trypticase peptone as a target of *Allobaculum* sialidase and as an essential medium component for *A. muciniphila* growth.** (A) *A. muciniphila* growth (OD<sub>600</sub>) after 48 h in variety of Gut Microbiota Medium formulations that lack one medium component at a time. (B) *A. muciniphila* growth (OD<sub>600</sub>) after 48 h in defined minimal medium (DMM) that was pretreated overnight with NanH1 (black bars) or a mock control (gray bars) and then size-fractionated. (C) *A. muciniphila* growth (OD<sub>600</sub>) after 48 h in NanH1 or mock pretreated >3 kDa DMM supplemented with 10 mM Neu5Ac. All results are based on at least three experimentally independent replicates, each with two or three technical replicates per condition. Bar plots represent the mean  $\pm$  SD. Statistical analysis for figure A was performed using GraphPad Prism, using a one-way ANOVA with Dunnett's multiple comparison test. Statistical significance in figure B was determined a *t* test. \* =  $P < 0.05$ , \*\* =  $P < 0.01$ , \*\*\* =  $P < 0.001$ , \*\*\*\* =  $P < 0.0001$ .

## DISCUSSION

Bacterial competition for nutrients and intermicrobial interactions are important determinants of the gut microbiota composition. In this study we set out to identify inhibitors of *A. muciniphila* growth that are secreted by bacterial competitors, as this may explain the reduced abundance of *A. muciniphila* in many diseases. Here we provide evidence that a sialidase from another intestinal mucin degrader, *Allobaculum*, can efficiently inhibit the growth of *A. muciniphila* through modification of the glycometabolic niche by targeting casein glycans that are required for growth.

We identified the sialidase-mediated inhibition of *A. muciniphila* by screening bacterial supernatants for inhibitory activity. The supernatant of *Allobaculum* clearly showed the most potent inhibition of *A. muciniphila* growth. Like *A. muciniphila*, *Allobaculum* secretes many glycosidases that can degrade (mucin) *O*-glycans (Chapter 3), showing that the metabolic programs of both bacteria are optimized for feeding on host glycans. This is important as it places these two anaerobic enteric bacteria in the same mucosal niche, where they would likely compete for space and nutrients. When competing for the same nutrients it can be imagined that bacteria evolve mechanisms to inhibit their competitors. However, as both *A. muciniphila* and *Allobaculum* are capable of producing sialidases, and sialidases are not known to act as inhibitors of bacterial growth, we did not anticipate to identify the *Allobaculum* NanH1 sialidase as the inhibitor of *A. muciniphila* growth<sup>33</sup>.

The NanH1 sialidase was identified as an inhibitor through a reductionist approach using multiple, consecutive fractionation methods. However, due to the sensitivity of mass spectrometric analyses this still left multiple candidate proteins, of which the majority were glycosidases that could be involved in mucin degradation. Due to the large number of candidate proteins we opted for an approach using the enzymes' putative cognate ligands, the mucin monosaccharides, to act as competitive inhibitors. This proved successful in identifying potential candidates as we were able to rescue the growth of *A. muciniphila* using Neu5Ac, GlcNAc and GalNAc. This suggested that the glycosidases that target these monosaccharides might be involved in the inhibition of *A. muciniphila*. Nonetheless, these findings could also point to the importance of GlcNAc and GalNAc in *A. muciniphila*'s metabolism, as exogenous supplementation of these metabolites was reported to be essential for *A. muciniphila* growth<sup>34</sup>. As multiple putative glucosaminidases were on our candidate list and, in this setup, it was difficult to delineate the

actions of these enzymes from the effects of the monosaccharides, we instead focused on the sialidase as the addition of Neu5Ac also rescued growth, but Neu5Ac cannot be metabolized by *A. muciniphila*<sup>35</sup>.

Multiple lines of evidence indicate that the NanH1 sialidase is able, and by itself sufficient to inhibit the growth of *A. muciniphila*. As a first step, using a sialidase activity reporter, we showed a near perfect inverse correlation between the levels of sialidase activity in the inhibitory fractions of the *Allobaculum* conditioned medium and the growth of *A. muciniphila*. Second, and most convincingly, we showed that recombinant NanH1 was capable of inhibiting *A. muciniphila* growth, but not when its sialidase activity was inhibited by Neu5Ac or inactivated through mutation of the catalytic site or by heat. As an additional confirmation of the central role of sialidase activity in the inhibitory process we showed that several other bacterial sialidases can also act as inhibitors of *A. muciniphila* growth. Bacterial sialidases often function as virulence factors and are known to play important roles in the degradation of mucin glycans. However, according to our knowledge, this is the first description of a sialidase that acts as an inhibitor of bacterial growth.

As a next step we identified the target of this sialidase. We demonstrated that pretreatment of the medium with NanH1 was sufficient to inhibit the growth of *A. muciniphila*. This indicated that the inhibition is mediated through modifications of sialoglycans in the growth medium rather than through direct effects on the cell surface of *A. muciniphila*. Then, using different growth media formulations, we showed that trypticase peptone was required for *A. muciniphila* growth and, importantly, that desialylation of this substrate was sufficient to inhibit the growth of this bacterium. Trypticase peptone is a pancreatic digest of bovine *k*-casein. Casein is a major glycoprotein in both bovine and human milk, and after digestion of *k*-casein by gastric and pancreatic proteases the glycosylated C-terminal part of this protein is also referred to as glycomacropeptide (GMP)<sup>37</sup>. GMP contains multiple *O*-glycans, which are made up of terminally located sialic acid residues and underlying residues of galactose, GlcNAc and GalNAc. GlcNAc and/or GalNAc, as well as L-threonine, which is abundantly present in the polypeptide backbone, are essential nutrients required for *A. muciniphila* growth<sup>34</sup>. The fact that GMP contains this tailor-made combination of essential metabolites likely explains the requirement for the substrate in the GMM growth medium and may provide clues about the mechanism underlying the sialidase-mediated growth inhibition of *A. muciniphila*.

Several scenarios can be envisioned as to how the sialidase may cause the inhibition of *A. muciniphila* growth on GMP. A first explanation could be that presence of sialic acid on the *O*-glycans is required for efficient hydrolysis of the glycan or the peptide backbone. However, this conflicts with the consensus view that the rate of glycoproteolysis is generally increased after the removal of terminal sialic acids<sup>38-40</sup>. An example of this is the much higher enzyme activity of the *A. muciniphila* *O*-glycopeptidase, OgpA, towards non-sialylated substrates<sup>41</sup>.

A second explanation could be that glycan-associated but not free sialic acid provides essential cues for the utilization of the casein GMP substrate, or that high concentrations of free sialic acid lead to catabolic repression. Transcriptional repression of the enzymes required for the sequential degradation of the underlying glycoprotein would then prevent further growth. However, catabolic repression by free sialic acid is not likely, as we were able to rescue growth of *A. muciniphila* in the presence of active *Allobaculum* conditioned medium by adding an excess of free sialic acid (Figure 2L). Moreover, *A. muciniphila* was also not able to grow on NanH1 pretreated DMM from which the liberated sialic acids were removed (Figure 5B). Although we cannot rule out the possibility that only complete, sialylated *O*-glycans may provide essential metabolic cues for *A. muciniphila*, it is difficult to envision how this would allow the bacterium to acquire essential nutrients, like GlcNAc and L-threonine, in situations when it actively secretes its own sialidases<sup>33</sup>. Although we have not verified the contribution of *A. muciniphila*'s own sialidases to this process, they are likely required for the degradation and growth on the fully sialylated GMP.

A third explanation for the growth inhibition could be that *A. muciniphila*, grown in the presence of fully sialylated GMP, tightly regulates its metabolic programme to match the rate at which monosaccharides are released from sialylated glycans, and that this rate is determined by *A. muciniphila*'s own sialidases. A suddenly increased rate of desialylation by an external sialidase, such as the *Allobaculum* sialidase, might disrupt this delicate balance and could lead to an increased rate of hydrolysis of the underlying glycan and a concomitant sudden increase in free *O*-glycan monosaccharides, such as galactose, GlcNAc and GalNAc. As the metabolic pathways for these substrates are highly intertwined, a sudden change in their availability could lead to metabolic dysregulation and a cessation of growth<sup>35,42</sup>. An example of this could be the toxic accumulation of sugar-phosphates, such as galactose-1-phosphate, which are linked to growth defects in wide variety of species

across multiple kingdoms of life<sup>43-45</sup>. Van der Ark *et al.* have also demonstrated that these metabolic pathways are intricately linked to processes of bacterial growth and cell morphology, as *A. muciniphila* requires exogenous GlcNAc or GalNAc for peptidoglycan synthesis<sup>34,42</sup>. Similar to our observation in sialidase-pretreated medium, this study also observed a highly elongated morphology of *A. muciniphila* when it was grown in synthetic PT medium<sup>42</sup>. The authors suggested that it could be caused by an imbalance between the availability of glucose and GlcNAc in this medium. The fact that these different growth media induce a similar elongated phenotype of *A. muciniphila* may point towards a similar underlying mechanism of metabolic dysregulation.

Besides valuable new insights into the intricate metabolism and cell biology of *A. muciniphila*, our findings also shed a new light on the role of sialidases in microbial ecology. First of all, we demonstrate that GMP supports the growth of *A. muciniphila*. The fact that this highly abundant milk protein supports growth may not be entirely surprising given the fact that the *O*-glycans present on GMP are similar to mucin *O*-glycans. Furthermore, it also aligns with a recent report by Kostopoulos *et al.*<sup>46</sup> who reported that *A. muciniphila* can also use human milk oligosaccharides for growth. Moreover, the fact that the highly abundant milk protein supports the growth of *A. muciniphila* can have important implications for the establishment of the early life microbiota. This notion is supported by the fact that GMP glycans also promote the growth of *Bifidobacterium longum* subsp. *infantis*, which colonizes the infant early after birth<sup>47</sup>. Many of the first bacterial colonizers in early life, including many of the *Bacteroides* and *Bifidobacteria* are known sialidase producers. Even though we did not see a significant inhibitory effect of these species on *A. muciniphila*'s growth *in vitro* (Figure 1A-C), sialidases from these bacteria or from pathobionts similar to *Allobaculum* could be important actors *in vivo* and affect *A. muciniphila*'s ability to establish itself within the neonatal intestinal ecosystem. Besides the effects on bacterial ecology, desialylation of GMP may also affect some of GMP's other biological functions. Sialic acid residues on GMP were previously shown to neutralize enteropathogens as well as inhibit the LPS-induced proliferation of spleen lymphocytes<sup>48-50</sup>. Sialidase-mediated removal of these sialic acids could therefore impact intestinal homeostasis.

In addition to demonstrating the inhibitory effect of the *Allobaculum* NanH1 sialidase, we also demonstrated that this effect can be exerted by sialidases from other bacteria, such as *C. perfringens*. This implies that the findings from *Allobaculum* could potentially also be extended to other sialidase-producing bacteria living in the intestinal mucosal niche. This hypothesis is in

line with findings by Png *et al.*<sup>24</sup> who reported inverse correlations between the abundance of *A. muciniphila* and the sialidase-producing mucin degraders *Ruminococcus gnavus* and *Ruminococcus torques*, which are known to occupy the same niche as *A. muciniphila*. We did not detect an inhibitory effect of the cell free supernatant of *R. gnavus* (Figure 1) but this might be explained by strain-dependent differences in the absence or presence of sialidase genes, or an inability of *R. gnavus* to sufficiently express the sialidases in the culture medium<sup>39</sup>.

The fact that multiple isolates of *A. muciniphila* seem to be susceptible to sialidase-mediated growth inhibition suggests that the mechanisms underlying this susceptibility are conserved and that this trait may be essential or beneficial *in vivo*. A reduced growth rate can have major negative consequences for bacterial fitness in complex multi-species bacterial communities, where competition for space and nutrients serves as a strong selective pressure. As such the question may arise why this trait is evolutionarily conserved among multiple strains of *A. muciniphila*, even though it makes them vulnerable to sialidase-mediated growth inhibition<sup>51</sup>. One possible explanation is that *A. muciniphila* does not commonly encounter “external” inhibitory sialidases. However, this is unlikely given the abundance of sialidase-encoding bacteria in the mucosal niche, even when considering not all sialidases may have the required specificity. Another explanation could be that *A. muciniphila* is incapable of adapting to sialidase inhibition, as the mutations or altered gene expression required to adapt interfere with processes that are essential for cell division and survival. The dependency on exogenous GlcNAc/GalNAc for peptidoglycan synthesis may support this notion. Alternatively, it can be imagined that successful adaptation to sialidase-mediated inhibition may alter the bacterium’s physiology (e.g., capsule or membrane structure) in such a way that this renders it more susceptible to other even stronger selective pressures such as phage predation or host immune responses<sup>52</sup>.

The question remains whether our findings also apply in a more complex *in vivo* setting. This will depend on whether *A. muciniphila* and *Allobaculum*, or other sialidase-producing bacteria do indeed encounter each other in the same (mucosal) niche, and whether the sialidase is produced and able to exert the inhibitory influence under these conditions. The fact that both *A. muciniphila* and *Allobaculum* have the ability to degrade mucins and the fact they are both found to be highly IgA coated suggests that they may inhabit the same niche *in vivo*. Regardless, our bottom-up *in vitro* approach allowed us to identify

and validate causal relationships between the growth of *A. muciniphila* and secreted products from other bacteria. This powerful approach can also be applied to any bacteria for which conditioned culture media are available. Moreover, the simplicity and efficacy of our experimental setup could allow for easy upscaling to a much larger number of bacterial supernatants, especially when combined with high-throughput culturomics techniques. Such a high-throughput screen will likely result in the identification of more growth inhibiting or growth promoting factors for *A. muciniphila* and other bacteria. As we have shown here, this approach can unveil hitherto unknown molecular mechanisms and provide important new insights in microbial cell biology and microbial ecology. These new insights may pave the way for new therapeutic approaches that prevent the loss of *A. muciniphila*.

## REFERENCES

1. THMPC. Structure, Function and Diversity of the Healthy Human Microbiome. *Nature*. 2013;486(7402):207–214. doi:10.1038/nature11234. Structure
2. Yassour M, Vatanen T, Siljander H, Hämäläinen AM, Härkönen T, Ryhänen SJ, Franzosa EA, Vlamakis H, Huttenhower C, Gevers D, *et al.* Natural history of the infant gut microbiome and impact of antibiotic treatment on bacterial strain diversity and stability. *Science Translational Medicine*. 2016;8(343). doi:10.1126/scitranslmed.aad0917
3. Rao C, Coyte KZ, Bainter W, Geha RS, Martin CR, Rakoff-Nahoum S. Multi-kingdom ecological drivers of microbiota assembly in preterm infants. *Nature*. 2021;591(7851):633–638. doi:10.1038/s41586-021-03241-8
4. Stewart CJ, Ajami NJ, O'Brien JL, Hutchinson DS, Smith DP, Wong MC, Ross MC, Lloyd RE, Doddapaneni HV, Metcalf GA, *et al.* Temporal development of the gut microbiome in early childhood from the TEDDY study. *Nature*. 2018;562(7728):583–588. doi:10.1038/s41586-018-0617-x
5. Proctor LM, Creasy HH, Fettweis JM, Lloyd-Price J, Mahurkar A, Zhou W, Buck GA, Snyder MP, Strauss JF, Weinstock GM, *et al.* The Integrative Human Microbiome Project. *Nature*. 2019;569(7758):641–648. doi:10.1038/s41586-019-1238-8
6. Vich Vila A, Imhann F, Collij V, Jankipersadsing SA, Gurry T, Mujagic Z, Kurilshikov A, Bonder MJ, Jiang X, Tigchelaar EF, *et al.* Gut microbiota composition and functional changes in inflammatory bowel disease and irritable bowel syndrome. *Science Translational Medicine*. 2018;10(472):eaap8914. doi:10.1126/scitranslmed.aap8914
7. Yachida S, Mizutani S, Shiroma H, Shiba S, Nakajima T, Sakamoto T, Watanabe H, Masuda K, Nishimoto Y, Kubo M, *et al.* Metagenomic and metabolomic analyses reveal distinct stage-specific phenotypes of the gut microbiota in colorectal cancer. *Nature Medicine*. 2019;25(6):968–976. doi:10.1038/s41591-019-0458-7
8. Zhao L, Zhang F, Ding X, Wu G, Lam YY, Wang X, Fu H, Xue X, Lu C, Ma J, *et al.* Gut bacteria selectively promoted by dietary fibers alleviate type 2 diabetes. *Science*. 2018;359(6380):1151–1156. doi:10.1126/science.aao5774
9. Yin Y, Mao X, Yang J, Chen X, Mao F, Xu Y. dbCAN: A web resource for automated carbohydrate-active enzyme annotation. *Nucleic Acids Research*. 2012;40(W1):W445–W451. doi:10.1093/nar/gks479
10. Honda K, Littman DR. The microbiota in adaptive immune homeostasis and disease. *Nature*. 2016;535(7610):75–84. doi:10.1038/nature18848
11. Chen H, Nwe P-K, Yang Y, Rosen CE, Bielecka AA, Kuchroo M, Cline GW, Kruse AC, Ring AM, Crawford JM, *et al.* A Forward Chemical Genetic Screen Reveals Gut Microbiota Metabolites That Modulate Host Physiology. *Cell*. 2019;177(5):1217–1231.e18. doi:10.1016/j.cell.2019.03.036
12. Donaldson GP, Lee SM, Mazmanian SK. Gut biogeography of the bacterial microbiota. *Nature Reviews Microbiology*. 2015;14(1):20–32. doi:10.1038/nrmicro3552
13. Tropini C, Earle KA, Huang KC, Sonnenburg JL. The Gut Microbiome: Connecting Spatial Organization to Function. *Cell Host & Microbe*. 2017;21(4):433–442. doi:10.1016/j.chom.2017.03.010
14. Martens EC, Neumann M, Desai MS. Interactions of commensal and pathogenic microorganisms with the intestinal mucosal barrier. *Nature Reviews Microbiology*. 2018;16(8):457–470. doi:10.1038/s41579-018-0036-x
15. Daniel N, Lécuyer E, Chassaing B. Host/microbiota interactions in health and diseases Time for mucosal microbiology! *Mucosal Immunology*. 2021;(January). doi:10.1038/s41385-021-00383-w
16. Atarashi K, Tanoue T, Ando M, Kamada N, Nagano Y, Narushima S, Suda W, Imaoka A, Setoyama H, Nagamori T, *et al.* Th17 Cell Induction by Adhesion of Microbes to Intestinal Epithelial Cells. *Cell*. 2015;163(2):367–380. doi:10.1016/j.cell.2015.08.058
17. Mazmanian SK, Round JL, Kasper DL. A microbial symbiosis factor prevents intestinal inflammatory disease. *Nature*. 2008;453(7195):620–5. doi:10.1038/nature07008
18. Palm NW, de Zoete MR, Cullen TW, Barry NA, Stefanowski J, Hao L, Degnan PH, Hu J, Peter I, Zhang W, *et al.* Immunoglobulin A Coating Identifies Colitogenic Bacteria in Inflammatory Bowel Disease. *Cell*. 2014;158(5):1000–1010. doi:10.1016/j.cell.2014.08.006
19. Derrien M, Vaughan EE, Plugge CM, de Vos WM. *Akkermansia muciniphila* gen. nov., sp. nov., a human intestinal mucin-degrading bacterium. *International Journal of Systematic and Evolutionary Microbiology*. 2004;54(5):1469–1476. doi:10.1099/ijs.0.02873-0
20. Derrien M, Belzer C, de Vos WM. *Akkermansia muciniphila* and its role in regulating host functions. *Microbial Pathogenesis*. 2017;106:171–181. (Microbiota and nutrition). doi:10.1016/j.micpath.2016.02.005
21. Derrien M. Mucin utilisation and Host Interactions of the Novel Intestinal Microbe *Akkermansia muciniphila*. 2007.
22. Planer JD, Peng Y, Kau AL, Blanton L V., Ndao IM, Tarr PI, Warner BB, Gordon JI. Development of the gut microbiota and mucosal IgA responses in twins and gnotobiotic mice. *Nature*. 2016;534(7606):263–266. doi:10.1038/nature17940
23. Bunker JJ, Flynn TM, Koval JC, Shaw DG, Meisel M, McDonald BD, Ishizuka IE, Dent AL, Wilson PC, Jabri B, *et al.* Innate and Adaptive Humoral Responses Coat Distinct Commensal Bacteria with Immunoglobulin A. *Immunity*. 2015;43(3):541–553. doi:10.1016/j.immuni.2015.08.007
24. Png CW, Lindén SK, Gilshenan KS, Zoetendal EG, McSweeney CS, Sly LI, McGuckin MA, Florin THJ. Mucolytic bacteria with increased prevalence in IBD mucosa augment in vitro utilization of mucin by other bacteria. *American Journal of Gastroenterology*. 2010;105(11):2420–2428. doi:10.1038/ajg.2010.281
25. Rajilić-Stojanović M, Shanahan F, Guarner F, De Vos WM. Phylogenetic analysis of dysbiosis in ulcerative colitis during remission. *Inflammatory Bowel Diseases*. 2013;19(3):481–488. doi:10.1097/MIB.0b013e31827fec6d

26. David LA, Maurice CF, Carmody RN, Gootenberg DB, Button JE, Wolfe BE, Ling A V, Devlin AS, Varma Y, Fischbach MA, *et al.* Diet rapidly and reproducibly alters the human gut microbiome. *Nature*. 2014;505(7484):559–63. doi:10.1038/nature12820
27. Sonnenburg ED, Smits SA, Tikhonov M, Higginbottom SK, Wingreen NS, Sonnenburg JL. Diet-induced extinctions in the gut microbiota compound over generations. *Nature*. 2016;529(7585):212–215. doi:10.1038/nature16504
28. Schulfer AF, Battaglia T, Alvarez Y, Bijmens L, Ruiz VE, Ho M, Robinson S, Ward T, Cox LM, Rogers AB, *et al.* Intergenerational transfer of antibiotic-perturbed microbiota enhances colitis in susceptible mice. *Nature Microbiology*. 2018;3(2):234–242. doi:10.1038/s41564-017-0075-5
29. Cox LM, Yamanishi S, Sohn J, Alekseyenko A V, Leung JM, Cho I, Rogers AB, Kim SG, Li H, Gao Z, *et al.* Altering the Intestinal Microbiota during a Critical Developmental Window Has Lasting Metabolic Consequences. *Cell*. 2014;158(4):705–721. doi:10.1016/j.cell.2014.05.052
30. Rappsilber J, Mann M, Ishihama Y. Protocol for micro-purification, enrichment, pre-fractionation and storage of peptides for proteomics using StageTips. *Nature Protocols*. 2007;2(8):1896–1906. doi:10.1038/nprot.2007.261
31. Schindelin J, Arganda-Carreras I, Frise E, Kaynig V, Longair M, Pietzsch T, Preibisch S, Rueden C, Saalfeld S, Schmid B, *et al.* Fiji: an open-source platform for biological-image analysis. *Nature Methods*. 2012;9(7):676–682. doi:10.1038/nmeth.2019
32. Gaskell A, Crennell S, Taylor G. The three domains of a bacterial sialidase: a -propeller, an immunoglobulin module and a galactose-binding jelly-roll. *Structure*. 1995;3(11):1197–1205. doi:10.1016/S0969-2126(01)00255-6
33. Huang K, Wang MM, Kulnich A, Yao HL, Ma HY, Martínez JER, Duan XC, Chen H, Cai ZP, Flitsch SL, *et al.* Biochemical characterisation of the neuraminidase pool of the human gut symbiont *Akkermansia muciniphila*. *Carbohydrate Research*. 2015;415:60–65. doi:10.1016/j.carres.2015.08.001
34. van der Ark KCH, Aalvink S, Suarez-Diez M, Schaap PJ, de Vos WM, Belzer C. Model-driven design of a minimal medium for *Akkermansia muciniphila* confirms mucus adaptation. *Microbial Biotechnology*. 2018;11(3):476–485. doi:10.1111/1751-7915.13033
35. Ottman N, Davids M, Suarez-Diez M, Boeren S, Schaap PJ, dos Santos VAPM, Smidt H, Belzer C, de Vos WM. Genomescale model and omics analysis of metabolic capacities of *Akkermansia muciniphila* reveal a preferential mucin-degrading lifestyle. *Applied and Environmental Microbiology*. 2017;83(18):1–15. doi:10.1128/AEM.01014-17
36. Lewis LA, Gulati S, Burrowes E, Zheng B, Ram S, Rice PA.  $\alpha$ -2,3-Sialyltransferase Expression Level Impacts the Kinetics of Lipooligosaccharide Sialylation, Complement Resistance, and the Ability of *Neisseria gonorrhoeae* to Colonize the Murine Genital Tract. *mBio*. 2015;6(1):1–11. doi:10.1128/mBio.02465-14.Editor
37. Neelima, Sharma R, Rajput YS, Mann B. Chemical and functional properties of glycomacropeptide (GMP) and its role in the detection of cheese whey adulteration in milk: A review. *Dairy Science and Technology*. 2013;93(1):21–43. doi:10.1007/s13594-012-0095-0
38. Tailford LE, Crost EH, Kavanaugh D, Juge N. Mucin glycan foraging in the human gut microbiome. *Frontiers in Genetics*. 2015;6(FEB). doi:10.3389/fgene.2015.00081
39. Crost EH, Tailford LE, Le Gall G, Fons M, Henrissat B, Juge N. Utilisation of Mucin Glycans by the Human Gut Symbiont *Ruminococcus gnavus* Is Strain-Dependent. *PLoS ONE*. 2013;8(10). doi:10.1371/journal.pone.0076341
40. Lewis AL, Lewis WG. Host sialoglycans and bacterial sialidases: A mucosal perspective. *Cellular Microbiology*. 2012;14(8):1174–1182. doi:10.1111/j.1462-5822.2012.01807.x
41. Trastoy B, Naegeli A, Anso I, Sjögren J, Guerin ME. Structural basis of mammalian mucin processing by the human gut O-glycopeptidase OgpA from *Akkermansia muciniphila*. *Nature Communications*. 2020;11(1):1–14. doi:10.1038/s41467-020-18696-y
42. van der Ark K. Metabolic characterization and viable delivery of *Akkermansia muciniphila* for its future application. Wageningen University; 2018. doi:10.18174/427507
43. Yarmolinsky MB, Wiesmeyer H, Kalckar HM, Jordan E. Hereditary defects in galactose metabolism in *Escherichia coli* mutants, II. Galactose-induced sensitivity. *Proceedings of the National Academy of Sciences*. 1959;45(12):1786–1791. doi:10.1073/pnas.45.12.1786
44. Gibney PA, Schieler A, Chen JC, Bacha-Hummel JM, Botstein M, Volpe M, Silverman SJ, Xu Y, Bennett BD, Rabinowitz JD, *et al.* Common and divergent features of galactose-1-phosphate and fructose-1-phosphate toxicity in yeast. *Molecular Biology of the Cell*. 2018;29(8):897–910. doi:10.1091/mbc.E17-11-0666
45. Demirbas D, Coelho AI, Rubio-Gozalbo ME, Berry GT. Hereditary galactosemia. *Metabolism: Clinical and Experimental*. 2018;83:188–196. doi:10.1016/j.metabol.2018.01.025
46. Kostopoulos I, Elzinga J, Ottman N, Klievink JT, Blijenberg B, Aalvink S, Boeren S, Mank M, Knol J, de Vos WM, *et al.* *Akkermansia muciniphila* uses human milk oligosaccharides to thrive in the early life conditions in vitro. *Scientific Reports*. 2020;10(1):1–17. doi:10.1038/s41598-020-71113-8
47. O'Riordan N, O'Callaghan J, Buttò LF, Kilcoyne M, Joshi L, Hickey RM. Bovine glycomacropeptide promotes the growth of *Bifidobacterium longum* ssp. *infantis* and modulates its gene expression. *Journal of Dairy Science*. 2018;101(8):6730–6741. doi:10.3168/jds.2018-14499

48. Nakajima K, Tamura N, Kobayashi-Hattori K, Yoshida T, Hara-Kudo Y, Ikedo M, Sugita-Konishi Y, Hattori M. Prevention of Intestinal Infection by Glycomacropeptide. *Bioscience, Biotechnology, and Biochemistry*. 2005;69(12):2294–2301. doi:10.1271/bbb.69.2294
49. Otani H, Monnai M. Inhibition of proliferative responses of mouse spleen lymphocytes by bovine milk  $\kappa$ -casein digests. *Food and Agricultural Immunology*. 1993;5(4):219–229. doi:10.1080/09540109309354801
50. Córdova-Dávalos LE, Jiménez M, Salinas E. Glycomacropeptide bioactivity and health: A review highlighting action mechanisms and signaling pathways. *Nutrients*. 2019;11(3). doi:10.3390/nu11030598
51. Hibbing ME, Fuqua C, Parsek MR, Peterson SB. Bacterial competition: Surviving and thriving in the microbial jungle. *Nature Reviews Microbiology*. 2010;8(1):15–25. doi:10.1038/nrmicro2259
52. Diard M, Bakkeren E, Lentsch V, Rocker A, Bekele NA, Hoces D, Aslani S, Arnoldini M, Böhi F, Schumann-Moor K, *et al.* A rationally designed oral vaccine induces immunoglobulin A in the murine gut that directs the evolution of attenuated *Salmonella* variants. *Nature Microbiology*. 2021. doi:10.1038/s41564-021-00911-1

# 05

---

5

## **Desialylation of secretory IgA increases IgA-mediated neutrophil activation**

Guus H. van Muijlwijk<sup>1</sup>, Bogdan Susca Jippa<sup>1</sup>, Piet C. Aerts<sup>1</sup>, Jos P.M. van Putten<sup>2</sup>  
& Marcel R. de Zoete<sup>1</sup>

<sup>1</sup>Department of Medical Microbiology, University Medical Center Utrecht, Utrecht, Netherlands

<sup>2</sup>Department of Biomolecular Health Sciences, Utrecht University, Utrecht, Netherlands.



## 05

## ABSTRACT

Secretory IgA (sIgA) plays a major role in maintaining gastrointestinal host-microbiota homeostasis. Besides being a highly abundant antibody, sIgA is also highly glycosylated. The role of serum IgA glycans is widely acknowledged and known to play an important role in aberrant immune responses, for instance in IgA nephropathy. Compared to this, the role of glycans on the effector functions of secretory IgA remains largely unexplored. Here we report that a sialidase released by the IgA-coated intestinal pathobiont *A. mucolyticum*, as well as several other bacterial sialidases, remove sialic acid from human colostrum sIgA and that sIgA desialylation results in increased sIgA-mediated neutrophil activation. The enhanced sIgA-mediated neutrophil activation is reduced in the presence of free sialic acid or sialic acid analogues but can be even further enhanced by desialylation of the neutrophil cell surface. IgA-coated, sialidase-producing bacteria as well as excessive neutrophil responses are known to play important roles in intestinal inflammation. Our findings indicate that bacterial sialidases may contribute to the inflammatory process.

## INTRODUCTION

Secretory IgA (sIgA) is the most abundant immunoglobulin in our body. The role of sIgA in governing gastrointestinal host-microbiota interactions has been a field of great interest in recent years<sup>1-5</sup>. Gut microbiota-reactive IgA is produced by plasma cells in the intestinal lamina propria where two, or occasionally more, IgA monomers are joined together by the joining chain and translocated across the epithelial cells by the polymeric Ig receptor (pIgR)<sup>6</sup>. Part of this receptor, the secretory component, is proteolytically cleaved and donated to the IgA dimer upon secretion into the lumen. The highly glycosylated IgA dimer is then called secretory IgA.

SIgA can exert a wide variety of functions. Most importantly, sIgA contributes to intestinal homeostasis by limiting microbial overgrowth, bacterial adhesion and invasion of host cells. More specifically, sIgA leads to immune exclusion by neutralizing bacterial toxins, blocking bacterial adhesins and through bacterial enchainment<sup>7-9</sup>. SIgA was shown to bind a wide variety of commensal bacteria but especially inflammatory intestinal bacteria were highly IgA coated<sup>13-15</sup>. The importance of sIgA as a regulator of intestinal homeostasis is illustrated by the overgrowth of inflammatory bacteria during sIgA deficiency<sup>10</sup>. Secondly, it was demonstrated that sIgA is key in establishing a diverse and balanced microbiota early in life and shaping appropriate mucosal immune responses<sup>11,12</sup>. While it is generally accepted that binding of sIgA is in principle disadvantageous to bacteria, for some sIgA binding actually increased their potential to colonize the mucus layer<sup>16</sup>.

Beside its effects on bacteria, sIgA also forms a bridge between the adaptive and innate immune systems. IgA-opsonized bacteria or antigens can be sensed by a variety of IgA-receptor expressing cells, such as M-cells, dendritic cells, monocytes and neutrophils<sup>17</sup>. These interactions are crucial for IgA-mediated antigen sampling and the initiation of both tolerogenic and inflammatory responses towards the gut microbiota and invasive pathogens<sup>17-21</sup>.

Palm and De Zoete *et al.*<sup>13</sup> demonstrated that many IgA-coated bacteria can penetrate deep into the mucus layer and are capable of inducing severe inflammation in mouse models of colitis. One of these bacteria is the highly IgA-coated and colitogenic Gram-positive bacterium *Allobaculum mucolyticum*. We previously demonstrated its ability to secrete a wide variety of mucin degrading enzymes, including sialidases (Chapter 3). We also demonstrated that one of these enzymes, the NanH1 sialidase, could inhibit

the growth of other bacteria by modifying the glycometabolic niche (Chapter 4). sIgA contains many sialylated glycans, located on the heavy chain, joining chain and the secretory component. The two sIgA subclasses, sIgA1 and sIgA2, have slightly different glycosylation profiles, with the presence of *O*-glycans on the extended hinge region of IgA1 being the major difference<sup>3,22</sup>. Although glycosylation of other antibody classes, such as IgG and serum IgA, is known to play an important role in the regulation of antibody-mediated immune responses, the role of glycans on sIgA has received little attention thus far<sup>22-25</sup>. As *A. mucolyticum* is capable of desialylating numerous glycoproteins and known to induce potent sIgA responses, we investigated the role of its sialidase on sIgA glycosylation and sIgA-mediated immune responses.

## RESULTS

### Bacterial sialidases desialylate human colostrum secretory IgA

To investigate whether sIgA could be affected by the sialidase of *A. mucolyticum*, human colostrum-derived sIgA was incubated with recombinant NanH1 sialidase (10 µg/mL, 16 h, 37°C). After sialidase treatment, the two IgA subclasses sIgA1 and sIgA2 were separated by affinity purification (Figure 1). The purity of the fractions was verified by SDS-PAGE (Figure 2A). To examine the presence of sialic acids on sIgA, lectin blotting was performed with lectins of different specificity. Probing of blotted mock-treated sIgA with the sialic acid-specific SNA lectin yielded a strong signal for the heavy chain (HC) of sIgA2, and weaker signals for the HC of sIgA1 and the secretory component (SC) of both sIgA1 and sIgA2 (Figure 2B). After treatment of sIgA1 and sIgA2 with NanH1, binding of SNA could no longer be detected, indicating an almost complete removal of sialic acids from sIgA1 and sIgA2 by the NanH1 sialidase (Figure 2B).

To further substantiate the loss of sialic acids, blotted sIgAs were probed with the ECA lectin that binds to galactose or N-acetylgalactosamine (GalNAc) residues that become exposed after removal of the terminal sialic acids. ECA blotting yielded an exact inverse signal pattern compared to blotting with SNA, with low levels of exposed ECA-detectable galactose/GalNAc in the mock-treated samples but high levels after treatment with the NanH1 sialidases (Figure 2C). The ECA lectin also bound to a ~25 kDa protein, but this was independent of sialidase treatment. As the IgA light chain is not glycosylated, the ~25 kDa protein may be the joining chain, which has a predicted molecular mass of ~16 kDa when not glycosylated<sup>26</sup>.

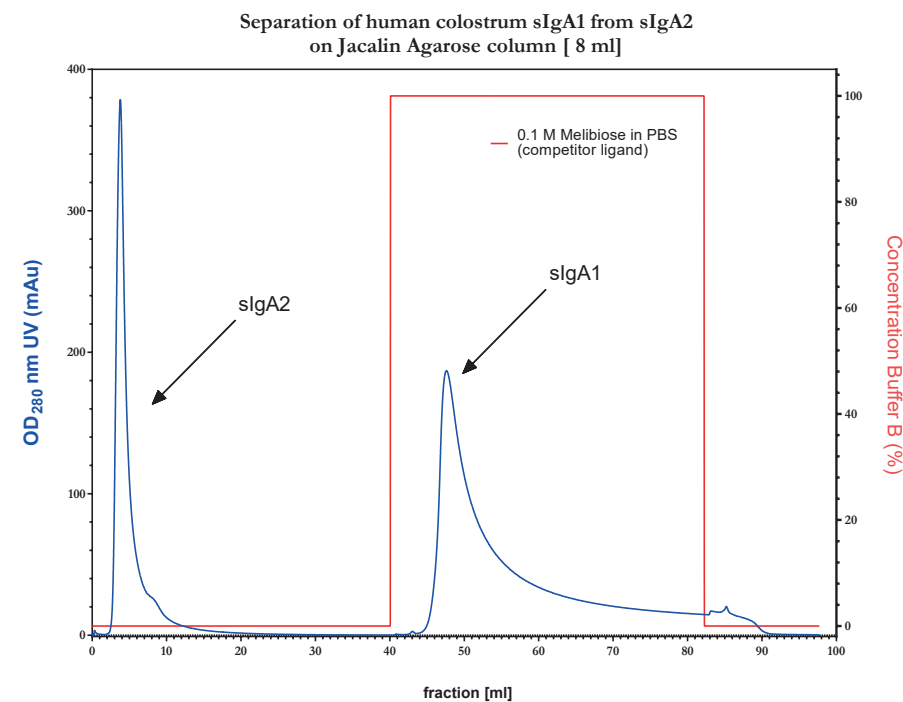


**Figure 1. Fractionation of human colostrum secretory IgA.** Chromatogram of human colostrum sIgA fractionation using a Jacalin agarose column. Retention volume is indicated on the X-axis and protein concentration was determined by measuring absorbance at 280 nm (blue, left Y-axis). The concentration of the elution buffer (0.1 M melibiose in PBS) is indicated on the right Y-axis in red.

To assess the uniqueness of the NanH1-mediated desialylation of sIgA, we repeated the experiment with three other, commercially available bacterial sialidases, CPNA, VCNA and AUNA, from *Clostridium perfringens*, *Vibrio cholerae*, and *Arthrobacter ureafaciens*, respectively. Colostrum-derived sIgA was treated with the enzymes after adjustment of their concentrations to match the enzyme activity of NanH1 used in Figure 1, as determined by a munana assay (data not shown). SNA and ECA-based glycan visualization showed a loss of SNA reactivity accompanied with an increase in ECA signal for each of the treated sIgA samples (Figure 2D-F). These results indicate that the NanH1 sialidase from *A. mucolyticum* (as well as other bacterial sialidases) can effectively remove sialic acids from sIgA.

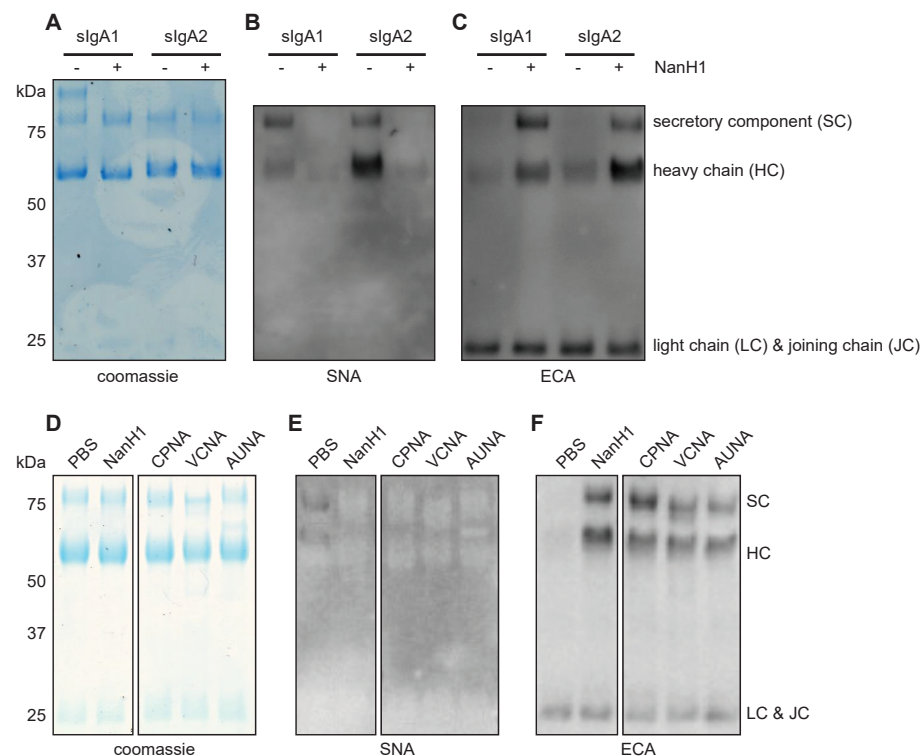


**Figure 2. Bacterial sialidases desialylate human colostrum secretory IgA.** (A) Coomassie blue staining after reducing SDS-PAGE of human colostrum slgA1 and slgA2 that was fractionated after treatment with 10 µg/mL NanH1 or PBS (control). Proteins from the same gel were blotted. The blot was stained with (B) SNA lectin (sialic acid detection) or with (C) ECA lectin (free terminal galactose detection). NanH1 treatment led to an increase in ECA signal and a decrease in SNA signal, indicating desialylation of slgA. The blots are representative of at least three independent experiments. (D-F) Coomassie blue staining and lectin blots of unfractionated human colostrum slgA treated with three commercially available sialidases, CPNA, VCNA and AUNA, from *Clostridium perfringens*, *Vibrio cholerae*, and *Arthrobacter ureafaciens*, respectively, of which the sialidase activity was adjusted to similar levels as NanH1 (10 µg/mL).

### Desialylation of slgA enhances slgA-mediated neutrophil activation

Next, we assessed whether sialic acids on slgA affect slgA-mediated neutrophil activation. Hereto we coated mock-treated and NanH1-treated slgA (both at 5 µg/mL) onto 96-well plates, after which freshly isolated human

polymorphonuclear leukocytes (PMNs), of which neutrophils are the most abundant cell population, were added to the wells. Neutrophil activation was assessed using a respiratory burst assay which follows the production of neutrophil-derived reactive oxygen species (ROS) for a period of 100 minutes. These experiments revealed a robust ROS production when the neutrophils were incubated with mock-treated slgA1 or slgA2 (Figure 3A-B), with a maximum response after approximately 25 minutes. Remarkably, stimulation of neutrophils with NanH1-treated desialylated slgA resulted in a markedly higher production of ROS. This effect was most pronounced when neutrophils were stimulated with desialylated slgA2 (slgA2-ds), which induced a two-fold higher maximum response compared to the fully glycosylated control (slgA2) (Figure 3B and E). The same trend could be observed for desialylated slgA1 (Figure 3A and E).

### Desialylation of slgA affects slgA-mediated neutrophil activation in a batch-dependent manner

Despite the fact that the slgA used for these experiments is pooled from multiple donors, variability in donors could still result in variations in different slgA batches. Therefore, a second batch of colostrum slgA was tested. Interestingly, the increased ROS production after sialidase-pretreatment of secretory IgA was indeed batch-dependent. When two batches of slgA were used in parallel in the same ROS production assay, the overall ROS production of batch #2 was lower than after stimulation with slgA batch #1. Furthermore, unlike what was observed with batch #1, no significant differences between slgA isotypes or NanH1-pretreatment could be observed (Figure 3C-E), even though slgA batch #2 was acquired from the same supplier and showed a similar ECA blot and Coomassie stain as batch #1 (Figure 3F). As the same fraction of PMNs was used and the differences in ROS production were observed when both slgA batches were tested in parallel, these batch-dependent effects may point towards slgA donor variability. Moreover, the batch-dependent effects on ROS production and the complete desialylation observed in both batches also indicate that the enhanced neutrophil activation can likely not be solely explained by the presence or absence of sialic acids on slgA alone.

### The role of FcαRI in slgA-mediated neutrophil activation

To further investigate the mechanism conferring the enhanced ROS production, we studied the interaction of slgA with its receptor. Although multiple IgA receptors exist, the FcαRI (CD89) is the principal IgA receptor on the surface of neutrophils<sup>17,27</sup>. To assess whether the observed slgA-driven activation of neutrophils is mediated by FcαRI, and whether the sialylation

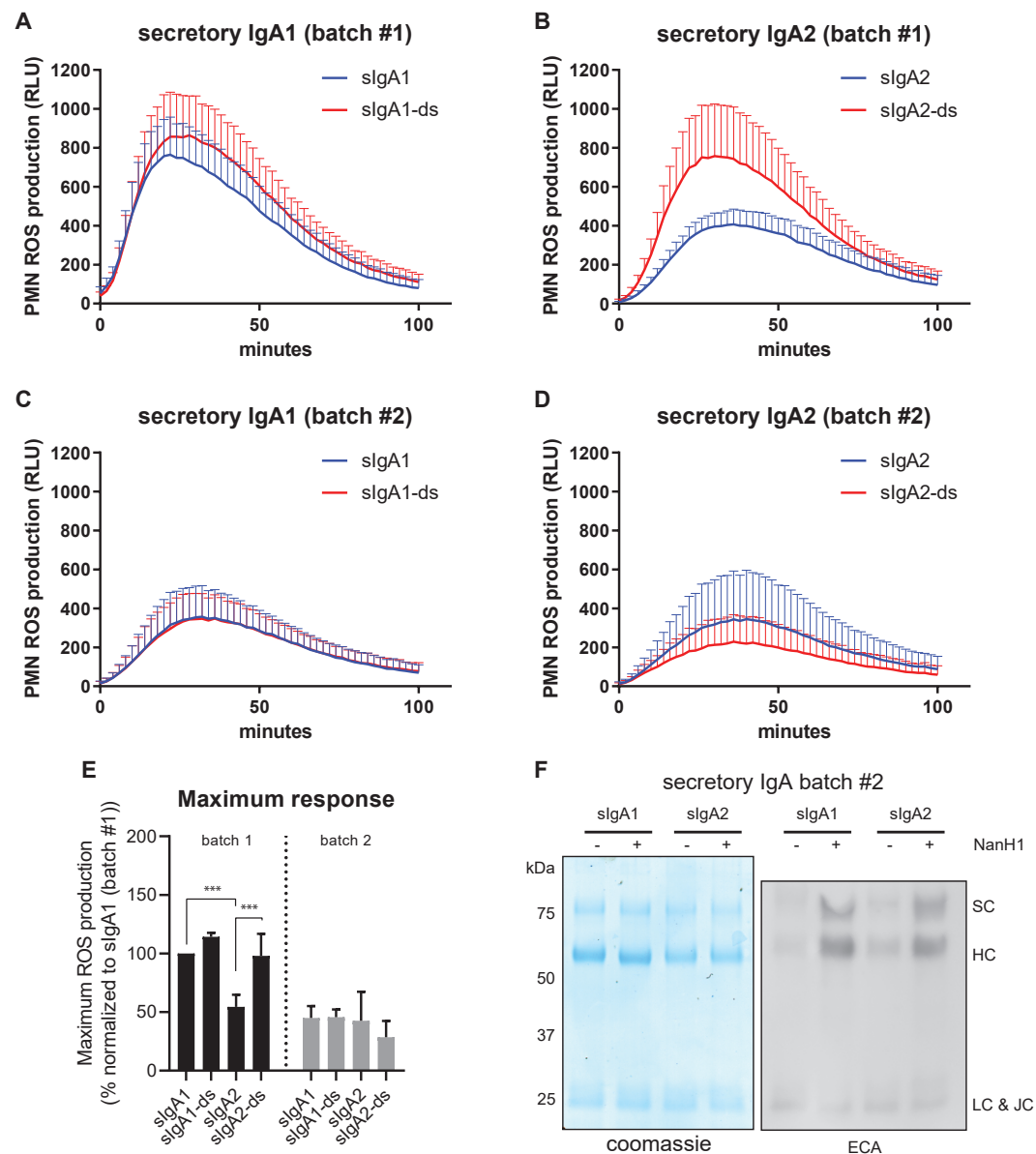


**Figure 3. SlgA desialylation affects slgA-mediated neutrophil activation.** Human Neutrophils isolated from fresh blood were mixed with luminol solution and added to a 96-well plate pre-coated with desialylated-slga1 (slgA1-ds), desialylated-slga2 (slgA2-ds), slgA1 or slgA2. Neutrophil activation was determined based on the production of reactive oxygen species (ROS) which in combination with luminol leads to luminescence. Time

course assay of ROS production by neutrophils stimulated with 5  $\mu\text{g}/\text{mL}$  of (A) slgA1 (batch #1), (B) slgA2 (batch #1), (C) slgA1 (batch #2) and (D) slgA2 (batch #2). The different slgA batches were tested in parallel using the same PMNs. Graphs represent mean. For clarity SD is only indicated in upward direction (E) Maximum luminescence achieved per condition during the 100 min long time course assay. (F) Coomassie blue staining and ECA lectin blot after reducing SDS-PAGE, of human colostrum slgA1 and slgA2 from slgA batch #2 that was fractionated after treatment with 10  $\mu\text{g}/\text{mL}$  NanH1 or PBS (control). All results are based on at least three experimentally independent replicates, each with two or three technical replicates per condition. Bar plots in E represent the mean  $\pm$  SD and are normalized to slgA1 (batch #1). Statistical analysis was performed using GraphPad Prism, using a one-way ANOVA with Tukey's multiple comparison test. Significant differences are indicated as follows: \* =  $P < 0.05$ , \*\* =  $P < 0.01$ , \*\*\* =  $P < 0.001$ , \*\*\*\* =  $P < 0.0001$ .

status of slgA affects this interaction, the respiratory burst assay was repeated in the presence of an Fc $\alpha$ R1 blocking antibody (MIP8a, 10  $\mu\text{g}/\text{mL}$ ) (Figure 4). The presence of the blocking antibody resulted in a trend toward less ROS production for all slgAs tested. This inhibitory effect was most pronounced with slgAs from batch 1, and reached statistical significance for sialylated slgA2, with >50% reduction in ROS production. While the effect of the blocking antibody was somewhat less pronounced with the desialylated slgAs, the sialylation status did not appear to be a major factor in the inhibition of ROS production. This suggests that while Fc $\alpha$ R1 contributed to the ROS production by slgA, the sialic acids on slgA do not play a significant role in receptor binding.

### Sialic acid and the NanH1 sialidase directly act on the neutrophil to modulate slgA-mediated neutrophil activation

In search for potential mechanisms that might explain the enhanced neutrophil activation after desialylation of slgA, we tested the effect of sialic acids on slgA-induced ROS production bearing in mind that sialic acids may target inhibitory sialic acid receptors (siglecs) on the neutrophil surface and thus limit ROS production<sup>30,31</sup>. Addition of 1 mM of Neu5Ac to the PMN medium resulted in a >50% reduction in maximum ROS production when stimulated with slgA1 as well as slgA1-ds. The same trend could be observed for slgA2 and slgA2-ds (Figure 5A). Addition of 1 mM of the sialic acid analogue oseltamivir phosphate, also known under the brand name Tamiflu, even resulted in a complete inhibition of neutrophil ROS production for all types of slgA tested. Together this showed that free sialic acids can act as a very potent inhibitor of slgA-mediated neutrophil activation, but this occurs independent of the sialylation status of slgA.

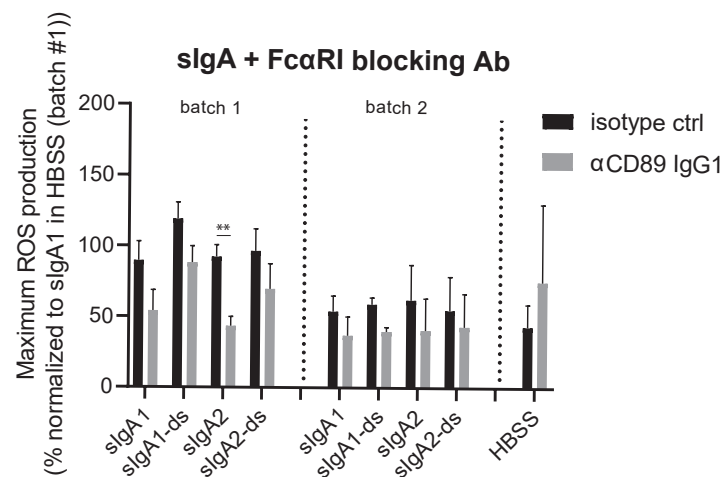


**Figure 4. Role of FcαRI in sIgA-mediated neutrophil activation.** Human PMNs isolated from fresh blood were mixed with luminol solution and added to a 96-well plate pre-coated with desialylated-sIgA1 (sIgA1-ds), desialylated-sIgA2 (sIgA2-ds), sIgA1 or sIgA2 from two different sIgA batches. Neutrophil activation was determined based on the production of reactive oxygen species (ROS) which in combination with luminol leads to luminescence. The different sIgA batches were tested in parallel using the same PMNs. Figure shows maximum luminescence with 5 μg/mL precoated sIgA in the presence of 10 μg/mL αCD89 blocking Ab or isotype control. Values are normalized to sIgA1 (batch #1). All results are based on at least three experimentally independent replicates, each with two or three technical replicates per condition. Bar plots represent the mean ± SD. Statistical analysis was performed using GraphPad Prism, using a two-way ANOVA with Tukey's multiple comparison test. Significant differences are indicated as follows: \* =  $P < 0.05$ , \*\* =  $P < 0.01$ , \*\*\* =  $P < 0.001$ , \*\*\*\* =  $P < 0.0001$ .

Besides activating siglecs directly, sialic acids may also act on siglecs indirectly by inhibiting exogenous (bacterial) and endogenous (NEU1) sialidases. Inhibition of such sialidases may prevent the disassociation of inhibitory siglecs with *cis*-acting, neutrophil-expressed sialoglycans or *trans*-acting exogenous sialic acids, as present on sIgA<sup>28,29</sup>. To assess whether sialidases can augment sIgA-mediated neutrophil responses, we added the NanH1 sialidase to the respiratory burst assay to target PMNs directly. The addition of the NanH1 sialidase (10 μg/mL) resulted in a great augmentation of sIgA-mediated neutrophil activation, with a >2-fold increase in maximum ROS production (Figure 5B). Heat-inactivation of NanH1 (30 min, 98°) completely abrogated this effect. Importantly, the presence of NanH1 alone was not sufficient for efficient neutrophil activation; this also required the presence of sIgA. Notably, the stimulatory effect of NanH1 was independent

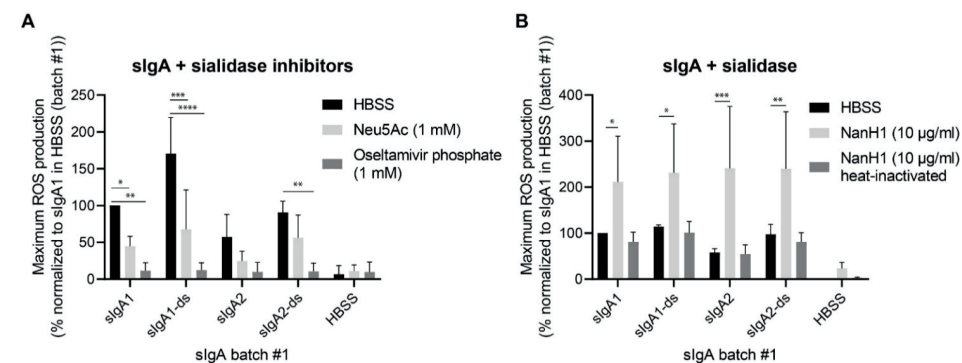


**Figure 5. Sialic acid and NanH1 sialidase modulate sIgA-mediated neutrophil activation.**

Neutrophils isolated from fresh blood were mixed with luminol solution and added to a 96-well plate pre-coated with desialylated-sIgA1 (sIgA1-ds), desialylated-sIgA2 (sIgA2-ds), sIgA1 or sIgA2 from batch #1. Neutrophil activation was determined based on the production of reactive oxygen species (ROS) which in combination with luminol leads to luminescence. (A) Maximum luminescence achieved after neutrophils were stimulated with 5 μg/mL sIgA in the presence of 1 mM sialic acid (Neu5Ac) and the sialic acid analogue osetamivir phosphate. (B) Maximum luminescence achieved after neutrophils were stimulated with 5 μg/mL sIgA in the presence of 10 μg/mL active or heat-inactivated (30 min, 98°C) NanH1. Values in A & B are normalized to sIgA1 in HBSS. All results are based on at least three experimentally independent replicates, each with two or three technical replicates per condition. Bar plots represent the mean ± SD. Statistical analysis was performed using GraphPad Prism, using a two-way ANOVA with Tukey's multiple comparison test. Significant differences are indicated as follows: \* =  $P < 0.05$ , \*\* =  $P < 0.01$ , \*\*\* =  $P < 0.001$ , \*\*\*\* =  $P < 0.0001$ .

of the sialylation status of sIgA, suggesting that removal of endogenous inhibitory sialoglycans on structures other than sIgA contributed to the effect. To exclude that, following desialylation, residual NanH1 remained bound to sIgA and caused the increased ROS production as seen in Figure 3, we assessed the presence of residual sialidase activity in the sIgA-coated wells using a 4-MU-NANA substrate. No sialidase activity could be detected in these assays (data not shown). Altogether, our findings suggest that *A. mucolyticum* NanH1 can independently target sialoglycans on sIgA as well as glycans on the neutrophil surface and that these endogenous sialoglycans can act as important regulators of IgA-mediated neutrophil responses.

## DISCUSSION

Here we report that the sialidase NanH1 from the IgA-coated intestinal pathobiont *A. mucolyticum*, as well as other bacterial sialidases, are capable of removing sialic acid from human secretory IgA. We provide evidence that the desialylation of sIgA glycans enhanced the sIgA-mediated neutrophil activation in a batch or donor-specific manner. In addition, we show that NanH1 regulates sIgA-mediated neutrophil activation through desialylation of neutrophil cell surface sialoglycans. Thus, the bacterial sialidase influences the host immune defence via multiple mechanisms.

The finding that the NanH1 sialidase from *A. mucolyticum*, as well as three other bacterial sialidases including the *C. perfringens* sialidase, removed sialic acid from sIgA became apparent after probing sIgA with SNA and ECA lectins, which detect penultimate sialic acid and galactose/GalNAc residues respectively. This showed loss of sialic acid reactivity that coincided with an unmasking of galactose/GalNAc reactivity. Although this lectin-based method did not allow analysis of individual glycosylation sites, for which a mass spectrometry-based approach would have been more suitable, we were able to determine that the sialoglycans on both the heavy chain and secretory component of colostrum IgA were efficiently desialylated. Our findings resemble to some extent the observation that the intestinal commensal *Bacteroides thetaiotamicron* uses its sialidase to remove sialic acids from sIgA *N*-glycans<sup>32</sup>. The bacterium *Gardnerella vaginalis*, which is associated with bacterial vaginosis, also efficiently desialylates sIgA<sup>33,34</sup>. This desialylation of sIgA in bacterial vaginosis increases IgA's susceptibility to further deglycosylation and proteolysis. We did not assess these effects in the current study, but we assume that desialylation by NanH1 also increases sIgA's susceptibility to proteolysis. The importance of these events is illustrated by the fact that the sialidase activity of the bacterial vaginosis-associated microbiota correlates with vaginosis disease severity<sup>35</sup>. This shows that the interaction between bacteria and sIgA glycans occurs in different mucosal compartments and that changes in its glycosylation can have major consequences for the function of sIgA.

It is well established that the glycosylation status of antibodies can have a major impact on their effector functions, e.g. by altering the antibody-Fc receptor interactions<sup>24,25</sup>. Intestinal inflammatory diseases, such as ulcerative colitis, are characterized by an influx of neutrophils as well as by increased

rates of pro-inflammatory, sIgA-coated bacteria, such as *A. mucolyticum*<sup>13,36,37</sup>. Therefore, we hypothesized that desialylation of secretory IgA might increase neutrophil activation. In Figure 3 we demonstrated that both sIgA1 and sIgA2 were able to efficiently activate neutrophil ROS production. Moreover, NanH1-mediated desialylation of sIgA increased neutrophil activation, suggesting a role for sIgA sialoglycans in regulating neutrophil responses. Our findings are in agreement with a recent report by Steffen *et al.*<sup>25</sup>, who demonstrated a differential neutrophil activation capacity between serum IgA1 and IgA2. Interestingly, this was related to the level of sialylation of the IgA *N*-glycans. The study demonstrated that removal of sialic acid from serum IgA1 increased its pro-inflammatory potential through increased neutrophil activation, which correlated with higher disease activity in rheumatoid arthritis patients. We also observe an inverse correlation between the level of sialylation and the rate of neutrophil activation.

An interesting result from our study was the sIgA batch-dependence of some of our results. We demonstrated that two batches of colostrum IgA were equally efficiently desialylated by the NanH1 sialidase (Figure 3F), but varied in their ability to activate neutrophils (Figure 3C-F). The presence or absence of sialic acid alone cannot explain the differences in neutrophil activation between the batches. Therefore, it might well be that sIgA-mediated neutrophil activation also depends on presence/absence or ratio of other glycans present on sIgA, for example fucose, which may act in concert with the sialoglycans. Through personal communication with the supplier (Sigma-Aldrich), we were informed that the batches of colostrum IgA were formulated using colostrum from only two or three donors per batch. This likely introduces large batch-to-batch differences, especially when considering glycosylation patterns can vary largely between individuals. An example of potential donor-variability is the *FUT2* secretor status, which determines the fucosylation of ABO blood group antigens. As about 20% of the Caucasian population are non-secretors, due to nonsense mutations, this could well affect fucosylation levels of different IgA batches. Our findings demonstrate both the complexity but also the necessity of validating results when using multiple antibody batches. Furthermore, investigation of the differences between batches with differential functionalities may provide important new insights in IgA effector functions. For instance, when differential sIgA functionalities correlate with altered glycosylation profiles, such profiles might serve as biomarkers for disease or can be used to optimize the design of therapeutic antibodies. Overall, this data demonstrated that the sialylation status of sIgA can modulate the neutrophil response in a batch-dependent manner.

How does the sIgA sialylation status affect neutrophil activation? In Figure 4, we show that FcαRI (CD89) plays a role in sIgA-mediated neutrophil activation. This is in line with previous research showing that FcαRI is the primary IgA receptor on phagocytic cells<sup>27,42</sup>. Although the role of sIgA glycans on sIgA-FcαRI interactions is unclear, it is known that the glycans on serum IgA do not contribute to binding to FcαRI<sup>43,44</sup>. Therefore, the increased activation of neutrophils after removal of sialic acid could possibly be mediated through interactions with other receptors on the neutrophil surface. Candidate receptors are the sialic acid-binding immunoglobulin-like lectins (siglecs), which act as inhibitory receptors by signalling through their ITIM domains<sup>30,31</sup>. Although siglecs are normally thought to interact *in cis* with self-expressed sialoglycans on the surface of neutrophils and other phagocytes, they can also act *in trans* with exogenous sialic acids and as such may interact with sialoglycans present on sIgA<sup>28,29,31,45</sup>.

Although we have not tested the involvement of siglecs directly, we do provide evidence that sialic acid interactions on the neutrophil surface are critical regulators of sIgA-mediated neutrophil activation. We demonstrate that sIgA-mediated neutrophil activation is greatly reduced in the presence of free sialic acid (Neu5Ac) or the sialic acid analogue oseltamivir phosphate (Figure 5A). This inhibition of neutrophil activation could happen in multiple ways. In one scenario free sialic acids interact *in trans* with the aforementioned inhibitory siglecs, thereby suppressing pro-inflammatory signalling through the sIgA-FcαRI axis. In a different scenario, free sialic acids inhibit the host endogenous sialidase (NEU1). NEU1 was previously shown to be an important regulator of neutrophil activation<sup>48-52</sup>. Upon neutrophil activation NEU1 is translocated to the neutrophil surface where it removes sialic acid from surface-attached host sialoglycans, thereby unmasking *cis*-acting siglec receptors which transduce inhibitory signals<sup>33</sup>. The potential regulatory role of sialidases was further supported by our own data in Figure 5B in which we showed that addition of an exogenous sialidase, in this case NanH1 from *A. mucolyticum*, can greatly enhance sIgA-mediated neutrophil activation. This is in line with previous reports showing that other bacterial sialidases can also promote increased neutrophil responses<sup>48,50,52,53</sup>.

Sialidase-enhanced activation via sIgA may be caused by modulation of sialic acid-siglec interactions, but it may also increase neutrophil activation through desialylation of FcαRI. Desialylation of FcαRI was shown to lead to a 3-fold increase in IgA binding, which was mainly attributed to removal of sialic acid

residues on N58<sup>54</sup>. Although it remains unclear whether binding of secretory IgA is also increased by desialylation of FcαRI, increased binding of IgA would likely result in higher neutrophil activation.

Our findings regarding the effects of free sialic acid and the NanH1 sialidase on modulation of sIgA-mediated neutrophil activation are in line with literature, in which it was reported that sialic acid (Neu5Ac) and the sialic acid analogues 2-deoxyNANA and oseltamivir phosphate were efficient inhibitors of PMA or LPS-induced neutrophil and macrophage activation due to their ability to inhibit the cell surface sialidase activity<sup>52,53</sup>. A recent pre-print also reported similar findings with the sialic acid analogue zanamivir in LPS-induced neutrophil activation<sup>48</sup>. Furthermore, they showed that NEU1-mediated shedding of the surface sialic acids is likely involved in a positive-feedback loop linked to exacerbated neutrophil responses in sepsis and COVID-19. Overall this shows that sialic acids can efficiently reduce neutrophil activation by acting as endogenous sialidase inhibitors<sup>48</sup>.

As sialidases are often considered virulence factors of pathogenic bacteria, early detection of sialidase activity could be an important danger signal to which the host should mount an appropriate immune response. We hypothesize a model (Figure 6) in which this detection of sialidase activity can be mediated through *in trans* interactions with the sialoglycans on secretory IgA as well as through *in cis* interactions with sialoglycans on the surface of neutrophils. Upon bacteria- or host-mediated desialylation of the glycans on sIgA or the neutrophil surface, the inhibitory sialic acid-siglec interactions are abrogated and neutrophil activation will be enhanced. However, this will only lead to neutrophil activation in the presence of a second signal such as IgA immune complexes on IgA-coated bacteria or a classical PAMP such as LPS (Figure 5). Such an enhanced neutrophil activation will be beneficial if it is sufficient to resolve bacterial infections. However, if bacteria are capable of evading this immune response and persist, this may lead to a chronic neutrophil overaction and the development of chronic inflammatory conditions such as inflammatory bowel disease.

Overall, our findings provide an important bridge between the IgA-coated intestinal microbiota, sIgA-mediated neutrophil activation and the intricate role that sialic acid plays in this interaction. This new and integrated perspective may pave the way for the development of novel therapeutic approaches.

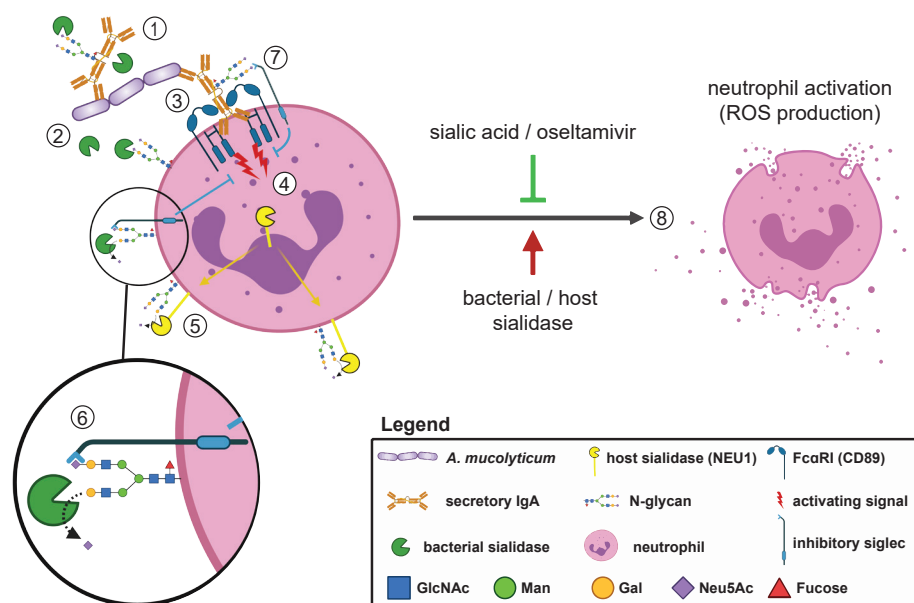


**Figure 6. Model of sIgA-mediated neutrophil activation and the role of sialic acids in this process.** (1) *A. mucolyticum* is bound by secretory IgA. (2) *A. mucolyticum* secretes a sialidase that targets sialoglycans on sIgA and the neutrophil surface. (3&4) Upon binding of the sIgA to the Fc $\alpha$ RI (CD89), the homodimeric receptor is cross-linked resulting in induction of pro-inflammatory signalling pathways. (5) This first sIgA-mediated signal, leads to the translocation of the endogenous sialidase NEU1 from granules to the neutrophil cell surface. (6&7) Here, NEU1 as well as NanH1 can remove sialic acids from surface expressed sialoglycans, thereby abrogating inhibitory *cis*-acting sialic acid-siglec interactions on the neutrophil surface or trans-acting sialic acid-siglec interactions with sIgA. (8) This results in an enhanced activation and increased production of reactive oxygen species (ROS). These pro-inflammatory responses can be counteracted by free sialic acid (Neu5Ac) or sialic acid analogues such as oseltamivir. This figure has been created with BioRender.com.

## MATERIALS AND METHODS

### Expression and purification of NanH1 sialidase

The *A. mucolyticum* NanH1 sialidase was recombinantly expressed and purified as described in Chapter 4 of this thesis.

### NanH1 treatment of secretory IgA and affinity purification

Two different human colostrum secretory IgA batches (I2636; Sigma-Aldrich) were used. Lot numbers of the two different sIgA batches were: batch #1 (027M4758V) and batch #2 (0000088074). One ml of human colostrum secretory IgA (1 mg/mL in PBS) was treated with 10  $\mu$ g/mL of NanH1, or mock-treated with PBS alone overnight at 37  $^{\circ}$ C in DPBS with calcium and magnesium (Gibco). Alternatively, a similar amount of IgA was pretreated with three commercial sialidases CPNA (Sigma), VCNA (Roche) and AUNA (Roche), of which the concentration was adjusted to match the sialidase activity of 10  $\mu$ g/ml NanH1, as also described in Chapter 3. Following NanH1 or mock treatment, the two sIgA preparations were separated into the sIgA1 and sIgA2 fractions by affinity chromatography using the ÄKTA Pure system (Cytiva). Samples were loaded on an 8 mL immobilized jacalin agarose column (20395; ThermoFisher Scientific) and washed with five column volumes of PBS. The IgA2 fraction was collected in the flow-through, whereas the IgA1 fraction remained bound to the jacalin agarose and was eluted with five column volumes of 0.1 M melibiose in PBS (Sigma-Aldrich). Pooled fractions were then dialysed twice against PBS and concentrated using a 100 kDa Amicon Ultra Centrifugal Filter (Merck). The concentration of purified sIgA was determined using the BCA protein assay kit (ThermoFisher Scientific) on a Qubit fluorometer.

### SDS-PAGE and lectin blotting

NanH1-treated or PBS-treated sIgA1 and sIgA2 (100  $\mu$ g/mL) were mixed with 3x Laemmli Sample Buffer (LSB) and denatured at 95  $^{\circ}$ C for 15 min. Samples were loaded in equal volumes (18  $\mu$ L) on a denaturing Bolt 4-12% Bis-Tris Gel (ThermoFisher Scientific), resolved at 150 V and then transferred to a PVDF membrane (BioRad) using the TurboBlot transfer system (with the predefined BioRad settings for 1.5 mm gels). Following transfer, the membrane was blocked in Tris-Buffered Saline (TBS; 150 mM NaCl; 20 mM Tris; pH 7.6) with 2% BSA for 1 h at room temperature on a rolling bench. Primary staining was done with either 1  $\mu$ g/mL biotinylated *Erythrina christagalli* (ECA) lectin (VectorLabs) for detection of free galactose, or 2  $\mu$ g/mL biotinylated *Sambucus nigra* (SNA) lectin (VectorLabs) for detection of sialic acids - diluted in TBS



with 2% bovine serum albumin and incubated for 1 h at room temperature on a rolling bench. After washing the membrane thrice in TBS (5 min/wash), secondary staining was done with streptavidin-HRP (1:10,000; 0.1 µg/mL; Jackson ImmunoResearch), diluted in TBS with 2% BSA and incubated for 1 h at room temperature on a rolling bench. The membrane was developed using the Pierce ECL chemiluminescent substrate according to the manufacturer's protocol (ThermoFisher Scientific) and imaged on a ImageQuant LAS4000 chemiluminescent imager (GE Healthcare). To ensure equal loading of samples, the Bis-Tris gel was stained with Coomassie InstantBlue (Expedeon) following blotting and imaged using a flatbed scanner (Epson).

### Neutrophil activation assay

A 96-well white plate (Greiner) was coated with 5 µg/mL or 10 µg/mL PBS-treated (normally sialylated) or NanH1-treated (desialylated) sIgA1 or sIgA2 in Hanks' Balanced Salt Solution (HBSS; Lonza) for 1 h at 37 °C 5% CO<sub>2</sub>. The plate was then washed twice with 200 µL HBSS after which 50 µL of HBSS was added to well as a negative control or 50 µL of HBSS supplemented with 5 µg/mL phorbol myristate acetate (PMA, Sigma-Aldrich) as a positive control. For other experimental conditions 50 µL HBSS was supplemented with the following: 40 µg/mL mouse IgG1 isotype control (AntibodyChain international, 026100), 50 µg/mL mouse IgG1 anti human CD89 (clone MIP8a, Sanbio, MCA1824), 4 mM sialic acid (Neu5Ac, Carbosynth), 4 mM oseltamivir phosphate (ThermoFisher Scientific), or 40 µg/mL of active or heat-inactivated (30 min at 98°C) NanH1 sialidase. As the IgG1 antibodies contain sodium azide, which is a potent quencher of luminescence, the antibodies were washed thrice with HBSS using a 10 kDa MWCO Amicon Ultra filters (ThermoFisher Scientific) prior to use.

For each assay, polymorphonuclear cells (PMNs) were isolated from fresh blood, using density gradient centrifugation according to published lab protocols<sup>55</sup>, and diluted to a concentration of 10<sup>7</sup> cells/mL in Gibco RPMI 1640 medium with phenol red (ThermoFisher Scientific) with 0.1% Human Serum Albumin (HSA; Behring Institut). PMNs were centrifuged at 1,200 rpm for 7 min at 4°C to remove the RPMI medium (which contains oxygen scavengers) and re-suspended in 4 volumes of HBSS with 0.1% HSA (final PMN concentration: 2.5 × 10<sup>6</sup> cells/mL). The PMNs were then mixed in a 1:2 (v/v) ratio with pre-warmed (37°C) luminol balanced salt solution (LBSS; HBSS with 0.3375 mM luminol and 0.05% HSA; filter-sterilized) and 150 µL of this mixture was added to the sIgA-coated 96-well plate. The plate was incubated in a plate reader

(ClarioStar) at 37 °C and luminescence was recorded every 2 min for a total time of 100 min. The experiments were repeated a minimum of three times with at least two technical replicates per condition every time.

## REFERENCES

1. Mantis NJ, Rol N, Corthésy B. Secretory IgA's complex roles in immunity and mucosal homeostasis in the gut. *Mucosal Immunology*. 2011;4(6):603-611. doi:10.1038/mi.2011.41
2. Sterlin D, Fadlallah J, Slack E, Gorochov G. The antibody/microbiota interface in health and disease. *Mucosal Immunology*. 2020;13(1):3-11. doi:10.1038/s41385-019-0192-y
3. de Sousa-Pereira P, Woof JM. IgA: Structure, Function, and Developability. *Antibodies*. 2019;8(4):57. doi:10.3390/antib8040057
4. Pabst O, Cerovic V, Hornef M. Secretory IgA in the Coordination of Establishment and Maintenance of the Microbiota. *Trends in Immunology*. 2016;37(5):287-296. doi:10.1016/j.it.2016.03.002
5. Palm NW, de Zoete MR, Flavell RA. Immune-microbiota interactions in health and disease. *Clinical Immunology*. 2015;159(2):122-127. doi:10.1016/j.clim.2015.05.014
6. MacPherson AJ, McCoy KD, Johansen FE, Brandtzaeg P. The immune geography of IgA induction and function. *Mucosal Immunology*. 2008;1(1):11-22. doi:10.1038/mi.2007.6
7. Moor K, Diard M, Sellin ME, Felmy B, Wotzka SY, Toska A, Bakkeren E, Arnoldini M, Bansept F, Co AD, et al. High-avidity IgA protects the intestine by enchainning growing bacteria. *Nature*. 2017;544(7651):498-502. doi:10.1038/nature22058
8. Perrier C, Sprenger N, Corthésy B. Glycans on secretory component participate in innate protection against mucosal pathogens. *Journal of Biological Chemistry*. 2006;281(20):14280-14287. doi:10.1074/jbc.M512958200
9. Ost KS, O' Meara TR, Zac SW, Chiaro T, Zhou H, Penman J, Bell R, Catanzaro J, Song D, Singh S, et al. Adaptive immunity induces mutually beneficial interactions with gut fungi. *Nature*. 2021. doi:10.1038/s41586-021-03722-w
10. Wang S, Charbonnier LM, Noval Rivas M, Georgiev P, Li N, Gerber G, Bry L, Chatila TA. MyD88 Adaptor-Dependent Microbial Sensing by Regulatory T Cells Promotes Mucosal Tolerance and Enforces Commensalism. *Immunity*. 2015;43(2):289-303. doi:10.1016/j.immuni.2015.06.014
11. Rogier EW, Frantz AL, Bruno MEC, Wedlund L, Cohen DA, Stromberg AJ, Kaetzel CS. Secretory antibodies in breast milk promote long-term intestinal homeostasis by regulating the gut microbiota and host gene expression. *Proceedings of the National Academy of Sciences of the United States of America*. 2014;111(8):3074-3079. doi:10.1073/pnas.1315792111
12. Koch MA, Reiner GL, Lugo KA, Kreuk LSM, Stanbery AG, Ansaldo E, Seher TD, Ludington WB, Barton GM. Maternal IgG and IgA Antibodies Dampen Mucosal T Helper Cell Responses in Early Life. *Cell*. 2016;165(4):827-841. doi:10.1016/j.cell.2016.04.055
13. Palm NW, de Zoete MR, Cullen TW, Barry NA, Stefanowski J, Hao L, Degnan PH, Hu J, Peter I, Zhang W, et al. Immunoglobulin A Coating Identifies Colitogenic Bacteria in Inflammatory Bowel Disease. *Cell*. 2014;158(5):1000-1010. doi:10.1016/j.cell.2014.08.006
14. Huus KE, Frankowski M, Pučić-baković M, Vučković F, Lauc G, Mullish BH, Marchesi JR, Monaghan TM, Kao D, Finlay BB, et al. Changes in IgA-targeted microbiota following fecal transplantation for recurrent *Clostridioides difficile* infection. *Gut Microbes*. 2021;13(1):1-12. doi:10.1080/19490976.2020.1862027
15. Bunker JJ, Flynn TM, Koval JC, Shaw DG, Meisel M, McDonald BD, Ishizuka IE, Dent AL, Wilson PC, Jabri B, et al. Innate and Adaptive Humoral Responses Coat Distinct Commensal Bacteria with Immunoglobulin A. *Immunity*. 2015;43(3):541-553. doi:10.1016/j.immuni.2015.08.007
16. Donaldson GP, Ladinsky MS, Yu KB, Sanders JG, Yoo BB, Chou WC, Conner ME, Earl AM, Knight R, Bjorkman PJ, et al. Gut microbiota utilize immunoglobulin a for mucosal colonization. *Science*. 2018;360(6390):795-800. doi:10.1126/science.aag0926
17. van Gool MMJ, van Egmond M. IgA and FcαRI: Versatile Players in Homeostasis, Infection, and Autoimmunity. *ImmunoTargets and Therapy*. 2021;Volume 9:351-372. doi:10.2147/ITT.S266242
18. Rochereau N, Drocourt D, Perouzel E, Pavot V, Redelinguhuys P, Brown GD, Tiraby G, Roblin X, Verrier B, Genin C, et al. Dectin-1 Is Essential for Reverse Transcytosis of Glycosylated SIgA-Antigen Complexes by Intestinal M Cells Nemazee D, editor. *PLoS Biology*. 2013;11(9):e1001658. doi:10.1371/journal.pbio.1001658
19. Rios D, Wood MB, Li J, Chassaing B, Gewirtz AT, Williams IR. Antigen sampling by intestinal M cells is the principal pathway initiating mucosal IgA production to commensal enteric bacteria. *Mucosal Immunology*. 2016;9(4):907-916. doi:10.1038/mi.2015.121
20. Hoepel W, Golebski K, van Drunen CM, den Dunnen J. Active control of mucosal tolerance and inflammation by human IgA and IgG antibodies. *Journal of Allergy and Clinical Immunology*. 2020;146(2):273-275. doi:10.1016/j.jaci.2020.04.032
21. van der Steen L, Tuk CW, Bakema JE, Kooij G, Reijerkerk A, Vidarsson G, Bouma G, Kraal G, de Vries HE, Beelen RHJ, et al. Immunoglobulin A: FcαRI Interactions Induce Neutrophil Migration Through Release of Leukotriene B4. *Gastroenterology*. 2009;137(6):2018-2029.e3. doi:10.1053/j.gastro.2009.06.047
22. Royle L, Roos A, Harvey DJ, Wormald MR, Van Gijlswijk-Janssen D, Redwan ERM, Wilson IA, Daha MR, Dwek RA, Rudd PM. Secretory IgA N- and O-glycans provide a link between the innate and adaptive immune systems. *Journal of Biological Chemistry*. 2003;278(22):20140-20153. doi:10.1074/jbc.M301436200
23. Kokubo T, Hiki Y, Iwase H, Tanaka A, Toma K, Hotta K, Kobayashi Y. Protective role of IgA1 glycans against IgA1 self- aggregation and adhesion to extracellular matrix proteins. *Journal of the American Society of Nephrology*. 1998;9(11):2048-2054.

24. Larsen MD, de Graaf EL, Sonneveld ME, Plomp HR, Nouta J, Hoepel W, Chen HJ, Linty F, Visser R, Brinkhaus M, et al. Afucosylated IgG characterizes enveloped viral responses and correlates with COVID-19 severity. *Science*. 2021;371(6532). doi:10.1126/science.abc8378
25. Steffen U, Koeleman CA, Sokolova M V., Bang H, Kleyer A, Rech J, Unterweger H, Schicht M, Garreis F, Hahn J, et al. IgA subclasses have different effector functions associated with distinct glycosylation profiles. *Nature Communications*. 2020;11(1). doi:10.1038/s41467-019-13992-8
26. de Haan N, Falck D, Wuhrer M. Monitoring of immunoglobulin N- And O-glycosylation in health and disease. *Glycobiology*. 2021;30(4):226–240. doi:10.1093/GLYCOB/CWZ048
27. Monteiro RC, Van De Winkel JGJJ. IgA Fc receptors. *Annual Review of Immunology*. 2003;21(1):177–204. doi:10.1146/annurev.immunol.21.120601.141011
28. Carlin AF, Uchiyama S, Chang YC, Lewis AL, Nizet V, Varki A. Molecular mimicry of host sialylated glycans allows a bacterial pathogen to engage neutrophil Siglec-9 and dampen the innate immune response. *Blood*. 2009;113(14):3333–3336. doi:10.1182/blood-2008-11-187302
29. Wielgat P, Rogowski K, Niemirowicz-Laskowska K, Car H. Sialic acid-siglec axis as molecular checkpoints targeting of immune system: Smart players in pathology and conventional therapy. *International Journal of Molecular Sciences*. 2020;21(12):1–18. doi:10.3390/ijms21124361
30. Lübbers J, Rodríguez E, van Kooyk Y. Modulation of Immune Tolerance via Siglec-Sialic Acid Interactions. *Frontiers in immunology*. 2018;9:2807. doi:10.3389/fimmu.2018.02807
31. Favier B. Regulation of neutrophil functions through inhibitory receptors: an emerging paradigm in health and disease. *Immunological Reviews*. 2016;273(1):140–155. doi:10.1111/imr.12457
32. Briliūtė J, Urbanowicz PA, Luis AS, Baslé A, Paterson N, Rebello O, Hendel J, Ndeh DA, Lowe EC, Martens EC, et al. Complex N-glycan breakdown by gut *Bacteroides* involves an extensive enzymatic apparatus encoded by multiple co-regulated genetic loci. *Nature Microbiology*. 2019;4(9):1571–1581. doi:10.1038/s41564-019-0466-x
33. Lewis AL, Lewis WG. Host sialoglycans and bacterial sialidases: A mucosal perspective. *Cellular Microbiology*. 2012;14(8):1174–1182. doi:10.1111/j.1462-5822.2012.01807.x
34. Robinson LS, Schwebke J, Lewis WG, Lewis AL. Identification and characterization of NanH2 and NanH3, enzymes responsible for sialidase activity in the vaginal bacterium *Gardnerella vaginalis*. *Journal of Biological Chemistry*. 2019;294(14):5230–5245. doi:10.1074/jbc.RA118.006221
35. Lewis WG, Robinson LS, Perry J, Bick JL, Peipert JF, Allsworth JE, Lewis AL. Hydrolysis of secreted sialoglycoprotein immunoglobulin a (IgA) in ex vivo and biochemical models of bacterial vaginosis. *Journal of Biological Chemistry*. 2012;287(3):2079–2089. doi:10.1074/jbc.M111.278135
36. Brazil JC, Louis NA, Parkos CA. The role of polymorphonuclear leukocyte trafficking in the perpetuation of inflammation during inflammatory bowel disease. *Inflammatory Bowel Diseases*. 2013;19(7):1556–1565. doi:10.1097/MIB.0b013e318281f54e
37. Therrien A, Chapuy L, Bsai M, Rubio M, Bernard G, Arslanian E, Orlicka K, Weber A, Panzini BP, Dorais J, et al. Recruitment of activated neutrophils correlates with disease severity in adult Crohn's disease. *Clinical and Experimental Immunology*. 2019;195(2):251–264. doi:10.1111/cei.13226
38. Plomp R, De Haan N, Bondt A, Murli J, Dotz V, Wuhrer M. Comparative glycomics of immunoglobulin A and G from saliva and plasma reveals biomarker potential. *Frontiers in Immunology*. 2018;9(OCT):1–12. doi:10.3389/fimmu.2018.02436
39. Phalipon A, Cardona A, Kraehenbuhl JP, Edelman L, Sansonetti PJ, Corthésy B. Secretory component: A new role in secretory IgA-mediated immune exclusion in vivo. *Immunity*. 2002;17(1):107–115. doi:10.1016/S1074-7613(02)00341-2
40. Maurer MA, Meyer L, Bianchi M, Turner HL, Le NPL, Steck M, Wyrzucki A, Orłowski V, Ward AB, Crispin M, et al. Glycosylation of Human IgA Directly Inhibits Influenza A and Other Sialic-Acid-Binding Viruses. *Cell Reports*. 2018;23(1):90–99. doi:10.1016/j.celrep.2018.03.027
41. Schrotten H, Stapper C, Plogmann R, Köhler H, Hacker J, Hanisch F-G. Fab-Independent Antiadhesion Effects of Secretory Immunoglobulin A on S-Fimbriated *Escherichia coli* Are Mediated by Sialyloligosaccharides. *Infection and Immunity*. 1998;66(8):3971–3973. doi:10.1128/IAI.66.8.3971-3973.1998
42. Breedveld A, Van Egmond M. IgA and FcαRI: Pathological roles and therapeutic opportunities. 2019. doi:10.3389/fimmu.2019.00553
43. Mattu TS, Pleass RJ, Willis AC, Kilian M, Wormald MR, Lellouch AC, Rudd PM, Woof JM, Dwek RA. The glycosylation and structure of human serum IgA1, Fab, and Fc regions and the role of N-glycosylation on Fcα receptor interactions. *Journal of Biological Chemistry*. 1998;273(4):2260–2272. doi:10.1074/jbc.273.4.2260
44. Gomes MM, Wall SB, Takahashi K, Novak J, Renfrow MB, Herr AB. Analysis of IgA1 N-glycosylation and its contribution to FcαRI binding. *Biochemistry*. 2008;47(43):11285–11299. doi:10.1021/bi801185b
45. MacAuley MS, Crocker PR, Paulson JC. Siglec-mediated regulation of immune cell function in disease. *Nature Reviews Immunology*. 2014;14(10):653–666. doi:10.1038/nri3737
46. SIGLEC5 protein expression summary - The Human Protein Atlas. <https://www.proteinatlas.org/ENSG00000105501-SIGLEC5>.
47. Blixt O, Collins BE, Van den Nieuwenhof IM, Crocker PR, Paulson JC. Sialoside specificity of the siglec family assessed using novel multivalent probes: Identification of potent inhibitors of myelin-associated glycoprotein. *Journal of Biological Chemistry*. 2003;278(33):31007–31019. doi:10.1074/jbc.M304331200
48. Wanderley CWS, Lorenzini CB, Santos AA, Fonseca FR, Aires L, Heck N, Starick MR. Neuraminidase inhibitors rewire neutrophil function. *bioRxiv*. 2020. doi:https://doi.org/10.1101/2020.11.12.379115

49. Razi N, Varki A. Cryptic sialic acid binding lectins on human blood leukocytes can be unmasked by sialidase treatment or cellular activation. *Glycobiology*. 1999;9(11):1225-1234. doi:10.1093/glycob/9.11.1225
50. Chang YC, Uchiyama S, Varki A, Nizet V. Leukocyte inflammatory responses provoked by pneumococcal sialidase. *mBio*. 2012;3(1):1-10. doi:10.1128/mBio.00220-11
51. Feng C, Zhang L, Almulki L, Faez S, Whitford M, Hafezi-Moghadam A, Cross AS. Endogenous PMN sialidase activity exposes activation epitope on CD11b/CD18 which enhances its binding interaction with ICAM-1. *Journal of Leukocyte Biology*. 2011;90(2):313-321. doi:10.1189/jlb.1210708
52. Cross AS, Wright DG. Mobilization of sialidase from intracellular stores to the surface of human neutrophils and its role in stimulated adhesion responses of these cells. *Journal of Clinical Investigation*. 1991;88(6):2067-2076. doi:10.1172/JCI115536
53. Amith SR, Jayanth P, Franchuk S, Finlay T, Seyrantepe V, Beyaert R, Pshezhetsky A V., Szewczuk MR. Neu1 desialylation of sialyl  $\alpha$ -2,3-linked  $\beta$ -galactosyl residues of TOLL-like receptor 4 is essential for receptor activation and cellular signaling. *Cellular Signalling*. 2010;22(2):314-324. doi:10.1016/j.cellsig.2009.09.038
54. Xue J, Zhao Q, Zhu L, Zhang W. Deglycosylation of Fc $\alpha$ R at N58 increases its binding to IgA. *Glycobiology*. 2010;20(7):905-915. doi:10.1093/glycob/cwq048
55. Surewaard BGJ, van Strijp JAG, Nijland R. Studying Interactions of *Staphylococcus aureus* with Neutrophils by Flow Cytometry and Time Lapse Microscopy. *Journal of Visualized Experiments*. 2013;(77). doi:10.3791/50788

# 06



## General discussion

## 06

## GENERAL DISCUSSION

The gut microbiota plays an important role in the development of IBD, but the molecular mechanisms underlying the microbiota-mediated intestinal pathology are still largely unclear. In order to advance our understanding of the role of the gut microbiota in IBD, the field needs to progress beyond association and correlation and should strive to attain new mechanistic insights into the microbial factors that drive disease development. Bacterial pathobionts are potentially pathogenic inhabitants of the intestinal tract and often take up residence close to or even in direct contact with the epithelium. These pathobionts have an outsized influence on host immune responses and as such can modulate inflammatory conditions such as IBD. Many pathobionts have evolved to interact with critical elements of the intestinal mucosal barrier, such as glycosylated mucins and sIgA, as well as other bacteria, which makes them critical modulators of the mucosal niche. However, many of the mechanisms underlying these interactions are still unclear. By studying pathobionts and their glycobiochemical interactions with the mucosal barrier, we aimed to identify pathways that drive pathological inflammatory conditions such as IBD.

This thesis describes our work on the chemical and genomic characterization of two novel IBD-associated pathobionts and their interactions with critical elements of the intestinal mucosal barrier, with a special focus on the role of the carbohydrate active enzymes (CAZymes) as modulators of the mucosal niche. In this final chapter we provide a summary of our findings and discuss these in a broader framework of (glycobiochemical) interactions at the host-microbial interface and the implications for human health.

### Identification of two IgA-coated *Allobaculum* species

In Chapter 2, we describe the isolation, identification and chemical and genomic characterization of two novel bacterial species: *Allobaculum filumensis* and *Allobaculum mucolyticum*. Both species were isolated from faecal samples of two different IBD patients and were shown to be highly IgA-coated. Moreover, *A. mucolyticum* was part of a consortium of IgA-coated bacteria that was strongly colitogenic when transplanted into mice<sup>1</sup> and both *A. mucolyticum* and *A. filumensis* drove intestinal inflammation in mono-colonized mouse models of IBD (personal communication). As such, both bacteria were considered potential novel pathobionts.

### Phylogeny

Phylogenetic analysis using 16S rRNA gene sequence and comparison of the percentage of conserved proteins indicated that the two bacteria were distinct species and closely related to the dog commensal *Allobaculum stercoricanis*. Therefore, we proposed to assign these species to the *Allobaculum* genus within the family of *Erysipelotrichaceae*. The relatively small family of *Erysipelotrichaceae* displays high phylogenetic heterogeneity and is characterized by multiple monotypic genera<sup>2</sup>. As such, this bacterial family is subject to frequent addition, removal and reannotation of member species. High-throughput 16S rRNA gene sequencing has identified many novel putative species belonging to this family, but as (partial) 16S rRNA gene-based identification rarely provides information beyond the genus level, this currently prevents accurate classification and taxonomic assignment. The rapidly falling costs of metagenomic shotgun sequencing will no doubt increase availability of high-quality metagenome-assembled genomes, including those from uncultured members of this family<sup>3,4</sup>. This will not only allow for an expansion of the number of *Erysipelotrichaceae* species but will also provide a much more accurate taxonomic characterization of the *Erysipelotrichaceae* family. Moreover, the increase in metagenomic data may provide an opportunity for a more in-depth exploration of the functional potential of the different species within this family.

Despite the phylogenetic heterogeneity, most of the *Erysipelotrichaceae* have been isolated from similar habitats; the feces or the intestinal tract of humans or other animals. This suggests that members of this family are well-adapted to and have a long-established relationship with the vertebrate host. Clear examples of this interaction and adaptation to the vertebrate host can be found in *Erysipelothrix rhusiopathiae* and *Turicibacter sanguinis*. The type genus and obligate pathogen *Erysipelothrix rhusiopathiae* is the causative agent of erysipeloid in humans and erysipelas in swine<sup>2,5</sup>. This microaerophile can colonize and invade host tissues through expression of virulence factors that are well adapted to its host, such as a sialidase and hyaluronidase enzymes<sup>6</sup>. The commensal *Turicibacter sanguinis* was shown to promote its own colonization by inducing the expression and secretion of the neurotransmitter serotonin by colonic enterochromaffin cells<sup>7</sup>. The serotonin was released on the basolateral side of the epithelial cells, but also apically into the lumen. Here, *T. sanguinis* could metabolize serotonin which promoted its colonization. Moreover, colonization with *T. sanguinis* greatly affected host lipid metabolism, showing complex bidirectional interactions between this microbe and the host<sup>8</sup>. Currently, besides *A. mucolyticum* and *A. filumensis*, only one other *Allobaculum* isolate has been used in colonization experiments: *Allobaculum* OTU002. This species was isolated from mice and shown to adhere to epithelial cells of the small intestine. *Allobaculum* OTU002 influenced the onset of experimental autoimmune encephalomyelitis, a model for multiple sclerosis development, through activation of intestinal Th17 responses<sup>9</sup>. These Th17 responses were previously shown to be induced upon bacterial adhesion to intestinal epithelial cells<sup>10</sup>. The induction of Th17 responses and the exacerbation of inflammation was also seen in mice that were colonized with the IgA-positive consortium that contained *A. mucolyticum*, suggesting this bacterium may also interact with the host intestinal epithelium<sup>1</sup>. All of these findings are in line with other reports showing that *Erysipelotrichaceae* have been increasingly associated with metabolic syndrome and intestinal inflammatory disorders in both humans and mice, suggesting that the ways in which several *Erysipelotrichaceae* species interact with their host are evolutionary conserved<sup>11</sup>.

### Morphology

The large phylogenetic diversity within the *Erysipelotrichaceae* family is also reflected in a large diversity in morphological and biochemical characteristics. Nonetheless, *A. filumensis* and *A. mucolyticum* share certain characteristics with their closest relatives. First of all, their appearance; these rod-shaped bacteria grow in long, slender chains or occasional pairs.

This filamentous morphology can also be seen in closely related members of this family, such as *A. stercoricanis* and *Eubacterium tortuosum*<sup>2</sup>. Although much is known about how bacterial cell shape is regulated, less is known as to why different bacteria differ in shape. Selective forces such as nutrient availability, attachment, motility and predation all affect bacterial cell shape<sup>12</sup>. It is also clear that cell shape can determine cell survival, and as such should be considered a critical selectable trait<sup>12,13</sup>. It is interesting to speculate on the selective advantage that a filamentous morphology may confer upon bacteria that reside in the intestinal tract of vertebrates, such as *A. mucolyticum*. The filamentous nature may contribute to bacterial adhesion as the elongated shape increases the number of potential contact points between the bacterial cells and other surfaces, such as mucins or host cells. This adhesion can help the bacterium to resist shear forces present in the intestine and allow stable colonization of the mucosal niche<sup>14</sup>. Another putative function of the filamentous morphology could be to resist predation by protists or, as was demonstrated for uropathogenic *Escherichia coli* (UPEC), phagocytosis by immune cells, such as neutrophils<sup>15,16</sup>. In this respect it is interesting to note that other inhabitants of the mucosal niche, such as the symbiont segmented filamentous bacteria (SFB or *Candidatus* Arthromitus) also have a filamentous morphology, suggesting that this morphology may confer an advantage to bacteria within this niche<sup>17</sup>.

### Metabolism

Besides morphological similarities there are also similarities in biochemical and metabolic capacity. In Chapter 2 we demonstrated that *A. mucolyticum* and *A. filumensis* have multiple active hydrolases such as esterases (C4) and ester lipases (C8), acid phosphatase and glycosyl hydrolases against different glycosidic linkages. In Chapter 3 we have also demonstrated that many of the *A. mucolyticum* glycosyl hydrolases, part of the family of CAZymes, are involved in mucus degradation and that the mucin glycans can be utilized for bacterial growth. The role of these CAZymes will also be discussed in the next section. This metabolic profile of the two *Allobaculum* species is largely similar to the activities observed in *A. stercoricanis*. A recent report identified *Allobaculum* spp. to be among the most active glucose utilizers of the murine gut microbiota<sup>18</sup>. Although we did not investigate the fermentation end products of glucose metabolism for the newly identified *A. mucolyticum* and *A. filumensis*, lactate, butyrate and/or acetate are the main end products of glucose fermentation in many closely related species such as *A. stercoricanis* and *C. innocuum*<sup>2</sup>. Moreover, the relative abundance of *Allobaculum* spp. has been correlated with the levels of butyrate in the murine gut<sup>19</sup>. These findings

may indicate an important role for *Allobaculum spp.* in intestinal homeostasis as butyrate is the preferred energy source for colonocytes and an important regulator of intestinal immune responses, although it has to be noted that the majority of butyrate in humans is likely produced by *Clostridia*, such as *Eubacterium rectale* and *Faecalibacterium prausnitzii*<sup>20,21</sup>.

Besides involvement in glucose and host-glycan metabolism multiple reports have indicated that the relative abundance of *Erysipelotrichaceae*, including that of *Allobaculum spp.*, was markedly increased after mice were fed a high fat diet<sup>11,22,23</sup>. Consistent with these reports, although not described in the experimental chapters of this thesis, we observed a strong growth reduction or even the complete absence of growth of *A. mucolyticum* when short-chain fatty acids (SCFAs; acetate, propionate and butyrate) or Tween-80, respectively, were omitted from the growth medium. This suggests that *A. mucolyticum* is auxotrophic for certain lipids and may require exogenous, dietary or even host-derived lipids for growth. Although it is unclear whether these findings extend to other *Erysipelotrichaceae*, auxotrophy has also been reported for other bacteria residing in the mucosal niche, such as SFB and *Akkermansia muciniphila*<sup>17,24</sup>.

Another characteristic metabolic function is the ability to metabolize L-tryptophan into indoles. This ability differentiates the two novel *Allobaculum* species from other members of the *Erysipelotrichaceae* family. L-tryptophan is an essential dietary amino acid and important for protein synthesis. It is also a precursor for serotonin and as such, the metabolism of L-tryptophan can have many local and systemic effects, for example on the enteric nervous system. Importantly, L-tryptophan and indole derivatives also play key roles in regulating intestinal immune responses. Indole derivatives are aryl hydrocarbon receptor (AhR) agonists and thereby modulate expression of important cytokines such as IL-22 and IL-17 as well as the expression of antimicrobial peptides. Hashimoto and Perlot *et al.*<sup>25</sup> have shown that dietary tryptophan levels alter the gut microbiota composition through mTOR-dependent pathways and this altered gut microbiota confers increased susceptibility to DSS-induced colitis. Interestingly, among the species of which the abundance was most affected by dietary tryptophan were three, as yet uncharacterized *Allobaculum* species. Upon tryptophan supplementation two of these *Allobaculum* species were reduced in abundance and one was increased. This differential effect on different *Allobaculum* species might be due to their differential tryptophan metabolizing activities, as we show that *A. filumensis* and *A. mucolyticum* can metabolize tryptophan, but the closely

related *A. stercoricanis* cannot, at least under the conditions and growth media tested<sup>26</sup>. Whether the effects of tryptophan on *Allobaculum* species are regulated through direct effects on *Allobaculum* metabolism or indirectly through the action of antimicrobial peptides or effects on other bacteria, or a combination of all above remains to be investigated. Nor is it clear whether the ability to produce indoles affects the ability to induce Th17 responses. To answer such questions colonization experiments with bacterial mutants with defects in the tryptophan metabolic pathway or an inhibition of host AhR signaling would be needed.

### Role of CAZymes in intestinal ecology

In Chapters 3, 4 and 5 we demonstrated that *A. mucolyticum* CAZymes, such as the NanH1 sialidase, are involved in many interbacterial and bacteria-host interactions.

### Nutrient acquisition

Humans possess a very limited amount of CAZymes, most of which are involved in intracellular functions such as processing of host glycans. In order to break down and absorb nutrients and energy from complex dietary carbohydrates, such as dietary fiber, we rely on the CAZymes expressed by the microbiota. The microbiota as a community encodes a tremendously diverse repertoire of CAZymes. This diversity is required to break down complex microbiota-accessible carbohydrates from dietary-derived sources such as plant cell wall polysaccharides and pectins, but can also be targeted towards host-derived carbohydrates such as the mucin O-glycans. The metabolism of such complex polysaccharides provides an important source of energy for the microbiota. Moreover, the fermentation end products, such as SCFAs, can be taken up by the large intestine and provide an estimated 5-10% of human caloric intake<sup>27</sup>. As already mentioned above, SCFAs, and in particular butyrate, also play crucial roles in intestinal homeostasis, like providing the main energy source for colonocytes as well as inducing the differentiation of T regulatory and IgA producing cells<sup>28</sup>.

Diet greatly affects gut microbiota composition and microbial CAZymes play an important role in dietary-derived nutrient acquisition for both the host and the microbes. As such they are important regulators of host-microbiota mutualism. People living in industrialized countries often consume so-called western diets, characterized by highly processed foods with a high sugar and fat content but low in fiber. Western diets can contain up to ten times less dietary fiber than diets from modern day hunter-gatherer civilizations. This is



reflected by a great reduction in microbiota diversity, a severe decline of the so-called VANISH (“volatile and/or associated negatively with industrialized societies of humans”) taxa and a concomitant decrease in the CAZyme diversity<sup>29</sup>. Studies in mice have shown that the intake of dietary fiber is critical for a successful maintenance and transmission of fiber-degrading microbes to the offspring. A low-fiber diet can greatly reduce the abundance of specific taxa, especially *Bacteroidales*, in mice and can even lead to complete extinction of certain species in as little as two to three generations<sup>30</sup>. Besides being essential for the production of SCFAs and the maintenance of microbial diversity, fibers also indirectly contribute to mucus barrier strength. Studies have shown that in mice kept on fiber free diets, certain species, such as *Bacteroides thetaiotamicron*, can instead resort to foraging on host mucin glycans through upregulation of mucin *O*-glycan specific CAZymes and this behaviour is crucial for bacterial persistence in the gut as well as vertical transmission<sup>31-33</sup>.

### **Mucus degradation**

Since mucus degradation is believed to be an important virulence factor of mucosal pathogens we investigated the CAZyme repertoire of *A. mucolyticum* and demonstrated that these CAZymes indeed enabled the bacterium to forage on mucin *O*-glycans (Chapter 3). With only an estimated 60 unique CAZyme genes, the *A. mucolyticum* CAZyme repertoire is not particularly large as compared to other species found within the human gut, like certain members of the *Bacteroidetes* phylum<sup>34</sup>. The genomes of *B. thetaiotamicron* and *Bacteroides vulgatus* each encode approximately 300 different CAZymes that allow them to degrade a tremendous diversity of glycans. Martens *et al.*<sup>35</sup> reported that CAZyme expression in *B. thetaiotamicron* is specifically induced by the presence of their respective substrates. When diet was devoid of dietary fibers, as is the case for suckling mice or mice fed a simple sugar diet, *B. thetaiotamicron* almost exclusively resorted to harvesting host glycans through expression of mucin-glycan targeting CAZymes. We observed a similar effect in *A. mucolyticum* when we grew this bacterium in gut microbiota medium (GMM). This GMM medium lacks fermentable plant polysaccharides but is rich in simple sugars and host-derived glycans from casein peptone, and as a result *A. mucolyticum* mainly expressed and secreted mucin-targeting CAZymes. Even in basal medium, which lacks the simple sugars and barely supports growth, *A. mucolyticum* still secretes a core set of host-targeting CAZyme genes, including the NanH1 sialidase. In Chapter 4 we demonstrated that NanH1 is able to degrade casein *O*-glycans, which makes these oligoglycans or the mono/disaccharides contained within them the

likely inducers of this core-set of CAZymes. As the casein glycans resemble host *O*-glycans, such as found on mucin, it is not surprising that the CAZyme repertoire on basal medium supplemented with mucin is largely similar to basal medium alone. Although we did not analyze the expression of the *A. mucolyticum* CAZyme repertoire in the presence of plant glycans, the fact that it is able to grow on inulin suggests that it is able to produce CAZymes that can degrade this plant polysaccharide.

Thus, although the CAZyme repertoire of *A. mucolyticum* is relatively small, it is highly specialized for the degradation of host-derived mucin *O*-glycans. This not only shows that *A. mucolyticum* is adapted to the human host and life in the mucosal niche, but may also mean that this bacterium has a selective advantage over bacteria that are unable to forage on host glycans, especially when dietary fiber intake is low. In this respect it is interesting to note that in industrialized microbiotas the number mucin-targeting CAZymes has been reported to be much higher than in microbiotas from hunter-gatherer societies<sup>36</sup>. Moreover, the industrialized microbiotas had a much higher relative abundance of *Verrucomicrobia*, such as *A. muciniphila*<sup>36</sup>. In Chapter 3 we demonstrated the CAZyme repertoire of *A. mucolyticum* is very similar to that of *A. muciniphila*. Multiple groups have demonstrated that a diet-induced expansion of mucolytic bacteria, including *A. muciniphila*, can cause degradation of the mucus layer and increase the susceptibility to enteric infections and colitis in mice<sup>33,37,38</sup>. Such degradation of the mucus layer, accompanied by increased numbers of mucosa-associated bacteria, is also seen in IBD patients<sup>39</sup>. Although industrialized microbiotas from healthy people are clearly different from IBD-associated, dysbiotic microbiotas, the increase in mucin-degrading bacteria may indicate a transition to a predysbiotic state. Albeit the role of other environmental factors such as hygienic practices, pollution, and the use of antibiotics should also be considered, these findings suggest that diet-induced alterations in the repertoire of microbial CAZymes play an important role in IBD development.

### **Sialidase-mediated modification of the glycometabolic niche**

The increase in relative abundance of *A. muciniphila* observed in industrialized microbiotas may have displaced other bacterial species. The factors underlying such a displacement are unknown but may be related to diet or use of antibiotics. Interestingly, many IBD patients have a reduced relative abundance of *A. muciniphila* but whether this is related to the

disease is unknown. In Chapter 4, we demonstrated that the sialidases from *A. mucolyticum*, as well as other bacterial sialidases, can greatly inhibit *A. muciniphila* growth through desialylation of milk-derived casein *O*-glycans.

### ***Sialidases and bacterial metabolism***

Sialidases liberate sialic acids from sialoglycans. As sialic acids are often located at the termini of cell surface expressed glycans they are prominent actors in host-microbe interactions and are utilized by various mucosal bacteria<sup>40,41</sup>. Sialidases can facilitate both interbacterial competition and cooperation and as such help shape the gut microbiota composition<sup>42,43</sup>. For example, *Ruminococcus gnavus* employs a specialized intramolecular trans-sialidase that prevents other bacteria from utilizing the liberated 2,7-anhydro-sialic acid, whereas other bacteria, such as *Bacteroides* species, release free sialic acid that allows the expansion of certain pathogens<sup>42,44,45</sup>. Our finding that bacterial sialidases can inhibit the growth of other bacteria, in this case *A. muciniphila*, by altering the glycometabolic niche has not previously been reported.

A still unresolved question is how a subset of bacterial sialidases inhibit *A. muciniphila* growth. Although we have not fully elucidated the underlying mechanisms, a likely scenario is that the metabolic program of *A. muciniphila* is tightly regulated to match the rate at which monosaccharides are released from sialylated glycans, and that this rate is determined by *A. muciniphila*'s own sialidases. A suddenly increased rate of desialylation by an external sialidase, such as the *A. mucolyticum* sialidase, might disrupt this delicate balance and could lead to an increased rate of hydrolysis of the underlying glycan and a concomitant sudden increase in free *O*-glycan monosaccharides, such as galactose, GlcNAc and GalNAc. As the metabolic pathways for these substrates are highly intertwined a sudden change in their availability could lead to metabolic dysregulation and a cessation of growth<sup>24,46</sup>. The fact that *A. muciniphila* requires exogenous *N*-acetylhexosamines and L-threonine for growth likely contributes to its sensitivity to sialidase-mediated disruption of its niche.

### ***Metabolism of casein glycans in the intestinal ecosystem***

Our results also indicate that milk-derived casein *O*-glycans play a crucial role in the growth inhibition of *A. muciniphila*. Casein is a major glycoprotein in breast milk, while casein-peptides are major glycopeptides in formula milk. Besides casein, *A. muciniphila* can utilize human milk oligosaccharides (HMO's) for growth<sup>47</sup>. These substrates are likely critical for facilitating

the efficient vertical transmission of *A. muciniphila*, and not only provide *A. muciniphila* with nutrients but also induce the expression of *O*-glycan targeting CAZymes required for successful colonization of the mucosal niche. Limited access to casein components or HMOs, e.g., through the action of an exogenous bacterial sialidase, can be envisioned to disrupt the dynamics of the fragile and still developing neonatal intestinal ecosystem. Genomic analysis of metabolic pathways may help identify members of the microbiota that are especially vulnerable to disruptions of their metabolic niche. Furthermore, resolving the genomic and molecular basis for diet-dependent metabolic interactions can aid the development of rationally designed therapies aimed at preventing or restoring microbiota dysbiosis.

### **Sialidase-mediated modulation of immune responses towards IgA-coated bacteria**

In Chapter 5, we reported that besides its ability to contribute to mucin degradation and modulation of the glycometabolic niche, the *A. mucolyticum* NanH1 sialidase also targets sialylated host proteins including sIgA. sIgA is a major component of the mucosal barrier and can exert a wide variety of functions<sup>48</sup>. Classically IgA is primarily considered for its role in exclusion and clearance of invading pathogens. More recent findings have also highlighted its critical role in establishing a diverse gut microbiota, by targeting both pathogens as well as commensal bacteria<sup>49</sup>.

### ***Effects of IgA binding***

Over the last decade multiple studies have charted the IgA-coated members of the gut microbiota<sup>1,50,51</sup>. However, why these bacteria are targeted and what the effects of sIgA binding are on bacterial physiology is much less clear. In a very recent paper, Rollenske *et al.*<sup>52</sup> demonstrated that sIgA binding to *E. coli* can have both generic and specific effects. A generic effect was that sIgA binding often led to downregulation of the target antigen, e.g., of the porin OmpC and type I fimbriae. A highly specific effect was that sIgA binding to different epitopes on the same antigen, OmpC, differentially affected *E. coli*'s capacity for glucose uptake. Individual dimeric monoclonal IgAs could also have varying functional effects; e.g., it could reduce glucose uptake as well as protect *E. coli* from a T4 bacteriophage. In general, surface-binding IgAs reduced *E. coli*'s motility and increased its protection against bile-acid-induced membrane permeabilization. These fascinating results shed a new light on the role of sIgA-mediated colonization of the mucosal niche.

In their hallmark paper, Donaldson *et al.*<sup>53</sup> demonstrated that Gram-negative *B. fragilis* can invite binding of sIgA through upregulation of capsular polysaccharides and this event is critical for adherence to epithelial cells and stable colonization of the mucosal niche. These findings were later corroborated and extended by Nakajima *et al.*<sup>54</sup> who demonstrated that aspecific binding of sIgA glycans to LPS of *B. thetaiotamicron* altered its gene expression *in vivo*, inducing specific polysaccharide utilization loci (PULs), essential for efficient mucin polysaccharide utilization. Moreover, they demonstrated that the sIgA binding was critical for establishing stable microbial communities, which included the expansion of butyrate-producing *Clostridiales*. Huus *et al.*<sup>55</sup> demonstrated a similar effect of sIgA binding on the Gram-positive *Lactobacillus*. Binding involved both sIgA- and bacterial-derived glycans and, similar to *Bacteroides* species, sIgA binding increased mucosal colonization of *Lactobacillus*. Importantly, sIgA binding was lost in undernourished mice and this was due to rapid, diet-dependent bacterial adaptation and was associated with mutations of carbohydrate utilization pathways. These studies beautifully demonstrated how some bacteria have adopted sIgA and its glycans to facilitate intimate associations with their host.

### **IgA glycosylation**

Besides the role of sIgA glycans in sIgA-bacteria interactions, the sIgA glycans may also influence sIgA effectors functions such as the activation of immune cells, although this is currently not well understood. In Chapter 5, we demonstrated that the glycosylation status of colostrum sIgA affects sIgA-mediated neutrophil activation. We also showed that bacterial sialidases, like the NanH1 sialidase from *A. mucolyticum*, can desialylate sIgA glycans and target the neutrophil surface, thereby altering the sIgA-mediated neutrophil response. Neutrophils are the most numerous leukocytes and are recruited to the intestine in large numbers during active phases of intestinal inflammation<sup>56</sup>. Disruption of the mucosal barrier allows pathogens and other bacteria to translocate into the lamina propria where they are targeted by neutrophils. Neutrophils can also transit into the lumen to encounter sIgA-coated bacteria. The resulting sIgA-neutrophil interactions could play a major role in driving pathological intestinal immune responses<sup>57</sup>. We observed for the first time an inverse correlation between the level of sIgA sialylation and the degree of neutrophil activation. These findings mimic observations on serum IgA<sup>58</sup>.

The translation from serum IgA to secretory IgA is not a trivial step, as the ontogeny, structure and localization of these two antibody classes are very different. Most notably, sIgA is expressed as a dimer and contains the heavily glycosylated secretory component<sup>48</sup>. We showed that multiple bacterial sialidases target the sIgA heavy chain, but also the secretory component. Interestingly, we also noted significant differences between different batches of colostrum IgA in the ability to activate neutrophils (Chapter 5). As both batches were efficiently desialylated, as demonstrated by the lectin blots, the sialylation status alone was not sufficient to explain the differences in neutrophil activation. It is likely that sIgA-mediated neutrophil activation also depends on presence/absence or ratio of other glycans present on sIgA, for example fucosylated glycans, which may act in concert with the sialoglycans. Personal communication with the supplier revealed that the batches of colostrum IgA were formulated using colostrum from only two or three donors per batch. This likely introduces large batch-to-batch differences, especially when considering glycosylation patterns can vary largely between individuals. An example of potential donor-variability is the *FUT2* secretor status, which determines the fucosylation of ABO blood group antigens. As about 20% of the Caucasian population are non-secretors, due to nonsense mutations, this could well affect fucosylation levels of different IgA batches, especially when these are formulated using such a limited number of donors. These variations in glycosylation can greatly affect an individual's ability to neutralize pathogens and, as our data indicate, may also alter the activation of immune cells and thus could have important clinical implications<sup>59-61</sup>.

As a next step, it would be important to delineate the role of site-specific glycosylation patterns on sIgA. One approach would be the production of recombinant sIgA, which would allow selective knock-out of glycosylation sites or components of the glycosylation machinery. A problem with this approach would be that recombinant sIgA production is currently limited to CHO-K1 or plant-based expression systems and the glycosylation machinery does likely not fully reflect that of human cells<sup>48,62,63</sup>. Another approach would be to analyse the glycosylation patterns of sIgA acquired from different sources that are known to have differential functional effects. The latter approach will likely help to elucidate the disparate functional effects we observe when using different sIgA batches. Such experiments will greatly increase our understanding sIgA glycosylation in sIgA-mediated neutrophil activation and could improve the design of IgA-based therapeutics.

### Sialylation of immune cells

Besides desialylation of sIgA glycans and its effect on sIgA-mediated neutrophil activation, we also observed a very potent, direct effect of the NanH1 sialidase on neutrophil activation. Desialylation of the neutrophil led to a two-fold increase IgA-mediated ROS production. This is most likely due to abrogation of *cis*-acting sialic acid and inhibitory siglec interactions on the neutrophil cell surface<sup>64-67</sup>. By using the sialidase inhibitor oseltamivir phosphate, we also demonstrated a role for endogenous sialidase activity in IgA-mediated neutrophil activation. In the presence of this sialidase inhibitor neutrophil activation was completely abrogated. This is in line with previous observations that reported a role for NEU1 in regulation of LPS-mediated immune responses<sup>65</sup>. The translocation of the endogenous sialidase NEU1 to the neutrophil surface may not only affect the neutrophil itself, but may also act on neighbouring cells. Shkandina *et al.*<sup>68</sup> indeed demonstrated that apoptotic neutrophils and Jurkat T cells were able to remove sialoglycans from erythrocytes and fibroblasts, *in vitro*. This was in agreement with previous data by the same group that demonstrated a caspase-dependent increase in NEU1 sialidase activity on the surface of apoptotic cells<sup>69</sup>.

While we have not investigated the effects on other aspects of neutrophil physiology, it could well be that the surface desialylation has a wide range of effects. For example, increased rates of desialylation of sialoglycoproteins expressed on the surface of enterocytes was reported to increase the rate of protein aging and rates of internalization and decrease protein half-lives<sup>70</sup>. Affected enterocyte proteins include IAP, DPP4, and lactase but could well extend to other sialoglycoproteins, such as EGFR or a multitude of receptors on immune cells<sup>71-74</sup>. It is important to note that besides affecting *cis*-acting sialoglycan-siglec interactions, desialylation may also affect similar interactions that act *in trans*. Such interactions occur in nearly all types of immune cells and can affect many different immune effector functions, such as cell migration, activation, and self/non-self-recognition<sup>73</sup>.

It is clear that both the bacterial sialidase and endogenous sialidases have the potential to change sialylation status and thereby act as a regulators of downstream effector functions of many different cell types. A potential outcome of such interactions could be that the encroachment of IgA-coated, sialidase producing bacteria, such as *A. mucolyticum*, *R. gnavus*, and *A. muciniphila* or LPS-containing Gram-negative bacteria leads to the recruitment and activation of neutrophils in the intestinal lamina propria. This IgA or LPS-mediated activation then results in increased levels of surface

expressed NEU1 on the neutrophil surface, which not only drives the neutrophil oxidative burst, but may also desialylate neighbouring immune cells, such as B-cells expressing CD22, an inhibitory siglec receptor. To come full circle, this then affects B-cell activation and the production, glycosylation and secretion of sIgA directed towards these sialidase producing microbes. Whether such hypothetical interactions do indeed occur in a more complex *in vivo* setting remains to be investigated, but investigation of such glycosylation dependent effects will no doubt shed a new light on host-microbiota interactions, the regulation of inflammatory and tolerogenic immune responses, and will likely provide opportunities for the development of novel biomarkers and therapeutic interventions.

### Perspective of glycosidases as biomarkers and druggable targets

#### Biomarkers

The increasingly appreciated impact of bacterial CAZymes, including sialidases, on the composition and functionality of the gut microbiota raises the question whether the detection of CAZymes could potentially be used as prognostic or diagnostic biomarkers. Their presence can be detected at the genomic, transcriptomic, proteomic and metabolomic level, which might warrant the development of easy-to-use diagnostic assays. Multiple studies have detected increased levels of microbiota-derived mucolytic activity in the faecal samples of IBD patients compared to controls<sup>39,75</sup>. A recent study also found an 8.3 fold increase of host NEU3 sialidase in IBD affected intestinal tissue compared to controls<sup>76</sup>. Despite multiple animal studies showing an important role for host and bacterial sialidases as drivers of intestinal inflammation, a recent, very extensive analysis of faecal samples of an IBD cohort over time did not indicate bacterial sialidases as a significant biomarker<sup>42,77</sup>. However, as the levels and types of glycosidases detected in faecal samples can be very different from what can be detected proximal parts of the intestine, the predictive value of bacterial glycosidases detected in faecal samples may be limited. Especially as multiple groups have already reported large differences between luminal versus mucosal bacterial transcripts, including those from CAZymes<sup>78,79</sup>.

An alternative detection method could be the use of CAZyme transcripts from mucosal biopsies that are sometimes acquired during colonoscopy. A comparison between biopsies from inflamed versus non-inflamed sites acquired from the same patients would allow a better correlation between inflammation and bacterial genomic, transcriptomic or proteomic signatures. A big technical hurdle to using mucosal samples, and especially for transcripts

and proteomics analysis is the overabundance of host-associated material. Donaldson *et al.*<sup>79</sup> used an elegant bacterial RNA-enrichment step using hybrid selection-RNA SEQ using a library of *B. fragilis* specific hybridization-probes. Although in this case this approach was limited to only a single bacterium, this same method could be applied to studying the transcription of CAZymes, and especially those targeting host glycans, by creating a CAZyme specific probe library. Given the rather conserved nature of many of the CAZyme active sites, this should be feasible. It is also probable that the application of ultra-deep sequencing methods might soon be a feasible alternative approach to tackling this problem. Another approach of detecting active CAZymes could be the development of specific activity-based probes<sup>80,81</sup>. Such studies can identify active members of the mucosal microbiota as well as detect the enrichment of bacterial CAZymes-of-interest. Identification of these active members and their actors could then serve as a first step towards developing intervention strategies, such as directed CAZyme inhibitors.

### Drug targets

Given their importance in establishing host-microbiota interactions, mucin-degrading CAZymes could be potentially interesting druggable targets. Generally, only a limited number of bacteria express mucus-degrading CAZymes. With specific CAZyme inhibitors one might therefore be able to selectively inhibit or even completely eliminate only those bacteria which negatively impact health. However, complete and specific inhibition of CAZymes is likely neither easy nor without risk of adverse effects. A first problem would be the redundancy; most species, including *A. mucolyticum*, encode multiple CAZymes of the same class. A second problem is that the specificity of most of the CAZymes is not known, as this cannot be easily inferred from the sequence alone, which may hinder the development of specific inhibitors as this requires laborious testing and validation. Therefore, if one would like to target an entire class of enzymes, one would likely opt for a broad-spectrum inhibitor. For bacterial sialidases, oseltamivir phosphate (Tamiflu) could be an attractive drug. Repurposing of this drug would be especially easy as this has already been approved for treatment and prophylactic use in influenza infections and generally has few side effects. In Chapter 4 we demonstrated that oseltamivir indeed can efficiently inhibit the *A. mucolyticum* NanH1 sialidase. Others have previously demonstrated efficient inhibition of *R. gnavus* NanH<sup>44</sup>. Oseltamivir may thus be used to target sialidases from pathobionts. However, a third problem may be the possible adverse effects of this approach as oseltamivir could also inhibit sialidases from commensals such as *B. thetaiotamicron*, *B. fragilis* or *A. muciniphila*. The

application of oseltamivir may therefore lead to a disruption of the mucosal microbiota. As a final problem we demonstrated that oseltamivir can also inhibit neutrophil activation, likely through inhibition of host neuraminidases. Although this may have very interesting therapeutic applications, e.g. the downregulation of excessive inflammatory responses, prolonged use could also have several unforeseen effects, for example on host protein turnover or progression of cancer cells<sup>65,70,82</sup>. Therefore, broad-spectrum sialidase inhibitors should only be applied with limited duration and accurate dosing.

An alternative, very specific approach, would be the application of bacterial CAZymes targeting vaccines. The swift and successful application of RNA-based vaccines against SARS-CoV-19 demonstrates the power and flexibility of such an approach. Using RNA-based vaccines it may be possible to much more specifically target bacterial proteins of interest, such as sialidases. Vaccination should then trigger an effective immune response with as important outcome the secretion of specific IgA antibodies into the intestinal lumen. Binding of this IgA to the target sialidase should then inhibit sialidase activity and might even completely downregulate its expression<sup>52,83,84</sup>. If the targeted sialidase is indeed critical for pathogenicity or colonization, such an approach could efficiently and specifically inhibit or remove sialidase-producing pathobionts and restore host-microbiota symbiosis.

### Conclusion and future perspectives

The aim of this thesis was to investigate intestinal pathobionts and their glycobiological interactions with critical components of the mucosal barrier. By studying the IgA-coated pathobiont *A. mucolyticum*, we aimed to identify novel molecular mechanisms that help elucidate the pathways that drive pathological inflammatory conditions such as IBD.

As shown in this thesis, the CAZymes of *A. mucolyticum* play important roles in mucus degradation and as modulators of the intestinal mucosal niche; these CAZymes contribute to degradation of host- and dietary-derived glycoproteins resulting in mucus degradation and alteration of the glycometabolic niche which favours competition with other mucus-colonizing microbes. Moreover, CAZymes also play a role in the modulation of neutrophil inflammatory responses. Therefore, under the right circumstances, CAZymes can likely act as drivers of intestinal dysbiosis and inflammation, as seen in IBD.

As bacterial CAZymes, but also host CAZymes, influence host-microbial interactions on so many levels, their role needs to be discussed in a broader ecological and evolutionary framework in which the reciprocal interactions between the gut microbiota, host immunity, and dietary factors are viewed from an integrative perspective that, importantly, also takes into consideration the effects of glycobiochemical interactions. It is evident that glycans and glycosidases are critical players at the host-microbe interface and that integration of glycobiochemistry in this research area will greatly enhance our understanding of the processes that govern intestinal homeostasis and disease.

## REFERENCES

1. Palm NW, de Zoete MR, Cullen TW, Barry NA, Stefanowski J, Hao L, Degnan PH, Hu J, Peter I, Zhang W, *et al.* Immunoglobulin A Coating Identifies Colitogenic Bacteria in Inflammatory Bowel Disease. *Cell*. 2014;158(5):1000-1010. doi:10.1016/j.cell.2014.08.006
2. Verbarq S, Göker M, Scheuner C, Schumann P, Stackebrandt E. The Families *Erysipelotrichaceae* emend., *Coprobaecillaceae* fam. nov., and *Turicibacteraceae* fam. nov. In: *The Prokaryotes*. Vol. 9783642301. Berlin, Heidelberg: Springer Berlin Heidelberg; 2014. p. 79-105. doi:10.1007/978-3-642-30120-9\_205
3. Almeida A, Mitchell AL, Boland M, Forster SC, Gloor GB, Tarkowska A, Lawley TD, Finn RD. A new genomic blueprint of the human gut microbiota. *Nature*. 2019;568(7753):499-504. doi:10.1038/s41586-019-0965-1
4. Pasolli E, Asnicar F, Manara S, Zolfo M, Karcher N, Armanini F, Beghini F, Manghi P, Tett A, Ghensi P, *et al.* Extensive Unexplored Human Microbiome Diversity Revealed by Over 150,000 Genomes from Metagenomes Spanning Age, Geography, and Lifestyle. *Cell*. 2019;176(3):649-662.e20. doi:10.1016/j.cell.2019.01.001
5. Wang Q, Chang BJ, Riley T V. *Erysipelothrix rhusiopathiae*. *Veterinary Microbiology*. 2010;140(3-4):405-417. doi:10.1016/j.vetmic.2009.08.012
6. Nakato H, Shinomiya K, Mikawa H. Adhesion of *Erysipelothrix rhusiopathiae* to Cultured Rat Aortic Endothelial Cells: Role of Bacterial Neuraminidase in the Induction of Arteritis. *Pathology Research and Practice*. 1987;182(2):255-260. doi:10.1016/S0344-0338(87)80114-0
7. Yano JM, Yu K, Donaldson GP, Shastri GG, Ann P, Ma L, Nagler CR, Ismagilov RF, Mazmanian SK, Hsiao EY. Indigenous Bacteria from the Gut Microbiota Regulate Host Serotonin Biosynthesis. *Cell*. 2015;161(2):264-276. doi:10.1016/j.cell.2015.02.047
8. Fung TC, Vuong HE, Luna CDG, Pronovost GN, Aleksandrova AA, Riley NG, Vavilina A, McGinn J, Rendon T, Forrest LR, *et al.* Intestinal serotonin and fluoxetine exposure modulate bacterial colonization in the gut. *Nature Microbiology*. 2019;4(12):2064-2073. doi:10.1038/s41564-019-0540-4
9. Miyauchi E, Kim S, Suda W, Kawasumi M, Onawa S, Taguchi-Atarashi N, Morita H, Taylor TD, Hattori M, Ohno H. Gut microorganisms act together to exacerbate inflammation in spinal cords. *Nature*. 2020;585(7823):102-106. doi:10.1038/s41586-020-2634-9
10. Atarashi K, Tanoue T, Ando M, Kamada N, Nagano Y, Narushima S, Suda W, Imaoka A, Setoyama H, Nagamori T, *et al.* Th17 Cell Induction by Adhesion of Microbes to Intestinal Epithelial Cells. *Cell*. 2015;163(2):367-380. doi:10.1016/j.cell.2015.08.058

11. Kaakoush NO. Insights into the Role of *Erysipelotrichaceae* in the Human Host. *Frontiers in Cellular and Infection Microbiology*. 2015;5(November):1-4. doi:10.3389/fcimb.2015.00084
12. Young KD. The Selective Value of Bacterial Shape. 2006;70(3):660-703. doi:10.1128/MMBR.00001-06
13. Young KD. Bacterial morphology: why have different shapes? 2007:596-600. doi:10.1016/j.mib.2007.09.009
14. McLoughlin K, Schluter J, Rakoff-Nahoum S, Smith AL, Foster KR. Host Selection of Microbiota via Differential Adhesion. *Cell Host & Microbe*. 2016:1-10. doi:10.1016/j.chom.2016.02.021
15. Matz C, Kjelleberg S. Off the hook - how bacteria survive protozoan grazing. 2005;13(7). doi:10.1016/j.tim.2005.05.009
16. Justice SS, Hung C, Theriot JA, Fletcher DA, Anderson GG, Footer MJ, Hultgren SJ. Differentiation and developmental pathways of uropathogenic *Escherichia coli* in urinary tract pathogenesis. 2004;101(5):1333-1338.
17. Sczesnak A, Segata N, Qin X, Gevers D, Petrosino JF, Huttenhower C, Littman DR, Ivanov II. The genome of Th17 cell-inducing segmented filamentous bacteria reveals extensive auxotrophy and adaptations to the intestinal environment. *Cell Host and Microbe*. 2011;10(3):260-272. doi:10.1016/j.chom.2011.08.005
18. Herrmann E, Young W, Rosendale D, Reichert-Grimm V, Riedel CU, Conrad R, Egert M. RNA-Based Stable Isotope Probing Suggests *Allobaculum* spp. as Particularly Active Glucose Assimilators in a Complex Murine Microbiota Cultured in Vitro. *BioMed Research International*. 2017;2017. doi:10.1155/2017/1829685
19. Balakrishnan B, Luckey D, Bodhke R, Chen J, Marietta E, Jeraldo P, Murray J, Taneja V. *Prevotella histicola* Protects From Arthritis by Expansion of *Allobaculum* and Augmenting Butyrate Production in Humanized Mice. *Frontiers in Immunology*. 2021;12(May):1-14. doi:10.3389/fimmu.2021.609644
20. Rivera-Chávez F, Zhang LF, Faber F, Lopez CA, Byndloss MX, Olsan EE, Xu G, Velazquez EM, Lebrilla CB, Winter SE, et al. Depletion of Butyrate-Producing *Clostridia* from the Gut Microbiota Drives an Aerobic Luminal Expansion of *Salmonella*. *Cell Host and Microbe*. 2016;19(4):443-454. doi:10.1016/j.chom.2016.03.004
21. Louis P, Flint HJ. Diversity, metabolism and microbial ecology of butyrate-producing bacteria from the human large intestine. 2009. doi:https://doi.org/10.1111/j.1574-6968.2009.01514.x
22. Turnbaugh PJ, Ridaura VK, Faith JJ, Rey FE, Knight R, Gordon JI. The effect of diet on the human gut microbiome: A metagenomic analysis in humanized gnotobiotic mice. *Science Translational Medicine*. 2009;1(6):1-12. doi:10.1126/scitranslmed.3000322
23. Cox LM, Yamanishi S, Sohn J, Alekseyenko A V, Leung JM, Cho I, Rogers AB, Kim SG, Li H, Gao Z, et al. Altering the Intestinal Microbiota during a Critical Developmental Window Has Lasting Metabolic Consequences. *Cell*. 2014;158(4):705-721. doi:10.1016/j.cell.2014.05.052
24. Ottman N, Davids M, Suarez-Diez M, Boeren S, Schaap PJ, dos Santos VAPM, Smidt H, Belzer C, de Vos WM. Genomescale model and omics analysis of metabolic capacities of *Akkermansia muciniphila* reveal a preferential mucin-degrading lifestyle. *Applied and Environmental Microbiology*. 2017;83(18):1-15. doi:10.1128/AEM.01014-17
25. Hashimoto T, Perlot T, Rehman A, Trichereau J, Ishiguro H, Paolino M, Sigl V, Hanada T, Hanada R, Lipinski S, et al. ACE2 links amino acid malnutrition to microbial ecology and intestinal inflammation. *Nature*. 2012;487(7408):477-481. doi:10.1038/nature11228
26. Greetham HL, Gibson GR, Giffard C, Hippe H, Merkhoffer B, Steiner U, Falsen E, Collins MD. *Allobaculum stercoricanis* gen. nov., sp. nov., isolated from canine feces. *Anaerobe*. 2004;10(5):301-307. doi:10.1016/j.anaerobe.2004.06.004
27. McNeil NI. The contribution of the large intestine to energy supplies in man. *The American Journal of Clinical Nutrition*. 1984;39(2):338-342. doi:10.1093/ajcn/39.2.338
28. Martens EC, Neumann M, Desai MS. Interactions of commensal and pathogenic microorganisms with the intestinal mucosal barrier. *Nature Reviews Microbiology*. 2018;16(8):457-470. doi:10.1038/s41579-018-0036-x
29. Sonnenburg ED, Sonnenburg JL. The ancestral and industrialized gut microbiota and implications for human health. *Nature Reviews Microbiology*. 2019;17(6):383-390. doi:10.1038/s41579-019-0191-8
30. Sonnenburg ED, Smits SA, Tikhonov M, Higginbottom SK, Wingreen NS, Sonnenburg JL. Diet-induced extinctions in the gut microbiota compound over generations. *Nature*. 2016;529(7585):212-215. doi:10.1038/nature16504
31. Sonnenburg JL, Xu J, Douglas L, Chen C-H, Westover B, Weatherford J, Buhler J, Gordon J. Glycan Foraging in Vivo by an Intestine-Adapted Bacterial Symbiont. *Science*. 2005;307(5717):1955-1959. doi:10.1126/science.1109051
32. Martens EC, Chiang HC, Gordon JI. Mucosal Glycan Foraging Enhances Fitness and Transmission of a Saccharolytic Human Gut Bacterial Symbiont. *Cell Host & Microbe*. 2008;4(5):447-457. doi:10.1016/j.chom.2008.09.007
33. Desai MS, Seekatz AM, Koropatkin NM, Kamada N, Hickey CA, Wolter M, Pudlo NA, Kitamoto S, Terrapon N, Muller A, et al. A Dietary Fiber-Deprived Gut Microbiota Degrades the Colonic Mucus Barrier and Enhances Pathogen Susceptibility. *Cell*. 2016;167(5):1339-1353.e21. doi:10.1016/j.cell.2016.10.043
34. Kaoutari A El, Armougom F, Gordon JI, Raoult D, Henrissat B. The abundance and variety of carbohydrate-active enzymes in the human gut microbiota. *Nature Reviews Microbiology*. 2013;11(7):497-504. doi:10.1038/nrmicro3050
35. Martens EC, Lowe EC, Chiang H, Pudlo NA, Wu M, McNulty NP, Abbott DW, Henrissat B, Gilbert HJ, Bolam DN, et al. Recognition and Degradation of Plant Cell Wall Polysaccharides by Two Human Gut Symbionts. *PLoS Biology*. 2011;9(12):e1001221. doi:10.1371/journal.pbio.1001221

36. Smits SA, Leach J, Sonnenburg ED, Gonzalez CG, Lichtman JS, Reid G, Knight R, Manjurano A, Changalucha J, Elias JE, *et al.* Seasonal cycling in the gut microbiome of the Hadza hunter-gatherers of Tanzania. *Science*. 2017;357(6353):802–806. doi:10.1126/science.aan4834
37. Khan S, Waliullah S, Godfrey V, Khan AW, Ramachandran RA, Cantarel BL, Behrendt C, Peng L, Hooper L V, Zaki H. Dietary simple sugars alter microbial ecology in the gut and promote colitis in mice. *Science Translational Medicine*. 2020;12(567). doi:10.1126/scitranslmed.aay6218
38. Chen L, Wang J, Yi J, Liu Y, Yu Z, Chen S, Liu X. Increased mucin degrading bacteria by high protein diet leads to thinner mucus layer and aggravates experimental colitis. *Journal of Gastroenterology and Hepatology*. 2021;36(10):2864–2874. doi:10.1111/jgh.15562
39. Png CW, Lindén SK, Gilshenan KS, Zoetendal EG, McSweeney CS, Sly LI, McGuckin MA, Florin THJ. Mucolytic bacteria with increased prevalence in IBD mucosa augment in vitro utilization of mucin by other bacteria. *American Journal of Gastroenterology*. 2010;105(11):2420–2428. doi:10.1038/ajg.2010.281
40. Tailford LE, Crost EH, Kavanaugh D, Juge N. Mucin glycan foraging in the human gut microbiome. *Frontiers in Genetics*. 2015;6(FEB). doi:10.3389/fgene.2015.00081
41. Lewis AL, Lewis WG. Host sialoglycans and bacterial sialidases: A mucosal perspective. *Cellular Microbiology*. 2012;14(8):1174–1182. doi:10.1111/j.1462-5822.2012.01807.x
42. Huang YL, Chassard C, Hausmann M, Von Itzstein M, Hennet T. Sialic acid catabolism drives intestinal inflammation and microbial dysbiosis in mice. *Nature Communications*. 2015;6:8141. doi:10.1038/ncomms9141
43. Agarwal K, Robinson LS, Aggarwal S, Foster LR, Id AH, Id HL, Tortelli BA, Id VPOB, Id LM, Id ALK, *et al.* Glycan cross-feeding supports mutualism between *Fusobacterium* and the vaginal microbiota. 2020. doi:10.1371/journal.pbio.3000788
44. Tailford LE, Owen CD, Walshaw J, Crost EH, Hardy-Goddard J, Le Gall G, De Vos WM, Taylor GL, Juge N. Discovery of intramolecular trans-sialidases in human gut microbiota suggests novel mechanisms of mucosal adaptation. *Nature Communications*. 2015;6:7624. doi:10.1038/ncomms8624
45. Ng KM, Ferreyra JA, Higginbottom SK, Lynch JB, Kashyap PC, Gopinath S, Naidu N, Choudhury B, Weimer BC, Monack DM, *et al.* Microbiota-liberated host sugars facilitate post-antibiotic expansion of enteric pathogens. *Nature*. 2013;502(7469):96–99. doi:10.1038/nature12503
46. van der Ark K. Metabolic characterization and viable delivery of *Akkermansia muciniphila* for its future application. Wageningen University; 2018. doi:10.18174/427507
47. Kostopoulos I, Elzinga J, Ottman N, Klievink JT, Blijenberg B, Aalvink S, Boeren S, Mank M, Knol J, de Vos WM, *et al.* *Akkermansia muciniphila* uses human milk oligosaccharides to thrive in the early life conditions in vitro. *Scientific Reports*. 2020;10(1):1–17. doi:10.1038/s41598-020-71113-8
48. de Sousa-Pereira P, Woof JM. IgA: Structure, Function, and Developability. *Antibodies*. 2019;8(4):57. doi:10.3390/antib8040057
49. Guo J, Ren C, Han X, Huang W, You Y, Zhan J. Role of IgA in the early-life establishment of the gut microbiota and immunity: Implications for constructing a healthy start. *Gut Microbes*. 2021;13(1):1–21. doi:10.1080/19490976.2021.1908101
50. Bunker JJ, Erickson SA, Flynn TM, Henry C, Koval JC, Meisel M, Jabri B, Antonopoulos DA, Wilson PC, Bendelac A. Natural polyreactive IgA antibodies coat the intestinal microbiota. *Science*. 2017;358(6361):eaan6619. doi:10.1126/science.aan6619
51. van der Houwen TB, van Laar JAM, Kappen JH, van Hagen PM, de Zoete MR, van Muijlwijk GH, Berbers R-M, Fluit AC, Rogers M, Groot J, *et al.* Behçet's Disease Under Microbiotic Surveillance? A Combined Analysis of Two Cohorts of Behçet's Disease Patients. *Frontiers in Immunology*. 2020;11(June):1–10. doi:10.3389/fimmu.2020.01192
52. Rollenske T, Burkhalter S, Muerner L, Gunten S Von, Lukasiewicz J, Wardemann H, Macpherson AJ. Parallelism of intestinal secretory IgA shapes functional microbial fitness. *Nature*. 2021;598(7882):657–661. doi:10.1038/s41586-021-03973-7
53. Donaldson GP, Ladinsky MS, Yu KB, Sanders JG, Yoo BB, Chou WC, Conner ME, Earl AM, Knight R, Bjorkman PJ, *et al.* Gut microbiota utilize immunoglobulin A for mucosal colonization. *Science*. 2018;360(6390):795–800. doi:10.1126/science.aaq0926
54. Nakajima A, Vogelzang A, Maruya M, Miyajima M, Murata M, Son A, Kuwahara T, Tsuruyama T, Yamada S, Matsuura M, *et al.* IgA regulates the composition and metabolic function of gut microbiota by promoting symbiosis between bacteria. *Journal of Experimental Medicine*. 2018;215(8):2019–2034. doi:10.1084/jem.20180427
55. Huus KE, Bauer KC, Brown EM, Bozorgmehr T, Woodward SE, Serapio-Palacios A, Boutin RCT, Petersen C, Finlay BB. Commensal Bacteria Modulate Immunoglobulin A Binding in Response to Host Nutrition. *Cell Host & Microbe*. 2020;27(6):909–921.e5. doi:10.1016/j.chom.2020.03.012
56. Therrien A, Chapuy L, Bsati M, Rubio M, Bernard G, Arslanian E, Orlicka K, Weber A, Panzini BP, Dorais J, *et al.* Recruitment of activated neutrophils correlates with disease severity in adult Crohn's disease. *Clinical and Experimental Immunology*. 2019;195(2):251–264. doi:10.1111/cei.13226
57. Brazil JC, Louis NA, Parkos CA. The role of polymorphonuclear leukocyte trafficking in the perpetuation of inflammation during inflammatory bowel disease. *Inflammatory Bowel Diseases*. 2013;19(7):1556–1565. doi:10.1097/MIB.0b013e318281f54e
58. Steffen U, Koeleman CA, Sokolova M V., Bang H, Kleyer A, Rech J, Unterweger H, Schicht M, Garreis F, Hahn J, *et al.* IgA subclasses have different effector functions associated with distinct glycosylation profiles. *Nature Communications*. 2020;11(1). doi:10.1038/s41467-019-13992-8



59. Günaydin G, Nordgren J, Sharma S, Hammarström L. Association of elevated rotavirus-specific antibody titers with HBGA secretor status in Swedish individuals: The FUT2 gene as a putative susceptibility determinant for infection. *Virus Research*. 2016;211:64–68. doi:10.1016/j.virusres.2015.10.005
60. Maurer MA, Meyer L, Bianchi M, Turner HL, Le NPL, Steck M, Wyrzucki A, Orłowski V, Ward AB, Crispin M, et al. Glycosylation of Human IgA Directly Inhibits Influenza A and Other Sialic-Acid-Binding Viruses. *Cell Reports*. 2018;23(1):90–99. doi:10.1016/j.celrep.2018.03.027
61. Larsen MD, de Graaf EL, Sonneveld ME, Plomp HR, Nouta J, Hoepel W, Chen HJ, Linty F, Visser R, Brinkhaus M, et al. Afucosylated IgG characterizes enveloped viral responses and correlates with COVID-19 severity. *Science*. 2021;371(6532). doi:10.1126/science.abc8378
62. Chintalacheruvu KR, Morrison SL. Production of secretory immunoglobulin A by a single mammalian cell. *Proceedings of the National Academy of Sciences*. 1997;94(12):6364–6368. doi:10.1073/pnas.94.12.6364
63. Vasilev N, Smales CM, Schillberg S, Fischer R, Schiermeyer A. Developments in the production of mucosal antibodies in plants. *Biotechnology Advances*. 2016;34(2):77–87. doi:10.1016/j.biotechadv.2015.11.002
64. Kiser ZM, Lizcano A, Nguyen J, Becker GL, Belcher JD, Varki AP, Vercellotti GM. Decreased erythrocyte binding of Siglec-9 increases neutrophil activation in sickle cell disease. *Blood Cells, Molecules, and Diseases*. 2020;81:102399. doi:10.1016/j.bcmd.2019.102399
65. Wanderley CWS, Lorenzini CB, Santos AA, Fonseca FR, Aires L, Heck N, Starick MR. Neuraminidase inhibitors rewire neutrophil function. *bioRxiv*. 2020. doi:https://doi.org/10.1101/2020.11.12.379115
66. Chang YC, Uchiyama S, Varki A, Nizet V. Leukocyte inflammatory responses provoked by pneumococcal sialidase. *mBio*. 2012;3(1):1–10. doi:10.1128/mBio.00220-11
67. Razi N, Varki A. Cryptic sialic acid binding lectins on human blood leukocytes can be unmasked by sialidase treatment or cellular activation. *Glycobiology*. 1999;9(11):1225–1234. doi:10.1093/glycob/9.11.1225
68. Shkandina T, Herrmann M, Bilyy R. Sweet kiss of dying cell: Sialidase activity on apoptotic cell is able to act toward its neighbors. *Autoimmunity*. 2012;45(8):574–578. doi:10.3109/08916934.2012.719951
69. Bilyy RO, Shkandina T, Tomin A, Muñoz LE, Franz S, Antonyuk V, Kit YY, Zirngibl M, Fürnrohr BG, Janko C, et al. Macrophages Discriminate Glycosylation Patterns of Apoptotic Cell-derived Microparticles. *Journal of Biological Chemistry*. 2012;287(1):496–503. doi:10.1074/jbc.M111.273144
70. Yang WH, Heithoff DM, Aziz P V., Sperandio M, Nizet V, Mahan MJ, Marth JD. Recurrent infection progressively disables host protection against intestinal inflammation. *Science*. 2017;358(6370). doi:10.1126/science.aao5610
71. Mozzi A, Forcella M, Riva A, Difrancesco C, Molinari F, Martin V, Papini N, Bernasconi B, Nonnis S, Tedeschi G, et al. NEU3 activity enhances EGFR activation without affecting EGFR expression and acts on its sialylation levels. *Glycobiology*. 2015;25(8):855–868. doi:10.1093/glycob/cwv026
72. Pillai S, Netravali IA, Cariappa A, Mattoo H. Siglecs and Immune Recognition. *Annual Review of Immunology*. 2012;30(3):357–392. doi:10.1146/annurev-immunol-020711-075018.Siglecs
73. MacAuley MS, Crocker PR, Paulson JC. Siglec-mediated regulation of immune cell function in disease. *Nature Reviews Immunology*. 2014;14(10):653–666. doi:10.1038/nri3737
74. Pshezhetsky A V., Hinek A. Where catabolism meets signalling: Neuraminidase 1 as a modulator of cell receptors. *Glycoconjugate Journal*. 2011;28(7):441–452. doi:10.1007/s10719-011-9350-5
75. Dwarakanath AD, Campbell BJ, Tsai HH, Sunderland D, Hart CA, Rhodes JM. Faecal mucinase activity assessed in inflammatory bowel disease using 14C threonine labelled mucin substrate. *Gut*. 1995;37(1):58–62. doi:10.1136/gut.37.1.58
76. Miklavcic JJ, Hart TD, Lees GM, Shoemaker GK, Schnabl KL, Larsen BM, Bathe OF, Thomson AB, Mazurak VC, Clandinin MT. Increased catabolism and decreased unsaturation of ganglioside in patients with inflammatory bowel disease. *World Journal of Gastroenterology*. 2015;21(35):10080–10090. doi:10.3748/wjg.v21.i35.10080
77. Lloyd-Price J, Arze C, Ananthakrishnan AN, Schirmer M, Avila-Pacheco J, Poon TW, Andrews E, Ajami NJ, Bonham KS, Brislawn CJ, et al. Multi-omics of the gut microbial ecosystem in inflammatory bowel diseases. *Nature*. 2019;569(7758):655–662. doi:10.1038/s41586-019-1237-9
78. Li H, Limenitakis JP, Fuhrer T, Geuking MB, Lawson MA, Wyss M, Brugiroux S, Keller I, Macpherson JA, Rupp S, et al. The outer mucus layer hosts a distinct intestinal microbial niche. *Nature Communications*. 2015;6(1):8292. doi:10.1038/ncomms9292
79. Donaldson GP, Chou WC, Manson AL, Rogov P, Abeel T, Bochicchio J, Ciulla D, Melnikov A, Ernst PB, Chu H, et al. Spatially distinct physiology of *Bacteroides fragilis* within the proximal colon of gnotobiotic mice. *Nature Microbiology*. 2020;5. doi:10.1038/s41564-020-0683-3
80. Kallemeijn WW, Li K-Y, Witte MD, Marques ARA, Aten J, Scheij S, Jiang J, Willems LI, Voorn-Brouwer TM, van Roomen CPAA, et al. Novel Activity-Based Probes for Broad-Spectrum Profiling of Retaining  $\alpha$ -Exoglucosidases In Situ and In Vivo. *Angewandte Chemie International Edition*. 2012;51(50):12529–12533. doi:10.1002/anie.201207771
81. Luijckx YMCA, Henselijn AJ, Bosman GP, Cramer DAT, Giesbers CAP, van 't Veld EM, Boons GJPH, Heck AJR, Reiding KR, Strijbis K, et al. Detection of bacterial  $\alpha$ -L-fucosidases with an ortho-quinone methide-based probe and mapping of the probe-protein adducts.

82. De Oliveira JT, Santos AL, Gomes C, Barros R, Ribeiro C, Mendes N, De Matos AJ, Vasconcelos MH, Oliveira MJ, Reis CA, *et al.* Anti-influenza neuraminidase inhibitor oseltamivir phosphate induces canine mammary cancer cell aggressiveness. *PLoS ONE*. 2015;10(4):1-22. doi:10.1371/journal.pone.0121590
83. Peterson DA, McNulty NP, Guruge JL, Gordon JI. IgA Response to Symbiotic Bacteria as a Mediator of Gut Homeostasis. *Cell Host and Microbe*. 2007;2(5):328-339. doi:10.1016/j.chom.2007.09.013
84. Joglekar P, Ding H, Canales-Herrerias P, Pasricha PJ, Sonnenburg JL, Peterson DA. Intestinal IgA Regulates Expression of a Fructan Polysaccharide Utilization Locus in Colonizing Gut Commensal *Bacteroides thetaiotaomicron*. *mBio*. 2019;10(6):1-13. doi:10.1128/mBio.02324-19

# SUMMARY

Microbial communities that colonize our bodies are collectively referred to as the microbiota, or the microbiome when referring to their total collection of genes. To date, thousands of microbial species and communities have been discovered and are known to exert profound effects on human physiology and health. Most microbes are found in our intestines and the intestinal microbiota is the most well studied in relationship to human disease. One of the diseases in which the composition of the intestinal microbiota is altered is inflammatory bowel disease (IBD). IBD pathogenesis is currently thought to occur from complex interactions involving genetic predisposition, environmental factors, aberrant immune responses, and alterations to the gut microbiota, also referred to as dysbiosis. This dysbiotic microbiota can then act as a driver of inflammatory responses, e.g., through increased levels of bacterial translocation.

The gut microbiota composition of IBD patients is often less diverse than in healthy controls. General patterns include a reduction in the relative abundance of the *Firmicutes* and *Bacteroidetes* phyla and an increase in the number of *Enterobacteriaceae*. Other notable changes include the increased number of encroaching, mucosa-associated bacteria as well as changes in the IgA-coated bacterial communities. Some of these immunogenic, IgA-inducing commensals are thought to have increased pathogenic potential compared to other symbionts and are referred to as pathogenic symbionts or pathobionts. Although many associations and correlations between the gut microbiota composition, pathobionts and IBD susceptibility have been reported to date, it has often been difficult to establish causality outside of mouse models. This is likely due to the complex, multifactorial nature of the disease. Moreover, a deeper understanding of these complex interactions is often hampered by the fact that most bacteria within the gut remain functionally unexplored. Therefore, if we aim to elucidate novel mechanisms that drive IBD development, a more detailed and functional characterization of dysbiosis-associated microbes and their interaction with the host is warranted. I focused my investigation on IgA-inducing pathobionts and their interactions with critical constituents of the mucus layer and the mucosal barrier, such as mucins and secretory IgA.

The intestinal mucus layer is an important part of the innate immune system and a first line of defence. It protects the underlying epithelium from dehydration, functions as a lubricant, and acts as a barrier to protect the epithelial cells and lamina propria from excessive exposure to foreign antigens and pathogens, including bacteria, and as such is crucial for maintaining

intestinal homeostasis. In the intestine, the largest part of the mucus layer is composed of the secreted and gel-forming mucin MUC2. Mucins, including MUC2, are heavily decorated with glycans. The glycans on MUC2 determine up to 80% of its mass and give the mucin a bottlebrush-like structure. These glycans have several important roles including the ability to attract water, prevent proteolytic cleavage of the mucin backbone, form a physical barrier to microbes as well as facilitate interactions with the microbiota.

Multiple bacterial species have evolved strategies to interact with mucins. For example, mucin-utilizing bacteria often degrade mucin *O*-glycans and acquire the released monosaccharides for growth. They degrade mucin glycans through the concerted action of carbohydrate active enzymes (CAZymes), which include a wide array of glycosidases that attack the glycosidic bonds within the glycan chain. The mucus layer is a unique nutrient niche and the ability of certain species to utilize host-derived mucins offers a competitive advantage over bacteria that lack this trait. However, whether and how different mucus-colonizing bacteria influence each other's growth remains to be explored.

Secretory IgA (sIgA) is another important component of the intestinal mucosal barrier. sIgA is the most abundant immunoglobulin class in our body and is ubiquitously secreted at mucosal surfaces. sIgA can exert a wide variety of functions. Most importantly, sIgA contributes to intestinal homeostasis by limiting microbial overgrowth and preventing microbes from invading underlying tissue. sIgA neutralizes toxins, limits bacterial motility, blocks adhesins and leads to immune exclusion through bacterial enchainment. IgA is also important for establishing a diverse and balanced microbiota early in life and shaping appropriate mucosal immune responses.

sIgA binds a wide variety of commensal intestinal bacteria but inflammatory pathobionts are especially highly IgA coated. It is interesting to note that many of these IgA-coated species are also considered mucus-colonizing and mucus-degrading bacteria. This suggests that colonization of the mucosal niche or the factors that influence colonization predispose these species to be targeted by sIgA. Even though these pathobionts elicit potent immune responses and can contribute to intestinal inflammation, it is largely unknown how these IgA-inducing pathobionts differ from other bacteria and which traits underly their immunogenic and inflammatory potential.

In order to advance our understanding of the role of the gut microbiota in IBD, the challenge of the field is to progress beyond association and correlation studies and to strive to attain new mechanistic insights into the factors that drive disease development. IgA-inducing pathobionts are critical modulators of the mucosal niche with an outsized influence on host immune responses, and as such can modulate inflammatory conditions such as IBD. Currently, many of the pathobionts remain functionally unexplored and many of the molecular mechanisms that govern their interactions within the mucosal niche remain uncharacterized. Importantly, many of these interactions are influenced by or even fully depend on glycans, a factor that is often underappreciated. In this thesis we studied pathobionts and their glycobiological interactions with critical components of the mucosal niche with the aim of identifying novel molecular mechanisms that help elucidate the pathways that drive pathological inflammatory conditions such as IBD.

In **Chapter 2** we describe two novel, strictly anaerobic, IgA-inducing bacteria isolated from the feces of humans with IBD. While being closely related to *Allobaculum stercoricanis*, the 16S rRNA gene sequences of the isolates shows a 91.95% and 93.25% similarity (95.49% similar to each other) and therefore phylogenetically cluster separately. Therefore, we propose to designate these two novel species as *Allobaculum mucolyticum* sp. nov. and *Allobaculum filumensis* sp. nov. We provide the first microscopic, genetic and chemical characterization of these two immunogenic and inflammatory bacterial species. Both species are strictly anaerobic, non-motile, rod-shaped and grow in long chains between 37°C and 42°C. Scanning electron microscopy did not reveal flagella, fimbriae or visible endospores. We also performed a biochemical analysis which showed that both species display nearly identical enzymatic activities with enzymatic activity of C4 and C8 esterases, acid phosphatase, Naphthol-AS-BI-phosphohydrolase,  $\beta$ -Glucuronidase, N-Acetyl- $\beta$ -Glucosaminidase and Arginine Arylamidase. In addition, both strains produced indole and reduced nitrate. These findings provide a foundation for the work described in later chapters as well as provide an important reference for others in the field.

*Allobaculum mucolyticum*, as characterized in chapter 2, is a newly identified, IBD-associated species that is thought to be closely associated with the host epithelium. A crucial prerequisite for bacterial survival and proliferation is the creation and/or exploitation of an own niche. For many bacterial species that are linked to IBD the inner mucus layer was found to be an important niche. In **Chapter 3** we explored how *A. mucolyticum* can effectively colonize

and interact with the mucus layer. We screened its genome for factors that may contribute to mucosal colonization. Up to 60 genes encoding putative Carbohydrate Active Enzymes (CAZymes) were identified. Mass spectrometry revealed 49 CAZymes of which 26 were significantly enriched in its secretome. Using functional assays, we also demonstrated the presence of CAZyme activity in *A. mucolyticum* conditioned medium. This enabled this bacterium to degrade human mucin O-glycans and utilize the liberated non-terminal monosaccharides for growth. These results support a model in which sialidases and fucosidases remove terminal O-glycan sugars enabling subsequent degradation and utilization of carbohydrates for *A. mucolyticum* growth. *A. mucolyticum* CAZyme secretion may thus facilitate bacterial colonization and degradation of the mucus layer and may pose an interesting target for future therapeutic intervention.

In **Chapter 4** we explore the molecular interactions between the probiotic *Akkermansia muciniphila* and other bacteria, in particular other mucin-degrading species, such as *A. mucolyticum*. In IBD, *A. muciniphila* is reduced in abundance while other, putative pathogenic, mucus colonizers bloom. We hypothesized that interbacterial competition may contribute to this observation. By screening the supernatants of a panel of enteric bacteria, we discovered that *A. mucolyticum* potently inhibits the growth of *A. muciniphila*. Mass spectrometry analysis and a large array of functional assays identified a secreted *A. mucolyticum* sialidase as an inhibitor of *A. muciniphila* growth. The sialidase targets sialic acids on casein O-glycans, present within the medium, thereby altering the accessibility of nutrients critical for *A. muciniphila* growth. The altered glycometabolic niche results in distorted *A. muciniphila* cell division and efficiently arrests its growth. Inhibition of *A. muciniphila* growth could also be detected when using other bacterial sialidases, indicating this mechanism of inhibition is not limited to *A. mucolyticum*. The identification of a novel mechanism of *A. muciniphila* growth inhibition by a competing bacterial pathobiont may provide a rationale for interventions aimed at restoring and maintaining a healthy microbiota symbiosis in patients with intestinal disease.

**Chapter 5** focuses on the role of sIgA glycosylation and the role of sialic acids in regulating neutrophil responses. Particular attention was given to the potential role of bacterial sialidases, including the NanH1 sialidase from *A. mucolyticum*, as modulator of sIgA function. We demonstrated that this NanH1 sialidase, as well as several other bacterial sialidases, efficiently remove sialic acid from human colostrum sIgA and that sIgA desialylation results in increased sIgA-mediated neutrophil activation. We also showed that the enhanced sIgA-

mediated neutrophil activation is reduced in the presence of free sialic acid or sialic acid analogues but can be even further enhanced by desialylation of the neutrophil cell surface. IgA-coated, sialidase-producing bacteria as well as excessive neutrophil responses are known to play important roles in intestinal inflammation. Our findings indicate that bacterial sialidases may contribute to the inflammatory process.

The aim of this thesis was to investigate intestinal pathobionts and their glycobiological interactions with critical components of the mucosal barrier. By studying the IgA-coated pathobiont *A. mucolyticum*, we aimed to identify novel molecular mechanisms that help elucidate the pathways that drive pathological inflammatory conditions such as IBD.

As shown in the different chapters of this thesis, the CAZymes of *A. mucolyticum* play important roles in mucus degradation and as modulators of the intestinal mucosal niche; these CAZymes contribute to degradation of host- and dietary-derived glycoproteins resulting in mucus degradation and alteration of the glycometabolic niche which favours competition with other mucus-colonizing microbes. Moreover, CAZymes also play a role in the modulation of neutrophil inflammatory responses. Therefore, under the right circumstances, CAZymes can likely act as drivers of intestinal dysbiosis and inflammation, as seen in IBD.

As bacterial CAZymes, but also host CAZymes, influence host-microbial interactions on so many levels, their role needs to be discussed in a broader ecological and evolutionary framework in which the reciprocal interactions between the gut microbiota, host immunity, and dietary factors are viewed from an integrative perspective that, importantly, also takes into consideration the effects of glycobiological interactions. It is evident that glycans and glycosidases are critical players at the host-microbe interface and that integration of glycobiology in this research area will greatly enhance our understanding of the processes that govern intestinal homeostasis and disease.

# NEDERLANDSE SAMENVATTING

Onze lichamen worden bevolkt door vele honderden miljarden micro-organismen. Deze verzameling van micro-organismen in en op het menselijk lichaam wordt de microbiota genoemd, en de verzameling genen die zij bij zich dragen het microbiom. Het onderzoek naar deze microbiota heeft in de laatste jaren een enorme vlucht genomen en het is duidelijk dat wij mensen bevolkt worden door vele duizenden verschillende soorten microben die samenleven in complexe verbanden. Gezamenlijk hebben ze een grote invloed op ons lichaam en onze gezondheid.

De meeste micro-organismen bevinden zich in de darm. De darmmicrobiota is het best bestudeerd in gevallen van ziekte, bijvoorbeeld bij chronische darmontstekingen zoals de ziekte van Crohn of ulceratieve colitis. Samen worden deze ook wel inflammatory bowel disease, of IBD genoemd. De ontstaanswijze van IBD is nog altijd niet precies bekend, maar bestaat vrijwel zeker uit een combinatie van factoren waaronder genetische aanleg, omgevingsfactoren, afwijkingen in de immunrespons en veranderingen in de darmmicrobiota. Deze veranderde samenstelling van de darmmicrobiota wordt ook wel dysbiose genoemd. De samenstelling van zo'n dysbiotische darmmicrobiota van IBD patiënten is vaak minder divers, met minder verschillende soorten bacteriën dan in gezonde mensen. Ook bevinden in IBD patiënten meer bacteriën zich dichtbij de darmwand. Sommige van de bacteriën hebben bovendien de neiging om het immuunsysteem te activeren en ontstekingsreacties in de darm te veroorzaken. De hypothese is dat deze bacteriën, ook wel pathobionten genaamd, de aanjager kunnen zijn van chronische ontstekingsreacties zoals bij IBD. De manier waarop ze dit doen is echter niet duidelijk omdat veel van deze bacteriën nog amper functioneel zijn bestudeerd. Daarom is een nader onderzoek van deze pathobionten nodig zodat we hun bijdrage aan de ziekteprocessen van IBD beter kunnen begrijpen. In mijn onderzoek heb ik met name gefocust op de interactie van pathobionten met cruciale onderdelen van de darmwand en de slijmvliesbarrière, zoals de slijmlaag zelf, mucine eiwitten en uitgescheiden IgA antilichamen.

De slijmerige mucuslaag is als eerste verdedigingslinie een belangrijk onderdeel van het immuunsysteem in onze darmen. Onze darmen kun je beschouwen als een buis waarbij de bacteriën zich in de holte van de buis bevinden en de buis zelf de darmwand is. De cellen in de darmwand, de zogenaamde darmepitheel cellen, zijn cruciaal voor de opname van water en voedingsstoffen en dienen dan ook beschermd te worden tegen schadelijke bacteriën, die als ze te dichtbij komen cel schade en ontstekingen kunnen veroorzaken. Hiervoor wordt aan de binnenkant van de darmwand een

beschermende slijmlaag gevormd, de zogenaamde mucuslaag. Deze is opgebouwd uit hele grote, langgerekte mucine eiwitten waaraan heel veel suikerketens zijn bevestigd. Deze suikerketens, ook wel glycanen genoemd, trekken water aan. Dit zorgt voor een smerende werking en beschermt de onderliggende epitheel cellen tegen uitdroging. Deze glycanen bevinden zich als een soort zijtakken aan een hoofdstam (het mucine eiwit) en vormen zo een soort van borstel. Veel van deze borstels samen vormen een bijna ondoordringbare barrière die bacteriën dient tegen te houden.

Desalniettemin hebben sommige bacteriën hebben zich zo aangepast dat ze toch aan de mucuslaag kunnen blijven plakken of hem zelfs kunnen afbreken. Ze doen dit onder andere door het uitscheiden van mucolytische enzymen, zogenaamde CAZymes, die de suikerketens van de mucine eiwitten kunnen afbreken. Vanwege de complexe structuur van deze glycanen bezitten mucolytische bacteriën vaak een groot arsenaal van deze enzymen. De losgeknipte suikers kunnen vervolgens door de bacterie worden opgenomen en gebruikt worden voor groei. Het kunnen afbreken van de mucuslaag biedt bacteriën een evolutionair voordeel omdat ze op die manier een unieke niche weten te benutten die voor veel andere bacteriën in de darm niet toegankelijk is. Voor veel van deze mucolytische bacteriën is nog niet goed in kaart gebracht hoe ze de mucuslaag kunnen afbreken, en hoe ze elkaar en de gastheer kunnen beïnvloeden.

IgA antilichamen zijn een ander belangrijk onderdeel van de slijmvliesbarrière. Antilichamen worden geproduceerd door onze immuuncellen en kunnen zich veelal specifiek binden aan bepaalde doelwitten. IgA is de meest geproduceerde antilichaam-klasse in ons lichaam en wordt voornamelijk uitgescheiden door onze slijmvliezen. IgA heeft veel uiteenlopende functies. De belangrijkste functie is het beschermen van het evenwicht in de darm door te verhinderen dat darmbacteriën te dichtbij de darmwand komen of die zelfs kunnen binnendringen. Het doet dit onder andere door te binden aan toxines of direct aan bacteriën waardoor deze zich niet meer kunnen binden, bewegen of zelfs worden samengeklonterd met andere bacteriën. Hierdoor draagt IgA ook bij aan een gebalanceerde en gezonde samenstelling van de darmmicrobiota.

Hoewel IgA veel verschillende bacteriën kan binden lijken de ontstekingsveroorzakende pathobionten het voornaamste doelwit te zijn. Interessant genoeg bevinden veel van deze pathobionten zich in de mucuslaag. Dit duidt er op dat hun aanwezigheid in de mucuslaag een immuun reactie veroorzaakt waardoor IgA tegen deze bacteriën wordt geproduceerd. Hoewel deze



pathobionten een sterke immuun reactie kunnen veroorzaken en kunnen bijdragen aan darmontstekingen is veelal nog niet duidelijk op welke manier pathobionten verschillen van andere bacteriën en welke eigenschappen bijdragen aan de ontstekingsprocessen.

Het is duidelijk dat pathobionten een belangrijke rol kunnen spelen bij het ontstaan en verergeren van darmontstekingen, maar veel van deze pathobionten zijn nog weinig bestudeerd en de moleculaire mechanismen die ze gebruiken in de interactie met de slijmvliesbarrière in de darm zijn nog grotendeels onbekend. Bovendien worden waarschijnlijk veel van de interacties beïnvloed door de aan- of afwezigheid van suikers, een cruciaal onderdeel van de biologie dat nogal eens over het hoofd wordt gezien. In het onderzoek beschreven in dit proefschrift hebben we daarom meerdere, al dan niet suiker-gemedieerde, interacties bestudeerd tussen pathobionten en cruciale onderdelen van de darmwand en de slijmvliesbarrière, met als doel om nieuwe moleculaire mechanismes te ontdekken die kunnen verklaren hoe deze bacteriën kunnen bijdragen aan darmontstekingsziektes zoals IBD.

In **Hoofdstuk 2** beschrijven we de eigenschappen van twee nog niet eerder beschreven pathobionten. Ze zijn beide geïsoleerd uit de ontlasting van IBD patiënten op basis van het feit dat ze door veel IgA antilichamen gebonden worden. Door middel van genoom analyse en vergelijking met naaste verwanten werd duidelijk dat ze beide sterk op elkaar leken en op de *Allobaculum stercoricanis*, maar dat het unieke soorten zijn binnen hetzelfde genus. Daarom stellen we voor deze twee nieuwe soorten *Allobaculum mucolyticum* sp. nov. and *Allobaculum filumensis* sp. nov. te noemen. Verdere microscopische en chemische analyses toonden aan dat deze bacteriën veelal in lange ketens groeien, niet beweeglijk zijn en beide een uniek chemisch profiel hebben. Deze gegevens vormen een belangrijke referentie voor het onderzoek beschreven in de andere hoofdstukken van deze thesis alsmede voor andere onderzoekers.

*Allobaculum mucolyticum*, zoals beschreven in hoofdstuk 2, is een nieuw beschreven bacterie die geïsoleerd werd uit een IBD patiënt en waarvan wordt vermoed dat die zich in de mucuslaag nestelt of aan de darmwand kan hechten. In **Hoofdstuk 3** hebben we onderzocht hoe *A. mucolyticum* de mucuslaag kan koloniseren en ermee kan interacteren. We hebben het genoom gescreend voor factoren die mogelijk kunnen bijdragen aan mucus kolonisatie. *A. mucolyticum* bleek meer dan 60 genen te bezitten die voor mucolytische enzymen, ofwel CAzymes, coderen. Met behulp van massa

spectrometrie konden we aantonen dat 49 enzymen ook daadwerkelijk geproduceerd worden, waarvan een groot deel ook wordt uitgescheiden. We konden met behulp van functionele testen aantonen dat de combinatie van enzymactiviteiten de glycanen van mucine eiwitten kan afbreken waarna de bacterie een deel van de vrijgekomen suikers kan gebruiken voor groei. Het uitscheiden van deze enzymen kan deze bacterie dus in staat stellen de mucuslaag af te breken en te koloniseren. Deze enzymen zijn daarom mogelijk een interessant doelwit voor toekomstige therapeutische interventies.

In **Hoofdstuk 4** hebben we de moleculaire interacties onderzocht tussen de probiotische, mucolytische bacterie *Akkermansia muciniphila* en andere darmbacteriën, en dan met name andere mucolytische bacteriën, zoals de pathobiont *Allobaculum mucolyticum*. In IBD patiënten is de hoeveelheid probiotische *A. muciniphila* verminderd, terwijl andere mucolytische bacteriën zich juist vermeerderen. We bedachten dat directe competitie tussen deze bacteriën hiervoor verantwoordelijk zou kunnen zijn. Om dit te testen hebben we de groei van *A. muciniphila* getest in aanwezigheid van de uitgescheiden fractie van andere darmbacteriën. Hieruit bleek dat de uitgescheiden fractie van *Allobaculum mucolyticum* de groei van *A. muciniphila* sterk kon remmen. Door middel van fractionering en massaspectrometrie en een aantal verschillende functionele testen konden we achterhalen dat een bepaald enzym, een sialidase, hiervoor verantwoordelijk is. Deze sialidase is een enzym dat bepaalde suikers, siaalzuren genaamd, kan losknippen van onderliggende glycanen. In dit geval gaat het om glycanen die aanwezig zijn op het caseïne melkeiwit, dat aanwezig is in het groei medium. Door het losknippen van de siaalzuren is *A. muciniphila* niet langer in staat om de resterende suikers te gebruiken waardoor deze stopt met groeien. We hebben ook aangetoond dat, behalve de sialidasen van *A. mucolyticum* ook sialidasen van andere bacteriën de groei van *A. muciniphila* op deze manier kunnen remmen. Deze manier van competitie tussen een pathobiont en een probiotische bacterie is niet eerder beschreven en kan een belangrijke basis vormen voor interventies die erop gericht zijn de balans in de darmmicrobiota van IBD patiënten te herstellen.

In **Hoofdstuk 5** hebben we de rol van suikers op IgA antilichamen onderzocht en met name hun rol bij neutrofiel activatie. Neutrofielen zijn de witte bloedcellen die als eerste worden opgeroepen bij bacteriële infecties. Ze vernietigen bacteriën door ze op te eten en te bestoken met zuurstofradicalen. Ze worden hierbij geholpen doordat bacteriën zijn gelabeld met antilichamen zoals IgA.

De rol van de suikers op dit proces van IgA-gemedieerde neutrofiel activatie is echter niet duidelijk. Om dit te onderzoeken hebben we gebruik gemaakt van het sialidase enzym van *Allobaculum mucolyticum*. Deze sialidase, alsmede de sialidases van andere bacteriën, waren in staat om efficiënt siaalzuren te verwijderen van de glycanen op menselijk colostrum IgA. De verwijdering van siaalzuren van IgA resulteerde in een toename van IgA-gemedieerde neutrofiel activatie. We konden ook aantonen dat deze activatie geremd kon worden door toevoeging van losse siaalzuren of siaalzuren-analogen, zoals de virusremmer oseltamivir fosfaat. Echter, als ook de siaalzuren van de neutrofiel zelf verwijderd werden werd de neutrofiel activatie nog sterker. IgA-gebonden pathobionten alsmede excessieve neutrofiel responsen spelen allebei een rol bij het ontstaan van darmontstekingen. Onze bevindingen wijzen erop dat bacteriële sialidases kunnen bijdragen aan het ontstekingsproces.

Het doel van het onderzoek beschreven in dit proefschrift was het ontdekken van darm pathobionten en het begrijpen van hun suiker-gemedieerde interacties met kritieke componenten van de slijmvliesbarrière. Door het bestuderen van de IgA-gebonden pathobiont *Allobaculum mucolyticum* hebben we nieuwe moleculaire mechanismen kunnen identificeren en zo een stap kunnen zetten in het ontrafelen van ziekmakende ontstekingsprocessen in de darm.

Omdat bacteriële suiker-afbrekende enzymen de interacties tussen de gastheer en bacterie op zoveel verschillende manieren kunnen beïnvloeden is het essentieel dat hun rol wordt besproken in een bredere, ecologische en evolutionaire context, waarbij de interacties tussen de microbiota, het immuunsysteem van de gastheer en voedingsfactoren worden gezien vanuit een integraal perspectief, waarin uitdrukkelijk ook de suiker-gemedieerde effecten in overweging worden genomen. Het is evident dat suikers en suiker-afbrekende enzymen een belangrijke rol vervullen in de uitwisseling tussen ons en onze microbiota. Verdere integratie van de glycobiologie in dit onderzoeksgebied zal daarom voor ontzettend veel nieuwe inzichten kunnen zorgen in de processen die betrokken zijn bij chronische darmziekten.

**DANKWOORD/  
ACKNOWLEDGEMENTS**

Na bijna zes jaar is het dan zover, ik mag eindelijk beginnen aan dit dankwoord.

In deze voorbije jaren heb ik ontzettend veel nieuwe mensen ontmoet en altijd mensen om me heen gehad die me steunden. Zoveel mensen zelfs dat ik het niet onmogelijk acht dat ik hier en daar een naam vergeet te noemen. Bij voorbaat mijn welgemeende excuses.

Laat ik beginnen diegenen te bedanken die vaak worden overgeslagen in het dankwoord. Dat bent u, de belastingbetaler en stemgerechtigde. Zonder uw steun was dit onderzoek en al het andere onderzoek in Nederland niet mogelijk geweest. Hartelijk dank daarvoor.

Ook wil ik bij deze gelijk de leden van de leescommissie hartelijk bedanken voor hun tijd, alsook de waardevolle feedback op m'n proefschrift.

Vervolgens wil ik graag **Marcel** bedanken. Eind 2015 zag ik je een presentatie geven over pathobionten en ik dacht gelijk: dat lijkt me wel cool onderzoek. Ik ben je dan ook ontzettend dankbaar dat je me de kans hebt gegeven om dit onderzoek te mogen doen. Je hebt me altijd alle ruimte gegeven om zowel het onderzoek als mezelf te ontwikkelen. Je wist me op jouw relaxte manier altijd te stimuleren om dieper de moleculaire mechanismes in te duiken, toch nog even dat experimentje te doen, of me toch weer aan het schrijven te zetten, ook als ik daar eigenlijk geen zin in had of er het nut niet van inzag. En als je weer eens die eeuwig terugkerende vraag stelde, 'En, data?' voelde dat dan ook niet als een verplichting, maar meer als aanmoediging. Met dit proefschrift heb ik eindelijk al die data bij elkaar gebracht en ik ben blij dat ik ook na al die jaren met volle overtuiging kan zeggen dat het wel cool onderzoek is.

**Jos**, het onmisbare tweede deel van het supervisorsoren-tandem, ook jij ontzettend bedankt voor al je tijd, aandacht en interesse. Het was fijn om te weten dat er naast Marcel nog altijd iemand was om bij aan te kloppen. Je fungeerde als waardevol klankbord en je vermogen om binnen een mum van tijd tot de kern van een persoonlijk of wetenschappelijk probleem door te dringen is bewonderingswaardig en heeft me een boel nieuwe inzichten opgeleverd.

Dan de overige leden van de voormalige infectiebiologie groep. **Marc** heel erg bedankt voor de goede discussies en adviezen tijdens labmeetings of bij de koffieautomaat. Ook waardeer ik al je pogingen om het woord erysipelotrichaceae goed uit te spreken. Ik ben er inmiddels zelf ook maar mee

gestopt. **Karin**, bedankt voor al het enthousiasme waarmee je het mucine-onderzoek bedrijft en aan de man brengt. Mijn interesse was natuurlijk al vroeg gewekt en dankzij jouw expertise heb ik mijn eigen mucine werk zeker kunnen verbeteren. Dan **Nancy & Linda**, de moeders en hoeders van het lab, zou ik wel durven stellen. Jullie wisten altijd van de hoed en van de rand, zowel op persoonlijk vlak als in het lab. Zonder jullie gezelligheid en gouden adviezen was het lab een stuk saaier en chaotischer geweest. Dan m'n mede PhD's. Ten eerste, **Mehdi, Claudia, Kasia**, en **Ax**; as a rookie in the lab, I could always turn to you for advice on anything. Be it bacterial culture, western blotting or general advice on how to deal with experimental problems. Thank you very much for creating such a welcoming atmosphere in the lab. It surely got me off to a good start. **Carlos**, van alle mensen heb ik met jou het langst een kantoor gedeeld en het was me een waar genoegen. Onze kantoorhumor was vaak van zeer bedenkelijk niveau en dat is natuurlijk ook precies hoe het hoort te zijn. Voor mij was met name het enthousiasme en de energie waarmee je op TLRs of woestijnschilpadden stortte altijd heel inspirerend. **Xinyue**, the true princess of the lab. You often came striding into the lab with all the calm and grace, while at other times with the raging fury of a Chinese dragon. I really admire your open mind as well the determination and persistence with which you threw yourself at your project. **Yaro**, je kon je ei misschien niet helemaal kwijt in je project, maar de energie en creatieve ideeën die je meebracht in de de Zoete groep waren altijd zeer welkom. **Xuefeng**, a.k.a. the master of campy phospholipids. Your energy and enthusiasm can rival Carlos'. The boardgame nights were a nightmare, because you always won. Good luck, bro! **Yvette & Hanna**, ik weet inmiddels niet meer wie er nou bij wie op het lab te gast was, maar het was altijd fijn om met jullie te sparren over de glycobioogie. Bedankt voor de gezelligheid en de waardevolle tips & tricks. **Emma & Bogdan**, mijn labminions, het was me een waar genoegen jullie te mogen begeleiden en te zien groeien in het lab. Jullie energie en enthousiasme werkte stimulerend en ik hoop dat ik jullie even veel hebben kunnen leren als ik van jullie heb geleerd. Ter afsluiting van de infectiebiologie sectie mag ik natuurlijk niet m'n paranympnen vergeten. **Jiannan**, the PhD life in times of corona was not always easy on you, but therefore I admire your hard work and determination even more. I'm sure you will do well and can defend your own thesis very soon! We'll drink a nice Chinese beer to that! **Coco**, eerst als student en later als mede-PhDer bracht je nieuw leven in de brouwerij. Je had veel nieuwe wetenschappelijke ideeën die je vervolgens enthousiast uitwerkte in het lab. Daarnaast wist je gelukkig ook altijd wel te vertellen of en waar er een al dan niet clandestiene borrel te vinden was, waarvoor dank.

Voor alle gezelligheid op de derde verdieping van het Androclus wil ik natuurlijk ook graag iedereen van de Molecular Host Defense groep bedanken. **Henk, Edwin, Albert, Martin, Hanne, Maaïke, Roel, Melanie en Lianci.** Bedankt voor het meedenken over experimenten, de leuke labuitjes, de voetbal-pouls, de cake-bake competities en spelletjesavonden.

Verder wil ik natuurlijk ook heel graag **Richard** en **Esther** van het Center for Cell Imaging bedanken. Zonder jullie adviezen en enthousiasme had ik nooit zoveel uur achter een microscoop in een donker kamertje willen besteden.

I would also like to thank my fellow members of the DGK Borrelcie. **Roel** (yes, once more), **Alberta, Malthe & Nathalie.** Thanks for the good times organizing the many great activities.

Many thanks go to my collaborators at Yale, **Noah** and **Tyler.** Our joint discussions about this fascinating *Allobaculum* were very valuable.

In september 2019 verhuisde ik met het lab van diergeneeskunde naar het UMC. Hoewel het niet lang duurde voordat de corona ellende begon voelde het mede dankzij het warme welkom binnen de Medische Microbiologie afdeling snel (weer) vertrouwd.

Many thanks go to all the members of the Willems group. **Rob, Fernanda, Janetta,** thanks for all your interest and tips & tricks for the experiments. **Irma,** bedankt voor je vriendelijke hulp bij alle administratieve taken. My fellow PhD's in the lab **Axel, Roos, Paul, Matteo,** it was a joy to work with all of you in the lab. My apologies for exposing you to all these smelly anaerobes. **Iris, Marco, Jelle en Moniek,** bedankt voor het handhaven van de orde en jullie gouden handjes in het lab en natuurlijk ook voor de gezelligheid.

Of course I would also like to give a big thanks to the entire Bio-IT crew. **Malbert, Anita, Rodrigo, Jesse, Julián.** Thank you for all of your suggestions and great help in doing the bioinformatics. If it wasn't for your help I would have lost at least one computer to techno rage.

Verder zijn de mannen van het magazijn, **Frank, Manolito & Loek** natuurlijk onmisbare schakels in de keten. Bedankt voor al jullie hulp bij het organiseren van bestellingen.

Dan alle mensen van het grote lab, ofwel het lab van de andere kant! Ten eerste **Piet.** Ontzettend bedankt voor al je hulp bij de eiwit opzuiveringen en het beantwoorden van eindeloos veel van mijn vragen. Zonder jouw hulp waren de projecten lang niet zo snel gegaan.

Natuurlijk wil ik ook **Maartje, Lisette, Ingrid, Anouk & Anneroos** bedanken. Bedankt voor het wegwijs maken in het lab, de strakke organisatie en jullie goede adviezen.

**Erik,** heel erg bedankt voor het managen van alle labruimtes en faciliteiten. **Kok & Carla,** eveneens heel erg bedankt voor jullie tips & tricks.

Last but not least of the MMB, I would of course like to thank all the other (ex-) postdocs & PhD's that I have not mentioned yet thus far. **Bart, Dani, Priscilla, Leire, Herr. Bellyrub de Buhr, Patrique, Dennis, Leonardo, Julia, Stephanie, Astrid, Sjors, Frerich, Remy, Rita, Eva, Marieke, Janneke, Shu, Ninée & Lianne.** Thanks for all the fun times in the lab, at borrels, and good parties at the PhD retreats.

Verder prijs ik mijzelf ontzettend gelukkig met de grote schare aan vrienden die ik al zo lang, en soms wat korter, om me heen heb.

**Marijn, Bart, Vincent, Thijmen en Bas.** Het is inmiddels bijna 20 jaar geleden dat ik aan jullie werd blootgesteld. M'n leven was nooit meer hetzelfde. Bedankt voor al jullie nerdheid, slechte grappen, goede grappen, nóg slechtere grappen, vakanties, festival-friet-fijnproeverij, klimsessies en (soms serieus) gelul. Ik hoop op nog vele jaren.

Lieve Nijmegenaren: **Toon, Marcel, Marga, Lieke, Chris, Joris, Janneke, Anneke, Marlies, & Guido.** Ik kan me nooit zo goed herinneren hoe onze vriendenkring is samengekomen, maar dat kan wellicht te maken hebben met de eindeloze kings-sessies. Gelukkig kan ik de MFV-feesten, stedentripjes, escape rooms, weekendjes weg, AoE-sessies, spelletjesavonden en fietstochten een stuk beter herinneren. Het is fijn dat iedereen altijd op zijn eigen manier lekker zijn gang kan gaan. Special shout out naar Guido voor z'n mass spec magic en bijdrage aan hoofdstuk 3 en 4.

Dan natuurlijk ook de lieve Utrechtse. Te beginnen met de VLL62: **Bart, Fiona, Marlies, Anne-Eva, Manon, Robert, Jonathan, Fransien, Madeline, Aart, Elise, Willemijn & Jonas.** Als kersverse Utrechter voelde ik me gelijk

ontzettend thuis in ons huisje met misschien wel het mooiste uitzicht van Utrecht. Bedankt voor de gezelligheid voor én na m'n tijd aan de VLL62. Ik hoop dat wel snel een zeer extravagante FM cooking experience in ons Toscaanse castello mogen beleven. Als het maar geen rauwe kip is...

Het andere thuis in Utrecht bevindt zich natuurlijk aan de Croeselaan 85. Met eerst **Vincent** (ja weer), en later met **Bas & Elske**. Ik heb er 4,5 heerlijke jaren gewoond. Zelfs de lockdowns waren in ons "Paradijsje" nog redelijk uit te houden en dat kwam toch zeker ook door jullie. Bedankt voor alle reuring, bankhang sessie, goede muziekkeuzes, gezelligheid, goede gesprekken, overheerlijke imam bayildi, en niet te vergeten de (tuin-)feestjes. Geniet er nog van zolang het kan en bedenk: ook na de verdrijving uit het Paradijs kan je nog een prima feestje geven.

Lieve Octopussers en Octoplussers. **Ria, Ernst, Margo, Sam, Floor, Lodewijk, en alle plussers**. Opgroeien in woongroep lijkt heel gewoon als je erin zit, maar is toch best wel bijzonder. Wie weet heeft de vroege uitwisseling van onze gastro-intestinale medebewoners wel de kiem gelegd voor m'n interesse in de microbiologie. Het samen opgroeien heeft hoe dan ook bijgedragen aan onze speciale band. Gelukkig is de uitwisseling tegenwoordig wat minder van fysieke aard, maar ik ben ontzettend blij dat ik altijd kan komen aanwaaien. En Lo, natuurlijk ook nog heel erg bedankt voor je ontwerp van de omslag.

**Miriam, Paulien, Tom & Fieke**. Het schrijven van een dankwoord kan soms een hele klus zijn. Als van Muijlwijk of Vos is het niet altijd even gemakkelijk om je te uiten, maar gelukkig liggen de gevoelens van dankbaarheid natuurlijk wél op mijn lippen bestorven. Hoe kan het ook anders. Desalniettemin hou ik het kort. Zonder jullie was ik er niet en mede door jullie ben ik wie ik ben. Ontzettend bedankt voor al jullie aandacht, steun en interesse, en natuurlijk bedankt voor jullie liefde, al dan niet geuit door een gevecht op de achterbank, een schop onder m'n kont, een gek dansje, of een heerlijke maaltijd. Bedankt voor jullie zelf.

# CURRICULUM VITAE

Guus van Muijlwijk werd op 15 maart 1990 geboren te Woerden. In 2008 runde hij succesvol het tweetalig VWO af aan het ORS Lek en Linge te Culemborg, waarna hij begon aan de Bachelor opleiding Biomedische Wetenschappen aan de Radboud Universiteit in Nijmegen. Als onderdeel van het honours programma doorliep hij in het voorjaar van 2011 een stage aan de Universiteit van Manchester, Engeland, en verkende daar de lokale antibiotica resistentie in de schimmel *Aspergillus fumigatus*. Later dat jaar behaalde hij zijn bachelor diploma om daarna t/m de zomer van 2013 al backpackend Australië en delen van Zuid-Oost Azië te verkennen. In september 2013 keerde hij terug naar de schoolbanken en begon aan een master Infection & Immunity aan de Universiteit Utrecht. Als onderdeel van deze opleiding bestudeerde hij in het UMC Utrecht, in het lab van Prof. Wiertz, de immuun evasie mechanismes van het humaan cytomegalovirus. Hierna volgde een stage in het lab van Prof. Kubes aan de Universiteit van Calgary, Canada, alwaar hij de in vivo immuun responsen tijdens hepatische infecties met de bacterie *Listeria monocytogenes* bestudeerde. In het voorjaar van 2016 ontving hij zijn Master diploma en begon hij aan zijn promotieonderzoek aan de Universiteit Utrecht. Eerst in de infectiebiologie groep aan de faculteit Diergeneeskunde en vanaf september 2019 in het UMC Utrecht. Onder begeleiding van Prof. van Putten en Dr. de Zoete, bestudeerde hij de moleculaire interacties van intestinale pathobionten met cruciale onderdelen van de darmwand en de slijmvliesbarrière. De bevindingen van dit onderzoek zijn beschreven in dit proefschrift. Vanaf november 2021 onderzoekt Guus als postdoc aan de Universiteit van Bern, Zwitserland, de rol van de darm microbiota op de ontwikkeling van het immuunsysteem.



# PUBLICATIONS

## Publications

### Related to this thesis:

**van Muijlwijk GH**, Bröring ECR, van Mierlo G, Jansen PWTC, Vermeulen M, Aerts PC, van Putten JPM, Palm NW, de Zoete MR. Growth inhibition of *Akkermansia muciniphila* by a secreted pathobiont sialidase. *bioRxiv*. 2022. doi:<https://doi.org/10.1101/2022.03.15.484512>

**van Muijlwijk GH**, van Mierlo G, Jansen PWTC, Vermeulen M, Bleumink-Pluym NMC, Palm NW, van Putten JPM, de Zoete MR. Identification of *Allobaculum mucolyticum* as a novel human intestinal mucin degrader. *Gut Microbes*. 2021;13(1). <https://doi.org/10.1080/19490976.2021.1966278>. doi:10.1080/19490976.2021.1966278

### Prior to this thesis:

van der Houwen TB, van Laar JAM, Kappen JH, van Hagen PM, de Zoete MR, **van Muijlwijk GH**, Berbers R-M, Fluit AC, Rogers M, Groot J, Hazelbag MC, Consolandi C, Severgnini M, Peano C, Elios MMD, Emmi G, Leavis HL. Behçet's Disease Under Microbiotic Surveillance? A Combined Analysis of Two Cohorts of Behçet's Disease Patients. *Frontiers in Immunology*. 2020;11:1–10. doi:10.3389/fimmu.2020.01192

van De Weijer ML, **van Muijlwijk GH**, Visser LJ, Costa AI, Wiertz EJHJ, Lebbink RJ. The E3 ubiquitin ligase TMEM129 is a tri-spanning transmembrane protein. *Viruses*. 2016;8(11). doi:10.3390/v8110309

Bromley MJ, **van Muijlwijk GH**, Fraczek MG, Robson G, Verweij PE, Denning DW, Bowyer P. Occurrence of azole-resistant species of *Aspergillus* in the UK environment. *Journal of Global Antimicrobial Resistance*. 2014;2(4):276–279. doi:10.1016/j.jgar.2014.05.004